Paving the foundation for precision medicine: Data-driven reconstruction of context-specific metabolic network models to elucidate pathomechanisms

Dissertation

Zur Erlangung des Doktorgrades (Dr. rer. nat.) der

Mathematisch-Naturwissenschaftlichen Fakultät der

Christian-Albrechts-Universität zu Kiel

Jonathan F. Josephs-Spaulding

Kiel | Dezember 2021

Erstprüfer:

Prof. Dr. Hinrich Schulenburg

Evolutionsökologie und Genetik, Evolutionary Ecology and Genetics,

Christian-Albrechts Universität zu Kiel

Zweitprüferin:

Prof. Dr. Christoph Kaleta

Medizinische Systembiologie, Institut für Experimentelle Medizin,

Christian-Albrechts Universität zu Kiel

Datum der mündlichen Prüfung: 10. March 2022

Nature is a language and every new fact one learns is a new word;
but it is not a language taken to pieces and dead in the dictionary,
but the language put together into a most significant and universal sense.
I wish to learn this language, not that I may know a new grammar,
but that I may read the great book that is written in that tongue.

-Ralph Waldo Emerson, "Nature (1836)"

TABLE OF CONTENTS

Summary

To further understand human biology to treat or intervene against the rise of modern diseases such as COVID-19, multidrug resistance UTIs, and Parkinson' Disease, there is a need to develop *in silico* clinical approaches that are based on personalized or precision medicine. Specifically, patient-derived "omics" approaches can be utilized to dissect the trajectory of pathology by gaining insight into molecular mechanisms underlying disease. For example, the application of transcriptome sequencing (RNA-Seq) provides insights into disease mechanisms at specific timepoints by characterizing the gene expression of cells, tissues, or host-associated microbiomes. However this technique is limited by the lack of approaches which extend or translate gene expression towards metabolic functions that are involved in disease onset. Therefore, the utilization of systems biology tools and frameworks combined with omics-based data can bolster our basic biological understanding of various diseases, towards developing cutting-edge interventions that are relevant to unique patient contexts. Specifically, datasets which utilize multi-omics (genomics, proteomics, transcriptomics, etc.) can be extended with systems biology approaches to develop context-specific models, thereby refining the assumptions which underlie predictive models of patient-specific disease mechanisms. To this end, precision medicine and systems medicine share a common goal: the need to identify and interpret fundamental pathomechanisms which influence disease onset or remission; a goal that is achieved through the development of *in silico* clinical trials. Prior to achieving this aim, one requirement is to develop bioinformatic and systems biology workflows upon clinical samples to effectively model adverse pathophysiological states. Specifically, these models ought to be informed by context-specific and patient-specific circumstances which underlie disease mechanisms. Therefore, this dissertation will investigate both biomedical and systems biology literature to support the argument that reductionist approaches in medicine are limited and remain as a constraint towards precision medicine. To address this issue, the methodology presented in this dissertation will employ various systems biology tools to develop two systems medicine workflows with the aim to reconstruct context-specific metabolic network models conditioned with two next-generation RNA-Seq datasets (single-cell and metatranscriptomics) to uncover novel pathway activity in various patient cases. First, single-cells were extracted from COVID-19 patients longitudinally over a timescale and used to reconstruct metabolic network models of individual immune cells from various patients. This metabolic modeling approach upon a wide-range of patient cells uncovered both cell- and patient-specific metabolic pathways which were used for the characterization of various disease states through metabolic reaction abundance. Second, metatranscriptomics samples derived from UTI patients were extended for the construction of patient-specific microbiome community models. By simulating the urinary tract microbiome in tandem with the gene expression of the individual bacteria which form the community, numerous patient-specific biomarkers of infection were identified. In summary, both approaches highlight that the results derived from metabolic network models provide insights into both metabolic pathomechanisms which accurately characterize disease phenotypes and the increased potential for identifying realistic targets for disease intervention. Overall, the development of computerized human models that are biologically relevant is a foundational requirement and precursor towards a future setting which allows for *in silico* clinical trials.

Zusammenfassung

Um die menschliche Biologie besser zu verstehen und akut zunehmende Krankheiten wie COVID-19, multiresistente Harnwegsinfektionen und Parkinson zu behandeln werden klinische in-silico-Ansätze benötigt, die auf einer personalisierten Präzisionsmedizin beruhen. Insbesondere können individuelle "Omics"-Datensätze von Patienten dazu genutzt werden, den Verlauf einer Krankheit durch die Analyse molekularer Mechanismen aufzuklären. Die Anwendung der Transkriptomsequenzierung (RNA-Seq) beispielsweise ermöglicht Einblicke in Krankheitsmechanismen zu definierten Zeitpunkten, zu denen die Genexpression von Zellen, Geweben oder wirtsassoziierten Mikrobiomen untersucht wird. Allerdings fehlt bei diesen neuen Verfahren eine Möglichkeit zur Übertragung von Genexpressionen auf Stoffwechselfunktionen, die an der Entstehung von vielen Krankheiten beteiligt sind. Daher kann der Einsatz von systembiologischen Werkzeugen und Verfahren auf Basis von Omics-basierten Daten das biologische Verständnis verschiedener Krankheiten grundlegend verbessern, um so neue Maßnahmen zu entwickeln, die zur individuellen Situation eines jeden Patienten passen. Die Verbindung von Multi-Omics-Daten (Genomik, Proteomik, Transkriptomik usw.) mit systembiologischen Ansätzen kann mittels kontextspezifischer metabolischer Modelle erfolgen, die quantitative Vorhersagen über patientenspezifische Krankheitsmechanismen ermöglichen. Präzisions- sowie Systemmedizin verfolgen daher das gemeinsames Ziel, durch die Entwicklung von klinischen in-silico-Studien diejenigen grundlegenden Pathomechanismen zu identifizieren und zu charakterisieren, die den Ausbruch oder die Remission von Krankheiten beeinflussen. Um dieses Ziel zu erreichen, müssen zunächst bioinformatische und systembiologische Verfahren auf der unmittelbaren Grundlage klinischer Proben entwickelt werden, um auch komplexe pathophysiologische Zustände hinreichend abbilden zu können. Dabei ist besonders wichtig, dass die entwickelten Modelle die kontext- und patientenspezifische Umstände, die den Krankheitsmechanismen zugrunde liegen, berücksichtigen. Die vorliegende Dissertation untersucht zunächst die biomedizinische und systembiologische Literatur, um die Schwachstellen von reduktionistischen Ansätzen in der Medizin offenzulegen und argumentiert, dass diese Hindernisse auf dem Weg zu einer Präzisionsmedizin bedeuten. Des Weiteren werden konkrete Lösungsvorschläge entwickelt, die durch den Einsatz von systembiologischen Werkzeugen moeglich werden: In zwei systemmedizinische Anwendungen werden daher kontextspezifische metabolische Modelle rekonstruieren, die auf Next-Generation-RNA-Seq-Datensätzen (Einzelzell-Sequenzierung sowie Metatranskriptomik) aufbauen, um so neuartige Reaktionswege aufzudecken. Estens wurden einzelne Zellen von COVID-19-Patienten über einen bestimmten Zeitraum extrahiert und zur Rekonstruktion von metabolischen Modellen einzelner Immunzellen der jeweiligen Patienten verwendet. Damit konnten sowohl zellspezifische als auch patientenspezifische Stoffwechselwege aufgedeckt werden, die anschließend zur Charakterisierung verschiedener Krankheitszustände anhand der Häufigkeiten von Stoffwechselreaktionen genutzt wurden. Darüber hinaus wurden zweitens Metatranskriptomproben von Harnwegsinfektionspatienten für die Konstruktion von patienten- und kontextspezifischen Bakterienmodellen genutzt, die dann als mikrobielle Gemeinschaften computergestützt simuliert wurden, was schließlich in der Ermittlung zahlreicher patientenspezifische Biomarker mündete. Zusammenfassend zeigen beide Ansätze, dass die aus kontextspezifischen metabolischen Modellen abgeleiteten Ergebnisse sowohl Einblicke in metabolische Pathomechanismen zur genauen Charakterisierung von Krankheitsphänotypen als auch ein erhöhtes Potenzial zur Identifizierung möglicher Krankheitsinterventionen bieten. Die Entwicklung biologisch relevanter, computergestützter Modelle des Menschen bildet somit eine grundlegende Voraussetzung für zukünftige klinische in-silico-Studien.

List of Figures

List of Tables

I. Introduction

"The single most unused person in healthcare, is the patient"

- David M. Cutler, MIT Review (2013)

While the central purpose of natural sciences as a field of inquiry is to explain the various phenomena of nature, the advancement of scientific knowledge is regularly constrained through the lens of reductionist approaches. While the approach of reductionism in science is useful to test hypotheses and ultimately develop theories in a systematic way to explain and predict biological phenomena, this approach quite often restricts the ultimate purpose of scientific inquiry, especially in medicine. For example, both microbiology and biomedical science have long-standing traditions in reductionist approaches in order to better understand microbiota and the onset of disease. To date, only 1% of all microbiota can be cultured and most therapies towards human disease employ a generalized approach to treat symptoms, but rarely to heal the entire human. This has led to long standing issues in how we understand the ever-lasting relationship between humans and microbiota. Human-associated microbiota occupy niches throughout the human body, both inside and out. The human microbiome is a dynamic community of intermingling bacteria which provide various ecosystem services with regards to health and disease, specifically this ecosystem is readily modulated by a wide-range of environmental factors, such as food (Josephs-Spaulding et al. 2016). More so, humans have not only a complicated genetic background, but also environmental or lifestyle influences which may drive disease mechanisms in various ways (Khoury et al. 2016). By applying a one-size or one drug fits all approach to patients and ignoring both the genetic and environmental uniqueness of patients, the development of therapies to treat patients likely overlooks foundational biology which controls both health and disease. This in turn has led to further misunderstandings of human complexities and the organisms which occupy various human niches; thus leading to the rise of global antimicrobial resistance, chronic inflammatory diseases, global pandemics, and the development of medical therapies which ignore the host-associated microbiome.

The present approaches of the medical to treat and interpret human medicine through holistic approaches which assess patients as a biological system is limited (Khoury et al. 2016). More so, traditional medical outlooks have stagnated the effectiveness of patient care, especially during the face of rising health crises such as the global Coronavirus disease 2019 (COVID-19) pandemic and the impending 'Superbug' (i.e bacteria which are resistant against last-resort antibiotics) pandemic which is probable in the near future. To solve these issues, numerous methods and engineered interventions are on the rise to improve human environments and mitigate disease, however basic understanding of the biological principles which mediate disease mechanisms remains limited, especially through the dissecting lens of sequencing technology which rapidly profiles molecular patterns. More so, the application of basic biology in a patient-specific or systems/precision medicine framework is lacking in a clinical setting. For example, human urinary tract infections (UTIs) have been understood and treated in clinics as a mono-infection caused by the uropathogenic *E. coli*. Rather, this dissertation acknowledges a uromicrobiome within patients that is diverse in both microbial species composition and metabolic function that is dependent on the host. Additionally, during the start of the COVID-19 pandemic, most believed that COVID-19 infections were tissue-specific, such as within the lungs, and the disease impacted mostly the elderly. The results in this dissertation support that various immune cells which circulate throughout the human have various roles within patients and diverse metabolic potential across age, sex, disease status, and other relevant characterisitics. Finally, Parkinson's Disease (PD) and other idiopathic neurodegenerative diseases which are manifested in motor impairment symptoms, require observations through the lens of systems toxicology. Specifically, the presented review of literature which is covered within this dissertation suggests that there is a great need to consider the strong effects of toxic metal exposure and the interaction of these compounds upon the host-associated gut microbiome to better understand the molecular mechanisms underlying disease. Overall, these three diseases highlight a significant complication of modern medicine and the need to advance clinical therapies with both precision and systems medicine approaches which keep patient-specific traits at the focus.

The primary research question presented in this dissertation is: “how do various pathologies (microbial or viral) drive cell or microbiome-specific metabolic pathways in a way that is either unique to the patient or closely-related groups or individuals?”. This question will be answered by deriving molecular information from next-generation sequencing (NGS) datasets to reconstruct metabolic network models during the course of the aforementioned diseases. Through this information, robust metabolic interventions or treatments may be suggested to individual patients, rather than through a generalized approach which may not bolster the health of all patients equally. During the course of this dissertation, three major diseases that have become significant to global public health will be discussed and used as models for human disease. The presented research question will be applied to all of these cases to better understand the current metabolic state of the respective diseases during disease trajectory. Therefore with the novel information provided from this dissertation, there will be increased evidence for future clinical practitioners to draw associations between the simulated findings and basic literature to better identify potential treatment regimens or interventions which directly impact cell or microbiome-specific metabolites.

The first presented application of metabolic model reconstructions will be utilized to describe the pathophysiology of COVID-19 infection on a longitudinal scale. This infection has been shown to demonstrate highly heterogeneous clinical symptoms and severity which may range from asymptomatic towards intense inflammatory responses which can lead to systemic organ failure and death. As COVID-19 has been strongly associated with dysfunction at the host level, our recent analysis has observed that specific cell-types are metabolically hyperactive during severe or critical cases and likely ‘steals’ nutrients from the patient environment, thus exacerbating a patient’s immune response (Bernardes et al. 2020). While this study provided much needed evidence of the molecular mechanisms underlying cell-specific trajectory, it did not investigate patient-specific similarities or differences. By using single-cell RNA-sequencing (scRNA-seq) data from a longitudinal cohort of patients, this dissertation seeks to derive metabolic pathway information about all assessed cell types from various patients during the

course of disease to identify unique molecular mechanisms for respective patients as they transition through disease states.

The next presented application of metabolic model reconstruction is in relation to recurrent urinary tract infections (rUTIs) in a small cohort of women. At present, UTIs are understood to be monoinfection; however through the lens of metatranscriptomics both the microbial community and their functional gene expression has been uncovered. By utilizing context-specific metabolic modeling, the findings from the presented simulations supports some observations and new knowledge with regards to metabolic uptake and crosstalk within the microbial communities which inhabit a patient's bladder. With regards to precision medicine and simulation of microbial communities, it has become clear that certain metabolites likely support pathogenesis, most are uptaken through microbial crosstalk to bolster recurrence in UTIs. Therefore, the results presented in the described study could bolster the effectiveness of UTI interventions in a clinical setting by suggesting the removal of specific dietary-derived metabolites which supports the growth of the pathogenic community. On the other hand, patients could also be supplemented with dietary metabolites to potentially inhibit the growth of the community by impairing specific metabolic pathways which were observed through the simulations that are later described in this dissertation.

Finally, the published knowledge detailing the crosstalk between both the host and associated microbiome interacts during the onset of PD, in tandem with environmental exposure of heavy metals was investigated. It is presently understood that dysbiosis of the gut microbiome negatively impacts the host, however the role of host-related factors such as diet and exposure to toxicants such as metals remains understudied. Therefore, the literature of the mechanisms underlying neurodegeneration and PD onset through the gut-brain axis in relation to toxic heavy metal exposures will be proposed as a future avenue for metabolic network model reconstruction by joining the host and microbiome, to create whole body metabolic models (WBMs). While it is essential to study how both systems function independently and mediate exposure of heavy metals, both also work in tandem to support patient health or exacerbate disease. More so, this review article will propose the development of a new

paradigm shift that includes the role of systems toxicology in precision medicine. This can be accomplished by modeling the effects of heavy metal exposures on the gut-brain axis through the application of WBMs.

This dissertation seeks to promote the interpretation and utilization of systems biology tools with NGS to improve the present understanding of pathomechanisms underlying disease, within a precision medicine context. Ideally, this study ought to further encourage clinicians to adopt next-generation approaches in collaboration with those who model disease to better decipher patient-specific differences and provide optimized treatment options. To reach this end, the methods in this dissertation apply bioinformatic and systems biology tools on NGS datasets derived from COVID-19 and UTI patients to investigate patient-specific disease differences rather than a generalized approach. Furthermore, these methods will extract relevant gene expression data from patient samples with bioinformatic tools to better inform the reconstruction of context-specific metabolic models, rather than generalized models. Presently, this dissertation will demonstrate the novel approach of reconstruction of context-specific metabolic models of human diseases that are derived from metatranscriptomics and scRNA-seq datasets, independently. The methods presented in this study can be readily applied to either the study of interactions in the human microbiome from a specific point of time or to investigate numerous human single-cells in parallel. From this information, future clinicians will have the opportunity to bolster precision medicine practices by expanding their understanding of diseases within specific contexts, but also at a phenotypic level through obtaining relevant metabolic information. The utilization of RNA-Seq for identifying counts of genes and transcripts of interest is a meaningful approach towards improving the understanding of various diseases where metabolism plays a significant role. More so, gene-level expression counts mapped to species genomes in the case of metatranscriptomics can help to improve the understanding of lowly expressed genes and metabolic functions that are expressed by host-associated microbiota during disease in a patient-specific fashion. However, due to the broad diversity and heterogeneity of environments and ecological niches that microbes or humans can occupy at any given time, this is a major limitation of conducting a study of this magnitude. While RNA-Seq may readily provide insight on transcriptional modifications and response to environments, this

heterogeneity provokes a challenge in comparing results across patients. However, this may be an advantage as these methods enforce an analytical rhetoric that is based on patient-specific understanding rather than comparing different groups who may or may not have similarities (as in the case for differentially expressed genes) that are assumed comparable by investigators. Furthermore, transcriptional changes that are host-pathogen specific may not be readily replicated in biological experiments, due to complexities when attempting to control specific environments. Thus, the application of context-specific genome-scale metabolic models for studying disease pathophysiology to predict an organisms' transcriptional and metabolic changes when primed by environmental stresses is a promising approach to unravel the complexities pathophysiology and predict treatment strategies to prevent or intervene against disease trajectory (Józefczuk et al., 2010). However, during the review of literature, especially on genome-scale metabolic models, there will be increased details on the limitations of this modeling approach and it's approach in medicine.

Overall, modern scientific practices have become significantly limited due to the application of reductionist approaches. These approaches have eventually spilled over and have come to negatively impact the translation of biomedical sciences towards the applications of medicine for clinical interventions. Specifically, modern medicine has diverted into a generalist approach to treat patients, rather there is a need to shift medicine for personalized design to take into account individual differences between patients. However, as more diseases become further complicated through the global emergence of antimicrobial resistance, the onset of the COVID-19 pandemic, and the debilitating long-term effects of chronic diseases, there is a need now more than ever to implement precision medicine approaches coupled with systems biology tools to better treat patients. In the course of this dissertation, the major employed method will be context-specific metabolic modeling on RNA-Seq datasets to provide a mechanistic snapshot into disease trajectory overtime. While these models are taken in the past of the patient's history, they will irregardless provide substantial support in understanding the biomedical foundations across disease within the framework of precision medicine.

II. Review of the Literature: Conceptual and Theoretical Framework

Human diseases cannot be cured by attempting to interpret symptoms alone, rather there are dynamic mechanisms which underlie disease onset and progression (Figure 1). Specifically, metabolism to a large extent underlies the health and disease of cells, microbial communities, and human health as a whole. The reprogramming of systemic metabolism is evolutionarily conserved and understood to play significant roles in the pathophysiology of numerous human diseases such as cancer, diabetes, immune dysregulation, and chronic inflammation (Cairns et al. 2011 ; Wang et al. 2019). Additionally, growing evidence is continuously demonstrating the extensive role that the crosstalk between the host metabolism and that of host-associated microbiome metabolism play in the onset or development of cardiovascular diseases, diabetes, various metabolic syndromes, and obesity (Tremaroli & Backhed, 2012). Furthermore, the applications of metabolic models can provide an avenue toward developing precision medicine by allowing a context-specific look into disease dynamics and trajectories. Overall, the presented perspectives covered in this review of the literature illustrate the need to withdraw from traditional reductionist perspectives in biomedical and translational sciences and instead, move towards a systems-view revolving around patient-specific pathophysiology during diseases.

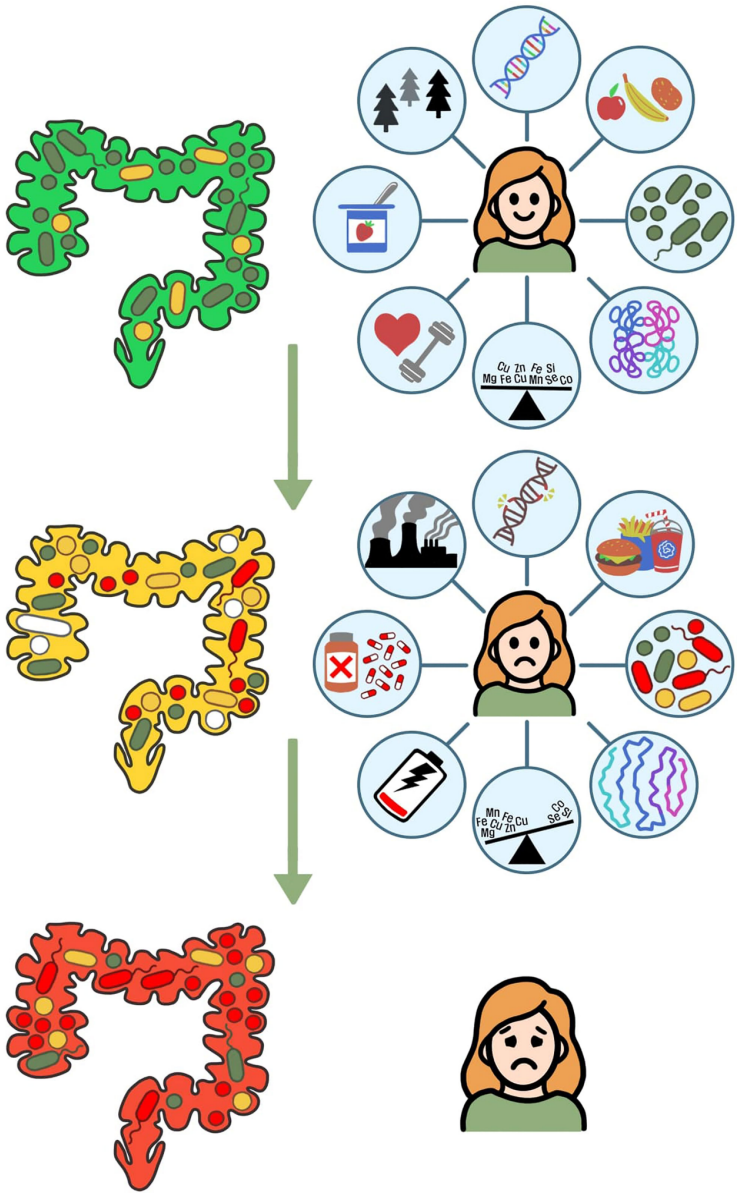

Figure 1: Host environment controls the transition from health to disease. A healthy host and associated commensal microbiota enforces an environment that prevents colonization by invasive pathogens. Environmental factors tend to influence the dysregulation of both host physiology and native microbial communities in tandem. Adverse community stressors such as DNA or protein damage, poor diet, depleted microbial diversity, excessive metals, an inactive lifestyle, antibiotic usage, and adverse environment. The two-pronged attack of dysregulation of both microbial communities and host homeostasis leads to dysbiosis of beneficial bacteria, thus leading to disease outcomes of individuals and formation of new microbial communities reflective of the pathology.

A. COVID-19 (Single Cells)

The spread of the novel coronavirus severe acute respiratory syndrome coronavirus 2 (SARS-CoV-2) which causes febrile respiratory symptoms has become a significant public health and precision medicine challenge for global communities. Presently, it is understood that the virus spread as a zoonotic outbreak from the Huanan Seafood Wholesale Market, as a consequence the market shut down on January 1st, 2020 to further mitigate spread of the virus (Hui et al. 2020). Within a few days, SARS-CoV-2 was obtained from the lower respiratory tract of a patient on January 7th. Subsequently, in a demonstration of the rapid and powerful response from the genomics community, SARS-CoV2 was isolated and fully sequenced to become available to scientists globally on January 12th; this rapid step allowed for the public to identify this novel virus strain as a Group 2B ß COV (Hui et al. 2020 ; Huang et al. 2020). From there, it was assessed that the novel SARS-CoV-2 strain has a 82% genomic similarity with a previous SARS virus which also originated from China and led to a significant outbreak in 2002 (Hui et al. 2020). However, the current SARS-CoV-2 virus is significantly more mild that the previous SARS virus, even though both viruses share similar symptoms of causing febrile illness and pneumonia in humans (Hui et al. 2020 ; Huang et al. 2020 ; Chen et al. 2020a). The previous virus only led to a peak of approximately 8000 cases with a high patient mortality rate of 9.6% (Hui et al. 2020 ; Huang et al. 2020). However, the rate of infections and deaths for the present SARS-CoV-2 have a high contrast between nations due to the fact that infection fatality rate/ number of true infections may have went unnoticed; some countries (such as Russia or India) were found to have failed to present thorough reports for death due to COVID-19 (Balashov et al. 2021; Karlinsky & Kobak, 2021).

It remains unclear why the manifestation of COVID-19 as a disease provokes heterogenous symptoms which can range from asymptomatic infections to massive cytokine storms or hyper-inflammation in the lungs, causing SARS. Hyperinflammatory COVID-19 has been characterized as the proliferation of type-1-IFN-activated $CD14^{+}$ suppressive monocytes in addition to granulopoiesis with a rapid increase in neutrophil counts in addition to the lack of production of T-cell lymphocytes as another hallmark of severe COVID-19 (Diao et al., 2020;

Giamarellos-Bourboulis et al., 2020; Guan et al., 2020; Huang et al., 2020; Zheng et al., 2020). Overall, severe COVID-19 cases in patients tend to share similar characteristics such as sepsis, the production of proinflammatory cytokines, activation of neutrophils, altered monocyte activation, lack of circulating lymphocytes, impaired functioning of natural killer cells, and general activation of circulating neutrophils (Laing et al. 2020 ; Li et al. 2020). Present studies have identified that the risk of developing severe COVID-19 is associated with age, numerous comorbidities (diabetes, high blood pressure, obesity, etc.), hyperactivated immune systems, and various other factors. This highlights the need to develop interventions in COVID-19 patients in a patient specific manner which considers molecular and cellular mechanisms which underlie the disease (Branchett et al. 2019; Wu et al. 2020 ; Guan et al. 2020 ; Huang et al. 2020; Mehta et al. 2020). Therefore it is essential to conduct detailed investigations to better understand the molecular mechanisms which underlies SARS-CoV-2 pathology, particularly disease severity progression, host-associated responses to infection, and constraints on viral replication rates. By progressing studies that go beyond the broad and heterogeneous cellular features of adaptive immune cells in response to infection from SARS-CoV-2, there is an opportunity for future studies to rapidly identify novel biomarkers for developing targeted treatments for patients through multi-omics and systems biology applications (Bernardes et al. 2020).

It has been hypothesized that one of the major sites for viral replication in humans is in the small intestines; viral proteins have been identified in patient small intestines several months following clearance of the virus from the respiratory tract indicating that SARS-CoV-2 likely incites mechanisms to evade host immune systems, further complicating the understanding of COVID-19 transmission (Zang et al. 2020 ; Cheung et al. 2021 ; Gaebler et al. 2021). Presently, animal-to-human transmission, from bats to humans, of SARS-CoV-2 was initially suggested by Paraskevis et al. based on initial whole-genome evolutionary analysis (Paraskevis et al. 2020 ; Zhou et al. 2020a). Specifically, viral reads of SARS-CoV-2 have been identified in the intestines of Chinese bats, where this organism acts as a long-term reservoir for various Coronaviruses without impairing the phenotypic fitness of the host (Tang et al. 2006 ; Watanabe et al. 2010). However, previous studies suggest that severe acute respiratory syndrome (SARS) viruses are known to be derived from animals such as the Chinese horseshoe bat, Himalayan

palm civets, raccoon dogs, and Chinese ferret badgers which are all found in live animal markets and are likely sources of reservoirs for various SARS viruses (Hui et al. 2020 ; Huang et al. 2020 ; Paraskevis et al. 2020 ; Ahmad et al. 2020). Interestingly, preliminary studies have not demonstrated an efficient proof of animal-to-human transmission (Hui et al. 2020). However, it has become quite clear that a rapid increase in cases over a short period of time and the presence of unique clustering of pneumonia symptoms associated with SARS-CoV-2, that human-to-human transmission of the virus is rather efficient and a cause for concern (Chan et al. 2020).

The zoonotic shift from animals to humans likely derives from a mutation found in the receptor binding domain of the virus spike protein, leading to increased binding potential to the human angiotensin-converting enzyme 2 (ACE2) which has become a significant point of study is delimiting the infectivity and pathogenicity of SARS-CoV-2 (Perlman et al. 2009 ; Huang et al. 2020). Specifically, the ACE2 receptor has been identified as the SARS-CoV-2 entry receptor for the initiation of infection and is mainly expressed in the cells of the nasopharynx and lungs (Letko et al. 2020 ; Zhou et al. 2020a). Specifically, the causative agent of SARS, both SARS-CoV-1 and SARS-CoV-2 are known to penetrate immune cells which do not express ACE2 (Gu et al. 2005). For example, a recent study in patients with COVID-19 demonstrated that patients treated with ACE inhibitors (for hypertension or diabetes treatment) may be at a significantly higher risk for SARS-CoV-2 infection, this is due to these drugs generally increase ACE2 expression (Fang et al. 2020; Wan et al. 2020). On the other, the virus may also infect dendritic or macrophages and use DC-SIGN (Cd209), CLEC4m (CD209L), and Fc-Gamma Receptor 1, which are alternative receptors for entering cells (Channappanavar et al. 2016 ; Zhou et al. 2020b). With regards to secretory cells, these cells typically have a three-times increase in the expression levels of ACE2 in comparison to controls with non-infected cells (Chua et al. 2020). It should be additionally noted that cells which are ACE2 positive are generally epithelial cells and are strongly overrepresented when assessing single-cell transcriptomics, viral cells have low numbers of viral reads during COVID-19 infection likely due to phagocytosis (Chua et al. 2020). While the number of secretory cells was not shown to increase after infection of COVID-19, this population does contain a high-number of cells that

are ACE2 positive, thereby highlighting that secretory cells may be one of the most susceptible cell types for COVID-19 infection (Chua et al. 2020). Recent studies have confirmed that ACE2 proteins become more localized with motility proteins found on secretory cells proximal to motile cilia with a high rate of infectivity on ciliated secretory cells when infected with SARS-CoV-2 (Lee et al. 2020 ; Ravindra et al. 2020). Overall, when employing scRNA-seq, both secretory and ciliated cells in general have been found to contain the highest fraction of viral RNA and act as the main site of infected cells in humans as compared to other cell types, further highlighting the need to investigate both as a potential mean to intervene against COVID-19 (Chua et al. 2020 ; He et al. 2020 ; Ravindra et al. 2020).

1. COVID-19 Inflammation at the Single-cell Level

Numerous longitudinal COVID-19 studies have sought to better understand the molecular pathophysiology of circulating immune cells during various stages of COVID-19. Yet these studies have only derived findings based on single information levels by employing techniques such as fluorescence-activated cell sorting to identify counts of specific cells. However, a recent study employed scRNA-seq to dissect COVID-19 disease severity trajectory by using a comprehensive and longitudinal approach with the support of multi-omics tools (Bernardes et al. 2020). The integration of a chronological ranking system of disease trajectory matched with multi-omics and systems biology applications has provided a powerful insight into disease pathophysiology at the single-cell level (Bernardes et al. 2020). Biomarkers derived from human single-cells can provide an early snapshot of disease trajectory from cells, towards the tissue level. While past studies investigate human medicine at the tissue level, there is a large-scale heterogeneity between cell-to-cell interactions that is controlled by various molecular mechanisms which require further investigation through scRNA-seq (Rajewsky et al. 2020). Specifically, scRNA-seq is a high-resolution method that has the potential to characterize the heterogeneity of individual cells over time, particularly during the course of infection where results may be hidden while comparing host response at the population level (Cristinelli and Ciuffi, 2018; Russell et al., 2018 ; Shnayder et al., 2018; Drayman et al., 2019; Wyler et al., 2019; Zanini et al., 2018).

When comparing host-specific transcriptional responses to a variety of respiratory viruses in human cells, it is readily noted that SARS-CoV-2 has a virus-specific inflammatory response as compared to other viruses (Blanco-Melo et al. 2020). Furthermore, scRNA-seq analysis has specifically demonstrated that genes such as IFIT1/IFIT2 tend to be broadly induced across most cell types, in contrast IFNB1 and IL6 have been assessed to be expressed in specific subset of infected cells during SARS-CoV-2 infection (Wyler et al. 2021). Therefore the application of scRNA-seq is not only a proven and promising technique within the realm of biomedicine, but it can further bolster our understanding of precision changes in heterogeneous populations by dissecting molecular mechanisms and further support our understanding in COVID-19 disease pathophysiology. At present, human single-cells during COVID-19 infection are studied at two levels: (1) as bronchoalveolar lavage fluid (BALF) which samples the bronchioles and lung alveoli, thereby providing information on the lung microenvironment (Liao et al. 2020) and (2) peripheral blood mononuclear cells (PBMC) which contain a wide-range of circulating blood cells that are susceptible to pathogenic infection. When investigating critical versus moderate cases through the lens of single-cell sequencing, it becomes evident that lung injury and tissue damage leading to respiratory failure is derived from individual cells which provoke inflammation (Chua et al. 2020). Overall, there is a great need to untangle individual host cellular features during various disease trajectories to not only predict severity outcome, but also to better define heterogeneous immune responses across patient groups (Bernardes et al. 2020).

Generally, the spread of the virus within human cells (epithelial and immune cells) is highly dependent on cytokine signaling, such as in the case for cell-to-cell interactions (Branchett et al. 2019). It has been previously understood that once an immune cell is activated, the host must destroy or remove the cell to prevent hyperactivation which can lead to additional tissue damage overtime through autoinflammatory mechanisms (Tisoncik et al. 2012 ; Branchett and Lloyd, 2019). It appears that in the case of severe lung injury linked to patients with COVID-19 the immune system is rather hyperactivated and therefore not likely linked to the inadequate clearance of viral infected cells (Mehta et al. 2020 ; Wen et al. 2020). Specifically, it appears quite likely that SARS-CoV-2 employs the strategy of hijacking the immune system of

the host to disrupt homeostatic antiviral immunity, thereby provoking chronic inflammation that is characterized by the aggregation of proinflammatory cytokines which eventually leads to acute respiratory distress disorder (ARDS) in severe COVID-19 patients (Bost et al. 2021). It is well-understood at the present that immune suppression of the host myeloid-derived cells, especially monocytes and their expression of immuno regulatory features such as arginase-1 is the hallmark of COVID-19 infection (Bost et al. 2021). Specifically, immune suppression of both monocytes and neutrophils has been associated with severe or fatal clinical outcomes across patients, highlighting a potential immunomodulating effect from COVID-19 (Bost et al. 2021). In terms of deciphering molecular mechanisms of COVID-19 in pathophysiology, several studies have investigated the how stepwise patterns of disease (i.e from healthy to mild, to moderate, to complicated, to severe) have demonstrated the underlying pathology of COVID induced ARDS, respiratory failure, and in several unfortunate cases, death (Huang et al. 2020 ; Zhou et al. 2020c). Through this analysis of COVID-19 severity it has become clear to identify unique features of severe disease outcome. For example, ARDS during COVID-19 is unique as compared to ARDS pathophysiology caused by infectious or physical damage to the lungs ; individuals with ARDS derived from COVID have significantly higher amounts to cytokines that are released into the peripheral blood, which is increased with disease severity (Li & Ma, 2020 ; Mehta et al. 2020). Furthermore, patients with severe cases of COVID-19 tend to have plasma interleukin (IL)-6 which is approximately 10 to 40 times lower than in patients with typical ARDS (Moore & June, 2020). Specifically, patients who are assessed to have adverse clinical outcomes at a severe stages of SARS-CoV-2 infection can be assessed to have low levels of lymphocytes in addition to great amounts and release of pro-inflammatory cytokines such CXCL10 (IP-10), IL-6, IL-8, IL-10, tumor necrosis factor, and the C-C motif chemokine ligand, thus leading to the name of “Cytokine Storm” (Chen et al. 2020b ; Huang et al. 2020; Laing et al. 2020). This specific immune response can also be characterized by a SARS-CoV-2 infection signature at assessed by both T-cell and B-cell responses to the virus (Braun et al., 2020; Grifoni et al., 2020; Long et al., 2020; Ni et al., 2020)

Sampling of PBMCs from patients of various levels of disease severity can provide a wide-range of sample accessibility for studies to identify novel biomarkers that are predictive of

disease (Bost et al. 2021). While single-cell sequencing of PBMCs is a tool to delineate the effect of systemic infection upon the host immune system, there are some preliminary limitations. For example, PBMC samples from COVID-19 patients generally lack viral RNA reads or contain low amounts, thus creating a larger challenge to decipher the crosstalk between host and pathogen (Bernardes et al. 2020; Chua et al. 2020 ; Xiong et al. 2020). Furthermore, studying PBMCs to investigate disease severity does not allow for the consideration of the local microenvironment during disease, as PBMCs are circulating. Therefore it is also useful to employ BALF samples, due to the fact that SARS-CoV-2 does not only infect cells within the lower respiratory tract, but the virus is also able to infect cells found in the pharyngeal region (Huang et al. ; Chen et al. 2020a). Specifically, it is known that coronaviruses tend to infect alveolar macrophages which highlights the dynamic role of the host cell-specific immunometabolism during SARS-CoV-2 infection (Cheung et al. 2005 ; Deng et al. 2017). Macrophages which are derived from proinflammatory monocytes tend to be abundant in patients with severe COVID-19 when investigated with single-cell sequencing (Liao et al. 2020). These observations support past assessments that proinflammatory macrophage microenvironments are indeed present during cases of severe COVID-19 during steady, inflammation, and recovery pseudotimes (Bonnardel & Guilliams, 2018). BALF samples from patients who are assessed to have a severe or critical state of COVID-19 infection typically have a higher proportion of neutrophils and macrophages within the samples, in contrast there is a lower proportion dendritic and T-cells in individuals with a moderate infection (Liao et al. 2020). Additionally, it was found that patients with critical cases of COVID-19 have a significant loss of basal cells and a high increase of neutrophils as compared to controls (Chua et al. 2020). Another cell-type of interest in COVID-19 infected BALF samples are epithelial cells, which on average demonstrate a three times higher increase in the SARS-CoV-2 entry ACE2 receptor as compared to moderate cases (Chua et al. 2020). In general, critical cases have been observed to demonstrate far greater interactions when observing epithelial and immune cells. Specifically, immune cells in severe or critical cases tend to have highly activated immune cells with inflammatory macrophages which express CCL3, CCL20, CXCL1, CXCL3, CXCL10, IL8, IL1B, and TNF (Chua et al. 2020). Additional studies have identified that

patients with severe COVID-19 tend to have higher than average expression of IL-6 secreting CD14/CD16 monocytes and a decrease of non-classical adaptive monocytes (Hadjadj et al. 2020 ; Schulte-Schrepping et al. 2020).

2. COVID-19 Immunometabolism

Human hosts and viruses are ultimately interconnected through host metabolic machinery; this connection can be exploited to develop potential antiviral targets (Aller et al. 2018; Moreno-Altamirano et al. 2019 ; Renz et al. 2020). The interconnectedness and reliance of viral metabolism upon humans is universal across most viruses and remains an active discussion with regards to the biological status of viruses as living organisms (Claverie, 2006 ; Peters et al. 2020 ; Kanehisa et al. 2021). Specifically, viroids require the cellular enzymes of the host for replication, further highlighting the need to better study host-associated cells as a target to limit the production of new virions (de Wilde et al. 2015 ; Dirmeier et al. 2020). Once virulence is initiated, several coronaviruses further regulate various host functions such as immune response cell cycle and checkpoints, cell-to-cell signaling, and general metabolism to develop an ideal environment for the replication of the virus (Perlman et al. 2009 ; de Wilde et al. 2015 ; Dirmeier et al. 2020). This occurs when a virus hijacks various host-associated cellular metabolic pathways including glycolysis, biosynthesis of nucleotides and lipids, thereby further driving an ideal environment for the proliferation of viral replication (Thaker et al. 2019). Initial studies with other human coronaviruses, specifically the HCoV-229E have suggested that increases or modifications in glycerophospholipids and fatty acid production in infected host cells, as compared to non-infected (Yan et al. 2019). Lipid metabolism and the regulation of this process is not only a specific pathway that may benefit from therapies, but also is essential for viral replication in host cells (Yan et al. 2019).

At the single-cell level, a recent longitudinal study which investigated COVID-19 severity through multi-omics found that plasmablasts in patients with inflammation have a high metabolic activity which could only be mitigated upon recovery (Bernardes et al. 2020). In comparison, the authors also demonstrated that the metabolic activity of both memory and naive B cells did not change between various disease trajectories (Bernardes et al. 2020 ; De Biasi et

al., 2020; Kuri-Cervantes et al., 2020; Mathew et al., 2020; Stephens and McElrath, 2020). Specifically, through the application of constraint-based metabolic modeling of single-cells during COVID-19 infection it was found that plasmablasts during inflammatory COVID-19 were highly metabolically active and displayed metabolic increases in dicarboxylate and glyoxylate metabolism, in addition to oxidative phosphorylation (Bernardes et al. 2020). In addition, the study also identified a significant increase in metabolic pathways which regulate the production of numerous amino acids such as alanine, glycine, isoleucine, leucine, serine, threonine, and valine. On the opposite end, it was identified that glycolysis activity had a low metabolic pathway abundance in during patients with hyperinflammation, this modification of metabolic pathways became highly active once the patient reached a recovery phase (Bernardes et al. 2020). These adverse metabolic pathways likely play a role in host immune response. For example, it has been hypothesized that plasmablasts have the potential to modify host immune response by acting as a nutrient sink and uptake these amino acids , such as in the case of other viral infections (Vijay et al. 2020). Overall, these study highlight that immunometabolic dsybiosis in plasmablasts and a variety of other cells during inflammatory COVID-19 infection which impairs the metabolism of amino acids is a contributing factor to the onset of severe COVID-19 (Bernardes et al. 2020).

3. Applying Metabolic Modeling Tools for COVID-19 Drug Targeting

Systems biology applications to biomedicine are becoming one of the most essential tools in the fight against outbreaks. There is an urgent need for the scientific community to understand the molecular mechanism underlying COVID-19 pathophysiology in relation to systemic effects for the development of precision therapy options. As previously mentioned, it is essential to analyze both the virus and host in tandem to better understand how infections drive immunometabolism pathophysiologies to identify new targets based on metabolic changes in cells that are infected with pathogens. Therefore there is value in improving the description of disease heterogeneity to identify drug targets at the molecular level; this approach starkly differs from classical reductionist approaches to drug discovery (Rajewsky et al. 2020 ; Yofe et al. 2020). Specifically, it is possible to identify novel targets for treatments by analyzing metabolic

changes from infected host cells (Renz et al. 2020). For example, a variety of coronaviruses have been identified to initially infect human macrophages and inhibit various antiviral responses such as interferon-stimulated genes, thereby increasing the viruses potential to evade the immune systems and induce pathogenicity in the host (Cheung et al. 2005) ; Deng et al. 2017; Huang et al. 2020 ; Chen et al. 2020).

Human immune cells such as macrophages are not applicable as dynamic models which can replicate *in vivo* features. Specifically, it is challenging to model macrophage plasticity, biologically this cell is able to fine-tune and diversify responses to promote crucial functions during pathogen infection to maintain homeostasis (Li et al. 2019). This plasticity is generally essential to generate heterogenous macrophage populations with diverse phenotypic complexity. Therefore there is a need to employ GEMs that integrate both humans and viruses to identify antiviral targets in numerous diseases caused by Chikungunya, Dengue, and Zika (Aller et al. 2018). The study integrated presently known targets of antiviral drugs as a confirmation, thereby demonstrating the potential of metabolic models to not only identify new targets, but also verify presently known targets (Aller et al. 2018).

In a recent study, Renz et al. simulated a human genome-scale metabolic model that was infected with SARS-CoV-2 (Renz et al. 2020). The authors employed a previously published alveolar macrophage from Bordbar et al. due to the fact that coronaviruses tend to infect this specific cell in humans (Cheung et al. 2005 ; Bordbar et al. 2010 ; Deng et al. 2017). In order to identify potential antiviral therapies for the host-virus model, the authors developed a novel virus biomass objective function for SARS-CoV-2 to investigate amino acids, energy requirements, and nucleotides that are relevant to viral replication in the host cell (Aller et al. 2018 ; Renz et al. 2020). The study identified that SARS-CoV-2 negatively impacts host cell metabolism disrupting the purine biosynthesis pathway, which the virus uses for replication. Specifically, the authors identified guanylate kinase to be an important target, during the author's analysis of the metabolic flux distribution, it was found that knocking-out of this gene reduced viral replication to almost 0, without negatively impacting the energy requirements of the host (Renz et al. 2020). However it should be noted that this approach is significantly

limited as metabolic models do not include information that may be relevant to host infections, such as cell-to-cell recognition for immune response, the production or release of lipids, or viral entry (Timm & Yin, 2012).

While there are numerous limitations with the reconstruction and use of genome-scale metabolic models for studying COVID-19, a recent longitudinal study investigating the metabolism of patient derived cells during COVID-19 infection demonstrated unique phenotypes. Primarily, the study identified stark changes in both energy and amino acid metabolism in specific cells during COVID-19 by employing novel tools to capture homeostatic metabolic functions to use for metabolic model reconstruction (Bernardes et al. 2020 ; Joshi et al. 2020). This study and others have supported evidence that reduced energy availability through the impairment of glucose metabolism may lead to not only the overshuttling of glucose to antibody glycosylation, thereby promoting the metabolic exhaustion of a wide-range of cells, thereby bolstering the effects of severe COVID-19 (Corcoran and Nutt, 2016; Bernardes et al. 2020 ; Hoepel et al., 2020; Larsen et al., 2020). Metabolic modeling of specific cells during COVID-19 disease has supported that hyperinflammatory states likely provoke cells towards a metabolic shift to increase pyruvate metabolism, thereby promoting glycolysis (Bernardes et al. 2020). This metabolic change may be the molecular mechanisms underlying the hallmark thrombosis symptoms in patients; glycolysis in cells typically sensitizes platelets and promotes activation and aggregation (Nayak et al. 2019).

B. Recurrent Urinary Tract Infections (Microbial Communities)

In the following section, details are presented which investigate our current understanding of microbial communities of the urinary tract, numerous excerpts were acquired from the published manuscript "Recurrent Urinary Tract Infections: Unraveling the Complicated Environment of Uncomplicated rUTIs" by Josephs-Spaulding et al. (2021). Specifically the literature which discusses the microbial communities of the female urogenital tract, host-microbial interactions preceding urogenital infections, dietary exposures and metabolism which underlie UTIs, and approaches on how to better interpret urogenital infections through the lens of systems biology are included in this manuscript. Furthermore, figures and tables from the aforementioned manuscript are again presented in this dissertation to support the theme of precision medicine and *in silico* modeling. Overall, the published manuscript seeks to improve the present understanding of UTIs as a complicated environment which is constrained by numerous host-factors. By studying UTIs as not one of the most common infections, but rather as a patient-specific disease, the manuscript presents an avenue to explore UTIs through a holistic and systems view which applies ecological principles to improve treatment of UTIs and further human diseases. My contribution to this manuscript included conceptualizing the manuscript idea, writing the manuscript, preparing all tables/figures, and acting as the corresponding author during the submission of the publication. For further information on this publication, please refer to the attached citation of the manuscript, specific remarks on the contribution of each author is detailed further in the manuscript.

Citation: Josephs-Spaulding J, Krogh TJ, Rettig HC, Lyng M, Chkonia M, Waschina S, Graspeuntner S, Rupp J, Møller-Jensen J and Kaleta C (2021) Recurrent Urinary Tract Infections: Unraveling the Complicated Environment of Uncomplicated rUTIs. *Front. Cell. Infect. Microbiol.* 11:562525. doi: 10.3389/fcimb.2021.562525

Recent advances in DNA and RNA sequencing contradicts prior assumptions that human urine is sterile; instead it harbors a unique microbiome with ecological interactions in health and disease (Wolfe et al., 2012; Hilt et al., 2014; Alteri and Mobley, 2015; Whiteside et al., 2015; de Vos et al., 2017; Aragón et al., 2018). As the physiological role of the bladder is to store nutrients and waste products in the form of urine, healthcare practitioners must consider the unique metabolism of bladder-associated microbial communities within this niche (Subashchandrabose et al., 2014; Alteri and Mobley et al., 2015; Conover et al., 2016; Horsley et al., 2018; Martín-Rodríguez et al., 2020). More so, with the emergence of pathogens that are resistant to first-line antibiotics, there is a pressing need to reinterpret uncomplicated UTIs, as an ever-changing and complicated pathology in humans (Mediavilla et al., 2016; Zilberberg et al., 2017). With the development of novel systems biology approaches and next generation methods, new viewpoints of UTIs and human-associated infections are being uncovered.

Most recently, the American Urological Association estimates that 150 million UTIs occur worldwide annually and cost up to $6 billion USD in healthcare costs (Flores-Mireles et al., 2015; AUA, 2020). This has led to the misapplication of antibiotics, likely resulting in long-term effects upon the interconnected gastrointestinal tract, vagina, and general urinary system (Kostakioti et al., 2012; Bartoletti et al., 2016; Nielsen et al., 2016; Gottschick et al., 2017; Thomas-White et al., 2018). Uropathogenic *Escherichia coli* (UPEC) primarily causes UTIs and is isolated from approximately 80% of patients (Flores-Mireles et al., 2015). Other pathogens such as *Enterococcus faecalis, Klebsiella pneumoniae, or Proteus mirabilis* can also be isolated from UTI patients (Abat et al., 2015; Thänert et al., 2019). UTIs begin at the urethra, colonize the bladder, and ascend to the kidneys through a multitude of mechanisms such as evading host protective factors or inhibiting host immunoglobulin A transport (Rice et al., 2005; Ashkar et al., 2008). The primary microbial strain causing the rUTI may originate from new colonizers deriving from various environmental reservoirs such as: a sexual partner, contaminated foods, or fecal/gut contamination of the urinary tract (Scholes et al., 2000; Nordstrom et al., 2013; Foxman, 2014; Gilbert et al., 2017; Thänert et al., 2019). While strains which initiate infection may cause a rUTI relapse, it is suggested that the initial infection caused by one UPEC strain primes the bladder for a new strain (or slightly similar) within several

hours, which is diagnosed by two separate cultures over a period of six months (Andersen et al., 2012; Luo et al., 2012; Schreiber et al., 2017; Anger et al., 2019). Specifically, uncomplicated UTIs are acute infections of urinary tracts without anatomical or physiological defects that would make a patient more susceptible to initial urinary tract infections (Hooton, 2012). Women are significantly at a higher risk for contracting a UTI as compared to men. Previous reports suggest that one-third of all women under the age of 26 will experience a UTI and 50% of those women will experience a subsequent UTI episode (Foxman, 2002; Brumbaugh et al., 2013).

As knowledge in modeling the fine-scale and dynamic changes in biological organisms increases, the context of personalized treatment strategies must also update with observations in molecular systems biology and microbiome sciences (Thiele et al., 2013; Thiele et al., 2020). Ideally, this includes withdrawing from reductionist approaches to diagnose UTIs and moving towards models that input multiple human data sources to create patient-specific models to characterize infection in a holistic view. Overall, our understanding of both host-microbiome interactions and rUTI pathophysiology elicits an update to the present concept of infection biology by redefining infectious diseases through a modern lens.

1. Microbiota of the Female Urogenital Tract

A culturable urinary tract microbial community exists within healthy individuals (Hilt et al., 2014). Specifically, the urobiome has been hypothesized to shift both microbial abundance and predicted metabolic pathways associated with various patient-specific urological morbidities or infections (Shoskes et al., 2016; Aragón et al., 2018). The urine of healthy females is characterized by the presence of *Corynebacterium, Lactobacillus, Staphylococcus*, and *Streptococcus* that tends to fluctuate abundance during periods of health and disease (Fouts et al., 2012; Aragón et al., 2018). Additionally when assessed by microbiome sequencing, it has been found that female urinary tract samples mainly consist of organisms from the phyla *Actinobacteria (Actinomyces* & Arthrobacter) and *Bacteroidetes (Bacteroides)*, which are typically absent from their male counter parts (Lewis et al., 2013). More so, *E.* coli is readily cultured from 91% of healthy women and only 25% of men, highlighting a stark difference in *E. coli* that is cultured as a residential bacteria from the female urobiome (Ipe et al., 2013).

When assessing cohorts by age, it becomes clear aging affects normal physiology and disease types (Irizar et al., 2018). Specifically a core female urine microbiota which parallels aging and age-related morbidities was identified and is manifested as asymptomatic bacteriuria (Lewis et al., 2013). In the case of patients with so-called asymptomatic bacteriuria, *E. coli* typically acts as symbionts (Godaly et al., 2016). Therefore, unnecessary and excessive application of antibiotics to "treat" asymptomatic bacteriuria in differing age groups leads to long-term consequences by depleting the resilient urinary system's microbiota, thus driving an increased prevalence of multidrug resistance (MDR) pathogens within the urinary tract across patients (Cai et al., 2015; Ipe et al., 2016; Zilberberg et al., 2017). This suggests that the definition of UTI diagnosis: 'the detection of a pathogen from not being sterile during all periods of health'. The dynamic exchange of microbiota, between the vagina and urinary tract illustrates a complex environment which is dependent on microbial composition. Probiotic strains of *Lactobacillus (L. crispatus, L. gasseri, L. iners, and L. jensenii)* that are the dominant bacteria of the vagina are demonstrated to repel or suppress non-native pathogens in environments through the production of secondary metabolites and control of environmental pH (Mirmonsef et al., 2014; Brubaker and Wolfe, 2017; Tachedijian et al., 2017; O' Hanlon et al., 2019). Specifically, recent metagenomic sequencing of both the female urinary tract an vagina have highlighted highly similar microbiota between both systems such as E. coli, Lactobacillus spp. and Streptococcus anginosus suggesting a degree of cross-talk between both environments (Thomas-White et al., 2018). These findings suggest a dynamic continuous interplay between beneficial commensals and invasive pathogens (Vodstrcil et al., 2017). For example, loss or depletion of one species of *Lactobacillus* spp. leads to other organisms invading the previously occupied niche (van de Wijgert et al., 2014). More so, loss of commensal microbial communities consisting of probiotic strains likely leads to dysbiosis and an increased risk for UTIs, rUTIs, or infections from other bacteria and viruses (Sewankambo et al., 1997; Martin et al., 1999; Lamont et al., 2011; Stapleton et al., 2011; Gilbert et al., 2017). While microbial dysbiosis is a known mechanism underlying bacterial vaginosis, it remains unknown how dysbiosis of microbial communities impacts the urinary tract (Zozaya et al., 2016; Liu et al., 2017).

While microbiota of the host urogenital system are ultimately connected, microbiota can also be shared between the urogenital systems of two hosts.Interestingly, microbiome studies of patients with bacterial vaginosis highlighted a shared microbiome between the penile/urethral microbiota and vaginal microbiota (Zozaya et al., 2016). Specifically, penile-vaginal sex is the primary driver for the sexual exchange and increase of *G. vaginalis* in individuals with or without bacterial vaginosis (Vodstrcil et al., 2017). Furthermore, the increased presence of *G. vaginalis* in tandem with biofilm-producing communities drives an intense competition for resources, leading to a decreased presence of *Lactobacillus* spp. and an increased risk for acquiring urogenital infections (Machado et al., 2013). This loss of *Lactobacillus* spp. shifts the host vagina towards a more alkaline environment to include more diverse microbial communities such as *Anaerococcus*, *Atopobium, Bacteroides* spp. *Gardnerella, Mobiluncus* spp, *Mycoplasma, Peptoniphilus, Peptostreptococcus* spp. *Prevotella, and Streptococcus* that is found in patients with bacterial vaginosis (Lamont et al., 2011; Ravel et al., 2011; Mirmonsef et al., 2014; Onderdonk et al., 2016).

2. Host-Microbial Interactions Leading to UTIs

Gut microbiota play a unique role in the hypothetical fecal-perianal-urethra transmission route:fecal-associated microbiota can contaminate patient urine during a UTI (Yamamoto et al., 1997; Jantunen et al., 2001; Paalanne et al., 2018). Microbiome sequencing of human feces revealed that high abundance of either *Escherichia* or *Enterococcus* is a risk factor for bacteriuria and symptomatic UTIs (Magruder et al., 2019). While previous evidence suggested that women with *E. coli* UTIs have a different strains in the urine and gut; Magruder and colleagues observed that E. coli strains between the gut and urinary tract are closely related, further supporting the hypothesis of a gut microbiota-UTI axis (Bahadori et al., 2019; Magruder et al., 2019). Interestingly, a study investigating genomic diversity of UTI patients between urine and feces strains observed two major patterns: the first case being that rUTIs are caused by the same strains and the opposite, there is a rapid and complete overtake of the bladder environment by another strain (Chen et al., 2013). These studies highlight the remaining lack of clarity in developing theories to describe the origins of gut-associated UTIs. Furthermore, all

present studies lack longitudinal data that would be useful in describing potential reservoirs that link gut microbiota changes before and after the onset of uncomplicated UTIs (Chen et al., 2013). With these observations in the interconnected urogenital ecosystem, we can begin to decipher ecological interactions and control mechanisms between hosts and microbes, which drive changes in microbiota composition. For example, Thänert et al. (2019) deciphered the core genomic relatedness among *E. coli*, suggesting that *E.coli* is well-adapted to transit between various environments within a host, such as between the human gut and bladder. For example, in a study investigating pairwise interactions from patient fecal-associated *E. coli* and UTI *E. coli*, the authors identified unique mutations for virulence and nutrient-uptake in addition to proteins for biofilm formation, these factors are necessary for transition between the gut and urinary tract (Nielsen et al., 2016). Figure 2 describes the normal female urogenital microbiome during health and how gut-associated pathogens transit to both the bladder and vagina during dysbiosis.

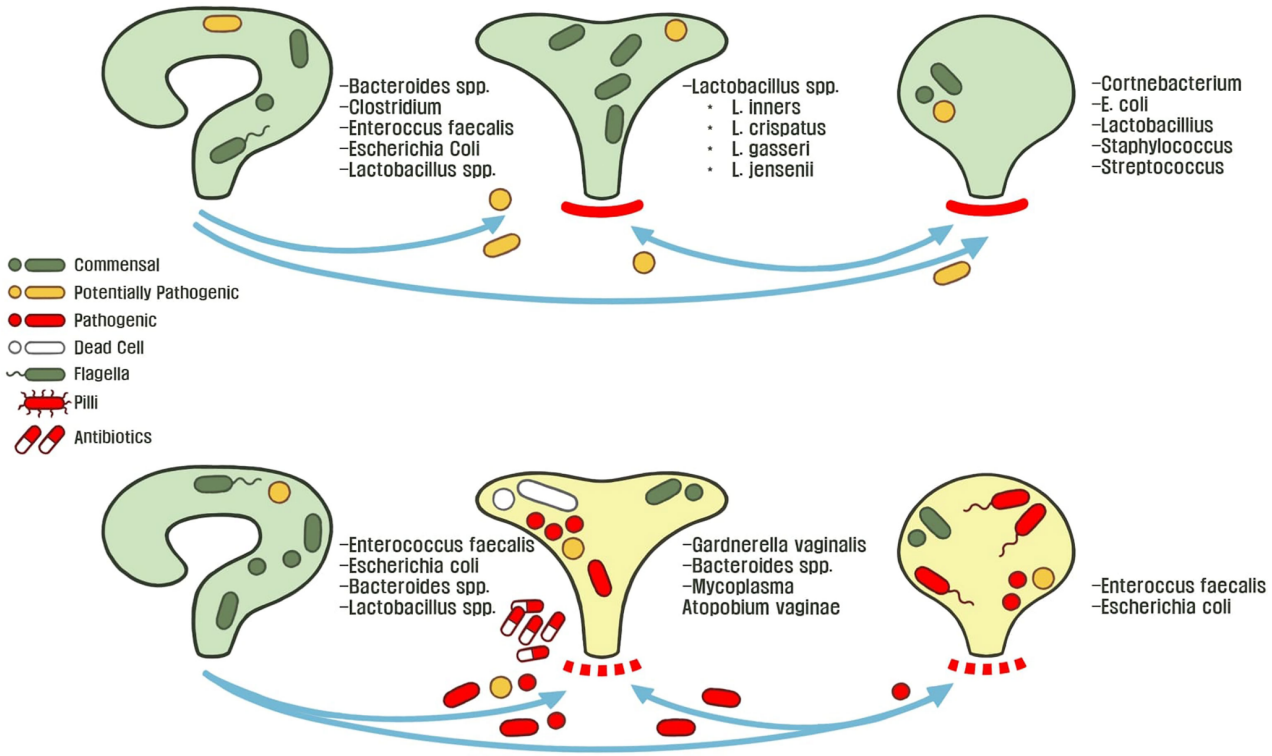

Figure 2: Microbial crosstalk in the gut-urogenital axis. The healthy or asymptomatic gut, vagina, and bladder microbiome is stable across individuals conditions. These microbiota protect their host-associated niche from foreign pathogens by controlling abiotic factors and outcompeting potentially invasive microbiota. Microbial dysbiosis and an adverse environment disrupts host homeostasis through various mechanisms such as: poor hygiene, metabolic changes (menopause, metabolic diseases, etc.), exposure to environmental metals or antibiotics, and consumption of food-borne pathogens. This allows for microbiota to transit between the perianal-urogenital pathway and in turn shapes other microbial communities towards dysbiosis and predisposes individuals to UTI pathophysiology.

A different aspect of the microbial reservoir route was revealed when Gottschick et al. (2017) hypothesized that the bladder and urethra have distinct microbiotas, in comparison to the vagina. It was found that abundant bacteria of the vaginal fluid from bacterial vaginosis patients were also increased in the urine. This suggests that biofilms in the urine persist for extended times as a reservoir for recurrent bacterial vaginosis infections (Gottschick et al., 2017). More so, this study highlights the need to clarify the underlying crosstalk and mechanisms of microbiota transition between the urethral and vagina. For example, it is understood that uropathogenic strains rapidly form biofilms to rapidly grow in human urine, as compared to other gut-associated *E. coli* strains (Anderson et al., 2003; Justice et al., 2004; Forsyth et al., 2018) (Figure 3). This evidence points to a major question: is there a microbial reservoir for the initial contamination and recurrence of UTIs? If so, what mechanisms is UPEC employing to invade the urinary tract when transiting from the gastrointestinal tract?

Urine is the primary source of information for identifying UTIs in patients. Analytical chemistry techniques use urine to detect biomarkers, such as excreted metabolites from pathogens (Smart et al., 2019). Specifically, urine is a waste product from various metabolic end-points of secondary metabolism whose concentration is determined by an individual's diet, lifestyle, and a variety of other environmental factors (Bouatra et al., 2013; Playdon et al., 2016; Tang, 2017). With regards to sex, the urine of females generally contains greater quantities of citrate, but not as much calcium or oxalate as males (Ipe et al., 2016). These metabolic differences likely favor a cohort of specific microbes which thrive in these niches. A large-scale multi-experimental mass spectrometry study of human urine samples was conducted to create the database of "The Human Urine Metabolome" to identify 2651 different metabolites and unique ionic species in healthy human urine (Bouatra et al., 2013). Overall, this study preliminary assesses the diversity of the urine metabolome in healthy humans and can be useful to predict metabolites which predisposes individuals to UTIs. However, there is a lack of data detailing the metabolic state of urine in various pathophysiologies and lack of knowledge regarding biomarkers that may predispose patients to various infection outcomes.

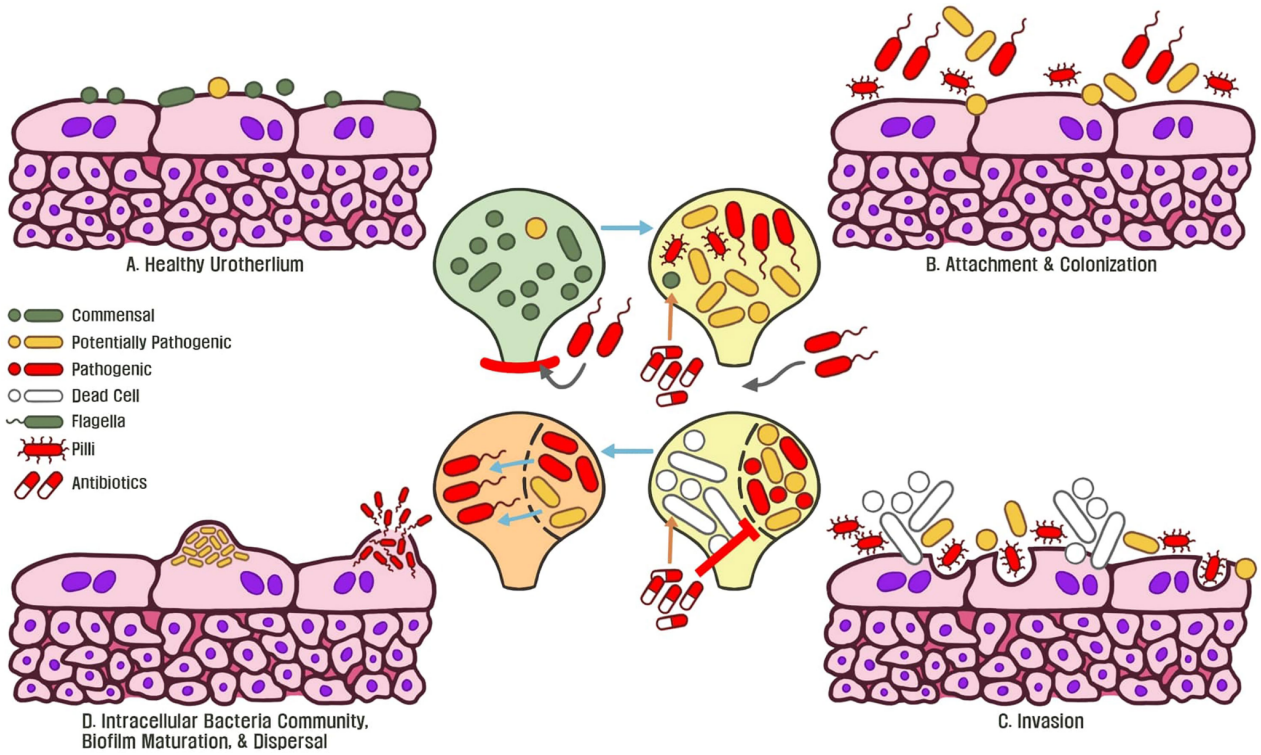

Figure 3: Antimicrobial stress drives *E. coli* virulence of the urogenital tract. (A) Commensal microbiota are associated with a healthy normal human urothelium and protect the host from invasive pathogens. (B) An initial course of antibiotics enforces bacteria to express flagella, type 1 pili, and adhesin proteins to attach and colonize the urothelium. (C) Continued antibiotic exposure eliminates commensal bacteria and surviving microbiota exposed to this stressor become resistant. Invasive bacteria begin to express virulence genes to colonize and replicate within tissue. (D) Following replication, intracellular bacteria communities are formed and antibiotic resistant biofilms become matured. Continued exposure to stressors such as antibiotics allows for the emergence of pathogenic, MDR biofilms, which underlines recurrent chronic UTIs of the host.

3. The Role of Dietary Exposures and Metabolism in rUTIs

Urine is a hostile environment for most bacterial species due to a pH range of 5.5 to 7, with an average of 6.2 (Rose et al., 2015). This biofluid is a patient-specific excretion containing a metabolomic profile, strongly dependent on health or disease (Beger et al., 2016). Advances in quantitative mass spectrometry have enabled the identification of specific metabolites as biomarkers of infections or inflammation. For example, a study identified unique biomarkers of UPEC-specific UTIs by identifying an increased ratio of acetic acid to creatinine and trimethylamine concentration in urine (Lam et al., 2014). While traditional methods such as a urine dipstick urinalysis have a variable sensitivity of 68 to 88% across different patient groups, employment of mass spectrometry was found to have a 92% true positive predictive value to diagnose urinary tract infections (Devillé et al., 2004; Lam et al., 2014). Table 1 illustrates directional changes in microbial abundances of the urinary tract associated with disturbances in host-metabolism. Microbiota adapt and uptake various energy sources from the host diet, likely leading to modifications of urine composition and metabolic profile (David et al., 2014; Playdon et al., 2016; Thiele et al., 2020). Generally, high quantities of glucose in the urine tends to favor bacterial growth and eventually a UTI (Wilke et al., 2015). For example *E. faecalis* is able to grow in urine containing greater concentrations of glucose and has enhanced recurrent biofilm formation potential, primarily in diabetic patients (Pillai et al., 2004). Such environments exacerbate the development of pathogenesis in patients who are affected by metabolic disorders.

State of dysbiosis	Metabolic Change	Microbiota Change	Citation
Follicular fluid during IVF	↑ Estradiol & progesterone	↑ Lactobacillus gassen, L. crispatus, L. jensenii	Pelzer et al., 2012
Kidney Transplant	↑ Folate metabolism	↑ E. coli & E. faecalis	Rani et al., 2017
N/A	↑ Levels of free glycogen	↑ Lactobacillus spp.	Mirmonsef et al., 2014
Post-Menopausal (Symptomatic)	↓ Estrogen & low glycogen	↓ Lactobacillus spp.	Muhleisen and Herbst-Kralovetz, 2016
Premenopausal	↑ Estrogen & glycogen	↑ Lactobacillus spp.	Muhleisen and Herbst-Kralovetz, 2016
Renal Tubular Acidosis	Hypercalciuria	↑ E. coli	Jamshidian et al., 2018
Type Two Diabetes Mellitus	↑ Fasting Glucose & hyperlipidemia	↑ Prevotella, Lactobacillus, and Shuttleworthia	Liu et al., 2016
Urinary Tract Infections	↑ Acetic Acid & trimethylamine	↑ E. coli	Lam et al., 2014
Urinary Tract Infections	↑ Ethanolamine	↑ E. coli	Sintsova et al., 2018
Urinary Tract Infections	↑ Acetate & Creatinine	↑ E. coli	Grochocki et al., 2017
Urosepsis	↑ Procalcitonin/Albumin ratio	↑ Increased E. coli	Luo et al., 2018

N/A, Not Applicable.

TABLE 1: Microbial changes of the urogenital tract are linked to host metabolic dysregulation. Various comorbidities directly impact the urogenital microbiome by inducing metabolic changes that are host-associated. These metabolic changes directly impact microbes of the urogenital tract by either reducing beneficial bacteria such as *Lactobacillus spp*. Or increasing the presence of pathogenic bacteria such as *E. coli* E. *faecalis*.

Metal	Pathogen	Gene Name (s)	Function	Citation
Cu II	UPEC	Ybt	Pathogenic siderophore	Chaturvedi et al., 2012
Cu 1+/2+	UPEC	cusC	Cu resistance & virulence mechanisms	Subashchandrabose and Mobley, 2015
Fe	UPEC	Iha	Fe siderophore uptake and virulence of bladder and kidney	Léveillé et al., 2006
Fe	UPEC	FyuA	Fe-Ybt siderophore uptake & increased virulence through biofilm in bladder	Hancock et al., 2008; Brumbaugh et al., 2013
Fe (Haem)	UPEC	ChuA	Heme receptor for iron transport and kidney invasion during UTI	Hagan and Mobley, 2009
Fe	UPEC	fepA, iroN*, iutA*, fyuA, chuA, hma, sitA	Iron uptake and metal transport*	Subashchandrabose and Mobley, 2015
Ni2+ &	UPEC	nikA	Nickel acquisition & urofitness	Subashchandrabose et al., 2014
Ni(II)	UPEC	Ybt	Metal acquisition, unknown purpose	Robinson et al., 2018
Zn2+	UPEC	ZnuACB & ZupT	Uropathogenic fitness & metal transport	Sabri et al., 2009
Ni	Uropathogenic S. aureus	NixA, NikA	Urinary tract colonization and increased fitness	Hiron et al., 2010
Ni & Co	Uropathogenic S. aureus	Cnt (Opp1)	Colonization of bladder & kidneys during UTI	Remmy et al., 2013

**Both the IutA and IroN have been observed to lead to bladder colonization.*

Table 2: Uropathogenic uptake of various metals incite virulence in host urothelium. Various uropathogenic bacteria utilize various genes to lyze and acquire host-associated metals such as Fe or Cu. By lysing and acquiring host biological metals, uropathogens can increase virulence and fitness through a wide-range of mechanisms.

Metals and their ions play major roles in human health and disease through electron exchange or redox reactions, thereby promoting cellular stress through reactive oxygen species. Chronic dietary exposure to metals in the food-chain has the potential to negatively impact human health, leading to a variety of nephron- and urinary-tract associated diseases (Zhao et al., 2017; Xu et al., 2018; Yen et al., 2018). Excessive exposure to dietary metals eventually reach the kidneys and bladder causing pathologies; heavy metals are also taken up by various microbiota to incite host infection (Subashchandrabose et al., 2014; Habibi et al., 2017; Hyre et al., 2017; Zhang et al. 2019). Therefore, interpretation of rUTIs must be updated to include the possibility that metal exposure from inhalation, diet, and cosmetics are potential risk factors for UTIs onset and recurrence (Table 2). Table 2 additionally describes uropathogenic mechanisms of siderophores and other transport mechanisms to acquire free metals from hosts, to elicit behaviors to colonize the urothelium. On the other hand, mitigation of urinary levels of heavy metals may prove to be an alternative treatment to rUTIs by depriving pathogens use of essential metals or nutrients in comparison to antibiotic usage (Subashchandrabose and Mobley, 2015; Bauckman et al., 2019).

Free iron (Fe) is necessary for most biological processes such as cellular respiration, DNA replication, and oxygen transport *via* hemoglobin. Therefore, there is an intense competition between the host and pathogens for Fe in which Fe deprivation from uropathogens may be a primary mechanism to mitigate virulence (Subashchandrabose and Mobley, 2015; Bauckman et al., 2019). For *E. coli* pathogenesis, invasion and disruption of the host urothelium to increase the availability of free Fe^{2+}/Fe^{3+} is essential to initiate and maintain virulence (Gao et al., 2012). This occurs through the promotion of the UPEC toxin **α**-hemolysin, which ruptures and degrades host membranes to promote hemoglobin release, thereby promoting bacterial growth and virulence (Dhakal and Mulvey, 2012). UPEC opportunistically adapts to Fe abundant conditions by increasing the expression of siderophores, to scavenge environmental metals (*ireA, irp-2, iucC)* (Zhao et al., 2009; Shields-Cutler et al., 2015). Additionally, the induction of evolved virulence genes (*chuA, fepA, fyuA*, *iroN, iucA, iutA, and sitA)* are required for Fe uptake and transport systems to incite UPEC virulence mechanisms (Subashchandrabose and Mobley, 2015; Khasheii et al., 2016; Habibi et al., 2017; Tang et al., 2018). Siderophore

biosynthesis and Fe acquisition from the host-environment allows UPEC to promote asymptomatic growth by overexpressing genes for growth, fitness, and colonization (Watts et al., 2012). Uptake and use of metals by uropathogens enforces an environmental niche for invasive microbiota to resist natural and artificial stressors, thus leading to persistent host infections (Hancock et al., 2007; Subashchandrabose and Mobley, 2015; Ipe et al., 2016). During UPEC-associated UTIs, copper (Cu) levels in the urine are elevated and play an underappreciated role in UTI pathophysiology (Subashchandrabose et al., 2014). Bacterial Cu-associated virulence is not as common as Fe-associated virulence in UTIs, though it is still observed in numerous organisms. The micronutrient Cu is necessary for a variety of aerobic organisms such as bacteria, fungi, plants, and animals by supporting metabolic processes through the maintenance of proteins and metalloenzymes; conversely, the interaction of Cu ions and free oxygen radicals can damage proteins (Festa and Thiele, 2011). Hyre et al. (2017) demonstrated that the gain or loss of electrons of Cu through oxidation-reduction reactions constitutes an active host response mechanism to infections with UPEC, *Klebsiella pneumoniae*, and *Proteus mirabilis*. Ceruloplasmin, a transport protein for Cu, serves as a molecular source for Cu in the urine (Hyre et al., 2017). This molecular mechanism can be observed in clinical patients who are affected by Menkes disease, a lethal hereditary disorder of Cu metabolism leading to Cu deficiency (Tümer and Moller, 2010). Consequently, those with this Cu deficiency are especially prone to developing rUTIs (Kim et al., 2019). In contrast, recent studies demonstrate that host-mediated mobilization of Cu into the urinary tract during UTIs occurs, this illustrates a potential novel approach to reduce bacteria which rely on Cu-virulence within the urinary tract (Hyre et al., 2017).

4. Exploring the Urinary Tract Environment With Systems Biological Approaches

The following represents recent advances in next-generation models and methods to examine UTI pathomechanisms. These methods reach endpoints that cannot be typically achieved through traditional *in vivo* or *in vitro* models. To understand the underlying environmental mechanisms which control host invasion, these methods are useful to develop novel treatment strategies for rUTIs. To achieve precision treatment options for UTIs, the

application of next-generation sequencing, genome-scale metabolic modeling, and the development of novel microfluidic or stem cells technologies to mimic the bladder is needed based on patient specifics, rather than generalizations. These next-generation methodologies foreshadow a future for treating UTIs from an ecological and systemic perspective, rather than through reductionist approaches. These examples bolster the argument for a necessary adjustment towards clinical diagnosis of infections and progression of host-specific diseases.

E. coli are flexible microbes that thrive in various niches and environments by tuning gene expression. These modifications allow *E. coli* to rapidly adapt to stressful environments for successive colonization during environmental stressors, like antibiotic exposure, to incite host pathogenicity (Schwartz et al., 2016; Erickson et al., 2017). While details of UPEC function in human urine exist, there is a lack of consistent information about UPEC acclimation to a rapidly changing environment (Hagan et al., 2010; Sintsova et al., 2019). Assessing UPEC gene expression from patients becomes convoluted due to patient-specific host factors which may induce various bacterial genes, bacterial behavioral responses, and gene expression in differing host environments (Subashchandrabose et al., 2014; Schreiber et al., 2017). Furthermore, a recent study which employed UPEC strains from humans, compared pathogenesis mechanisms from humans in mice and found a similar gene expression pattern associated with metabolic machinery (Frick-Cheng et al., 2020).The complexity to assess human UPEC infections requires updating and clarifying definitions of bacterial virulence in heterogeneous human patients for optimized precision health outcomes (Mobley 2015). This aspect of biology underlies the deepening complexity of systems-oriented interaction needed to understand patient-specific disease outcomes.

Presently, the “Tolerome” describes transcriptome-level information detailing *E. coli* tolerance and resistance response to over 89 different stressful conditions (Erickson et al., 2017). Understanding the Tolerome and environmental stress response of uropathogens at a global transcriptomic level can enable a realistic understanding of the functions underpinning microbial colonization in urine. The undertaking of this study translates to 56263 events of up- or down-regulation in 5049 different genes (Erickson et al., 2017). Comparative studies of this

nature can further elucidate unique bacterial signatures of microbial communities necessary for maintaining physiological equilibrium in human hosts. For example, global pathogenic transcriptional responses are potential biomarkers of infection. For example, a recent study by Sintsova and colleagues (2019) identified a novel and universal transcriptional response which controls various transcriptional regulators, thus driving rapid growth of UPEC during infection. While these studies assess *E. coli* response to various known or stable environments, investigations of rapidly changing environments is not well understood. *E. coli* response to environments is not well-characterized (i.e during dynamic disease processes and pathophysiologies), there is a need to quantify microbial communities phenotypic reactions to host-specific perturbations and interpret how these changes impact human health or disease in real-time.

Shotgun metatranscriptomics profiles the transcriptome of all present strains of a microbial community in an environment and their functions (Shakya et al., 2019). While metagenomic sequencing provides information on the assembled genome and potential genes of organisms which comprise microbial communities, it cannot provide real-time information on the functions or metabolic diversity of these communities (Mick and Sorek, 2014). More so, while metagenomics can identify active or inactive microbial members of a community, it does not provide much information towards the function of a microbial community like metatranscriptomics (Brown et al., 2017; Shakya et al., 2019). While metagenomics can provide information on all functional possibilities of the microbiome, metatranscriptomics provides a snapshot of the present infection state of the patients. Particularly, application of metatranscriptomics deciphers both function and diversity of microbial communities in responsive and non-responsive individuals. Further advances in next-generation sequencing has led to the development of scRNA-seq of microbial communities as a novel approach to elucidate functional interactions among microbial species, mixed microbial communities, and within the host-associated microbiome (Lloyd et al., 2018; Imdahl et al., 2020; Kuchina et al., 2021). While scRNA sequencing for microbial communities is developing, metatranscriptomics is becoming readily available to identify present organisms in microbial communities from human samples in tandem with microbe-specific gene expression changes host responses

(Shakya et al., 2019). Metatranscriptomics was applied to study the vaginal microbiota during bacterial vaginosis, following antibiotic treatment (Deng et al., 2018). Subjects were divided into responsive and non-responsive groups to identify potential mechanisms underlying response to the drug. The authors observed that *G. vaginalis* upregulated CRISPR-Cas genes as a stress response to mitigate DNA strand breakage from metronidazole by inducing DNA repair mechanisms. Female patients colonized by *G. vaginalis* with this unique change in gene expression were shown to be non-responsive to antibiotic treatment. Overall the observations from this study cast doubt on previous assumptions regarding microbial communities and pathogenesis progression. Metatranscriptomics for assessing the functional roles of diverse microbial strains in various environmental conditions of humans is growing in the literature (Shakya et al., 2019). But to date, metatranscriptomics has not been applied to urine or patient samples with UTIs *in vitro* or *in vivo*. Application of metranscriptomics for the bladder microbiome would clarify perspectives of not only the microbiota occupying the bladder, but also their community interactions in respect to UTI pathophysiology.

Organisms adapt their metabolism to maintain homeostasis in ideal or adverse environments by selecting either rapid growth or resistance phenotypes (Ewald et al., 2017). Specifically, the metabolic flux of prokaryotes dynamically adjusts during growth alterations, thus optimal adaptation of protein production depends on pathway expression that constrains or allows growth (Bartl et al., 2013). Fulfillment of metabolic requirements to maintain physiological balance is a strategy employed by pathogens in rapidly changing environments to thrive or survive (Wessely et al., 2011). Depending on required response time, *E. coli* employs transcriptional or post-transcriptional mechanisms to regulate metabolic pathways for stress adaptation (Wessely et al., 2011). Identification and understanding of stress-response regulatory networks illustrates the role of environmental sensing and non-genetic changes in the emergence of disease phenotypes or MDR in pathogens. During this phase, the rapid acclimation of bacteria can be exploited to innovate treatment options for infectious human diseases (Conover et al., 2016).

By assessing the remarkable flexibility and diversity of differentially expressed genes between different stressful conditions, we can decipher UPEC adaptation towards colonization and persistence within differing human hosts (López-Maury et al., 2008). Transcriptional responses to various environmental cues are understood, less is known about UPEC response to heterogenous humans with regards to UTIs (Erickson et al., 2017). Furthermore, transcriptional changes that are host-pathogen specific may not be readily replicated in biological experiments, due to complexities when attempting to control specific environments. Thus, the application of genome-scale metabolic models for uropathogens which predicts an organisms' transcriptional and metabolic changes when primed by environmental stresses is a promising approach to unravel the complexities pathophysiology and predict treatment strategies to prevent or intervene against rUTIs (Józefczuk et al., 2010). The mapped genomes of various wild-type and mutant *E. coli* strains have been defined and applied to predict or engineer various metabolic capabilities through reconstruction of constraint-based genome-scale models. Modeling metabolic systems has been constantly updated since the original metabolic network reconstruction of *E. coli* in 2000 (Edwards and Palsoon, 2000; Orth et al., 2011; King et al., 2015; O'Brien et al., 2015). Genome-scale metabolic modeling is useful for creating genome-wide transcriptional networks to illustrate transcriptional response to various environmental stresses. By integrating both transcriptomics and metabolomics to identify conserved responses for various environmental stressors, such as oxidative stress, acid, cold, heat, and shifting glucose to lactose in media which are necessary for the maintenance of homeostasis (Józefczuk et al., 2010; Seo et al., 2015; Du et al., 2019). Application of genome-scale metabolic models that incorporate environmental stressors provides inspiration to interpret uropathogenic transcriptomes which are associated with chronic infections.

In silico community metabolic models of microbiota provide valuable insights into the ecological interactions within a microbial consortia. In brief, metabolic models of microbial species are constructed based on the organism's annotated genome sequence. Enzymes, for which genes were predicted, are assigned to reactions, which the enzymes can catalyze. By connecting the individual reactions to a metabolic network, *in silico* representations of the organism's catalytic capabilities allow predictions of metabolic phenotypes, for instance

environmental context-dependent growth rates, nutrient utilization, and metabolic by-products release (O'Brien et al., 2015). Through the use of gene expression data, sets of reactions from an organism's metabolic network can be limited to represent the current experimental condition. Models of community metabolism are constructed by connecting species-specific models and allowing the exchange of metabolites between cells as well as the competition for shared resources. To our knowledge, there are no applications of community metabolic models of the urinary tract microbiome, the results of this dissertation will present the first one. The rationale behind such models is that microorganisms not only adjust their metabolism in response to abiotic stresses and chemical composition of the environment, but also depend on the presence or absence of other microbial cells in their vicinity (Klitgord and Segrè, 2011).

In systems medicine, these models are applicable to generate hypotheses of factors that promote ecosystem colonization with a potential pathogen. Thereby providing potential treatment options, as well as prevention strategies against resistant pathogens. Thus with the growing appreciation of the role of the urinary tract microbiome in rUTIs, *in silico* models of community metabolism could potentially expand clinical understanding of rUTI pathophysiology and foster the development of novel therapeutic strategies to target the urobiome specifically.

C. Parkinson's Disease (Host-Microbiome)

In the following section which details our present understanding of how our gut-associated microbiome interacts with heavy metal toxicants in the onset of Parkinson's Disease. Specifically, the manuscript was co-written by Ms. Forero-Rodriguez and I, the first-authors of this study, seeks to answer how our gut microbiome acts as a friend or foe in initiating or preventing neurodegeneration. Numerous excerpts from the next presented section are acquired from the submitted manuscript "Parkinson's Disease and the Metal-Microbiome-Gut-Brain Axis: A Systems Toxicology Approach" by Josephs-Spaulding & Forero-Rodriguez et al. (2021). While the literature surrounding the role of environmental microbes and their interactions with heavy metal bioremediation is sizable, there is a lack of studies which investigate the role of human-associated microbiota duringin metal sequestration. Furthermore, figures and tables from the aforementioned manuscript are again presented in this dissertation to support the overall theme of precision medicine and *in silico* modeling. Overall, the submitted manuscript seeks to connect the literature and present understanding of neurodegeneration as a disease that is driven by environmental metals and can be mediated by the host-associated gut microbiome. By studying PD as not simply a genetic disease, but rather as a patient-specific disease, the manuscript presents an avenue to explore PD through a holistic and systems view which applies the lens of systems toxicology to develop and bioremediate individuals who are in a cycle of chronic inflammation and neurodegeneration. My contribution to this manuscript included conceptualizing the original manuscript idea, writing the manuscript and preparing all tables/figures with Ms. Forero-Rodriguez, and acting as the corresponding author during the submission of the publication. For further information on this publication, please refer to the attached citation of the manuscript, specific remarks on the contribution of each author is detailed further in the manuscript.

Citation: Forero-Rodríguez, Lady Johanna, **Jonathan Josephs-Spaulding**, Stefano Flor, Andrés Pinzón, and Christoph Kaleta. "Parkinson's Disease and the Metal–Microbiome–Gut–Brain Axis: A Systems Toxicology Approach." *Antioxidants* 11, no. 1 (2021): 71.

PD is a neurodegenerative disease, leading to motor and non-motor complications. Autonomic alterations including gastrointestinal symptoms precede motor defects and act as early warning signs. Chronic exposure to dietary environmental heavy metals impacts the gastrointestinal system and host-associated microbiome, eventually affecting the central nervous system. The correlation between PD and dysbiosis suggests a functional and bidirectional communication between the gut and the brain. Bioaccumulation of metals promote stress mechanisms through increasing reactive oxygen species, likely altering the bidirectional gut-brain link. To better understand differing molecular mechanisms underlying PD, integrative modeling approaches are necessary to connect multifactorial perturbations in this heterogeneous disorder. By exploring the effects of gut microbiota modulation on dietary heavy metal exposure in relation to PD onset, modification of the host-associated microbiome to mitigate neurological stress may be a future treatment approach against neurodegeneration through bioremediation. The progressive movement towards a systems toxicology framework for precision medicine can uncover molecular mechanisms underlying PD onset such as metal regulation and microbial community interactions by developing predictive models to further understand disease etiology to identify novel PD treatments options and beyond. Several methodologies have recently addressed the complexity of this interaction from different perspectives, to date a comprehensive review of these approaches is still lacking. Therefore, our main aim through this manuscript is to fill this gap in scientific literature and at the same time address the surrounding questions regarding the underlying molecular mechanisms between metals, microbiota, and the gut-brain-axis and the regulation of this system to prevent neurodegeneration.

PD is the second most common neurodegenerative disorder and affects nearly 1% of the population above 60 years of age (Tysnes & Storstein, 2017). PD is characterized by motor and non-motor symptoms, caused by striatal dopamine depletion and alterations in neurochemicals (Qamar et al. 2017). Although motor symptom impairment is critical to disease development, the non- motor symptoms may become evident years before the emergence of motor dysfunction (Pfeiffer, 2016). PD is preceded by non-motor symptoms related to gastrointestinal (GI) dysfunction, followed by motor dysfunction such as excess salivation, dysphagia, nausea,

and constipation in approximately 30% - 80% of patients (Mulak & Bonaz, 2015 ; Brudek, 2019). PD onset is unknown and is loosely related to genetic background (5% to 10%), environmental factors in idiopathic PD are postulated to trigger pathogenesis (Bellou et al. 2016; Chen & Ritz, 2018 ; Kouli et al. 2018).

1. The Gut-Brain Axis: Braak's Hypothesis

The GI microbiome is a dynamic ecosystem comprising microbial communities impacted by individual diet, host-derived metabolites, and environmental exposures. More so, the human microbiome is essential in bidirectional gut–brain communication; brain and intestinal development, function and homeostasis are likely mediated by the gut microbiome (Sampson et al. 2016 ; Quigley, 2017 ; Calvani et al. 2018 ; Cryan et al. 2019 ; Suganya et al. 2020). Braak and colleagues developed a hypothetical framework to explain the influence of environmental factors on PD development (Braak et al. 2003). For example, invasive microbiota from the gut during dysbiosis may induce a pro-inflammatory environment, thereby promoting PD onset (Hawkes et al. 2007 ; Ghaisas et al. 2016). This pathological agent could retrogradely promote alpha-synuclein formation and spread to the brainstem, locus coeruleus complex, substantia nigra, and the cerebral cortex (Visanji et al. 2013 ; Chung et al. 2016; Oertel, 2017). Overall, in PD patients the microbiota-gut-brain axis communication could beimpaired, where GI dysfunction symptoms are observed in over 80% of PD subjects (Lebouvier et al. 2009 ; Mulak et al. 2015) . However general research is necessary to elucidate communication mechanisms between gut microbiota in relation to the gut-brain axis (Cryan et al. 2019).

The GI tract is a highly interactive surface area between host and environment, and as a barrier it plays a pivotal role in regulating immune homeostasis (Vancamelbeke & Vermeire, 2017). Six major host cell types comprise the GI barrier: enterocytes, entero-endocrine cells, goblet cells, paneth cells, microfold cells, and additionally stem cells which form a monolayer barrier that restricts microbial transport and metal ion movement by the expression of transporters (Turner, 2009 ; Takiishi et al. 2017). Approximately 80% of the cells in the GI barrier are enterocytes, thus epithelial cells are intermediates between host and luminal interactions in homeostatic functions (Turner et al. 2009 ; Pott & Hornet, 2012 ; Hiippala et al.

2018). The GI has three major roles as a semipermeable barrier: selective absorption of nutrients, regulation of environmental antigens, and the transport of microorganisms (Takiishi et al. 2017 ; Salvo-Romero et al. 2015). First, the mechanical barrier consists of intestinal epithelial cells and capillary endothelial cells connected with tight or adherens junctions and desmosomes which regulate nutrients (Vancamelbeke & Vermeire, 2017). Second, the GI barrier is an immune barrier to control environmental antigens. The third which is extensively covered in this review, is the biological barrier colonized by gut microbiota. However, recent studies highlight that heavy metal exposure alters native gut microbiota and intestinal physiology (Breton et al. 2013 ; Li et al. 2019). Specifically, additional damage due to heavy metals to the gut epithelium leads to a heightened inflammatory response, disrupting GI tight junctions and promoting systemic inflammation by inciting changes in microbial abundance leading to downstream metabolic changes (Tinkov et al. 2018).

The gut-brain axis concept is a key factor fundamental to interpreting the bidirectional communication and mechanisms modulating gut-brain homeostasis, especially during oxidative stress (Cryan et al. 2019). The central nervous system (CNS), autonomic nervous system (ANS) and enteric nervous system (ENS) influence GI smooth muscle mobility, mucus secretion, and blood flux, thereby modifying intestinal microbiota abundance which in turn impacts brain homeostasis and function (Cryan et al. 2019 ; Quiglez, 2017). Microbiome-gut-brain communication is carried out through pathways involving nervous, endocrine, and immune signaling mechanisms (Martin et al. 2018). The GI tract is controlled by both intrinsic and extrinsic innervation, in which intrinsic innervation is regulated by the ENS. The ENS is innervated with extrinsic ANS (parasympathetic and sympathetic systems) (Carabotti et al., 2015). Alteration of microbial communities at the gut epithelial barrier modulates both inflammatory responses and metabolic pathways (Corywell et al. 2019 ; Assefa & Köhler, 2020).

Communication between the brain and gut microbiome is likely modulated through the vagus nerve (Breit et al. 2018). The commensal relationship between microbiota and host neurotransmitter synthesis in enteric nerves is likely an evolutionary adaptation (Galland, 2014 ;

González et al. 2021). Various GI microbiota produce metabolites that are identical to the chemical structure of host-derived metabolites (Cryan et al. 2019). For example, *Bacillus*, *Escherichia*, and *Proteus* are able to produce the neurotransmitters dopamine and norepinephrine which are uptaken by the host, molecular signals modulate communication between the microbiota-gut-brain axis and have implications for host physiology (Tsavkelova et al. 2000 ; Özoğul, 2004 ; Shishov et al. 2009 ; Strandwitz, 2018). Human vagus nerve stimulation is therapeutic to treat various pathologies, such as refractory depression, IBD, and Crohn's disease (Breit et al. 2018 ; Bonaz et al. 2016). The microbial secondary metabolite indole stimulates the vagus nerve by inducing the expression of c-Fos proteins in the dorsal vagal complex, indicating that vagus nerve activation leads to enhanced anxiety-like behaviors (Jaglin et al. 2018). Within the gut barrier, enteroendocrine cells (EECs) represent 1% of the total epithelial cells and are critical for gut maintenance (Cryan et al., 2019). Type-L enterochromaffin cells are the most common EECs and directly interact with the intestinal lumen, microbiota, and microbially-derived metabolites (Woźniak et al. 2021). EECs produce glucagon-like peptide-1 (GLP-1) and peptide YY (PYY) which stimulates satiation and regulates food intake behaviors (Latorre et al. 2016) . Release of these molecules activates food-derived nutrients in addition to bacteria-derived metabolites such as short-chain fatty acids (SCFAs) and indole which likely induce GLP-1 secretion in colonic L-cells during acute exposure (Chimerel et al. 2014 ; Cryan et al. 2019). Studies in rats and *in vitro* models highlighted that the SCFA propionate stimulates the secretion of PYY and GLP-1 through free fatty acid receptors 2 and 3 (Psichas et al. 2015). Human organoid cultures have identified that bacteria-derived secondary bile acids such as lithocholic acid stimulate GLP-1 release by activating the G–protein–coupled bile acid receptor 1 (Lund et al. 2020). Gut microbiota, such as Lactobacillus strains in co-culture with EECs increase GLP-1 secretion by downregulating expression of adaptor proteins involved in TLR signaling such as MyD88 and CD14 (Panwar et al. 2016). This may demonstrate the direct effect of lactic acid bacteria (LAB) on host physiology (Figure 4).

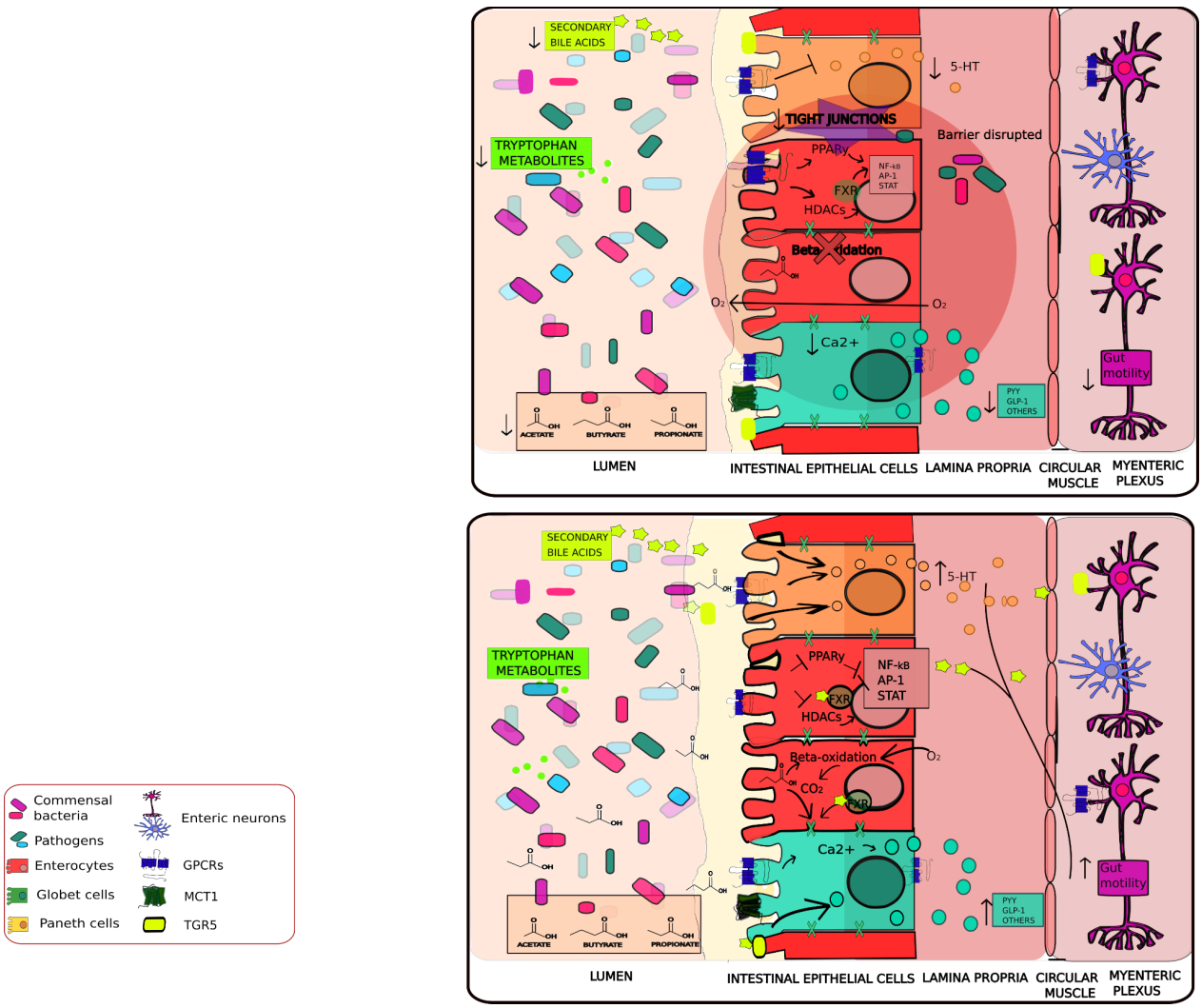

Figure 4: Bacterial metabolite signaling in the intestine. (Top panel) Secondary bile acids, SCFAs and tryptophan metabolites are microbially-derived metabolites. Secondary bile acids in the colon activate FXR and TGR5. Bacterial fermentation of dietary fibers leads to the reduction of luminal pH and produces SCFAs. (Bottom panel) Under dysbiosis a limited availability of SCFAs decreases the amount of available substrate for the colonocytes. The metabolic switch to anaerobic glycolysis and lactate production. The amount of oxygen increases of HIF1 and the expression decreases the expression of tight junctions and degenerates the gut barrier. The bacterial pathogen interacts with the

cells and increases their translocation to lamina propria promote inflammation and oxidative stress events.

2. Metal Neurotoxicity & Parkinson's

Biological organisms require 13 metals, nine of which are essential trace metals for creating organic building blocks and regulating homeostasis such as catalyzing enzymes for basic metabolic or biochemical processes. Approximately one-third of biological proteins and 40% of enzymes rely on metal ions to function (Andreini et al. 2008). The brain generally contains the greatest concentrations of metals in the human body, including Fe, Cu, Zn, and Mn (Genoud et al. 2017) . For example, both Zn and Mn are found in the midbrain and are essential for neuronal excitement, synaptic transmission, creation of new myelin, and regulation of oxidative stress (Bhattacharyya et al. 2014 ; Möller et al. 2019) . Conversely, when these metals are above normal homeostatic balance, they are associated with PD (Barnham & Bush, 2008) . Specifically, increased occupational exposure to Fe or Mg has been found to double the risk of developing PD (Hegde et al. 2004).

Various nutrients, vitamins, and reactive metals are consumed daily by humans through the ingestion of contaminated foods or water (Xuan et al. 2017 ; Miranda et al. 2005 ; McConnell et al. 2008 ; Petersen et al. 2008 ; Hadayat et al. 2018 ; Fu et al. 2019; Miclen et al. 2019). Simultaneously, the influx of global industrial emissions of heavy metals into environments is linked to environmentally-derived brain pathologies, this likely occurs first through direct interactions with the gut-associated microbiome (Tshala-Katumbay et al. 2015 ; Duan et al. 2020) (Figure 3) . Once metals enter the GI system, the gut microbiome, can potentially mediate metal toxicity through biochemical reactions of oxidation or reduction. However, heavy metals promote oxidative stress and disrupt healthy microbiomes in humans, thereby promoting dysbiosis (Assefa & Köhler, 2020) (Figure 5). Dysbiosis of protective microbial communities increases the toxic effects of heavy metals (Hashim et al. 2014) and long-term oxidative stress insults, which in turn is associated within neurobehavioral and neurological pathologies. Heavy metals toxicants, which are not modulated by the

host-associated microbiome, transit to the brain, leading to a wide-range of deleterious effects, such as neuroinflammation and neurodegeneration (Peter et al. 2018).

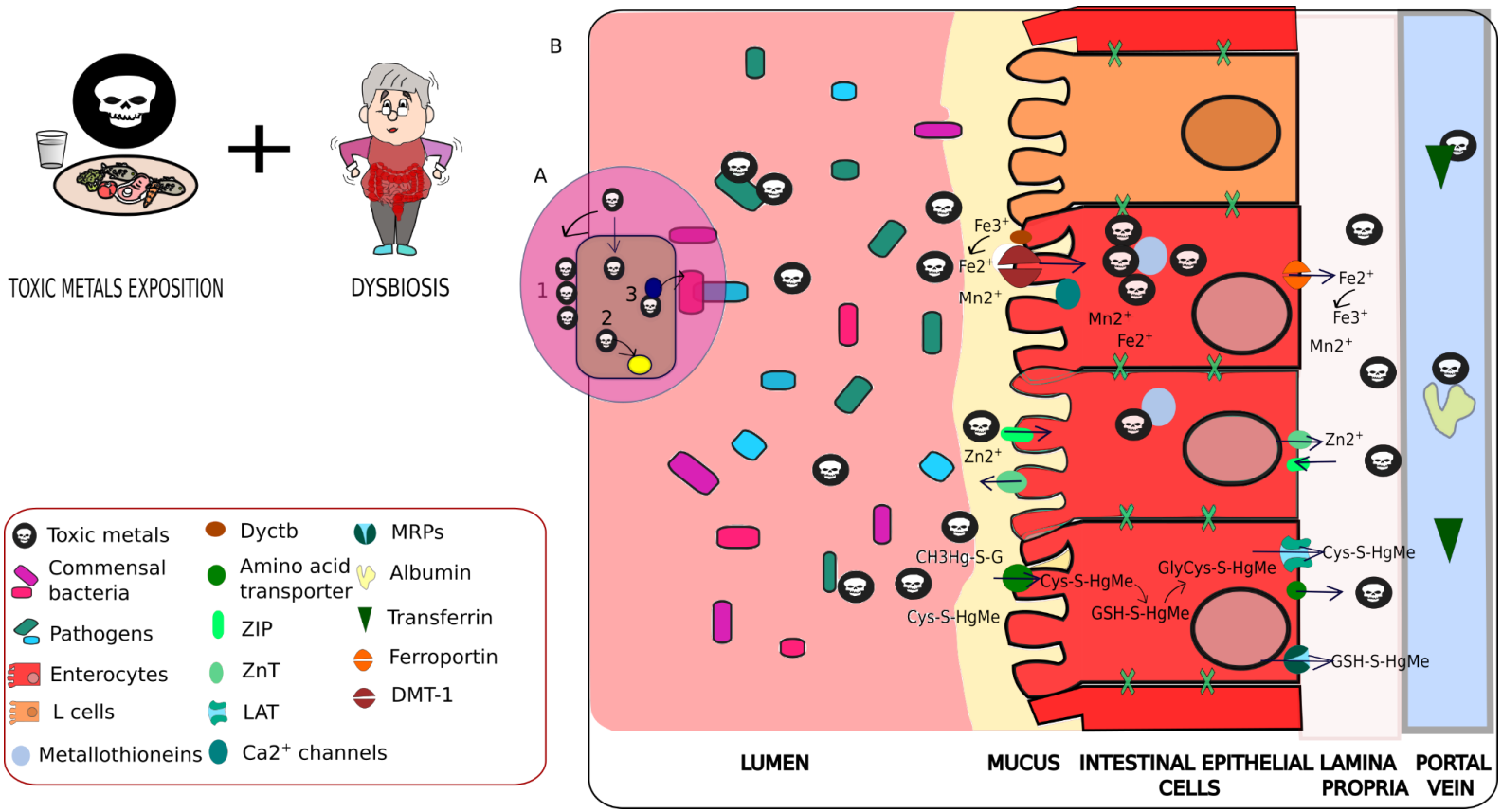

Figure 5. Gut-Microbiome Metal uptake. A) Mechanisms of microbial heavy metal bioremediation in the gut: 1. Biosorption, 2. Bioaccumulation, 3.Biotransformation. B) The primary mechanisms by which iron and other divalent metals are taken up by the enterocyte is through DMT-1 on the luminal membrane. In the case of $Fe^{3+,}$ this metal is reduced to Fe^{2+} by Dyctb. Other receptors for Zn^{2+} (ZIP, ZnT), Ca^{2+} and amino acids transporters (b0,+ , PepT1) are utilized to uptake MeHg or other metal ions. Iron has also been suggested to be transported with heme through HCP1 and as ferritin. Once entering the intracellular space, metals are readily stored as ferritin (Fe^{2+}) with metallothioneins and exported into the body circulation through ferroportin or other transporters (LAT, ZIP, ZnT).

Clinical and epidemiological characterization of PD suggests that environmental risk factors such as heavy metal toxicity, occupational farming, and pesticide exposure play major roles in PD pathophysiology (Priyadarshi et al. 2001 ; Dick et al. 2007). These environmental stressors lead to the production of reactive radicals such as ROS or NOS that are normally observed in PD progression (Breton et al. 2016) (Figure 3). Specifically, acute exposure to divalent metal ions incites oxidative stress and oligomerization risk for α-synuclein formation in the brain (Jinsmaa et al. 2014). Furthermore, Mn, Pb, and Cu ions increase α-synuclein fibrils formation which leads to Lewy Body formation, a major pathophysiological characteristic of PD (Zhang et al. 2012 ; Kwakye et al. 2015 ; Ingrassia et al. 2019). Due to the vulnerability of the CNS to metals and the lack of means to detoxify, excrete, or eliminate metals, neuronal energy homeostasis and antioxidant balance are perturbed leading to neurodegeneration (Ratner et al. 2017 ; Bridges et al. 2005 ; Fujishiro et al. 2009 ; Vesey, 2010). This is the case for the dopaminergic nerves of the nigrostriatal system, which when stressed by heavy metal exposure, can be associated with PD onset (Caito & Aschner, 2015). Thus the study of the prodromal phase underlying the pathomechanisms of PD is necessary to interpret disease etiology.

Improper metal binding associated with oxidative stress leads to protein misfolding and aggregation (Abramov et al. 2020). Metals with a high affinity to sulfhydryl groups, alter dopamine neurotransmission, reduce expression of D2 dopamine receptor sites, and impair proteins essential for maintaining cellular homeostasis (Carmona et al. 2021). Abnormal protein misfolding is the hallmark of numerous neurodegenerative diseases such as Alzheimer's Disease, Lewy Body Dementia, Huntington's Disease, prion diseases, and similarly during metal stress (Harischandra et al. 2019) . The association between metal exposure, abnormal accumulation of misfolded proteins (especially α-synuclein) found in Lewy bodies, and PD is not well understood at the mechanistic level and is likely associated with an increase in ROS (Abramov et al. 2020). Regardless, the potential to control metal exposure and maintain cellular homeostasis in PD may prevent improper neuroprotein folding prior to apoptosis. There is a need to determine the underlying metabolic outcome from heavy metals exposure, oxidative stress, and neuropathology.

Mn is a trace metal found throughout various tissues and is essential for enzymatic processes, biosynthesis of amino acids, protein formation, and carbohydrate metabolism (Fitsanakis et al. 2007 ; Harischandra et al. 2019). Environmental exposure to Mn primarily occurs by ingesting leafy vegetables, rice, grains, and nuts and enters the circulatory system through passive diffusion (Chen et al. 2018) . Presently, chronic exposure to Mn is positively correlated with dopaminergic nerve deterioration impaired basal ganglia including globus pallidus, substantia nigra, subthalamic nucleus and striatum, a hallmark characteristic of PD pathology (Bouabid et al. 2014) . Different valence states or species of Mn (Mn^{2+} or Mn^{3+}) play significant roles in Mn neurotoxicity, in which Mn^{3+} is more toxic than Mn^{2+} (O'Neal & Zheng, 2015). Typically, Mn is found in portal circulation, 80% of Mn^{2+} is found associated with α-macroglobulin or albumin. Toxic Mn^{3+} species account for 1% of total Mn found in the body; Mn^{3+} associates with transferrin endosomes during tissue circulation and Mn^{2+} diffuses through tissues including kidneys, bones, liver, and the brain (Gunter et al. 2013).

Within the brain, Mn^{3+} accumulates and enters neurons by binding to transferrin endosomes and localizes within brain tissue (Fitsanakis et al. 2007 ; Martinez-Finley et al. 2012) . Specifically, DMT1 is highly expressed in brain tissue, especially dopamine rich areas of the basal ganglia and cortex, explaining Mn association with the brain (Tai et al. 2016 ; Ingrassia et al. 2019). Mn exposure affects the transcription and translation of α-synuclein and through the activation of MAPK, beginning apoptosis cascade signals, resulting in dopaminergic neuron apoptosis (Prabhakaran et al. 2011) . Mn stress leads to the dysregulation of key homeostatic functions which are essential to degrade proteins (such as autophagy, proteasomes, and endosomal trafficking) (Moons et al. 2020). Chronic metabolic dysequilibrium linked to Mn initiates conformational changes leading to the aggregation of α-synuclein, becoming harmful to brain neuronal cells (Cai et al. 2010). This suggests that Mn and other metal ions incite the production of ROS and thereby impact the confirmation and aggregation of α-synuclein (Martinez-Finley et al. 2012 ; Moons et al. 2020). Recent observations of human α-synuclein have identified a neuroprotective role in the mitigation of dopaminergic degeneration linked to acute Mn exposures (Harischandra et al. 2015).

Conversely, neuroprotective effects are lessened when neurons are exposed to Mn chronically, leading to accelerated oxidation and misfolding of α-synuclein (Harischandra et al. 2015).

Hg is a metal that shifts between organic and inorganic phases, thereby having differing modes of toxicity. Hg not only bio-accumulates within both plants and animals in ecosystems, but is also transported over long distances as a gas following combustion. Hg vapor is stable as a gaseous and accounts for 90% of Hg within the environment (Yin et al. 2012). Inorganic Hg is not physiologically necessary in humans and is toxic in low concentrations. Hg becomes fat-soluble within the tissues of animals after methylation by microbes to become methylmercury (MeHg), prior to organism consumption and bioaccumulates from the bottom of food chains. Contaminated fish with a high biomass of fatty acids rapidly accumulate MeHg within tissues as compared to other fish which share the same environment. Hg is found to accumulate within the nervous tissue of deceased individuals with neurodegenerative diseases in comparison to healthy controls (Fung et al. 2012). Individuals poisoned by chronic MeHg suffer from numerous symptoms linked to CNS impairment such as visual impairments, lethargy, tremors, lack of coordination, and inability to recall memories (Finkelman et al. 2002).

Hg differs from other metals, it does not require human macrophages or other immuno-transport mechanisms, rather MeHg is readily able to penetrate the blood brain barrier (BBB) (Cariccio et al. 2019). Hg uniquely binds to sulfhydryl groups with high affinity in comparison to other metals in the human body. Specifically, MeHg binds to cysteine groups through molecular mimicry, is transported through the BBB, and directly interacts with glial and neuronal cells (Cariccio et al. 2019). From there, Hg is taken up through the nerve endings and accumulates in the CNS ganglia where it cannot be detoxified, leading to systemic effects upon the substantia nigra dopaminergic neurons through disruption of tubulin molecules (Sarafian et al. 1996 ; Pendergrass et al. 1997). Dopaminergic neurons consist of axons composed of tubulin molecules, however in presence of inorganic Hg, these neurons bind to the 14 sulfhydryl groups of tubulin. Through this mechanism Hg interacts with α-tubulin and β-tubulin, inhibiting tubulin structural formation of neurons, prevents tubulin from binding to GTP, and halts motor neural functions by blocking neurotransmission (Pendergrass et al. 1997). Hg promotes the formation of amyloid-β proteins, the predecessors for amyloid plaques and neurofibrils in the brain, which

have been associated with the onset of both Alzheimer's disease and PD (Breydo et al. 2012 ; Wallin et al. 2020). Through these pathomechanisms, MeHg exposure leads to apoptosis and neurotoxicity by abnormal cellular narrowing, chromatin condensation, modification of cytochrome C flux, and well-described oxidative stress insults to the mitochondria (Ceccatelli et al. 2010).

Fe is a common dietary metal that is essential in humans, assisting in oxygen transport and mitochondrial respiration (Sian-Hülsmann et al. 2011). Conversely, the over or under abundance of free Fe in humans is associated with several pathophysiologies (Muñoz, 2012). Low Fe, anemia, or low hemoglobin levels throughout the course of one's life has been correlated with an increased risk of developing PD (Savica et al. 2009). Irregular Fe metabolism in humans leads to lack or excess Fe in the brain, causing deleterious effects in the PNS or CNS (Dev et al. 2017). Incidentally, the argument that Fe accumulation precedes PD and other neurodegenerative diseases has been discussed in detail elsewhere (Sian-Hülsmann et al. 2011 ; Hare et al. 2015 ; Hare et al. 2017).

Fe metabolism regulates brain uptake, sequestration, accumulation, release, and movement of Fe into the substantia nigra pars compacta; dysfunction of Fe metabolism and is associated with PD (Anzai et al. 2017). Specifically, PD patient ferritin, transferrin, and total serum Fe is lower than healthy controls, illustrating that Fe metabolism and movement is adverse in PD patients (Logroscino et al. 1997). In healthy patients, Fe provides pigmentation and other essential neurophysiological roles, in PD patients Fe is released from neuromelanin (Fasano et al. 2006). Approximately 20% of Fe in the substantia nigra is bound to neuromelanin. Impaired Fe metabolism is assessed by loss of neuromelanin of dopaminergic neurons in PD patients as observed by MRI (Gerlach et al. 2006 ; Lotfipour et al. 2012). Overall, adverse Fe metabolism highlights the role of metal exposure and dysregulation in individuals, especially for neurodegeneration and idiopathic PD (Levi et al. 2014).

Fe accumulates within graymatter of both the basal ganglia and midbrain, this is positively associated with PD onset (Xuan et al. 2017). Neuronal Fe accumulates in the substantia nigra pars compacta of PD patients, but not in other regions of the brain in

post-mortem PD patients (Dexter et al. 1989). High quantities of Fe and lack of Cu in the substantia nigra pars compacta are typical features of PD onset (Ottman et al. 2017). When tracking PD patients over 3 years, it was found that Fe increases in the substantia nigra pars compacta and simultaneously Fe decreases in the white matter (Ulla et al. 2013). A down regulation of DMT1 perturbes Fe metabolism in the brain and is typically found in PD brains postmortem. Irregularities of this gene leads to chronic ferritin release and neurotoxicity (Yu et al. 2013).

3. Oxidative Stress & Inflammation in the Gut-Brain Axis

Reactive oxygen species (ROS) (superoxide, hydrogen peroxide, and hydroxyl) produced from metals generate deleterious products which impairs key enzymes of the mitochondrial electron transport chain, leading to alterations in protein functions (Chtourou et al. 2011 ; Prakash et al. 2016 ; Trist et al. 2019). Numerain regions in patients with PD are affected (Hawkes et al. 2007). For example, the hippocampus which is associated with memory, is impacted by heavy metals. Metal-stress of the hippocampus is linked to accelerated aging, memory loss, and dementia (Schneider et al. 2017 ; Lamtai et al. 2020). The hippocampus contains higher than average glutamate and glucocorticoid receptors, predisposing the hippocampus to metal stress (Cobley et al. 2018).

Heavy metals induce oxidative stress by generating ROS, which impair tight junctions that regulate barrier and permeability functions of both the GI tract and BBB by modifying phosphorylated junction proteins, thereby inducing chronic inflammation (Vandeputte et al. 2016 ; Bridge et al. 2005 ; Rao et al. 2000 ; Jaishankar et al. 2014 ; Ferruzza et al. 2002 ; Valko et al. 2005 ; Rao, 2008). ROS can be counteracted via antioxidants. Across various organisms, glutathione (GSH) mitigates cellular damage by ROS. Metal ions accelerate hydroxyl radical production through fenton reactions, leading to GSH reductase inhibition and decreased GSH concentration (Bonetto et al. 2014) (Figure 6). Specifically, when ROS levels are greater in relation to antioxidant capacity, oxidative stress is generated. Thus, the increase of ROS triggers cell damage through lipid peroxidation, DNA fragmentation, mitochondrial damage, and other cellular alterations that disrupt barrier tight junctions (Rao, 2008).

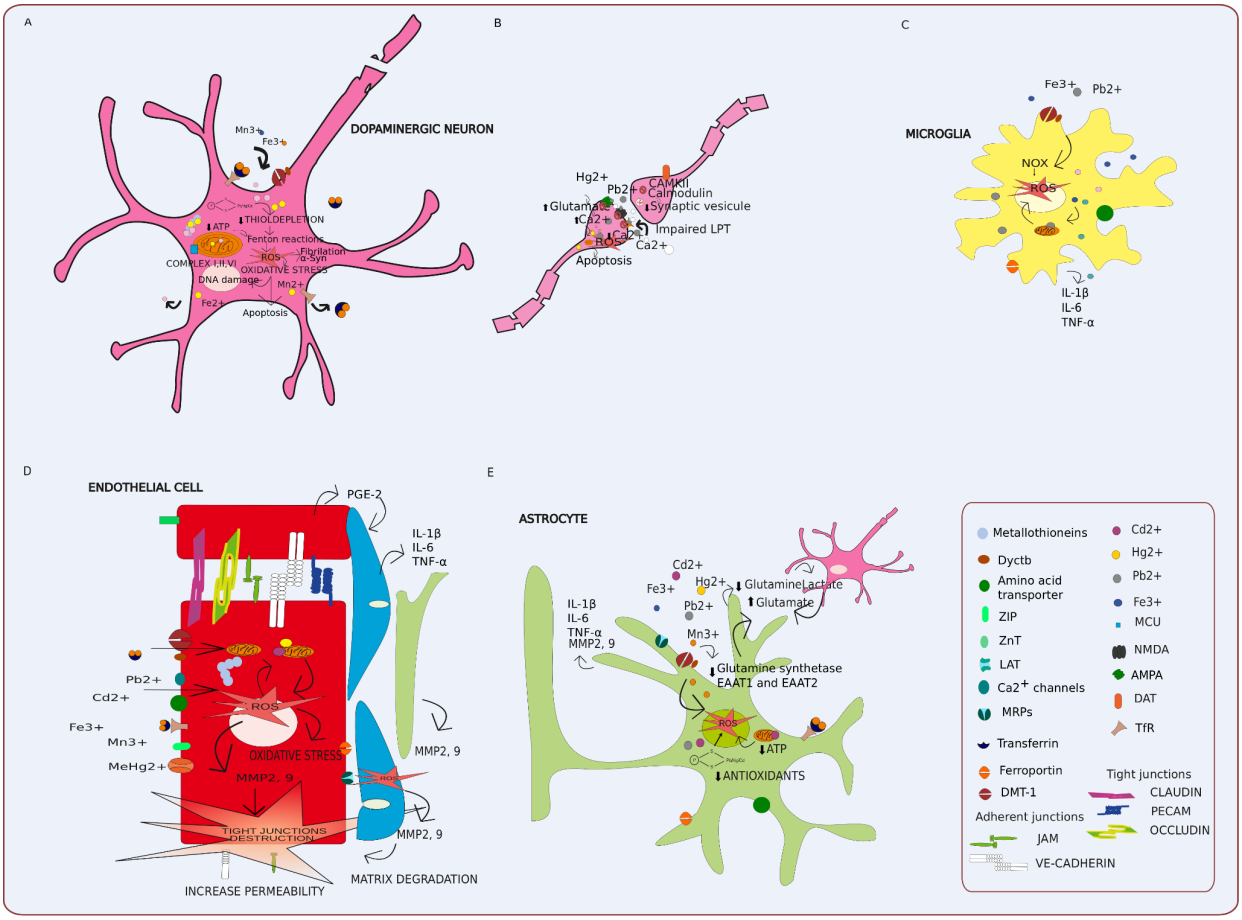

Figure 6: Cell-specific disruption of the blood-brain barrier through metal neurotoxicity and molecular mimicry. A) Mn, Fe and other toxic metals accumulate in the mitochondria, leading to damage of the mitochondrial electron transport chain dysfunction by. decreasing antioxidative functioning and increasing oxidative stress, leading to cellular damage. B) In the neuronal synapses, Pb, Cd and Mn impair Ca^{2+} channels and alter ion signaling. C) Glial cells increase the production of ROS through mitochondrial damage, alterations in antioxidant levels and metal reactions, promote the activation of the NF-kB pathway and release of proinflammatory cytokines (TNF-α, IL-1, IL-6) leading to excitotoxicity in neurons. D) In endothelial cells, the increased production of ROS promotes the release of metalloproteinase-9 and PGE-2 by endothelial cells, which stimulates pericytes and glial cells to promote pro-inflammatory signals. E) The interaction of Glial cells with ROS leads to mitochondrial damage and release of proinflammatory cytokines which are further bolstered by heavy metals.

The human GI tract contains a diversity of metabolites produced by host-associated microbiota. These microbiota-metabolites mediate gut-brain communication by transiting to the CNS where they can modulate oxidative stress and promote microglia activation (Kwon et al. 2020 ; Giambò et al. 2021). Local oxidative stress disrupts gut and BBB barriers, leading to synuclein misfolding, aggregation, and subsequent neuronal damage in both ENS and CNS (Chen et al. 2019). Increased intestinal permeability allows for heavy metal ion translocation and bacterial antigens which are critical in intestinal neuronal oxidative injury. Synthesis of nitric oxide (NO) in the GI tract by inhibitory motor neurons, translocates to the brain through the vagus nerve (Sanders et al. 2019). On the other hand NO produced by the gut microbiota, is scavenged by hemoglobin and is later diffused, providing free radicals that interact with α-synuclein, microbial, immune signaling, leading to a perturbed BBB and neurodegenerative disorders (Dumitrescu et al. 2018).

Microbial dysbiosis of the GI system promotes a pro-inflammatory environment and alters barrier permeability. This factor in addition to free heavy metal ions leaking from the gut likely induces downstream oxidative stress in the enteric nervous system (ENS), leading to α-Syn misfolding and aggregation (Friendland et al. 2017 ; Ingrassia et al. 2019). Altered microbiota stimulate ROS production by activating the cytoplasmic NLRP3 associated inflammasome, regulating the maturation and secretion of pro-inflammatory cytokines, such as IL-1β in epithelial cells, promoting Th17 cell differentiation (Tschopp et al. 2010 ; Cheng et al. 2019). Gut-mucosa Th17, an inflammatory subset of T helper cells, are associated with the development of autoimmune disorders, in addition to PD (Campos-Acuña et al. 2019 ; Lee et al. 2011 ; Kustrimovic et al. 2018)). Caspase-1-deficient stressed mice which lack inflammasome activation, present reduced depressive-like behaviors and altered fecal microbiome. The microbiome changes were related with beneficial effects in rebalancing the gut microbiota and attenuating the inflammation, highlighting that gut microbiota via inflammasome signaling likely alters brain functioning (Wong et al. 2016). Proinflammatory signaling from LPS and TNF-G directs nitric oxide synthase (iNOS) upregulation induces oxidation and nitration of actin cytoskeleton, thereby disrupting the GI mucosal barrier by depleting both occludin and zonula occludens-1 (Banan et al. 2001 ; Byndloss et al. 2017 ; Litvak et al. 2018 ; Hu et al.

2019). Due to the fact that the GI submucosal neurons and terminal axons are proximal to the gut lumen, this may lead to the spread of α-Syn from the ENS to the CNS through the vagus nerve pathway (Friedland et al. 2017). Chronic oxidative stress exposure to dopaminergic cells eventually leads to characteristic motor symptoms of PD (Lebouvier et al. 2009 ; Blaecher et al. 2013). These tandem reactions trigger neuroinflammation and the onset of neurodegeneration and eventually PD onset through a well-established timeline of disease (Hawkes et al. 2010).

Heavy metal exposure and ROS by-products promote neurotoxic disturbances such as cognitive impairments, learning/memory dysfunction, movement disorders, loss of language skills, nervousness, and emotional instability (Caito et al. 2015 ; Vandeputte et al. 2016). Human brains are especially susceptible to fatty acid oxidation due to high rates of oxygen consumption and ROS stress caused by heavy metals. Specifically, when fatty acids contained in vascular endothelial cells, neurons, and astrocytes are exposed to MeHg, these cells become impaired and cannot uptake antioxidants leading to chronic oxidative stress, inflammation, and endothelial dysfunction (dos Santos et al. 2018 ; Takahashi et al. 2019).

Mn exposure has systemic effects on ROS regulation and production, primarily enzymes which control both protein folding and transcription (Fernandes et al. 2017 ; Fernandes et al. 2019). A recent RNA-Seq study investigating the acute and chronic effects of Mn on human-derived neuroblastoma cells found that Mn at any dose incites damages to nervous system by upregulating oxidative stress, leading to mitochondrial dysfunction and inflammatory response (Fitsanakis et al. 2007). Mn prevents neurotoxin clearance by promoting cellular oxidative stress and impairing neuron and astrocyte crosstalk by dysregulating calcium signaling , glutamate- glutamine pathway, glutamate-GABA cycle (Farina et al. 2013 ; Sidoryk-Wedrzynowicz et al. 2013; Ke et al. 2019; Kwon et al. 2020. These metabolic disturbances drive oxidative stress, mitochondrial dysfunction by mitigating ATP levels, induce protein misfolding, finally neuroinflammation and neurotoxicity, which could lead to nigrostriatal cell death (Farina et al. 2013 ; Genoud et al. 2017). Mitochondrial stress exacerbates ROS production and drives neuroinflammation in the brain by perturbing muscarinic and dopaminergic receptors (Fernandes et al. 2012 ; Raj et al. 2021). Furthermore, Mn^{3+} oxidation of dopamine increases the relative concentration of localized oxidized

dopamine,thus, resulting in increased oxidative stress (Harischandra et al. 2015). While Mn impacts neurotransmitter uptake and trafficking through neuronal oxidative stress leading to impaired cellular metabolism, this is shared between both Mn neurotoxicity and PD onset, there is a lack of mechanistic evidence connecting Mn exposure to PD causation (Fitsanakis & Aschner, 2005 ; Racette et al. 2017).

Inorganic Hg^{2+} that is oxidized by ROS has an increased half-life in the brain and binds to sulfhydryls of thiols, leading to disruptions in protein conformation or enzyme functions (Clarkson, 2002 ; Rooney, 2007). By binding to GSH and cysteine residues of hormones, essential functions such as GSH upregulation, mitochondrial functions, and inhibition of the NFkB pathway are blocked, thereby leading to neuronal damage (Kim et al. 2002 ; Fonnum et al. 2004). MeHg causes apoptosis within 18 hours of exposure by impairing mitochondrial mRNA expression, mutation of mtDNA, and promoting excessive production of ROS (Castoldi et al. 2000 ; Wang et al. 2016).When heavy metals damage mitochondria and GSH concentrations are inhibited, Hg concentrates in the midbrain and promotes ROS prior to PD onset through dopamine depletion of dopaminergic cells (Hsu et al. 2005). This mechanism of neurodegeneration occurs because Hg has a high affinity for dopamine receptors compared to other metals and prevents GSH from mitigating ROS, leading to the impairment of numerous neuronal cellular processes and eventually neurological pathologies preceding PD (Ballatori et al. 2009).

Fe exerts neurotoxic effects through ROS production that react with hydroxyl radicals, producing hydrogen peroxide which interacts with ferroptosis to release Fe ions that oxidize dopamine and incite dopamine catabolism (Hare et al. 2014 ; Hare & Double, 2016 ; Guiney et al. 2017). Tandem increase of Fe and ROS in the brain of PD patients is associated with substantia nigra damage (Ma et al. 2021). This oxidative stress cascade results in: neural degeneration, loss of dopaminergic cells, and apoptosis exacerbating neuroinflammation in PD patients (Tiwari et al. 2017). Chronic inflammation perpetuates Fe ion accumulation in the brain and modifies proteins which metabolize Fe further driving neuronal apoptosis by inhibiting mitochondrial complex I (Collins et al. 2012 ; Hare et al. 2013 ; Urrutia et al. 2013 ; Niranjan et al. 2014). Over time, chronic inflammation by free Fe ions creates ROS, increases the presence

of IL-6 and L-Ferritin in the cerebrospinal fluid, and finally neurodegeneration through neuronal apoptosis which is presented as recurrent tremors (Sian-Hülsmann et al. 2011 ; Lian et al. 2019).

BBB disequilibrium allows metal entry and increased peripheral immune cells infiltration into the CNS, further promoting PD development (Kortekaas et al. 2005). Microglia sense a diverse stimuli that disrupts CNS homeostasis such as toxicants, neuronal damage, microbial infection, α-synuclein (Hanisch et al. 2007). Initial microglial activation allows leukocyte to enter the BBB, thereby recruiting Th1 and Th17 cells to produce cytokines that secrete inflammatory molecules such as cytokines, chemokines, reactive free radical, and others (eg. iNOS, NO, IL-1beta, IL-6, TNF-α, IFN-γ, IL-8, TGF-b, prostaglandins, cyclooxygenases), which may worsen neurodegenerative conditions by inducing neuronal inflammation thereby stimulating the inflammatory M1 phenotype in the microglia and thereby contributing to neuroinflammation and neurodegeneration (Mosley et al. 2012 ; Devos et al. 2013; Tanaka et al. 2013; Wang et al. 2015; Troncoso-Escudero et al. 2018; Campos-Acuña et al. 2019). Chronic activation of M1 microglia is implicated as a key component in the development of neurodegenerative diseases (Troncoso-Escudero et al. 2018).

Astrocyte activation through chronic metal exposure promotes secretion of pro-inflammatory TNF-α, IL-6, and IL-10, resulting in BBB tight junction impairment (Liu et al. 2015 ; Liu et al. 2017). The protective role of astrocytes, which clear alpha-synuclein and neurotrophic factors, is impaired when metals alter glycogen consumption and induce ROS production, further promoting astrogliosis and dopaminergic neuron degeneration (Jozefczak et al. 2012). This is essential because the overproduction of alpha-synuclein, if taken up by astrocytes, leads to astrogliosis and neurodegeneration (Cabezas et al. 2013). Thus the over-activation, abnormal influx and loss of regulatory astrocyte activity contributes to progression of immune-mediated PD (Gu et al. 2010 ; Gelders et al. 2018).

4. Microbial Dysbiosis and Inflammation in the Gut-Brain Axis

CNS disorders are often accompanied by intestinal inflammation (Fond et al. 2014 ; Fung, 2020). Gut-associated microbiota modulate immune function and oxidative stress at the local and systemic level (Dumitrescu et al. 2018 ; Fung, 2020). The mucosal immune system is

composed of the GI tract, lamina propria dendritic cells, gut-associated lymphoid tissue, LP-lymphocytes, and intraepithelial lymphocytes (Takiishi et al. 2017). Hosts tolerate commensal antigens by constantly recognizing and reacting to microbes ensuring the mutualistic nature of the host-microbial relationship (MacDonald & Monteleone, 2005 ; Hooper et al. 2012). Therefore, the immune system is integrated as a bidirectional signaling hub between the CNS and the gut (Powell et al. 2017). Microbiota are essential in lymphoid structure development, epithelial, and innate lymphoid cells function, and T-cell subsets at a systemic level. These cells maintain gut mucosa homeostasis by signaling for proinflammatory (Th1, Th2 and Th17 cells) and anti-inflammatory (Foxp3+ regulatory T cells (Tregs)) differentiation and response (Sommer & Bäckhed, 2013 ; Fung, 2020). Tregs cells are concentrated in the colon and are influenced by intestinal microbiota (Hall et al. 2008). Commensal microbiota likely influence Treg cell generation and immune responses through production of both butyrate and propionate, thereby limiting oxidative stress induced inflammation and promoting gut homeostasis Fung et al. 2020 ; Venegas et al. 2019 ; Cheng et al. 2019). In murine models, the application of *Bifidobacterium*, *Lactobacillus*, and *Clostridium* genera increase Foxp3(+) T regulatory cells, which are associated with the protection and attenuation of allergic responses and the ensure immune homeostasis (Karimi et al. 2009 ; Lyons et al. 2010 ; Atarashi et al. 2011 ; Lu et al. 2017).

PD specifically is associated with intestinal inflammation, in which 80 % of patients are observed to have gut microbiota composition and abundance differences compared to non-PD controls (Brudek et al. 2019 ; Chen et al. 2019). For example, an overgrowth of Enterobacteriaceae and decreases in Prevotellaceae or families associated with SCFAs production are observed in PD (Keshavarzian et al. 2015 ; Scheperjans et al. 2015 ; Unger et al. 2016 ; Li et al. 2017 ; Barichella et al. 2019). Enterobacteriaceae such as *E.coli*, induce Th17 inflammatory responses through inflammasome mechanisms, leading to the production of IL-1β. Induction of Th1 and Th17 crosses the BBB, stimulates the microglia, and consequently promotes brain inflammatory reactions (Mosley et al. 2012 ; Campos-Acuña et al. 2019).

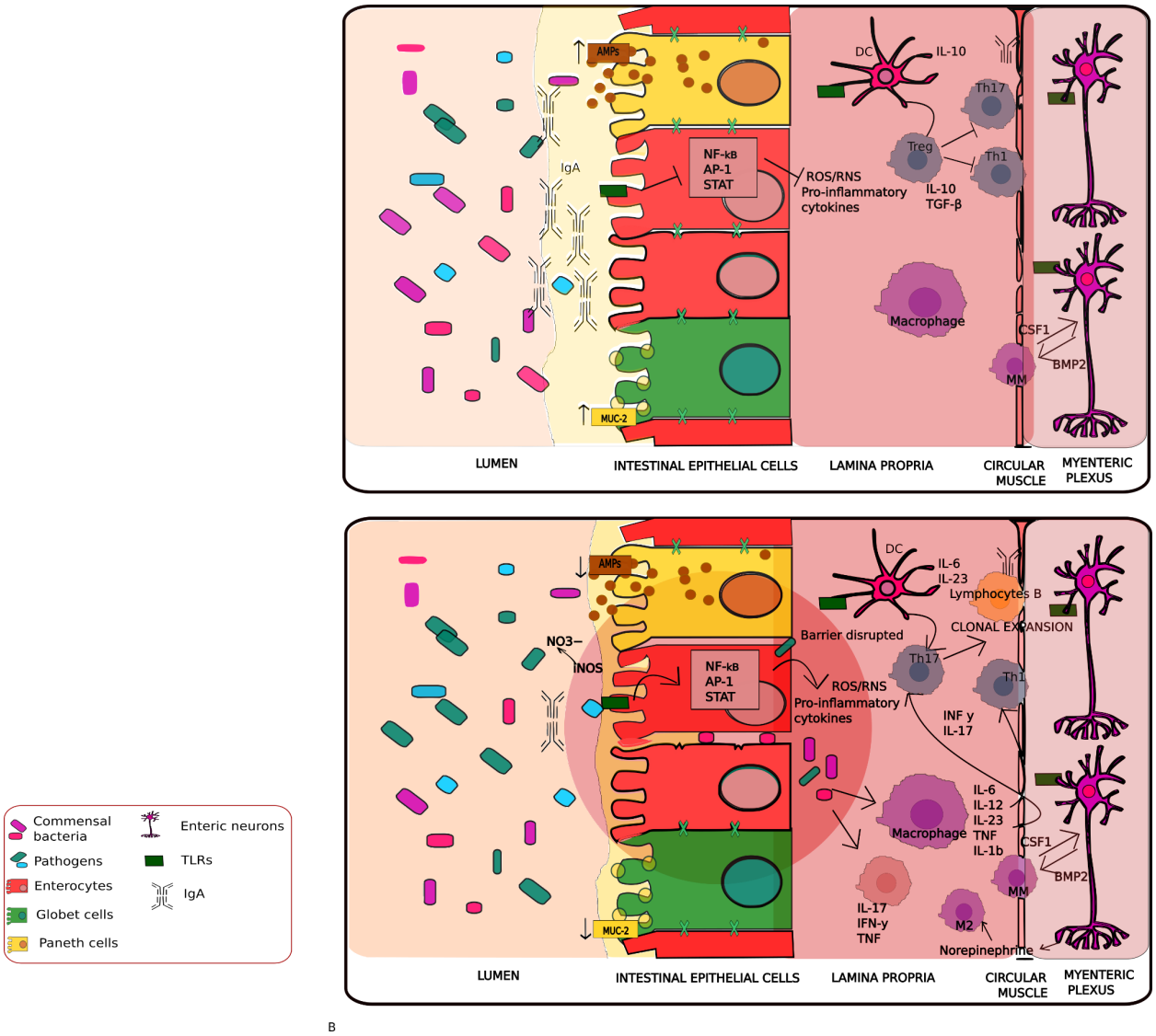

B

Figure 7: Neuro-Immune Crosstalk. A) Neuronal enteric cells play essential roles in gastrointestinal motility. Crosstalk between these cells with macrophages in the longitudinal and circular smooth muscle where the MMs incite the production of growth factor bone morphogenetic protein 2 (BMP2) to stimulate motility that is directed by the neurons. In turn, the enteric neurons through the production of survival factor (CSF1) promote the maintenance of macrophages B) Under dysbiotic conditions the epithelial barrier is impaired leading to the translocation of microbiota, toxins, and deleterious exposures as suggested by Braak's Hypothesis, thereby leading to the activation of the host immune response. Thus, macrophages decrease the expression of BMP2, and enteric neurons decrease the expression of Csf1 and the motility.

PD patients display high levels of proinflammatory cytokine expression (TNF-α, IFN-γ, IL-1β and IL-6) and glial activation markers (GFAP and Sox-10) in the colon (Devos et al. 2013). TNF-α enters the brain and induces inflammation by activating microglia or astrocytes, oligomeric protofibrils are uptaken and presented to CD4+ by antigen presenting cells (Benner et al. 2008 ; Campos-Acuña et al. 2019). Oral administration of Proteus mirabilis promotes α-synuclein aggregation in the gut and SN, impairing the colonic barrier, and contributes TNF-α and TLR4-mediated macrophage activation (Choi et al. 2018). Thus, dysbiosis of the gut microbiota induce PD-related pathological changes by increasing gut permeability, promoting TNF-α transit via blood to the SN, triggering α-synuclein aggregation, and dopaminergic neuronal damage (Choi et al. 2018 ; Campos-Acuña et al. 2019; Chen et al. 2019).

Microbial dysbiosis of the GI system promotes a pro-inflammatory environment and alters barrier permeability. This factor in addition to free heavy metal ions leaking from the gut likely induces downstream oxidative stress in the enteric nervous system (ENS), leading to α-Syn misfolding and aggregation (Friedland & Chapman, 2017 ; Ingrassia et al. 2019). Altered microbiota stimulate ROS production by activating the cytoplasmic NLRP3 associated inflammasome, regulating the maturation and secretion of pro-inflammatory cytokines, such as IL-1β in epithelial cells, promoting Th17 cell differentiation (Cheng et al. 2019 ; Tschopp & Schroder, 2018). Gut-mucosa Th17, an inflammatory subset of T helper cells, are associated with the development of autoimmune disorders, in addition to PD (Lee et al. 2011 ; Kustrimovic et al. 2018 ; Campos-Acuña et al. 2019). Caspase-1-deficient stressed mice which lack inflammasome activation, present reduced depressive-like behaviors and altered fecal microbiome. The microbiome changes were related with beneficial effects in rebalancing the gut microbiota and attenuating the inflammation, highlighting that gut microbiota via inflammasome signaling likely alters brain functioning (Wong et al. 2016). Proinflammatory signaling from LPS and TNF-G directs nitric oxide synthase (iNOS) upregulation induces oxidation and nitration of actin cytoskeleton, thereby disrupting the GI mucosal barrier by depleting both occludin and zonula occludens-1 (Byndloss et al. 2017 ; Litvak et al. 2018 ; Hu et al. 2019). Due to the fact that the GI submucosal neurons and terminal axons are proximal to the gut lumen, this may lead to the spread of α-Syn from the ENS to the central nervous system

(CNS) through the vagus nerve pathway (Friedland & Chapman, 2017). Chronic oxidative stress exposure to dopaminergic cells eventually leads to characteristic motor symptoms of PD (Lebouvier et al. 2009 ; Blaecher et al. 2013). These tandem reactions trigger neuroinflammation and the onset of neurodegeneration (Hawkes et al. 2010).

5. Towards Next-generation Systems Toxicology

Foundational understanding of complex disease mechanisms are expanded with computational and mathematical modeling of biological systems through a systems approach. By integrating and modeling multiple biological properties which underlie metabolic networks, the properties of biological systems are readily uncovered. Metabolic profiles and respective concentrations are useful for biomarker identification and have an extended value in the creation of metabolic models for systems biology applications (Graspeunter & Waschina, 2019 ; Marinos et al. 2020). While systems biology methods have numerous applications, in the case of this manuscript they provide a novel outlook to investigate the cross-talk between the host and microbiome with regards to toxicology. However, within a larger metabolic network, this results in significant changes in terms of metabolic capacities (Li et al. 2019). These findings suggest that human-associated microbiota modulation impacts human health at the metabolomic level and likely interacts with neurodegenerative mechanisms. Modeling of microbiome interactions with the host within the systems toxicology paradigms may highlight mechanisms to remediate free metal cations within the human GI tract. Advancements in meta-modeling and application to humans in a clinical setting would provide novel evidence to use this intervention successfully.

Humans are likely exposed to an environmental cocktail of heavy metals through their diet. Conversely, toxicity testing and risk assessment of metals typically investigate a singular exposure through reductionism (Rice et al. 2008). Therefore the consideration of metal mixtures on multiple target organs simultaneously is lacking in detail. While metal mixtures upon human health have been investigated, progress has been significantly limited by the traditional reductionist approach in toxicology, rather than a systems level approach (Kortenkamp et al. 2009 ; van Vliet, 2011). For example, reductionist toxicology risk assessment on multiple

exposures tends to be imprecise and provides uncertainty as to what molecular biomarkers require to be investigated (Sarigiannis & Hansen, 2012 ; Sharma et al. 2017). Specifically, the application of "Omics" methods can increase the mechanistic understanding of metal mixture toxicity such as how metals disturb the systemic interacting biological pathways such as oxidative stress, mRNA splicing, and electron transport chain dysfunction in relation to neurodegeneration (Zhang et al. 2005 ; Karri et al. 2020)). Therefore, there is a need to decipher the underlying toxicomechanisms of metal neurotoxicity leading to PD in humans through the application of multi-omics technology to measure cellular responses to stress. While it is possible to obtain quantitative information on a variety of molecular functions which underlie neurodegeneration, a major hurdle still exists to integrate omics data and microbiome into a large-scale systems toxicology analysis through modeling approaches (Wanichthanarak et al. 2015).

Systems toxicology integrates data from both *in vitro* or *in vivo* studies with computational modeling to derive novel insights to inform toxicity risk assessments; this is in contrast to risk assessments that are derived from reductionist toxicity testing methods. Naturally, systems toxicology relies both on big data derived from high-quality experiments that are analyzed with multi-omics technology to create information that is both reliable and relevant to studies. These approaches are key in the creation of a systems toxicology study to investigate the mechanistic underpinnings of toxic exposures (Knudsen et al. 2015 ; Hartung et al. 2017). Due to the high quantity of toxicity data being produced in previous years, systems toxicology and bioinformatics have provided novel methods to assess disturbances in biological networks to further understand molecular mechanisms. While multi-omics is valuable to understand the molecular systems of biological homeostasis and disturbances, it is important to note that significant hurdles still remain in the measurement, testing, and integration of dynamic datasets, which closely resemble biological phenotypes (van Vliet, 2011 ; Bouhifd et al. 2015). For example, the Human Toxome Project has been a valuable assessment of disturbances within several pathways as identified by multi-omics technology to verify and increase the confidence of toxicity study (Bouhifd et al. 2015). To achieve the goals in satisfying the Human Toxome Project, there is a great need to develop and validate novel systems toxicology tools that are

inspired from systems biology or medicine through the modeling of dynamic systems towards a more realistic representation of human toxicity outcomes.

As extensively discussed previously, heavy metals toxicity influences neurodegeneration via the microbiota through a wide variety of pathomechanisms. Utilization of different "omics" technologies such as transcriptomics and metagenomics to generate large "molecular snapshots" of various conditions underlying neurodegeneration in the gut-brain axis is essential (Tilocca et al. 2015; Stilling et al. 2018). While these approaches provide the means to obtain sizable quantitative datasets describing a variety of molecular functions which underlie neurodegeneration, a major hurdle still exists; the integration of multi-omics and microbiome data into a large-scale systems toxicology analysis through modeling approaches (Wanichthanarak et al. 2015). Systems biology knowledge-bases and models can be readily employed to integrate and interpret this data at a systems level, providing mechanistic hypotheses about the interactions between the large variety of biological components involved. For example, the alterations that metal toxicants induce between different biological processes such as oxidative stress responses, mRNA splicing, and energy metabolism and their relation to neurodegeneration (Zhang et al. 2005; Karri et al. 2020) can be characterized at the level of gene and protein expression and metabolome. Systems biology models can be employed in this case to infer systems-level activity changes to characterize the interplay between metal toxicants, gut bacteria, and human tissues.

D. **Genome-scale Metabolic Network Models**

Genome-scale metabolic models (GEMs) are used to identify and analyze changes in metabolism under specifically defined constraints such as the irreversibility of various reactions (thermodynamic constraints), steady-state conditions (mass-balance constraints) and minimum or maximum values as decided for certain metabolic fluxes (capacity constraints) (Fouladiha & Marashi, 2017). These changes include quantitative measurements of cellular phenotypes such as biosynthesis of cellular components, secretion of secondary metabolites, cellular energetics, and growth rates which can demonstrate how changes in one of these aspects impacts metabolic pathways and thereby interact other phenotypes within a network (Lewis et al. 2012). At present there are hundreds of manually-curated GEMs, all are representatives of various prokaryotic and eukaryotic species. These network models have been employed to investigate evolutionary relationships (Pál et al. 2006 ; Marashi et al. 2013), model endosymbiosis (Yizhak et al. 2011), identify potential drug targets (Oberhardt et al. 2013), metabolically engineer relevant strains (Feist et al. 2009 ; Garcia-Albornoz et al. 2013), and study basic genotype-phenotype relationships (Thiele et al. 2005 ; Durot et al. 2008).

To create such models, metabolic network reconstruction methods are employed to either automatically or manually collect these reactions and their data of specific cells to make an *in silico* model of metabolic activity and cross-talk (Mo et al. 2007 ; Zimmermann et al. 2021). Metabolic network reconstruction generally employs various biochemical reactions encoded in an organism's genome and thus provides models for stoichiometric analysis (Thiele & Palsson, 2010). The reconstruction of GEMs acts as a valuable method to systematically analyze large-scale multi-omics data and further provides mechanistic information about molecular processes through *in silico* approaches (Hyduke et al. 2013). Metabolic networks of an individual cell for example, is reconstructed to include numerous interwoven biochemical reactions where extracellular nutrients are uptaken or consumed to achieving a energy or biomass reaction to synthesize metabolites which form the building blocks of cells, while excreting secondary metabolites back into the extracellular environment (Fouladiha & Marashi, 2017). The greatest advantage of employings GEMs for the integration of diverse multi-omics

datasets is the potential to catalog all metabolic reactions derived from an organism in addition to the reactions which allows for the correspondence of reactions to active enzymes (Opdam et al. 2017).

A major limitation of this approach is that only metabolic changes can be analyzed. Therefore, it is not possible to investigate signaling or regulatory pathways through kinetic analysis which may be used to provide further information on cellular signal transduction or regulatory mechanisms in biological organisms (Palsson et al. 2011 ; Fouladiha & Marashi, 2017). However, there are some cases of investigation in this area within classic systems biology model organisms such as *Escherichia coli* and *Saccharomyces cerevisiae* (Shlomi et al. 2007). This is due to the fact that these organisms have well-studied and comprehensive assessment of organismal regulatory data, humans presently do not have such information available. Another significant limitation of GEMs is the personal bias for the selection of objective function for various context-specific metabolic models. For example, most unicellular prokaryotes or eukaryotes typically aim to maximize growth or biomass, this concept can not be simply applied to human specific cells or tissues (Feist & Palsson, 2016). While there have been approaches to identify objective functions for human livers or kidneys, it becomes more challenging to decide this function for more dynamic cells, such as in the case for cancer or stem cells while they are still transforming towards a state of "normality" (Chang et al. 2010 ; Gille et al. 2010 ; Agren et al. 2012). Furthermore, as there may be a lack of bibliographic metabolic information or errors in the construction of metabolic network models which may be manifested as gene products that are not compatible with some metabolic networks, this may induce "gaps" in the metabolic pathways (Zimmermann et al. 2021). These gaps are a significant limitation in metabolic model reconstruction and are linked to inconsistencies when predicting phenotypic features in *silico* cells (Bernstein et al. 2021). While this information is useful to identify at what level metabolic knowledge is lacking in terms of reactions and pathways, it does prevent the thorough prediction of metabolic phenotypes. Recently, Zimmermann and colleagues published *gapseq* which automatically predicts metabolic pathways from genomes and reconstructs microbial metabolic models by employing a

gap-filling algorithm to predict enzyme activity within microbial communities (Zimmermann et al. 2021).

The field of GEMs as expanded into humans is relatively new. In 2007, the first manually reconstructed GEMs, RECON1, which is based on human metabolism, was published and found to describe most of the known functions that are metabolically relevant in any human cell (Duarte et al. 2007). Specifically, RECON1 comprises 1496 unique metabolic genes which code for specific metabolites spread across eight cellular compartments and 3311 reactions that are relevant for metabolism and transport (Duarte et al. 2007). A major strength of RECON1 is the identification of gene-protein-reaction rules which can be exploited to better understand pathological conditions. Specifically, by rendering a gene inactive, the resulting metabolic reaction will become blocked, this approach has been used to understand reactions which underlie hemolytic anemia (Duarte et al. 2007). Subsequently, RECON 2 includes 2191 unique metabolic genes which produce 5063 metabolites that are characterized with 7440 different reactions (Thiele et al. 2013). The most recent RECON version is RECON3D which includes 3288 metabolic genes that produce 4140 metabolites, that are catalyzed by 13543 different metabolic reactions (Brunk et al. 2018). Since the initial publication of RECON and subsequent updates, this human metabolic reconstruction has been widely employed as a starting point for creating both tissue- and cell- reconstructions (Bordbar et al. 2012 ; Fouladiha & Marashi, 2017). As the RECON models are richly curated and contain analogous metabolites, these models have also been expanded upon various other mammals, such as for mouse metabolic reconstructions (Selvarasu et al. 2010 ; Sigurdsson et al. 2010).

A popular and diverse approach for building GEMs for computational modeling in accordance with a molecular mechanistic framework that is standardized across systems biology is the constraint-based reconstruction and analysis (COBRA) approach (Heirendt et al. 2019). Specifically, this approach seeks to defines biochemical transformations and the stoichiometry or chemical properties of reactions by deriving information from various datasets such as known biochemistry, genome annotations, physiological data, and phenotypic information from next-generation sequencing experiments (Heirendt et al. 2019 ; McGarrity et al. 2020). The

process to convert a metabolic reconstruction of an organisms into a metabolic model requires transformation of a list describing biochemical reactions into a computer-readable mathematical matrix; this is further constrained by physiochemical constraints derived from thermodynamic conservation of mass and flux boundaries of the system (i.e the upper and lower limits of enzyme reaction velocities) (Fouladiha & Marashi, 2017). All of these constraints are then used for the prediction of metabolic phenotypes. Depending on the goal of the model, further constraints can be added such as nutritional uptake rates or the maximum rate of enzyme reactions to create a calculated solution space that is biologically relevant within a specific condition (Thiele et al. 2013). To specify, optimization of this goal can only be achieved under constraints. Regardless, the COBRA approach does not require complete knowledge of the previously described constraints (in addition to enzyme kinetics, metabolite or enzyme concentrations, and generation reaction rates) to reconstruct GEM that are phenotypically and physiologically relevant (Feist & Palsson, 2008 ; Oberhardt et al. 2009). Overall, assumptions that are imposed by various model reconstruction algorithms likely influences not only the quality, but also the physiological accuracy and relevancy of predictive models (Machado et al. 2014 ; Correia et al. 2015 ; Pancheco et al. 2016 ; Ferreira et al. 2017 ; Opdam et al. 2017). However, it is clear that utilizing the systems biology approach for medicine can be used to not only improve understanding the molecular mechanisms of disease, but allow for the discovery of novel therapeutic options (Mardinoglu et al. 2012 ; Thiele et al. 2020). Precision medicine as an emerging field requires the development of mechanistic models that are biologically relevant and are able to capture the complexity of human functions at a patient-specific level (Thiele et al. 2020). Specifically, the development of *in silico* human clinical trials requires the development of personalized computer models of human physiology that are biologically relevant (Viceconti et al. 2016).

1. Context-specific Metabolic Models

While GEMs are able to illustrate all metabolic reactions within an organism, not all enzymes are active within specific cells or tissues at a given timepoint as demonstrated by tissue-level proteomics studies (Uhlen et al. 2015). Therefore, there has been a wide-range of

growing methodology to extract cell, tissue, microbiome, etc. specific GEMs that are representative of the metabolic pathways of within a specific context (thus, context-specific metabolic models) (Becker & Palsson, 2008 ; Zur et al. 2010; Wang et al. 2012; Heinken et al. 2021). Specifically, in the case of MBA-like algorithms (such as FASTCORE), the algorithm reconstructs context-specific metabolic models that are specified as core reactions, this subset is extracted from the original GEMs and effectively removes reactions that are not active in the model (Jerby et al. 2010; Vlassis et al. 2014). The removal of these still remains highly debated in the field and is dependent on the algorithm employed, gene expression levels as determined by sequencing technology, availability of proteins or metabolites, integration of literature-based knowledge, and known essential functions that are necessary for the model within a biological context (Opdam et al. 2017). While these numerous liabilities may compromise the interpretability of context-specific metabolic models, it is generally understood that context-specific models do provide a more realistic view of an organism or community's metabolism within a specific situation.

The mapped genomes of various wild-type and mutant *E. coli* strains have been defined and applied to predict or engineer various metabolic capabilities through reconstruction of constraint-based genome-scale models. Modeling metabolic systems has been constantly updated since the original metabolic network reconstruction of *E. coli* in 2000 (Edwards and Palsoon, 2000; Orth et al., 2011; King et al., 2015; O'Brien et al., 2015). Genome-scale metabolic modeling can be further extended towards context-specific models with the addition of genome-wide transcriptome data to illustrate metabolic responses to various environmental stresses. By integrating both transcriptomics and metabolomics to identify conserved responses for various environmental stressors, such as oxidative stress, acid, cold, heat, and shifting glucose to lactose in media which are necessary for the maintenance of homeostasis (Józefczuk et al., 2010; Seo et al., 2015; Du et al., 2019). Application of genome-scale metabolic models that incorporate environmental stressors provides inspiration to interpret pathogenic transcriptomes which are associated with chronic infections. Another fascinating case of employing context-specific metabolic models was used to simulate the infection of human macrophages with *Mycobacterium tuberculosis.* The authors identified three states of infections

(latent, pulmonary, and meningeal) by mapping transcriptome data to known metabolic pathways; the results led to not only a stronger predictive power of the three aforementioned infection states, but also a significant improvement of drug targeting in a context-specific manner (Bordbar et al. 2010).

2. Single-Cell-specific Metabolic models

While it is possible to extract omics data that is derived from tissues or organs (i.e tissue-specific models), cell-specific models are generally reconstructed with omics data based from an isolated and defined cell-type that is not from a mixed media (Fouladiha & Marashi, 2017). The reconstruction of cell-specific models typically employs a reductive approach during reconstruction to create a model that is reflective of the active reactions within a specific cell-type. For example, this approach may include using a general GEMs such as RECON1 and then exclude inactive reactions based on cell-specific transcriptome or proteome data by using CORDA, FASTCORE, GIMME, MBA, or mCADRE (Becker & Palsson, 2008 ; Jerby et al. 2010 ; Wang et al. 2012 ; Vlassis et al. 2014 ; Schultz et al. 2016).

In order to identify biomarkers and to predict therapeutic targets, a high-quality model for hepatocytes was created by integrating a wide-range of biological metrics such as clinical, biochemical, gene expression, and functional characterization of proteins as a means to accurately represent biological function (Mardinoglu et al. 2014). This approach demonstrated that metabolic network reconstruction can be utilized to annotate various experimental data to derive more insight on not only physiological biological function, but also better determine the molecular understanding of complicated pathophysiologies such as hepatitis, cirrhosis, liver cancer, and non-alcoholic fatty liver disease (Baffy et al. 2012 ; Mardinoglu et al. 2014). Specifically, this study has illustrated that diagnosing the onset and monitoring the further progression of non-alcoholic fatty liver disease through GEM identified metabolic biomarkers is a probable approach to promote the application of systems biology tools in medicine.

Previously, Lewis et al. (2010) developed a simplified, but large-scale mechanistic approach to model metabolic interactions between various cell types in the brain by integrating both gene expression and proteomic data from various cell types to better understand brain

energy metabolism. Uniquely, the authors created *in silico* compartments that are representative of both cell types and organelles independently, both were linked together with transport reactions which are known from both literature and experimental data to create context-specific reconstructions; overall this represented a combination of cells derived from various cell types to form a brain metabolic model. This approach gave rise to a novel approach to create a tissue-specific/multicellular metabolic model which is built upon both gene expression and proteomic knowledge from various neurons and astrocytes to obtain a systems-level view of brain energy metabolism.

3. Microbiome Community Metabolic Models

The human-associated microbiome is presently a cutting-edge field of precision medicine; the advent of NGS and development of systems biology tools have rapidly driven the emergence of this field. Specifically, systems biology applications allow for the investigation of the connected relationship between the host and host-associated microbes as part of a holistic biological system (Thiele et al. 2013). Most recently, this field is closing in on the development of *in silico* clinical trials through the creation of large-scale databases and models of the human gut microbiota that are then utilized as an integrated compartment in virtual humans models (Magnúsdóttir1 et al. 2017 ; Noronha et al. 2019 ; Thiele et al. 2020). However, there remains a need to continue the utilization of human microbiome sequencing data for the metabolic reconstruction of microbiome models that are representative of the ecosystems that they occupy in hosts (Abubucker et al. 2012 ; Thiele et al. 2013 ; Heinken et al. 2021). Constraint-based *in silico* community metabolic models of microbiota provide valuable insights into the ecological interactions within a microbial consortia, thus providing valuable clues into the complex dynamics between individual organisms within communities. Systems biology applications towards microbial communities seek to identify the underlying molecular mechanisms which bolster our understanding for the organization and function within microbial communities (Zengler & Palsson, 2012). In brief, metabolic models of microbial species are constructed based on the organism's annotated genome sequence (Zimmermann et al. 2021). Enzymes which catalyze biochemical reactions are identified by selecting genes and their predicted proteins that are assigned to reactions. By connecting the individual reactions to a metabolic

network, *in silico* representations of the organism's catalytic capabilities allows for the prediction of metabolic phenotypes, for instance environmental context-dependent growth rates, nutrient utilization, and metabolic by-products release (O'Brien et al., 2015). For example, in one of the earliest *in silico* reconstruction of a microbial community, Klitgord and Segrè utilized seven previously published reconstructions of microbes with various supplementary mediums and investigated microbial interactions in a pair-wise fashion (Klitgord and Segrè, 2010). Thus, preliminary studies of this nature allow for the network reconstruction of microbial communities for the simulation of microbial species to species or community-wide interactions such as collaborative competition or cross-feeding based on various metabolic environments (Thiele et al. 2013).

Models of community metabolism are constructed by connecting species-specific models and allowing the exchange of metabolites between cells as well as the competition for shared resources. The *in silico* connection of species can be achieved by treating individual species in a spatio-temporal setting (Bauer et al. 2017) or by joining individual bacteria models and optimizing aforementioned variables under coupling constraints (Heinken et al. 2013). Cross-feeding interaction or simply, the exchange of nutrients between microbes is a metabolic process that both modulates and organizes microbial community structure (Stewart & Franklin, 2008). The rationale behind such models is that microorganisms not only adjust their metabolism in response to abiotic stresses and chemical composition of the environment, but also depend on the presence or absence of other microbial cells in their vicinity (Klitgord and Segrè, 2011). For example, *in silico* modeling of the human gastrointestinal microbiota revealed specific metabolic processes, including fermentation and metabolic cross-feeding interactions that are altered in disease when compared to healthy controls (Bauer and Thiele, 2018; Graspeuntner et al., 2018; Aden et al., 2019; Pryor et al., 2019). Specifically, when microbial communities which consist of a high diversity of unrelated species metabolically interact with one another within the human gut, there is a potential to improve human health by supplementing indigestible dietary components that can be fermented by the occupying microbial community (Wong et al. 2006).

4. Integration of Host-Microbiome Metabolic Models

The human gut-associated microbiome impacts host metabolism directly and indirectly; this has led to the development of various theories within the field of microbiome which connects microbes to host organ systems (i.e gut-brain axis, gut-liver axis, etc.) (Clarket et al. 2014). The advent of numerous systems biology tools which have been successfully integrated into automated softwares have presented powerful approaches to investigate not only microbe-microbe interactions, but also support efforts to investigate the interactions between host's and their associated microbial communities in health and disease (Bauer et al. 2017 ; Heirendt et al. 2019 ; Thiele et al. 2020;). For example, the application of constraint-based modeling of microbial communities is a progressive approach to investigate metabolic interactions between host and their associated microbiome during various stages of health and disease, thereby providing novel information for potential therapeutic targets against pathogens (Chavali et al. 2012 ; Thiele et al. 2013). Over time, these applications have led to the development of personalized whole body metabolic models (WBMs) which are the integration of physiological, metabolome, and microbiome data to assess the cross-directional effects of microbial metabolism upon host organ systems, in a person-specific manner (Thiele et al. 2020). These models represent multiple individual tissues of an organism by their respective metabolic network along with their unique metabolic connections (e.g. via the bloodstream or the lymphatic system). The most complete model of WBM that is based on GEMs integrates the metabolism from 20 organs, six sex organs, six types of blood cells, the GI tract lumen, systemic blood circulation, and the blood-brain barrier (Thiele et al. 2020).

Depending on specific questions to be answered, physiological constraints can be integrated into these models to include information such as blood flow and kidney filtration (Thiele et al. 2020). For example, the integration of WBM with classic physiologically-based pharmacokinetic (PBPK) models have been used to create novel physiologically and stoichiometrically constrained models (PSCM). The creation of PSCM allows for the combination of both physiological attributes and quantitative metabolomics inputs to constrain the rates of organ-specific metabolite uptakes that are physiologically relevant and sex-specific

(Thiele et al. 2020 ; Zhu et al. 2021). While PBPK models are useful to predict the kinetics of drugs such as ethanol, WMB has the powerful predictive potential to simulate ethanol metabolism across multiple organ and metabolic pathways (Zhu et al. 2021). The combined application towards PSCM is useful to develop a novel human relevant framework to model patient-specific metabolism of ethanol and other relevant drugs for future applications, such as for *in silico* clinical trials (Viceconti et al. 2016 ; Thiele et al. 2020 ; Zhu et al. 2021). Furthermore, these applications have also led to the recapitulation of inter-organ interactions between both the lactic acid and alanine/glucose-alanine cycles through simulations by using the WBM approach (Thiele et al. 2020). Overall, WBM models highlight a promising approach to predict the interactions between multiple organ systems and microbes within specific contexts.

However, it must be noted that approaches such as WBM cannot be possible without the development of systems biology databases such as the Virtual Metabolic Human (VMH) or the Metabolic Atlas which are all-inclusive databases which integrate the present understanding of human metabolism with five major linked resources such as: 'Human metabolism', 'Gut microbiome', 'Disease', 'Nutrition', and 'ReconMaps' (Noronha et al. 2019 ; Robinson et al. 2020). Specifically, this database allows for the metabolic reconstruction of human and our associated gut microbiome by providing 5180 unique metabolites, 17,730 unique reactions, 3695 human genes, 632,685 microbial genes, and metabolite information from 8790 food items. Most importantly, the metabolic reconstructions developed from VMH can be converted into biologically relevant computational models by utilizing transcriptomics, proteomic, or metabolomic datasets through approaches such as the COBRA Toolbox or MetaboTools (Yiyhak et al. 2014 ; Heirendt et al. 2018 ; Aurich et al. 2016). The VMH database also hosts the most complete and detailed human metabolic network model reconstruction which has been developed for more than a decade; Recon3D utilizes 13,343 metabolic reactions than is associated with 104 metabolic subsystems which can produce 4140 unique metabolites that are coded by 3288 genes (Duarte et al. 2007 ; Thiele et al. 2013 ; Swainston et al. 2016 ; Brunk et al. 2018). Furthermore, the Virtual Human Physiome project is another comprehensive database which details the human body and organ processes, but has yet to be integrated with

molecular-level or omics datasets which use gene, protein, and reaction rules to reconstruct metabolic networks (Hunter et al. 2013 ; Tan et al. 2017).

E. Study Objectives

The aim of this dissertation is to assess major human disease models through the lens of systems biology tools, specifically context-specific metabolic modeling. This dissertation will apply next-generation sequencing in tandem with systems biology approaches to highlight patient-specific differences which are helpful in understanding underlying disease mechanisms. To this end, I seek to not only develop novel systems biology and bioinformatics pipelines to study patient-specific disease processes, but also develop a theoretical framework to support the need for precision medicine in a clinical setting. The core methods in the following sections of this dissertation make use of next-generation sequencing approaches, namely scRNA-seq and metatranscriptomics. While both methods are widely used, both methods are utilized uniquely in the respective cohorts of this study to extend next-generation data with modeling approaches to derive information on patient-specific alterations in the disease. Uniquely, this study aims to expand on these two approaches by further extrapolating their standard RNA-seq analysis with systems biology tools to reconstruct context-specific metabolic models. The techniques in this dissertation can be applied in the future to develop context-specific metabolic models which could be applied to a wide-range of human metatranscriptome and scRNA-seq studies, thereby allowing for patient-specific models.

1. **Single-cell metabolic model reconstruction**. Individual metabolic network models require context. This will be done by considering not only patient-specific gene expression across disease status with scRNA-seq, but also constraining models with a developed blood medium. Patient-derived models will be assessed to characterize the role of individual cell types in relation to COVID-19 disease status and trajectory.
2. **Microbiome community model reconstruction**. The urinary tract microbiome of humans is poorly understood. By utilizing taxonomic and functional knowledge of this niche through metatranscriptomics, this approach seeks to reconstruct a model to better understand urinary tract microbiome form and function. By further integrating a virtual urine medium with context-specific microbiome community models, the activity of the community as a whole is simulated to identify disease pathomechanisms.

III. Methodology

A. (COVID-19)

1. Introduction

In the following methodology section, details are presented to investigate the current understanding of COVID-19 by analyzing the single-cell transcriptomes (358,930 cells) of patient PBMCs over five different timepoints during the course of disease. While scRNA-seq provides high-resolution information which describes cell-specific gene expression across conditions, this study sought to disseminate unique or conserved metabolic phenomena during COVID-19 pathophysiology. While this dissertation utilizes data from the manuscript of "*Longitudinal Multi-omics Analyses Identify Responses of Megakaryocytes, Erythroid Cells, and Plasmablasts as Hallmarks of Severe COVID-19*" by Bernardes et al. (2020), an extension of that study is presented as a major method for this dissertation. As a second-author in the aforementioned manuscript, my efforts sought to reconstruct metabolic models across three major patient cell-types (Erythroid cells, Megakaryocytes, and Plasmablasts) to better understand metabolic phenotypes across various pseudotimes. This was achieved by reconstructing cell-specific metabolic models by integrating scRNA-seq data with a human GEM from individual single-cells that were obtained from the cohort. However, as analyzing and interpreting only three major cell-types from patients was a limitation of this study, an additional contribution to reconstruct models for the remaining cell types. Overall, a supplementary bioinformatic analysis of the scRNA-seq datasets, reconstructions of all single-cells that were produced during this study, and analysis of cellular metabolic activity across patients and their respective pseudotimes are presented as an extension of Bernardes et al. (2020). All GEMs will be analyzed in a patient-specific manner to identify the effects of disease severity and other known phenotypes upon disease status. For further information on this publication, please refer to the attached copy of the manuscript with this dissertation, specific remarks on the contribution of each author is detailed further in the manuscript.

Citation: Bernardes, J. P., Mishra, N., Tran, F., ……. **Josephs-Spaulding, J**. et al. (2020). Longitudinal Multi-omics Analyses Identify Responses of Megakaryocytes, Erythroid Cells, and Plasmablasts as Hallmarks of Severe COVID-19. Immunity 53, 1296-1314.e9. doi:10.1016/j.immuni.2020.11.017.

2. scRNA-Seq Quality Control

The single-cell libraries utilized in this study were previously generated by Bernardes et al. (2020), more details on the library preparation, sequencing machines, and read depth are described there. Furthermore, Bernardes et al. (2020) describes the processing of sequences with CellRanger (v.3.1.0 ; 10x Genomics) to map the genome of individual samples to GRCh38 *Homo sapiens* reference, and using cell-type-specific markers to create a raw count matrix for each patient and their respective cell-types for further analysis. Seurat (version 3.1.5) was employed to remove low-quality or duplicate cells that were likely disrupted by using with either the number of features (i.e the number of reads which can map to unique genes) or by the percentage of mitochondria reads which mapped to cells (Butler et al. 2018 ; Stuart et al. 2019). The entire object was further normalized and scaled with the *LogNormalized()* and *ScaleData()* function for further analysis.

Next, principal component analysis (PCA) was employed across the Seurat object to identify similarity of features for individual cell types**.** A clustering analysis employs the standard k-nearest neighbors (KNN) graph which is based on euclidean distance in which edges of the network weights were refined between any two cells. This analysis was utilized to identify shared overlap between clusters based on Jaccard similarity coefficient. This method was based on 20 dimensions within the samples at a resolution of 0.5. This in total produced 23 clusters, these clusters were then visualized as Uniform Manifold Approximation and Projection (UMAP)**.** Additionally UMAPs were further created to assess the heterogeneity for the 23 clusters, the cell-types which were used for metabolic network model reconstruction, and for three cell-types (erythroid, megakaryocytes, and plasmablasts).

3. Identification of Highly Variable Genes & Cell Targets

As Bernardes et al. (2020) reported, severe cases of COVID-19 are associated with metabolically hyper-active cell types, especially plasmablasts. Therefore, various cell-types were investigated to further decipher the link between highly variable gene expression, cell-types, and disease status. Following quality control and standardization, the number of

individual features within the dataset were checked against the level of gene expression per cell. Through this analysis, it was found that plasmablasts have a wide range of gene expression across features and was therefore further investigated. The top 100 most variable features within the dataset were identified for later clustering. These genes were then plotted against cell-type identity to predict hyperactive cells. More so, this analysis additionally points out erythroid and megakaryocytes as potential cells of interest. Furthermore, the top 100 highly variable genes were plotted against patient pseudotimes to identify at what disease status do these genes belong to. Erythroid cells, megakaryocytes, and plasmablasts were then extracted from the Seurat object for further investigations. Specifically for each of the aforementioned cell-type, a UMAP projection was created to check cell heterogeneity and a figure which plots the average cell expression against patient pseudotime was produced.

4. Single-cell Metabolic Modeling

a. Preprocessing and Identification of Core Reactions for Metabolic Modeling

Prior to the reconstruction of single-cell metabolic models, gene expression scRNA datasets were further processed for the purpose to identify metabolic core reactions which are likely active in respective metabolic models with the StanDep algorithm (Joshi et al. 2020). The process to identify core reaction sets for individual cells was initiated in various steps. First, normalized gene-level counts were extracted from the previously described Seurat object and converted into transcripts per kilobase million (TPM) values. These values were then normalized in accordance to human ENSEMBL gene lengths, whereis these ENSEMBL gene names were further mapped to RECON 2.2 to identify human genes which are relevant for metabolism (Swainston et al. 2016 ; Cunningham et al. 2019). Gene-level counts mapped to RECON 2.2 for individual single-cells were extracted from the Seurat object as an output, in addition to respective meta-data (i.e conditions), gene names, and cell barcodes. These four sets of data were then used with the StanDep approach to identify cell-specific core reactions which are relevant for metabolism.

Standep was employed within the COBRA Toolbox (v.3.0) by using pre-processed gene expression data and various patient conditions to identify core reaction genes across cell types, specifically the algorithm identified enzyme type and the level which that was expressed with respect to RECON 2.2 (Heirendt et al. 2019 ; Joshi et al. 2020). In order to identify the number of k-clusters to be used in the StanDep algorithm, a representative sample size was calculated. The entire population of single-cells was utilized (n= 358930). The margin of error was set to 1% with a confidence level of 95%. Enzyme expression was then log10 transformed into a binary matrix with rows representing enzymes and columns as bins, to identify both minimum and maximum enzyme expression. Core reaction matrices were assembled, defined, and used as an input in FastCore (Vlassis et al. 2014) to reconstruct single-cell, context-specific metabolic models which would be further used for a metabolic pathway analysis.

b. Reconstruction of Cell-specific Metabolic Models

Context-specific metabolic models were constructed based on metabolic network models from human metabolic network Recon 2.2. These models were further extended with gene expression data derived from patients during various timepoints across during COVID-19 infections. All models were further conditioned with a human blood medium with metabolic information derived from the human metabolome database. First, the CobraPy package was employed to further process and constrain the core reactions for each cell that were produced from StanDep (Ebrahim et al. 2013 ; Joshi et al. 2020). Specifically, core reaction tables were further constrained with a predefined human blood medium to identify metabolic core reactions which are likely active than those that are not while interacting with the blood medium. Next, the function *fastcc* from the FASTCORE suite was used to identify inconsistent reactions within the model and remove them to create a consistent model. With the consistent models, FASTCORE was used on individual core reactions derived from cells to reconstruct context-specific metabolic network models.

c. Patient-Specific Metabolic Subsystem Analysis

Subsystems reactions were extracted for all models by matching the names of all metabolic subsystems across the reconstructed models to define pathway abundance during COVID-19 infection within individual patients and their respective cell-specific expression, at various pseudotimes or state of disease. Subsystems or the grouping of pathways which are associated with biological processes were selected for analysis in this study. Due to the nature of FASTCORE to reconstruct a core metabolic network which includes reactions that are connected to core metabolites, these pathways are clearly represented and describe the core reduced metabolic model (Vlassis et al. 2014 ; Masid et al. 2020). Subsystems are typically recommended to analyze GEMs because due to their large size and complexity, assessing individual reactions can become both functionally challenging and time-consuming to analyze. Thus, the abundance of various metabolic subsystems were extracted from each individual cell-specific GEMs and grouped by patient and their respective pseudotimes.

Cell-specific models were reconstructed for all patients during various pseudotimes, information with regards to the average metabolic subsystem abundance for each patient during conditions was assessed. Metabolic subsystems were then counted for all reconstructed cell models and the total number was matched to specific subsystems names. Both the overall metabolic subsystem activity for each patient was averaged across the total number of cell models of that patient for each pseudotimes to correspond with the average cell pathway abundance. Specifically, only the four patients who were assessed with four pseudotimes are included in the following section to readily compare the change of cell-specific metabolic activity across pseudotimes. Only erythroid, megakaryocytes, and plasmablasts were included in the presented investigation as these cells were identified as cells of interest in the preliminary bioinformatics assessments. All cell-specific pathway activity derived from the metabolic models from all patients can be found in the supplementary data section (Supplementary Figures 1-33).

B. Urinary Tract Infection (UTI)

1. Introduction

In the following section, metatranscriptomics sequencing was employed on the urine of five patients to reconstruct patient-specific microbial community models for each patient. This manuscript is in preparation "Patient-specific Metabolic Reconstruction of Microbial Community Models of UTIs identifies Biomarkers of Infection Onset and Recurrence" by Josephs-Spaulding et al. UTIs are one of the most common human infections which are typically diagnosed by a positive culture of a uropathogenic bacteria from the urine and supplemented with clinical markers of inflammation from the urinary tract; *E.coli* are identified in 80% of UTIs (Flores-Mireles et al., 2015). However, the bladder is constantly challenged by adverse environmental stimuli which influence urinary tract physiology, contributing to a dysbiotic environment (Josephs-Spaulding et al. 2021). Simultaneously, pathogens are primed by environmental stressors such as antibiotics, favoring rUTIs, resulting in chronic illness. Due to different confounders for UTI onset, a greater understanding of the fundamental patient-specific environmental mechanisms and microbial ecology of the human urinary tract is required. Such advancements could promote the tandem translation of bench and computational studies for precision treatments and clinical management of UTIs. Therefore, there is an urgent need to understand the ecological interactions of the human urogenital microbial communities which influence recurrence in UTIs. My contribution to this manuscript included conceptualizing the manuscript idea, writing the manuscript, preparing all tables/figures, and acting as the corresponding author during the submission of the publication. For further information on this publication, please refer to the attached citation of the manuscript, specific remarks on the contribution of each author is detailed further in the manuscript.

Citation: **Josephs-Spaulding J**, Rettig HC, Chkonia M, Marinos G, Zimmermann J, Graspeuntner S, Rupp J, Møller-Jensen J and Kaleta C (*In-Preparation*) Patient-specific Metabolic Reconstruction of Microbial Community Models of UTIs identifies Biomarkers of Infection Onset and Recurrence

2. Research Design

For this purpose, a large number of clinical samples from patients with urinary tract infections were characterized in detail through functional and molecular analysis such as culturing and metatranscriptomics to describe microbiome function. A novel bioinformatics pipeline was developed that utilizes metatranscriptomics to reconstruct metabolic models which are reflective of context-specific microbiomes during a UTI. Patient-specific models consisting of host-associated microbial pathogens were simulated in the software BacArena and further constrained with a developed urine medium with information derived from the Human Urine Metabolome database (Bouatra et al. 2013 ; Bauer et al. 2017). This was essential to determine not only the impact of gene expression upon patient-specific microbiomes, but also to understand how an *in silico* urine metabolome further interacts with the urine microbiome.

The main goal of this project is to develop a novel approach to predict various metabolic phenotypes in clinical isolates which are suggestive of virulence and recurrence. This assessment will be acquired by applying first metatranscriptomics to identify both invasive pathogens which cause UTIs and their gene expression during infection. Once gene expression is mapped back to all known species, this information will be extended with context-specific metabolic modeling to reconstruct metabolic network models of patient-specific community microbial models. Furthermore, these patient-specific models will be simulated in BacArena and further constrained with a generic developed urine medium. This approach would be beneficial to optimize treatment strategies in a strain- and patient-specific way. Thus, based on the metabolic information extracted from our simulations which can suggest whether a UTI is causing an infection by specific metabolite uptake or production, different modes of action for curing the infection and follow-up treatment may be suggested through dietary supplementation. However a major limitation still persists in the aforementioned approach: while phenotypes can be strain specific, it is also possible that they are strongly influenced by patient-specific factors (e.g. diet, comorbidities) in addition to micro-environmental factors (e.g. local microbiome, pH, nutrient availability) which will be challenging to model in this study. However, a future

prospect of this approach would be to acquire dietary information from the respective patients and use the metabolic information from foods in their diets to further constrain the simulations.

3. Population and Sample

All patients in this study were selected from a group of patients with an acute, uncomplicated UTI. The inclusion group that will be investigated in this study is prospective with the occurrence of described symptoms of an uncomplicated UTI (see inclusion criteria) and ends formally on day 3 after taking a second sample. All participants of the study provided a sample of midstream urine on days 1 and 3, in additon to both urethral and peri-anal smears. Furthermore, a scoring was used to assess the severity of acute cystitis. These results were used to interpret pathogen-related factors which could be later used in the prediction of UTI presence and to better define risk factors for rUTIs.

a) Inclusion criteria for the patient group:

This study selected patients from UKSH Lübeck over the course of three years (2018 - 2021) with who were > 60 and <80 years of age. To determine eligibility for this study on uncomplicated UTIs, various clinical signs of a lower or upper urinary tract infection were assessed such as: pain when urinating (alguria), imperative urgency, pollakiuria, pain above the symphysis, flank or kidney pain, and / or fever (> 38 degrees C). We further assessed the patients who had potential rUTIs. There patients were included within the rUTI cohort if they had > 3 UTIs within 12 months and > 2 urinary tract infections within six months in addition to leukocyturia and the detection of a UPEC.

b) Exclusion criteria for the patient group:

Patients were excluded from the study if they were assessed to have physical malformation or comorbidities which could be classified as a complicated UTI which include: anatomical urogenital malformations such as a urethral stricture and bladder stones or tumors, a known previous surgery at the site of the urinary tract, and patients with any neurological or other type of underlying diseases that could lead to a disturbed bladder emptying. We further excluded patients with any known previous irradiation of the small pelvis, cytostatic treatment

during the study period or within the last year, presence of immunosuppression, type 1 or 2 diabetes mellitus, the status of being pregnant status, the presence of recent use of vaginal probiotic therapies or the use of vaginal spermicides, asymptomatic bacteriuria, and finally known participation in clinical studies which could influence urinary or renal function for 30 days before or during the study.

c) Inclusion criteria for the control group:

Inclusion into the control group was similar to the patient group, except for the presence of a rUTI. Specifically, women younger than 18 years of age with an uncomplicated UTI. To determine eligibility for this study on uncomplicated UTIs, various clinical signs of a lower or upper urinary tract infection were assessed such as: pain when urinating (alguria), imperative urgency, pollakiuria, pain above the symphysis, flank or kidney pain, and / or fever (> 38 degrees C). We further assessed the patients who had potential recurrent urinary tract infections. There patients were included within the rUTI cohort if they had > 3 UTIs within 12 months and > 2 urinary tract infections within six months in addition to leukocyturia and the detection of a uropathogenic UPEC. The outage charters meet the exclusion criteria for the patient group.

4. Data Collection

a) Patient group (with evidence *E.coli* associated UTI)

Patients who were identified to develop an acute, uncomplicated UTI with cultured evidence of uropathogenic *E. coli* at UKSH Lübeck and who meet the inclusion criteria were offered to participate in the study. The urine already collected is processed according to the procedure described below, otherwise the procedure is the protocol for the control group.

b) Control Group

All female medical students were invited to participate in this study after completion of their fifth or sixth semester of studies and provided info-materials on the study. Specifically, these materials described the goals of the study and sample vessels for the acquisition of midstream urine were provided, free of charge. Furthermore, with the info-material was also

provided a telephone number so potential probands can report clinical symptoms, receive further information on the study, and ask further details about preparing the urine sample. Finally, two sets of smears were provided in the kit for obtaining both urethral and peri-anal smears that were issued with instructions for self-examination.

5. Library Prep and Sequencing

Total RNA was then extracted by use of the both the MICROBEnrich and MICROBExpress mRNA enrichment kits to reduce the presence of any human contamination of the samples and isolate only bacterial RNA. The samples were then shipped and further processed by the CCGA at the Christian-Albrecht University, Kiel. Here, the total RNA was further purified with the TruSeq stranded total RNA kit and sequenced with shotgun metatranscriptomics to characterize the local microbiome and respective functions. All libraries for metatranscriptomic sequencing of the urine microbiome were conducted at the CCGA. In total, 5 samples of total RNA (without human contamination) were sequenced on an Illumina MiSeq with 2x75bp with paired-end reads.

6. Raw Read Quality Control

In a standard quality control pipeline raw reads were initially processed by using FASTQC to report sequence quality to identify low quality reads which require removal (Andrews, 2010). From there, raw reads were processed for quality trimming by using *prinseq-lite* with a variety of settings detailed in Table 4. Next *CutAdapt* was to further remove any adapters or repetitive sequences based on previously known i7 & i5 indexes as detailed in Table 3 (Martin, 2011). FASTQC was used again to compare the before and after process from the quality control step.

Name	Barcode	i7-index	i5index
H25361-L1	L122834	GTTAATTG	CGAGATAT
H25362-L1	L122835	CTACAGTT	ACGCCGCA
H25363-L1	L122836	GTGCGATA	CTTAGTGT
H25364-L1	L122837	ACCGGCCA	TAGAGCGC
H25365-L1	L122838	TCGTGACC	GTATTATG

Table 3: Sample names, barcodes, and adaptor sequences used in this study.

Filter/Trim Options	Value	Description
min_len	3	Filters sequence shorter than minimum length
ns_max_n	5	Filters sequence with more than the maximum number of N's
min_qual_mean	10	Filters sequences with a quality score below minimum quality mean threshold
trim_qual_left	10	Trim sequence by quality score from the 5'-end at defined threshold
trim_qual_right	10	Trim sequence by quality score from the 3'-end at defined threshold
trim_tail_left	10	Trim poly A/T tail with a minimum length at the 5' end
trim_tail_right	10	Trim poly A/T tail with a minimum length at the 3' end

Table 4: Metrics used for preprocessing raw metatranscriptome reads

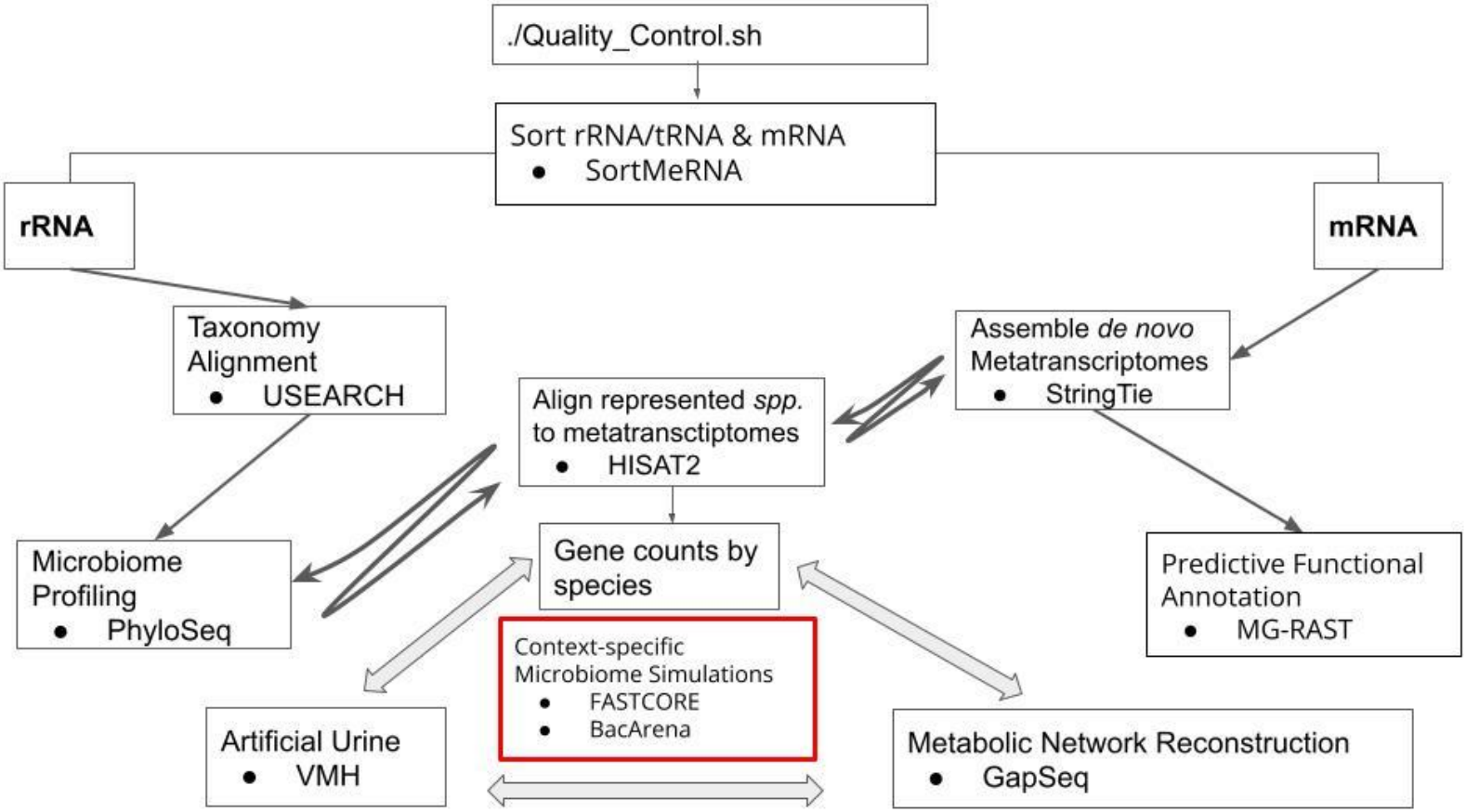

Figure 8: Overview of context-specific microbiome community model reconstruction pipeline.

7. Mapping and Sorting mRNA/rRNA

The sorting and mapping of preprocessed metatranscriptome reads were completed by utilizing the software *SortMeRNA* (Kopylova et al. 2012). First, forward and reverse reads were combined into pair-end reads with the *SortMeRNA* script *merge-paired-reads.sh* for filtering the samples with various RNA databases. A variety of RNA index database, based on FASTAs from SILVA rRNA database (Yilmaz et al. 2014) and Rfam (Griffiths-Jones et al. 2003) were employed to create indexes for sorting patient-derived total RNA using the *'indexdb_rna'* function in SortMeRNA. Next, individual pair-end libraries were merged using the SortMeRNA script 'merge-paired-reads.sh'. From there, the merged paired ends were mapped to seven different RNA indexes to assess mapping rates for each microbial dataset. As the aim of this study is to investigate only prokaryotic communities within the urine in the BacArena simulation software, only bacterial rRNA & mRNA was extracted. Therefore, following databases were used: Silva-Bac16s, Silva-Bac23s, Silva-Arc16s, Euk18s, Euk28s, rfam-5s, and rfam-5.8s. To specify, mapping to the Silva databases allowed for the extraction of both rRNA and tRNA, only Bacteria 16s rRNA was relevant for the later presented taxonomy analysis.

8. rRNA Taxonomy Analysis

Following the split from SortMeRNA, remaining rRNA was used in preparation for a taxonomy analysis. The *USEARCH* tool and it's suite of algorithms was used for the rRNA sequence analysis and clustering (Edgar, 2010). Pair-end reads were remerged and converted into *fasta* files for smaller computational size. All samples were then concatenated into a master file which includes the rRNA sequences from all patients that were investigated in this study. Next, the *USEARCH* function *fastx_uniques* was used to independently identify common sequences across all samples that would be used for clustering operational taxonomic units (OTUs). Specifically this algorithm finds all unique sequences, thereby dereplicating the samples with any redundant sequences. Then the command *cluster_otus* was used to expand the present list of identified OTUs by further denoising samples and by performing a 97% OTU clustering, however these OTUs will be further processed. Next, all OTUs and remaining amplicons were then subject to error correction and all chimeras were removed with the *unoise3*

command to produce zero-radius OTUs (zOTUs). OTUs were formed into a table with the *otutab* command. And finally, all potential taxonomy was predicted with the *sintax* command in which the bootstrap values for confidence in the taxonomy was set to 97%. To better understand the amount of unique species or OTUs found within each sample, a rarefaction curve was plotted as a function against the total number of reads per sample.

Next the CRAN package PHYLOSEQ with it's dependencies was used to determine the taxonomy and abundance of each patient-specific community (McMurdie et al. 2013). First, after a matrix containing OTU abundance and taxonomic information was formed into *PhylosSeq* objects, the data was normalized by the number of reads and low abundance was removed. To visualize this data, non-metric multidimensional scaling (NMDS) was utilized across the five main taxa within the population to visualize similarities. This approach was selected to demonstrate the clustering of OTUs or counts of abundance in terms of potential microbial communities.

Next, alpha diversity was calculated to investigate the appropriate community abundance and microbial species diversity for the simulation of the reconstructed metabolic community model through the *PhyloSeq* command '*estimate_richness*'; specifically both the diversity measures Chao1 and Shannon diversity index were used. First Chao1 was investigated across all species to interpret the general abundance or the number of organisms that are representative in that sample within a poisson distribution and corrected for sample-specific variance**.** Shannon diversity index was then calculated to measure the number of species across abundance. Next, the Shannon index was utilized to calculate the Effective Number of Species (ENS) as a means to attempt to transform and more effectively translate these indices into a true measure of diversity (Jost, 2006 ; Jost, 2007). This calculation was then used to decide for the number of individual species to add into the metabolic models. Furthermore, abundance distribution was further studied at various taxonomic levels. Specifically, the genus level diversity of the samples were assessed to identify potentially dominant groups. *Enterobacter* was further investigated due to *Escherchia coli* being identified as the dominant inciting species in patients with UTIs (Flores-Mireles et al., 2015). Based on the results acquired from the alpha diversity analysis, a filtered count matrix was formed with the top 10 species based on

abundance. From there, this list of species was cross-checked with the USEARCH taxonomy bootstrapped confidence interval of 97% to select the dominant species to utilize for metabolic modeling. Whole-Genome Sequences (WGS) of the most abundant species with respect to the patient were acquired from NCBI to be further employed in the mRNA analysis and for creating *gapseq* genome-scale metabolic models (Zimmermann et al. 2021).

9. Functional mRNA analysis

Following the split from SortMeRNA, remaining mRNA was used in the following analysis. First, mRNA was uploaded to the open-source web application Metagenomic Rapid Annotations using Subsystem Technology (MG-RAST) (Glass et al. 2010) for a functional analysis. Specifically, predicted protein function was assessed by mapping mRNA to a wide-range of functional databases for microorganisms. Finally, annotation of the mRNA to both the Kyoto Encyclopedia of Genes and Genomes (KEGG) and RAST metabolic subsystems (Kanehisa et al. 2000 ; Aziz et al. 2008) annotation was employed. mRNA mapping, alignment, and counting was conducted in *HISAT2* (Kim et al. 2019), *SamTools* (Li et al. 2009), and *HtSeq* (Anders et al. 2015) respectively. First, genomes from all identified species from the previously described taxonomy analysis were downloaded from NCBI and used to build a genome index with HISAT2. Next, remaining mRNA reads were aligned to respective indexes which were identified in each patient-specific sample. SamTools was then employed to convert aligned reads to SAM files for filtering, sorting, and removing single-end reads from the samples. Prepared samples were then converted into BAM files, sorted by gene position, and finally used to acquire all pair-end reads which were mapped to the species. *Stringtie* was then used with respective species level gene annotations to form a species-specific *de novo* transcriptome for later mapping purposes (Pertea et al. 2015). Finally, all patient-specific counts of relevant species were mapped to this *de novo* transcriptome and counted with *Htseq* to obtain species gene-level counts which were relevant to patients.

10. Microbiome Community Metabolic Modeling

A) Selection of Microbial Community

Following assessment of the taxonomy data, species which were used to form the microbial community model were selected. Specifically, taking information from the Shannon index that was derived from the alpha diversity analysis, the effective number of species was calculated (Jost, 2006 ; Jost, 2007). Calculating the effective number of species or ENS is essential due to the fact that alpha and beta diversities are identified directly from the frequencies of both species and their quantity within a community, but do not take into account true or effective diversity within an ecosystem. This information suggested that three unique species on average were dominant in the patients and this information was therefore used to decide the inclusion of three species in the simulations. From there, any species with a high confidence interval of at least 90% were initially selected. Next, based on the results from the effective number of species analysis, which observed species abundance as the lowest being 2.66 and up to 3.52, the three of the most abundant species with the highest confidence interval were selected.

B) Creation of Artificial Urine

To further constrain all context-specific models of microbial communities, a urine metabolic medium was developed based on The Urine Metabolome (Bouatra et al. 2013). Specifically this study employed NMR, GC-MS, DFI/LC-MS/MS, ICP-MS, and HPLC on numerous healthy human urine samples, thereby identifying 445 metabolites and providing quantitative readings for 378 urine metabolites or species. This is the largest attempt to accumulate known metabolites found within pooled samples, thereby creating a consensus database for this study. All metabolites were verified and converted into microbial exchange reactions to match additional data points from the VMH database. Next the observed concentrations of each metabolite from The Urine Metabolome were calculated into millimolar. A completed database with VMH compatible urine metabolites and respective concentrations was then utilized for gap filling or adding the minimum number of essential metabolites required for microbial growth. This step was employed in *gapseq* and later in BacArena to

further constrain the presented microbial community models. However, it is understood that the metabolic composition of human urine directly affects the composition and function of urine-associated microbiota (Josephs-Spaulding et al. 2021).

C) Gapseq

The *gapseq* software was used to automatically reconstruct GEMs of three bacterial species (*Escherichia coli, Shigella flexneri,* and *Salmonella dysenteriae*) and further constrain those models with the aforementioned developed urine medium (Zimmermann et al. 2021). Specifically this approach was utilized to predict metabolic pathways based on WGS, thereby reconstructing GEMs based on known reactions in addition to gap-filling with a defined medium (i.e urine medium). After identifying all relevant patient-specific microbiota from the taxonomy analysis, genomes from each bacteria were acquired from NCBI. Next, the commands *find -p all* and *find-transport* were used to identify all metabolic reactions, transport reactions, and metabolic pathways associated with the obtained bacteria WGS. A draft metabolic model of the bacteria was then reconstructed by using the following described information. This draft metabolic model was then additionally curated with the metabolic fluxes obtained from the developed *in silico* urine medium based on the aforementioned metabolome data to create a refined metabolic model.

D) Preprocess Context-specific Metabolic Models

Matching and preprocessing of species-specific mRNA to match with *gapseq* metabolic models were obtained with a custom in-house script. First, the start and end of chromosome position in addition to gene count levels of expression was extracted from the species files to create a count matrix. Next, gene lengths were calculated, normalized by both sample sequencing depth and gene length, then finally transformed into TPM. The R package *sybil* was used to read and extract both metabolic reaction attributes and chromosome start and stop position from the metabolic models. After obtaining chromosome position and gene-level expression, pattern matching was employed to concat and merge relevant counts with matched chromosome position.

Gapseq models that were previously created were then imported into CobraPy (Ebrahim et al. 2013) and transformed into MATLAB compatible files which are representative of species WGS. The new files were then loaded into MATLAB in addition to patient-derived gene expression which matches the employed *gapseq* model. The COBRA Toolbox version 3.3 in MATLAB (Heirendt et al. 2019) was then employed for mapping gene expression to metabolic reactions with the command *'mapExpressionToReactions'*. This output was defined as the reaction activity of all included pathways within the model, that is associated with gene expression. Furthermore, the reaction activity was further pre-processed as suggested by Richelle et al. (2019) to identify the core set of reactions found within the models. Specifically, 25% of reactions with the highest levels of expression were further selected to define the core reactions.

E) Reconstruction of Microbiome-specific Metabolic Models

Context-specific metabolic models were reconstructed by first extending GEMs of UTI bacteria species as created by, models were constrained with UTI microbial-specific gene expression and then further conditioned with the aforementioned urine medium. Prior to model reconstruction and simulation, a consistent model with the potential to allow for all metabolic reactions to carry a flux must be created. Specifically, inconsistent reactions within the model were identified and removed by utilizing the function *fastcc,* from the FASTCORE suite. Then with the consistent models, FASTCORE was employed on the previously defined core reactions that were selected from the top 25% of all patient-derived microbiota reactions to finally reconstruct context-specific metabolic network models. These context-specific models were saved as MATLAB files and then loaded into BacArena to conduct patient-specific community analysis of microbially communities.

F) BacArena

Patient-specific community models were created with standard genome-derived *gapseq* models in addition to *gapseq* models that are constrained with gene expression to compare the metabolic effects of context-specific modeling approaches. GEMs of the representative species either as metabolic models without a context (obtained directly from GapSeq) or

context-specific (constrained with bacteria-specific gene expression) were converted into an R compatible format and added into BacArena with artificial urine to simulate individual patient-specific microbial communities. A 100 by 100 arena was created and added with patient-specific representative microbiota, in addition to the *in silico* urine medium to further constrain the environment. The total arena was set with a high diffusion rate, allowing for the simulated environment to mix both substrates and organisms randomly. Specifically, bacteria are allowed to move to random positions within the arena and metabolic substances are allowed to have a uniform value respective to their concentration. The entire community was allowed to grow and simulate for a total of 5 iterations or hours to maximize bacterial growth. As suggested by the ENS analysis, an average of three different species were added to the respective communities, the predicted species with the highest abundance and confidence interval were added into simulations. Specifically, Table 5 describes the species relative abundance from the rRNA analysis and the value scaled by a factor for 1000 which were then added into the microbial community simulations. Values of the added microbiota to seed the community were rounded up or down. With microbiota and a urine medium added into the arena, the entire community was simulated over ten hours to study growth, metabolic production/consumption, and cross-feeding within the microbial community.

Sample	Species	Relative Abundance	Simulation Abundance	Final Abundance	
				Non-context	Context-specific
H25361	*Escherichia coli*	80623	80	167	179
	Shigella *flexneri*	77628	80	169	161
	Salmonella dysenteriae	76523	80	158	172
H25362	*Escherichia coli*	132446	130	275	274
	Shigella flexneri	18567	20	47	45
	Salmonella dysenteriae	15387	20	39	36
H25364	*Escherichia coli*	28375	30	55	65
	Shigella flexneri	24573	20	43	37
	Salmonella dysenteriae	22392	20	37	47
H25365	Escherichia coli	7398	10	20	16
	Shigella flexneri	18024	20	41	34
	Salmonella dysenteriae	17692	20	44	43

Table 5: **Species-specific relative abundance and simulation start/end abundance across studied samples.**

Chapter IV: Results, Discussion, and Interpretation

A. COVID-19

1. scRNA-seq Preprocessing

Specifically, the selected threshold for pre-processing the raw reads of the scRNA count matrix datasets for quality control for the number of features which mapped to genes (> 200 & < 5000) and percentage of mitochondrial (< 25%) reads was standardized across all datasets. This preprocessing produced 358,930 cells which contained the expression of 22574 human genes. Clustering analysis and utilization of KNN graphs based on the euclidean distance identified 23 unique clusters that are displayed in a UMAP graph in Figure 9. An additional UMAP was created only for cell-types that were distinguishable by FACS and will be used for metabolic model reconstruction (Figure 10). UMAP analysis with a KNN graph was employed within a PCA space to identify shared overlap across cell types and unique features. Overall, individual cell-types appear to be heterogeneous due to patient bias and various pseudo times. However, it is likely that there are more unique cell type clusters than those initially used for metabolic model reconstruction.

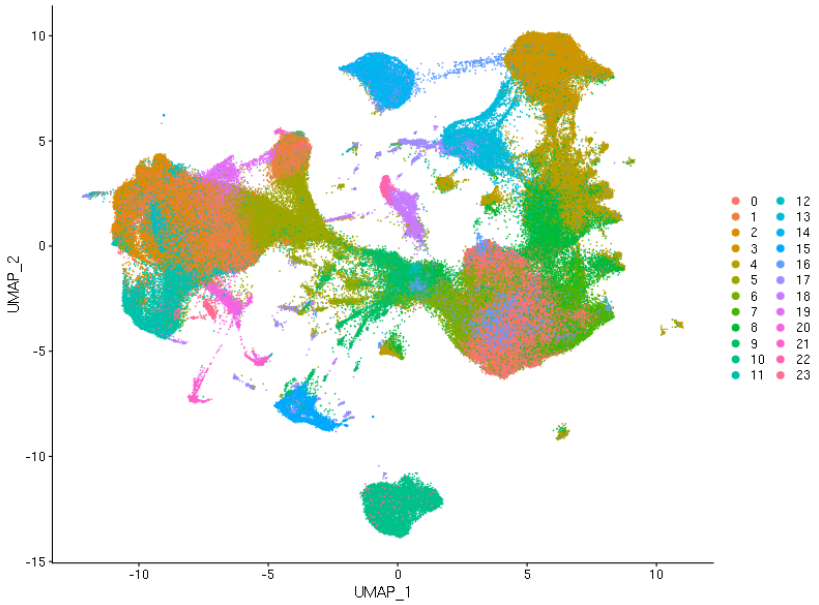

Figure 9: UMAP of unique cell clusters based on KNN.

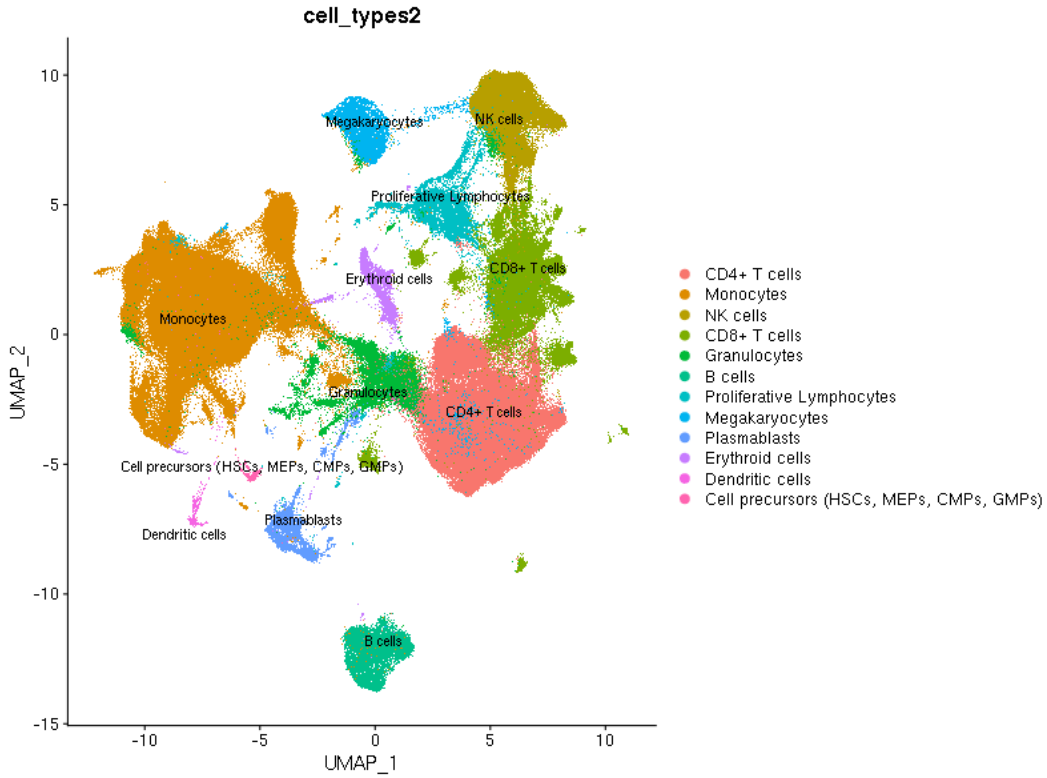

Figure 10: UMAP of 12 cell-types identified by FACS.

2. Identification of Highly Variable Genes

Following quality control and standardization, the number of individual features within the dataset were checked against the level of gene expression per cell (Figure 11)**.** When plotting the number of features within the RNA compartment against the gene expression counts across cell-types, plasmablasts are highlighted as the cell-type with a high quantity of highly-expressed cells However, such observations may be expected due to the fact that plasmablasts tend to secrete high amounts of antibodies. Furthermore, the top 100 most variable features within the dataset were investigated and clustered (Figure 12). The results from the presented clustering of the top genes highlight the presence of numerous immunoglobulin heavy chain variable region (IGHV) genes. Specifically these genes are essential in various immune cells for class switching within the early stages of viral infection. Notably, class switching in IGHV genes which provoke B-cells to switch from IgG to IgA subclasses appears to be shared as a human response to both SARS-CoV-2 and SARS-CoV (Nielsen et al. 2020). More so, modulation of IGHV gene expression in various immune cells, such as B-cells is potentially disease specific. For example, IGHV1-69 tends to be increased in response to exposure of antigens from various influenza virus (Avnir et al. 2016) while COVID-19 may upregulated IGHV1-24, IGHV3-13, and IGHV3-20 (Nielsen et al. 2020). The top 100 gene features were then plotted against cell-type identity to assess which cells contained hyper- or hypo-activated cells (Figure 13). This grouping identified that the top 100 most highly variable cells belonged to Plasmablasts and Erythroid cells. The hyperactivation of plasmablasts is not surprising, this has become a classic example to characterize severe COVID-19, in addition to the loss of memory B-cell abundance (De Biasi et al. 2020). When assessing the group of the top 100 cells against patient pseudotime, average expression of the top genes was shown (Figure 14**).** Patients who are deemed healthy, recovered, or recovery/asymptomatic had a low expression of disease. However, patients at any other course of disease and within the pseudotimes mild (recovering), complicated (recovering, incremental, or hyperinflammatory syndrome) in addition to critical were found to have a high level of gene expression of their highly variable cells expressed.

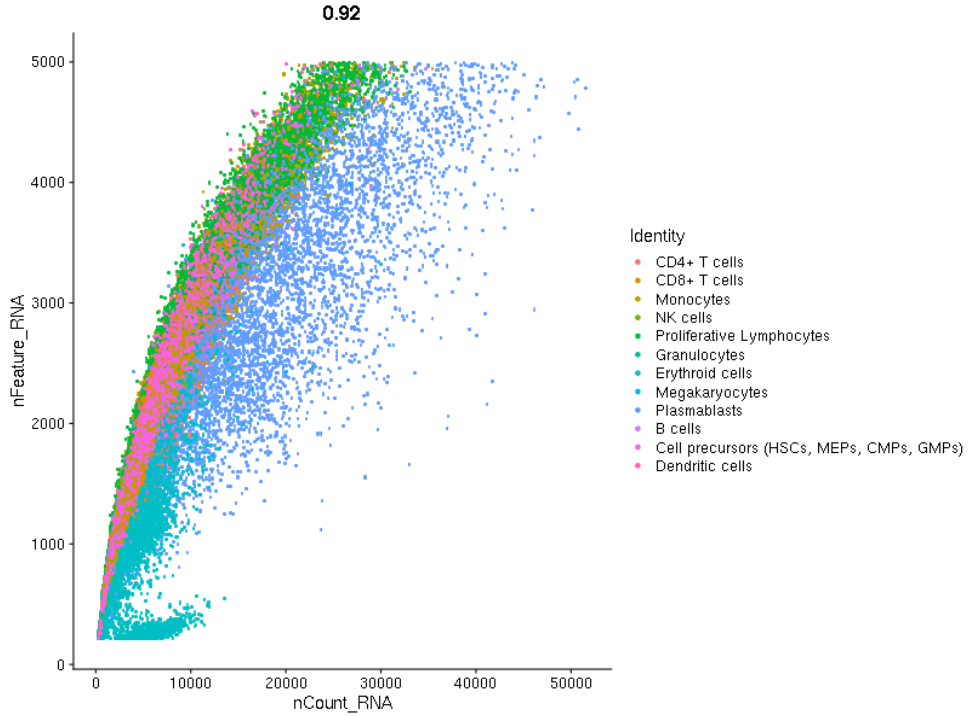

Figure 11: Cell-type gene expression abundance plotted against number of gene features.

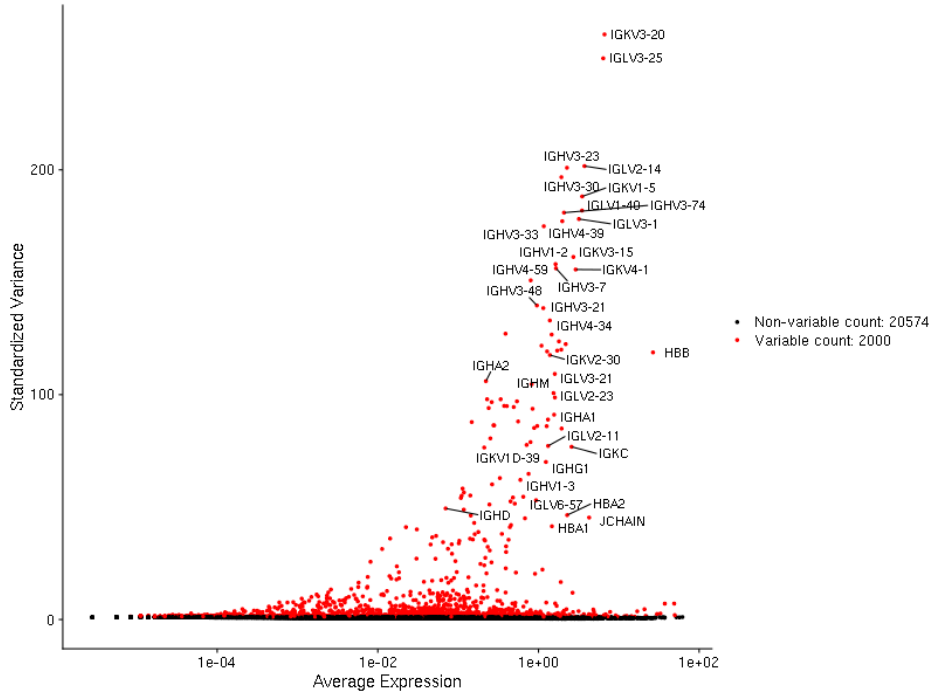

Figure 12: Top 100 highly variable genes in COVID-19 dataset.

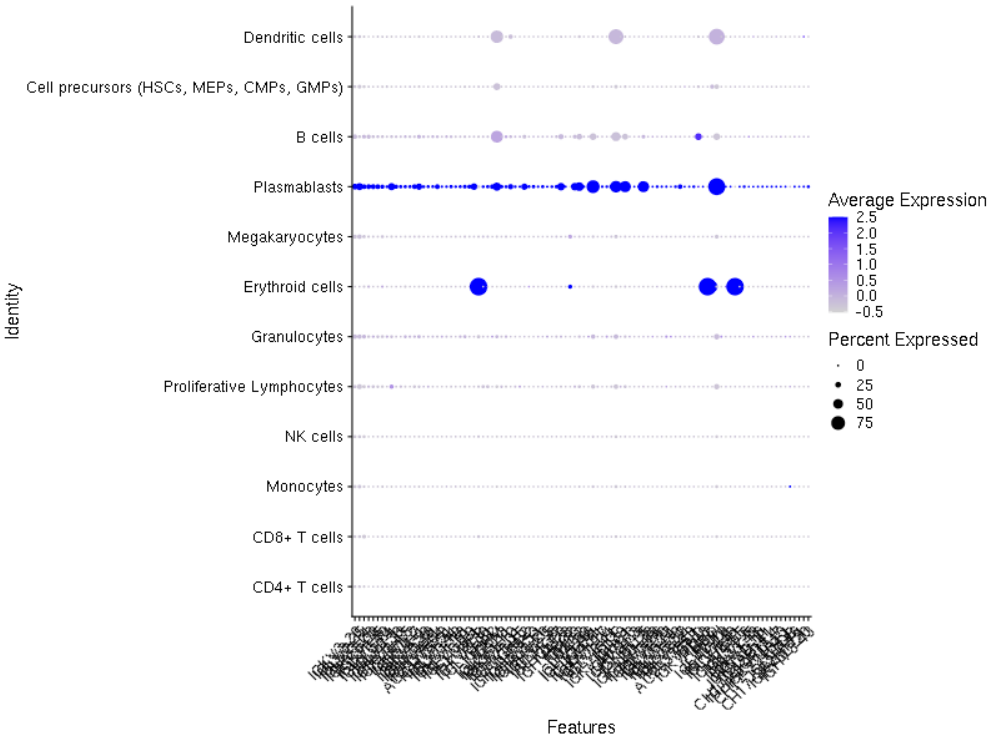

Figure 13: Top 100 genes in the COVID-19 dataset plotted against cell-type.

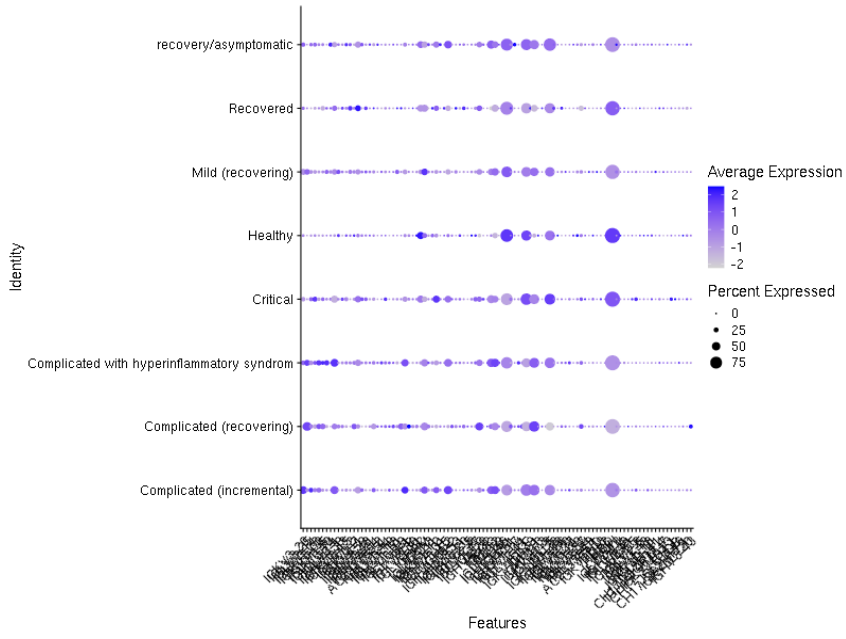

Figure 14: Top 100 genes in the COVID-19 dataset plotted against psuedotimes. The top 100 highly variable genes were plotted against patient pseudotimes

3. Cell-specific gene expression and heterogeneity

By assessing a UMAP projection of the distribution of erythroid cells, plasmablasts, and megakaryocytes, cell heterogeneity was investigated by creating cell-specific UMAP projections and plotting the average gene expression of various genes across patient disease states (Figure 15). Erythroid cells had one significant cluster and several outlier cells. This difference was highlighted when plotting individual gene features against the average gene expression. Specifically, erythroid cells appeared to have a conserved average gene expression across most disease status. However there were some exceptions with unique gene expression markers in patients that were either in a recovery/asymptomatic state or in a complicated (incremental) state. With regards to megakaryocytes, the UMAP projection highlights one major cluster and several smaller clusters which may describe hyperactivity during severe disease status. When mapping the average gene expression of various features across disease status for megakaryocytes, most patient disease status had unique signatures with the exceptions of those that are healthy, recovered from illness, or are in a recovery/asymptomatic state. Specifically, those with a complicated disease status in any of the 3 pseudotimes which describe this status, all demonstrated a unique signature of highly active cell expression. Finally, with regards to plasmablasts the UMAP projection showed two major clusters with two smaller clusters. Most interestingly, plasmablasts cells had one of the most heterogeneous UMAP projections and contained cells within a wide-range of dimensions. When plotting the average gene expression from plasmablast cells across disease status, it appears that all classes of disease have a similar conserved average gene expression. However, when noting those with critical or any of the three complicated status, there is an outlier of several genes which are likely highly expressed during severe disease.

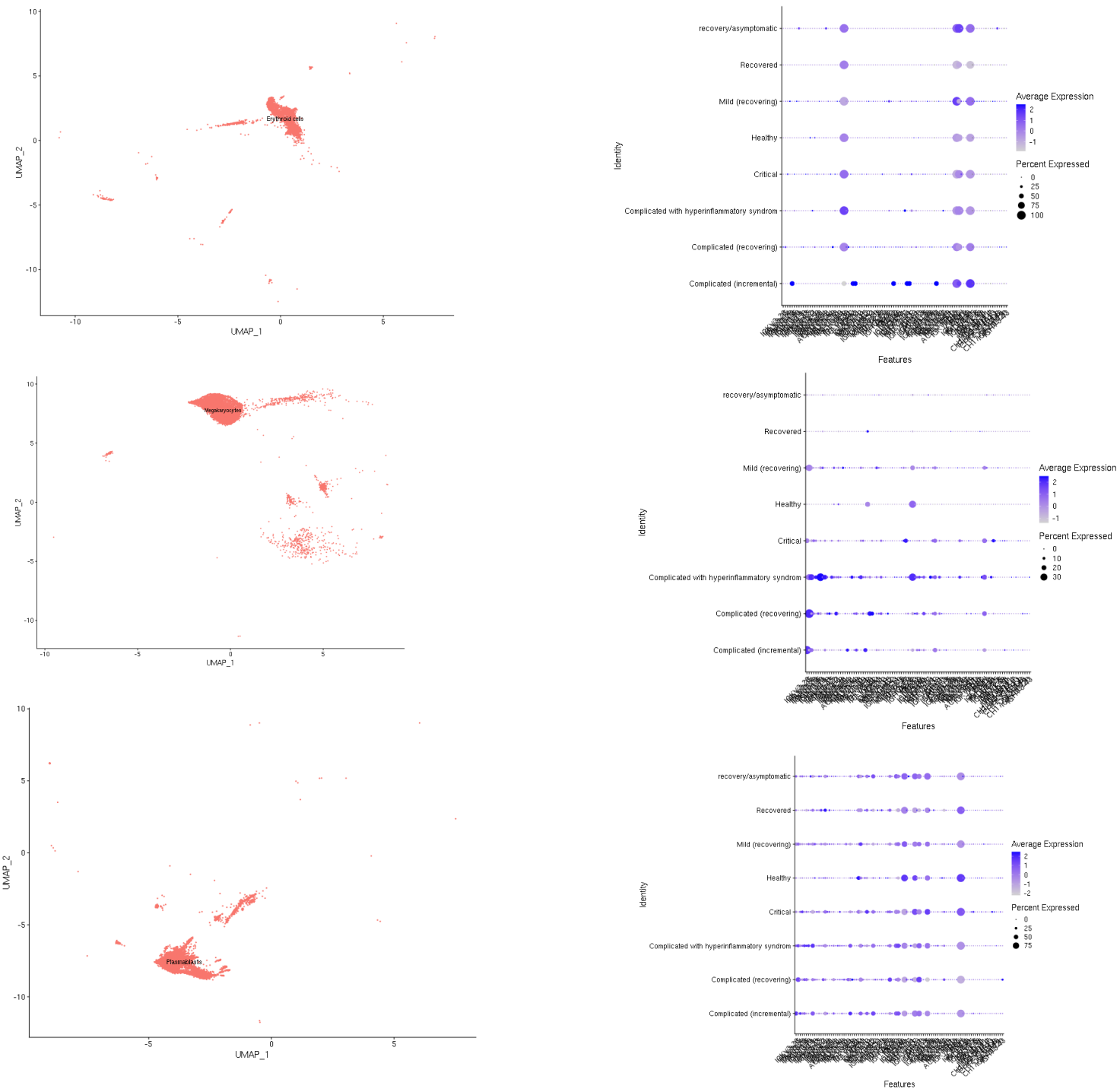

FIGURE 15: Cell-specific UMAP projections and comparison of psuedotime gene expression of three target cells (erythroid (top), megakaryocytes (middle), and plasmablasts (bottom)).

4. Patient-Specific Metabolic Subsystems

Cell-specific metabolic models for each patient across disease status were reconstructed by use of both *StanDep* and *FastCore* (Vlassis et al. 2014 ; Joshi et al. 2020**)**. Normalized gene-level counts were extracted, converted into TPM-values, normalized according to human ENSEMBL gene lengths, and ENSEMBL gene names were mapped to Recon 2.2 (Thiele et al. 2013). *StanDep* was employed with the pre-processed expression data to identify core reaction genes across cell types, identifying both enzyme type and expression concerning Recon 2.2. Enzyme expression was then $\log_{10}$ transformed into a binary matrix with rows representing enzymes and columns as bins to identify minimum and maximum enzyme expression. A complete linkage metric with hierarchical clustering and Euclidean distance was used to cluster (number of clusters = 40) genes concerning their expression. Core reaction matrices were assembled, defined, and used as an input in *FastCore* (Vlassis et al. 2014) to reconstruct single-cell, context-specific metabolic models.

After applying all constraints that were imposed from the blood medium and scRNA gene expression, all cells which were identified to have less than 30 core reactions per individual cell were removed. While only 358930 cells were initially employed in the initial bioinformatics analysis and preprocessed for metabolic model reconstruction, only 299163 models were reconstructed with a total success rate of 82% (Table 6). While metabolic models were reconstructed for 15 patients across 33 conditions, representing 12 cell types; only four patients with four pseudotimes with the three previously described cell targets will be investigated in the following cases. All patients with their associated pseudotimes and total cell models can be found plotted in the supplementary section of this dissertation. The total number of subsystem reactions for each cell-type were summed for each metabolic model based on patient-specific timepoints. The average number of subsystem reactions was then compared between timepoints. While assessments and discussion of all patient timepoints are possible, it would be cumbersome to assess the changes in metabolic subsystems across all patients and their respective disease timepoints; therefore only two transitions were assessed in patients with four pseudotimes. For example, if a patient with four disease timepoints transitioned from

healthy to mild (transition 1) and then from complicated to critical (transition 2), only these changes were initially interpreted.

Patient ID	Status	# Sequenced Cells	# of Metabolic Models	Model Reconstruction Success Rate (%)
Co_002_TA	Complicated w/ Hyperinflammatory Syndrome	9776	8901	0.91049509
Co_003_TA	Complicated (Recovering)	13349	10888	0.8156416211
Co_c003_TB	Recovery / Asymptomatic	12389	11042	0.8912745177
Co_c004_TC	Mild (Recovering)	13942	11854	0.8502366949
Co_c011_TA	Recovery / Asymptomatic	9656	9536	0.9875724938
Co_c011_TB	Recovery / Asymptomatic	12710	12261	0.9646734854
Co_c012_TA	Critical	10662	9146	0.8578127931
Co_c012_TB	Complicated w/ Hyperinflammatory Syndrome	13511	11179	0.8273998964
Co_c012_TC	Mild (Recovering)	1579	1336	0.8461051298
Co_c012_TE	Mild (Recovering)	14471	8983	0.6207587589
Co_c022_TA	Complicated (Recovering)	11051	8431	0.762917383
Ki_001_TA	Complicated (Recovering)	4334	3540	0.8167974158
Ki_001_TA2	Critical	11658	10827	0.9287184766
Ki_001_TB	Mild (Recovering)	9637	8119	0.8424821002
Ki_001_TC	Recovery / Asymptomatic	8056	6203	0.7699851043

Ki_002_TA	Complicated (Incremental)	8516	7089	0.8324330672
Ki_002_TA2	Critical	11027	9502	0.8617030924
Ki_003_control	Healthy	3293	1667	0.5062253265
Ki_004_TA	Complicated (Incremental)	2520	2324	0.9222222222
Ki_004_TA2	Complicated w/ Hyperinflammatory Syndrome	6185	5992	0.9687954729
Ki_004_TB	Mild (Recovering)	9534	8664	0.90874764
Ki_005_control	Healthy	7869	3006	0.3820053374
Ki_005_TA	Complicated (Incremental)	18783	15836	0.8431028057
Ki_005_TA2	Complicated w/ Hyperinflammatory Syndrome	14643	13422	0.9166154477
Ki_005_TB	Recovery / Asymptomatic	21263	19080	0.897333396
Ki_006_TA	Mild (Recovering)	18279	14666	0.8023414848
Ki_006_TA2	Mild (Recovering)	13727	13325	0.97071465
Ki_006_TB	Recovery / Asymptomatic	14234	13349	0.9378249262
Ki_006_TE	Recovered	8954	8374	0.9352244807
Ki_007_control	Healthy	11351	4793	0.4222535459
Ki_007_TE_rec	Recovered	9353	9080	0.9708115043
Ki_009_control	Healthy	10511	9299	0.8846922272
Ki_010_control	Healthy	12107	7449	0.6152638969

Table 6: Details of patient samples, disease status, total number of cells, and successful metabolic model reconstruction from the COVID-19 cohort.

a. **Case 1**

Patient 1 with the code ‘Co_012’ had four timepoints in which the individual transitioned from critical, to complicated with hyperinflammatory syndrome, and remained with mild disease as they were observed to be recovering for the final two timepoints. Across the four timepoints, this patient had 7661 cells on average and a metabolic model reconstruction rate of 78.8% (Figure 16). While the graphs for metabolic activity appear similar, there were some differences between this patient during the first two timepoints: critical and complicated with hyperinflammatory syndrome. First, it should be noted that there were approximately 3000 more sequenced cells for the patient during hyperinflammation. Another surprising observation was between the last two timepoints, which were both defined as a mild disease status. Primarily, the second mild time point had approximately 6600 more cells sequenced; this difference is likely related to phenotypic variability of effects in sequencing quality and is therefore, not a major issue However there was a major difference in the success rates for metabolic model reconstruction. The first mild time point showed an 84.6% success rate while the second mild condition only had 62%.

When comparing erythroid cell metabolic activities, the metabolic subsystem of ‘Keratan sulfate synthesis' was doubled in this patient with a critical disease status. Additionally, erythroid cells within the critical status also were found to have a higher average metabolic activity of fatty acid oxidation in comparison to the timepoint with complicated symptoms. Specifically, this increased fatty acid metabolism may be mediated by erythroid cells which produce erythropoietin, a cytokine which promotes both the proliferation and across various cells; this cytokine is effective at mediating against stress and promoting anti-inflammation by regulating the metabolism of fatty acids (Wang et al. 2014). The number of erythroid cell activity associated with inositol phosphate significantly decreased when the patient transitioned from critical to hyperinflammatory symptoms. Increased amounts of inositol in addition to products of pentose phosphate metabolism are known to increase during the inhibition of heme synthesis; this uptake of inositol products in turn leads to the inhibition of erythropoietic synthesis of heme products (Marcero et al. 2021). Most interesting, the metabolic models of the critical timepoint in erythroid cells identified a low activation of heme synthesis, while there

was no observation of heme synthesis when the patient experienced hyperinflammatory symptoms.

Megakaryocytes in this patient case were significantly lower during critical conditions as compared to the complicated hyperinflammatory syndrome status. As megakaryocytes play a significant role in the production of blood platelets which are necessary for blood clotting (Nayak et al. 2019); the role of blood clotting with regards to COVID-19 pathophysiology is presently being discussed within the community (Lemke & Silverman, 2020). When the patient was in a critical disease status, it was observed in the metabolic models that the average bile acid synthesis activity by megakaryocytes was approximately doubled as compared to the patient's status during complicated disease. Interesting, it was recently found that bile acid synthesis inhibits the aggregation of platelets (Cheng et al. 2020). The increased production of bile acids prior to hyperinflammation by megakaryocytes may be a preventative mechanism to reduce platelet formation and thus severe disease.

When assessing the average metabolic pathway abundance in this patient among plasmablast cells between a critical and complicated with hyperinflammatory disease status, several stark differences can be noticed. With regards to a critical status of disease severity there were several metabolic pathways that were over expressed. For example, bile acid synthesis, blood group synthesis, cholesterol metabolism, eicosanoid metabolism, fatty acid oxidation, glycerophospholipid metabolism, heme synthesis, inositol phosphate metabolism, keratan sulfate degradation, N-Glycan synthesis, nucleotide interconversion, o-glycan synthesis, purine synthesis, sphingolipid metabolism, steroid metabolism, extracellular transport, mitochondrial transport, and tryptophan metabolism appear to be highly upregulated in critical plasmablasts as compared to critical with hyperinflammatory syndrome. In contrast the same patient has highly expressed metabolic pathways in the plasmablasts during complicated with hyperinflammatory syndrome. It was observed that biotin metabolism, butanoate metabolism, citric acid cycle, cysteine metabolism, folate metabolism, fructose and mannose metabolism, glycosphingolipid metabolism, limonene and pinene degradation, nucleotide salvage pathway, phenylalanine metabolism, squalene and cholesterol synthesis, taurine and hypotaurine metabolism, golgi

apparatus transport, peroxisomal transport, and vitamin A metabolism are all highly active in this patient's plasmablasts during their complicated hyperinflammatory status.

One study has observed that plasmablasts, when exposed to viruses or vaccines, tend to have a higher gene expression which codes for both heme biosynthesis and inositol phosphate metabolism (Li et al. 2017). Both were observed in this patient's plasmablasts during critical disease status as they were transitioning towards hyperinflammation. More so, this was observed soon after the patient became ill with COVID-19. Furthermore, a recent immunometabolic study identified that enhanced glycolysis is a metabolic feature during COVID-19 which provokes memory B-cells to transition into plasma cells, this is further associated with a heightened inflammation in monocytes and improved cell survivability in plasma cells derived from COVID-19 patients with a severe disease status (Qi et al. 2021). While it is not significant, this patient was observed to have a three fold increase in plasmablast cells which were associated with glycolysis and gluconeogenesis during critical disease status, as compared to complicated with hyperinflammatory syndrome. Furthermore, a recent study in plasmablast metabolism has suggested that during parasitic infection, plasmablasts may act as a competitive nutritional sink for uptaking L-glutamine; this may strongly influence parasitic infection success and the transition of early plasmablasts towards B cells to help in infection control (Rodda & Pepper, 2020). These observations may be supported from the metabolic models which observed that plasmablasts have a higher rate of glutamate metabolism during complicated hyperinflammation as compared to critical disease status. However, the metabolic activity of plasmablasts with regards to glutamate metabolism was unchanged when comparing the final two mild timepoints.

While it can be assumed that both mild disease status timepoints in this patient ought to be the same, there was a significant difference in the number of sequenced single-cells as previously described; this is in addition to the discrepancy of model reconstruction success rate. However, the patient may be transitioning to an asymptomatic disease status which may lead to some miniscule differences between both timepoints, even if they were clinically defined to be the same. For example, while not significant, it was found that erythroid cells in the first mild

timepoint had a minor increased metabolic activity in bile acid synthesis, CoA catabolism, fatty acid oxidation, glutathione metabolism, glyoxylate and dicarboxylate metabolism, inositol phosphate metabolism, and vitamin B6 metabolism. In contrast, there were not any metabolic subsystems which were significantly more active in the second mild timepoint as compared to the first mild timepoint. However, when comparing megakaryocytes metabolic activity between both mild timepoints there were some significant differences. First, the initial mild timepoint had an almost double metabolic activity in cholesterol metabolism and fatty acid oxidation. On the other hand, the second mild disease status had a significantly higher metabolic activity with regards to the citric acid cycle, glutamate metabolism, heme synthesis, methionine and cysteine metabolism, purine synthesis, steroid metabolism, and the urea cycle. Most of these cases were interesting as these metabolic pathways were not expressed or lowly expressed in the first mild timepoint. Finally with regards to plasmablasts, these cells appear to be metabolically active in this patient's mild disease status; however only pyrimidine synthesis was found to be highly expressed in the second mild timepoint as compared to the first.

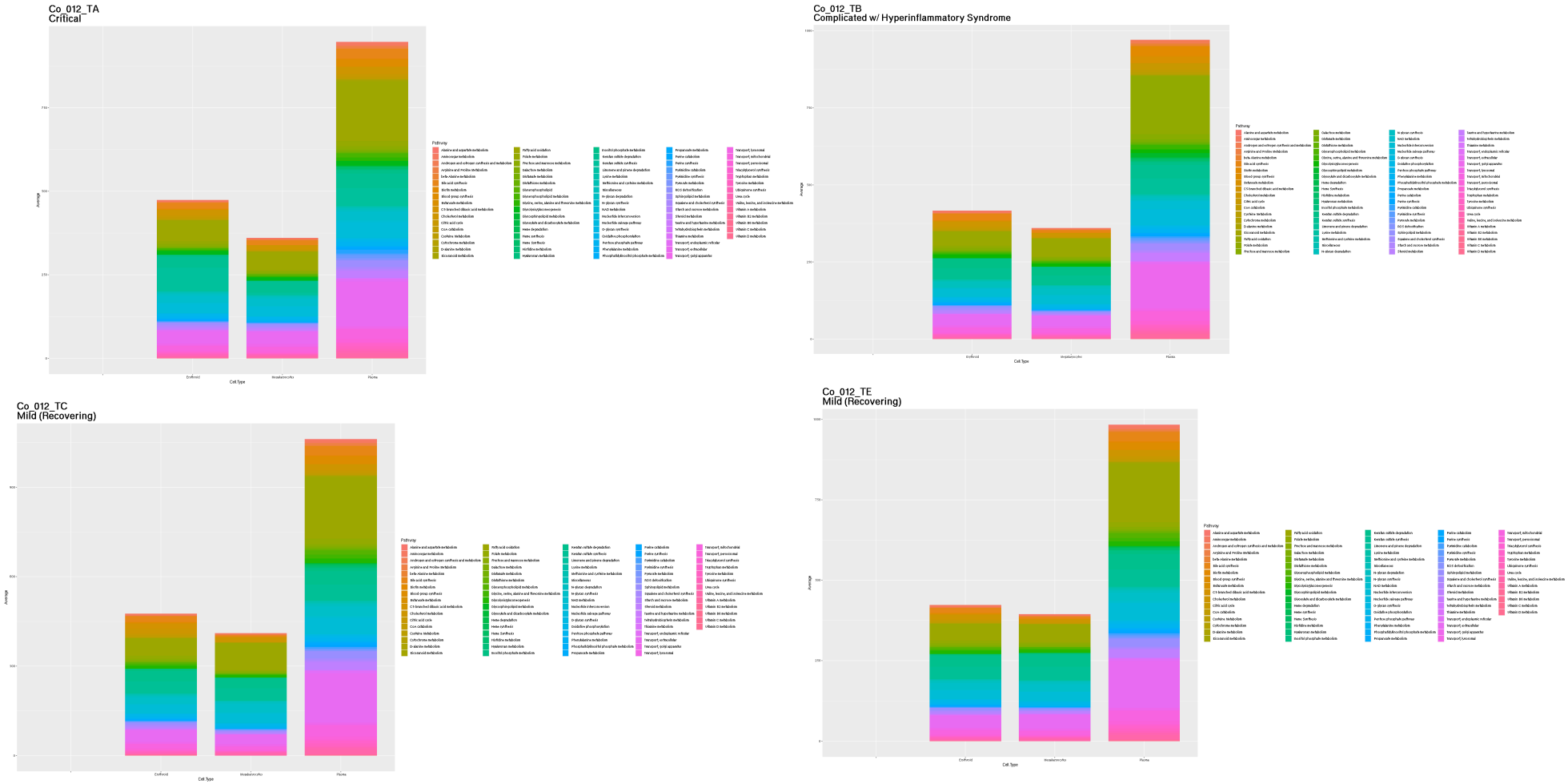

Figure 16: Metabolic subsystem activity of Case 1 from the COVID-19 cohort.

b. Case 2

Patient 2 with the code 'Ki_001' had four timepoints in which the individual transitioned from complicated (recovering) to critical, and finally towards mild (recovering) and then recovery/ asymptomatic for the final two timepoints. Across the four timepoints, this patient had 8421 cells on average and an average metabolic model reconstruction rate of 83.9% (Figure 17). In this specific case, there are significant differences between each disease timepoint. First, it can be observed that both erythroid and megakaryocytes had an increased average metabolic activity when transitioning from complicated (recovering) towards a status of complicated with hyperinflammatory syndrome. This can be expected as the patient will have more highly active cells during hyperinflammation. However what is most surprising is the complete lack of erythroid cells in this patient during both mild (recovering) and the recovery / asymptomatic disease status. While it is possible that this may simply be a technical issue in association with the sequencing technology used, it is also possible that these cells are no longer active in a mild or recovered disease status. However this seems unlikely as the previously defined case (Co_c012) has metabolically active erythroid cells during a mild course of disease. It is also possible that there were minor differences in the preparation of the samples prior to sequencing, as some samples were received from Cologne (Co_xxxx) and others from Kiel (Ki_xxx). Furthermore, the quantity of metabolically active erythroid cells during complicated and critical status of the disease also remains to be low as compared to other patients, in which this patient only had a single metabolic model for erythroid cells for each of the first pseudotimes.

When comparing the metabolic activity of erythroid cells during the transition between complicated / recovering and critical in this patient, there are some aspects of metabolism which are unique between each context. For example, sphingolipid metabolism, tryptophan metabolism, ubiquinone synthesis, urea cycle metabolism, and valine/leucine/isoleucine metabolism are all uniquely active only in the complicated / recovering context rather than critical. Upregulation of sphingolipid pathways may control the cellular differentiation of erythroid cell lineages (Xie et al. 2016). This mechanism has been uncovered in a recent study that has suggested that bioactive sphingolipids can lead towards the inhibition of erythropoiesis

by upregulating tumor necrosis factor alpha (Orsini et al. 2019). Tryptophan metabolism plays an important role in the immune system, in which enhanced metabolic activity of tryptophan in addition to serotonin is physiologically relevant for healthy erythropoiesis, especially during anemia (Sibon et al. 2019). When assessing erythroid cells during critical conditions against complicated (incremental) disease status, there were also several metabolic related activities which were unique in this certain context. Specifically, bile acid synthesis, cholesterol metabolism, folate metabolism, glyoxylate and dicarboxylate metabolism, keratan sulfate degradation, keratan sulfate synthesis, and steroid metabolism were all found to be unique. With regards to unique metabolic update of cholesterol metabolism in erythroid cells during a critical disease status, it is presently understood that cholesterol uptake and metabolism is necessary in erythroid cells for both self-renewal and maintenance (Meja-Pous et al. 2011). Furthermore, reduction in low-density lipoprotein cholesterol has been found to lead to alterations in human erythroid differentiation (Schmelzer et al. 2011). This critical mechanism occurs when cholesterol biosynthesis is downregulated and leads to the reduction of intracellular cholesterol and directly promotes a defect in erythroid differentiation (Lu et al. 2021).

With regards to megakaryocyte metabolic activity as the patient transitions from complicated/ recovering towards critical disease status, there appears to be few differences. This is besides the fact that metabolic activity is significantly higher in a complicated case with hyperinflammatory syndrome. During hyperinflammation, it was observed through the metabolic models that CoA catabolism is heightened. In contrast, steroid metabolism is also increased in the critical case. Interesting, with regards to the complicated case, alanine and aspartate metabolism, blood group synthesis, fatty acid oxidation, various transport reactions (golgi apparatus, lysosomal, and mitochondrial). For example, fatty acid metabolism is essential for megakaryocytes, they are necessary to allow for megakaryocytes to communicate with adipocytes which regulate the maturation of megakaryocytes in the production of platelets (Valet et al. 2020). With regards to the significant upregulation of metabolic pathways associated with lysosomes, these organelles may play an important role in how patient-derived megakaryocytes heal during COVID-19 infection or further promote disease trajectory. Overall, while the pathophysiological role of lysosome secretions are not well-understood within

megakaryocytes, there are some speculations that can be made. First, it is known that the megakaryocytes and their associated platelets do possess lysosomes which contain various hydrolases, this includes both proteases and glycosidases (Bentfiel & Bainton, 1975 ; Bentfeld-Barker & Bainton, 1982). However, when these platelets are activated through immune stimulation, they are able to release lysosomal contents which can have a double-edged effect on humans (Ciferri et al. 2000). Depending on the context, the megakaryocyte platelets may release lysosomal enzymes which may promote remodeling of extracellular material during wound healing (Rendu et al. 2001). In contrast, the lysosomal enzymes may lead to an assumed local injury of lung vascular arteries, thus further promoting chronic inflammation (Muir et al. 1984). Thus, the correct metabolic regulation of lysosomes that are mediated by megakaryocytes are required for not only proper healing but also necessary to prevent both chronic inflammation and thrombosis (Min et al. 2014). Furthermore, the heightening of mitochondria transport in the megakaryocytes may be of interest with regards to disease severity trajectory while the patient is in a complicated disease state. For example, the increased transport of mitochondrial ROS levels is able to incite the production of platelet biogenesis from mature human megakaryocytes, this provokes a positive feedback loop which is necessary for beginning thrombosis as a phenotype (Poirault-Chassac et al. 2021).

However, the metabolic models revealed that reconstruction of plasmablasts during complicated / recovering disease state is significantly more active than during a critical disease status. For example, various vitamin metabolisms (A, B2, B6, C, and D) appear to be highly active. Vitamin availability, especially vitamin D, has been hypothesized to confer advantages to patients with severe COVID-19 (Notz et al. 2021). For example, vitamin A plays a significant role in mediating host adaptive immunity, this occurs when vitamin A induces the differentiation of plasmablasts (Scholz et al. 2021).Furthermore, vitamin A deficiency has been associated with the reduction of the production of IgA+ ; however, plasmablasts do not require vitamin D to induce the same function (Sigmundsdottir & Butcher, 2008). In general, plasmablasts appear to be greater in patients with greater levels of vitamin D, in which these cell types support the establishment of both immune memory and the accumulation of specific

antibodies which may be effective against pathogens such as SARS-CoV-2 (Notz et al. 2021 ; Fink, 2012).

Finally, the assessment of metabolic reaction potential when assessed from the disease status of mild (recovering) to recovery / asymptomatic was not as robust as other modeled cells. Specifically, there were no erythroid cells found in this patient. Additionally, the metabolic activity between megakaryocytes and plasmablasts between both patient contexts did not highlight any significant differences. Regardless, there are some noticeable differences. The first is that when the patient is in a state of mildc COVID-19, they have low levels of eicosanoid metabolism which is not present during recovery / asymptomatic. The cells which are within the recovery / asymptomatic context also show a high level of transport reactions that are associated with the lysosomes. As previously discussed, the lysosomes of megakaryocytes play a major role in modulating both wound healing (Rendu & Brohard-Bohn, 2001) and inciting chronic inflammation (Muir & Bowyer, 1984). Thus playing a significant role in the regulation of both inflammation and thrombosis (Min et al. 2014).

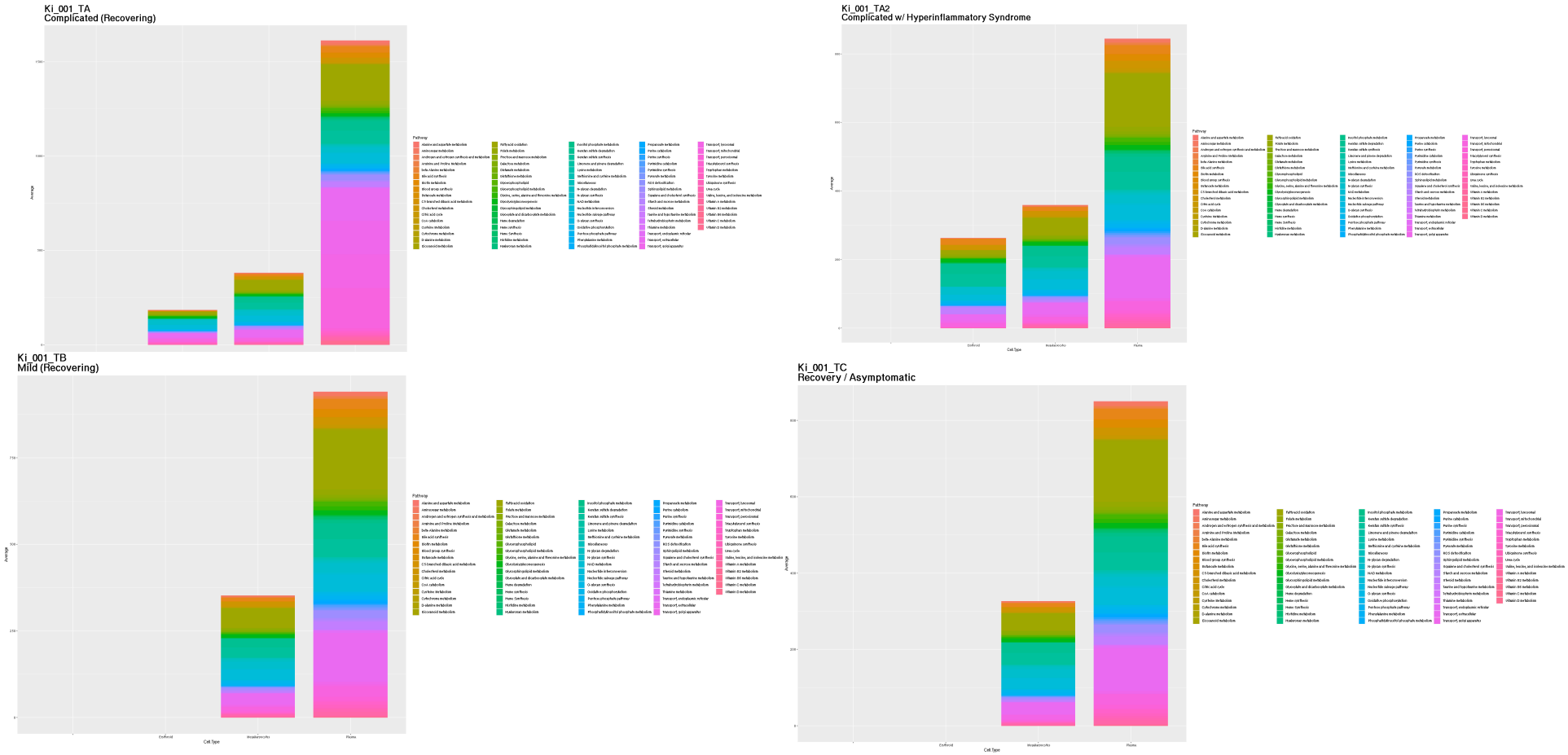

Figure 17: Metabolic subsystem activity of Case 2 from the COVID-19 cohort.

c. Case 3

Patient 3 with the code ‘Ki_005’ had four timepoints in which the individual transitioned from healthy to complicated /incremental, and finally from complicated with hyperinflammatory syndrome into a state of recovery / asymptomatic for the final two timepoints.Across the four timepoints, this patient had 15640 cells on average and an average metabolic model reconstruction rate of 75.97% (Figure 18). While the graphs for metabolic activity appear similar, there was one stark common feature: there were no erythroid cells sequenced in this patient across any timepoint, this is likely a technical bias. First, it should be noted that there were approximately 3000 more sequenced cells for the patient during hyperinflammation. Another surprising observation was between the last two timepoints, which were both defined as a mild disease status. Primarily, the second mild time point had approximately 6600 more cells sequenced. However there was a major difference in the success rates for metabolic model reconstruction. The first mild time point showed an 84.6% success rate while the second mild condition only had 62%.

When this patient transitioned from healthy towards a complicated / incremental state of COVID-19, there are several significant changes that ought to be highlighted; numerous metabolic subsystems which were not active in megakaryocytes during health, were active as symptoms changed. For example, biotin metabolism, blood group synthesis,C5- branched dibasic acid metabolism, cytochrome metabolism, eicosanoid metabolism, glutathione metabolism, glycosphingolipid metabolism, glyoxylate and dicarboxylate metabolism, heme degradation, heme synthesis, histidine metabolism, hyaluronan metabolism, phosphatidylinositol phosphate metabolism, purine synthesis, ROS detoxification, taurine and hypotaurine metabolism, tetrahydrobiopterin metabolism, thiamine metabolism, and five types of vitamin metabolism (A, B2, B6, C, and D) subsystems became active during a complicated / incremental state of disease as compared to the control. Some metabolic pathways such as bile acid synthesis, CoA catabolism, squalene and cholesterol synthesis, steroid metabolism, ubiquinone synthesis, and urea cycle increased as the patient’s disease status became complicated. Interestingly, several metabolic pathways such as methionine and cysteine

metabolism, N-glycan degradation, N-glycan synthesis, nucleotide interconversion, oxidative phosphorylation, pentose phosphate pathway golgi apparatus transport, and triacylglycerol synthesis were found to decrease.

To clarify these changes and their modification on disease status, it was previously described in another patient that the increased biosynthesis of bile acids can impair platelet aggregation (Cheng et al. 2020); increased bile acid synthesis by megakaryocytes prior to hyperinflammation seems to be a viable pathomechanisms to reduce platelets from sticking together and thus, mitigate the risk of severe disease. Cytochrome metabolism, ROS detoxification, and mitochondria transport reactions were all found to increase simultaneously when transitioning towards a complicated / incremental disease status, it is possible that there are present oxidative stress which is damaging host mitochondria (Ceccatelli et al., 2012). Additionally, glutathione metabolism is also increased during complicated disease status, this enzyme is typically expressed to mitigate cellular damage which occurs through ROS that may impact host mitochondria functions (Bonetto et al. 2014). Furthermore, there is a tandem increase of pentose phosphate metabolism, inositol metabolism, and heme synthesis when the healthy patient is transitioning to complicated (incremental); all are related with regards to platelet formation. Furthermore, NADPH that is produced through pentose phosphate metabolism plays a role as an essential cofactor to mitigate ROS during inflammation. For example, by increasing the biosynthesis of inositol with pentose phosphate, both lead to the inhibition of heme synthesis, this may in turn be a mechanism to mitigate platelet formation as the patient is transitioning to a severe disease status. The presented metabolic models also identified an increase of purine biosynthesis while the patient reached a complicated / incremental disease status. Metabolic models of SARS-CoV-2 from another study which employed metabolic models to study viral replication capacity identified that the virus employs host purine biosynthesis pathway for replication (Renz et al. 2020).

Finally, the metabolic activity of plasmablasts within this patient as they transitioned from health towards a complicated disease status were compared. Primarily, there were few metabolic pathways which were highly expressed during the complicated disease status of

plasmablasts. For example, beta-alanine metabolism, bile acid synthesis, blood group synthesis, butanoate metabolism, C5-branched dibasic acid metabolism, eicosanoid metabolism, fatty acid oxidation, glycerophospholipid metabolism, glycine/serine/alanine metabolism, heme degradation, histidine metabolism, inositol phosphate metabolism, keratan sulfate synthesis, limonene and pinene metabolism, methionine and cysteine metabolism, NAD metabolism, N-glycan degradation, phenylalanine metabolism, phosphatidylinositol phosphate metabolism, purine synthesis/catabolism, pyrimidine synthesis, pyruvate metabolism, ROS detoxification, sphingolipid metabolism, taurine and hypotaurine metabolism, extracellular transport, tryptophan metabolism, tyrosine metabolism, and vitamins B2 and B6 were observed to have minor increases in metabolic subsystem activity as compared to healthy. Most interestingly, the transport reactions of plasmablasts during health were highly active and were drastically reduced when the patient transitioned to a complicated disease status.

Next, this case was further assessed in their transition from a phenotype that can be described as complicated with hyperinflammation towards a state of recovery / asymptomatic. Similarly with the previous disease status, erythroid cells are also not present in this patient. Interestingly, there were not any major differences in the metabolic activity for the remaining two cell types (megakaryocytes and plasmablasts) when comparing the patient disease status of complicated hyperinflammatory syndrome to recovery / asymptomatic. However with regards to megakaryocytes, it should again be noted that the complicated with hyperinflammatory syndrome disease status had some unique metabolic activity which was not observed during recovery. For example, bile acid synthesis, blood group synthesis, C5-branched dibasic acid metabolism, glycosphingolipid metabolism, glyoxylate and dicarboxylate metabolism, histidine metabolism, and vitamin C metabolism were all active only in the megakaryocytes during complicated with hyperinflammation and not in the recovery state. Another interesting observation is with regards to plasmablasts. While comparing the metabolic subsystem activity of plasmablasts between complicated hyperinflammation and recovery / asymptomatic, there were not any significant or noticeable changes between either contexts, suggesting that metabolic activity of the plasmablasts remains highly active following inflammatory illness.

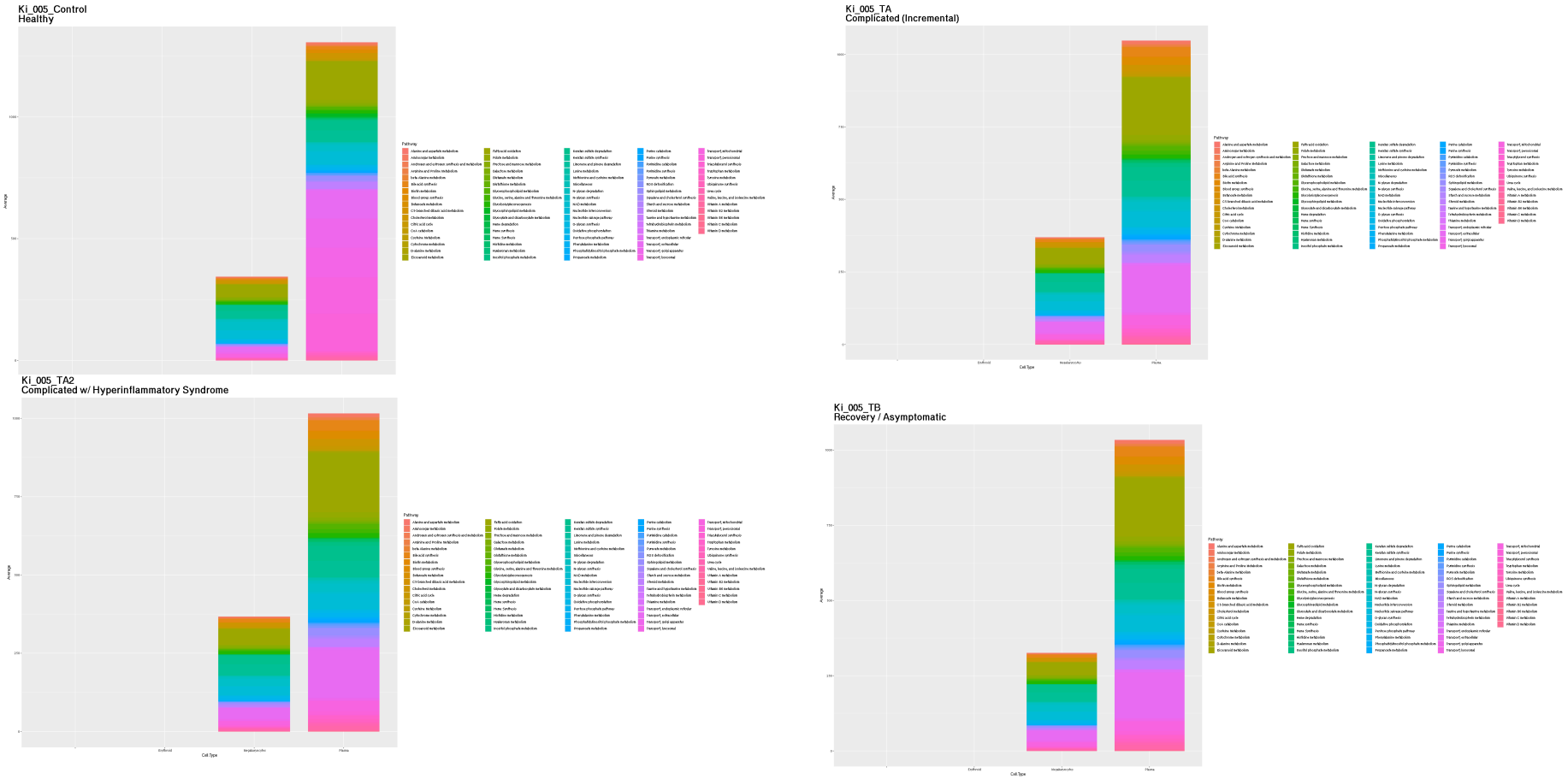

Figure 18: Metabolic subsystem activity of Case 3 from the COVID-19 cohort

d. Case 4

Patient 4 with the code ‘Ki_006’ had four timepoints in which the individual transitioned from mild and remained in mild condition for the first two timepoints, the next transition was from recovery / asymptomatic towards fully recovered for the final two timepoints. Across the four timepoints, this patient had 13798 cells on average and an average metabolic model reconstruction rate of 91.15% (Figure 19). While the graphs for metabolic activity appear similar, the major difference is that erythroid cells were only identified in the final timepoint. Interestingly, this timepoint hosted erythroid cells which had a significant amount of fewer cells than the other timepoints (approximately 5000 less). Another surprising observation was that between the first two timepoints, which were both defined as a mild disease status, there is a significant difference in the model reconstruction success rate (80% vs. 97%).

With regards to cell-specific metabolic changes across disease contexts, there are minor changes in this patient with the exception of erythroid cells in the recovering time point. As aforementioned, there is a complete lack of erythroid cells in the first three timepoints. As the first two timepoints are both mild disease status, it is expected that there may not be too many changes that are noteworthy. However with regards to megakaryocytes, there is a slight increase in cytochrome metabolism in the second mild time point. Cytochrome metabolism is generally overexpressed as a means to metabolize drugs or toxins, however it also plays a significant role in mediating oxidative stress during inflammation (Bhattacharyya et al. 2014). Interestingly, CoA catabolism was also greatly increased, however the reason for why this occurred is not clear.

With regards to erythroid cells, the patient appears to have metabolically active erythroid cells only when the patient is fully recovered from COVID-19. As this may be a technical bias in the sequencing technology, these results cannot be compared to others from this patient effectively. However with regards to megakaryocytes, there are not any noticeable metabolic pathway differences for interpretation, this could simply mean that patients who are in a state of recovery/ asymptomatic are closely related to the phenotype of those who are fully recovered. This observation is similar for plasmablasts of the same patient. However, it was noted that

glycosphingolipid metabolism is the only metabolic subsystem which is active in plasmablasts during recovery, that is not active when the patient is fully recovered.

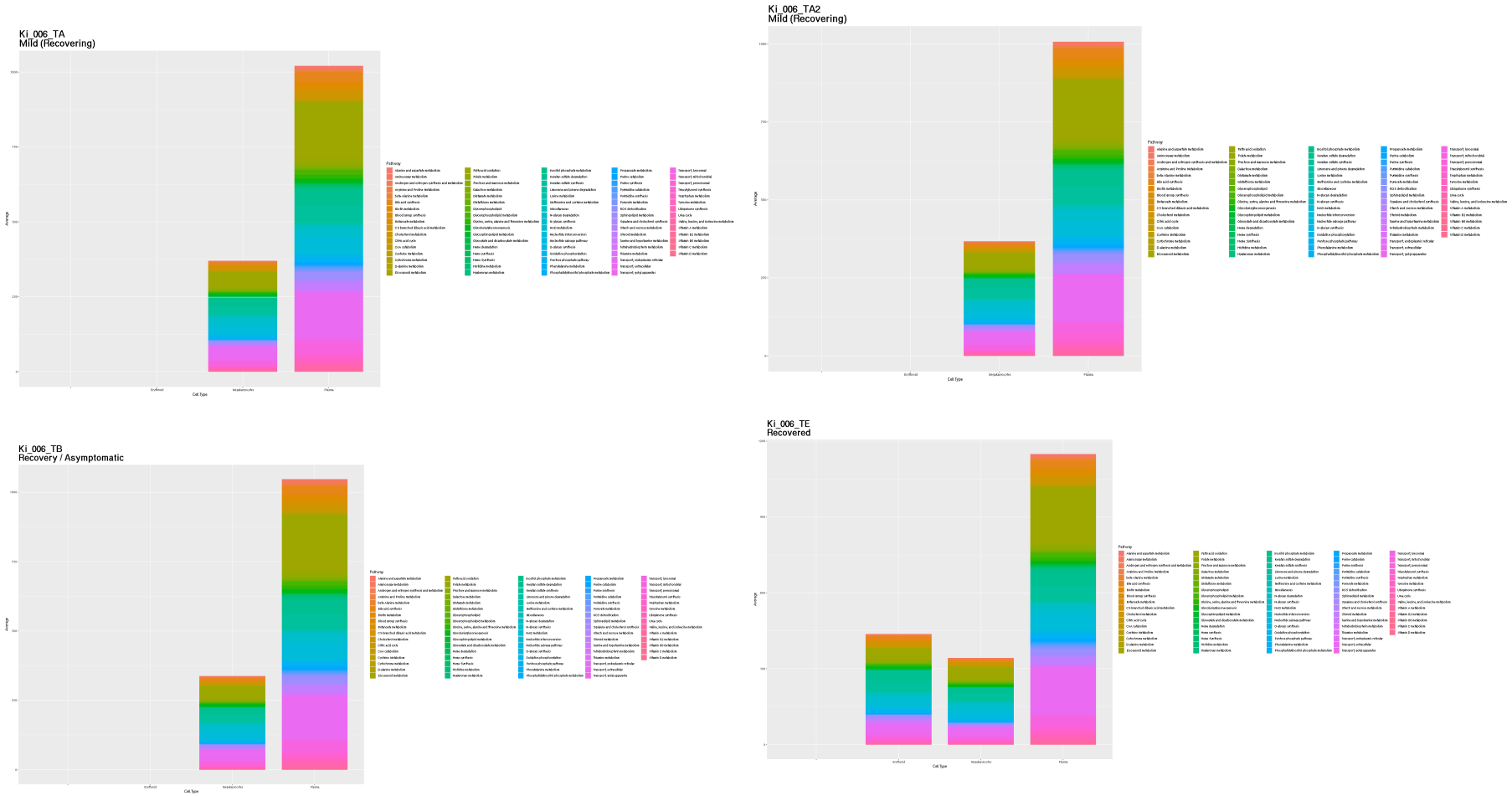

Figure 19: Metabolic subsystem activity of Case 4 from the COVID-19 cohort.

B. Urinary Tract Infection

1. Mapping and Sorting mRNA / rRNA

Following quality control and preprocessing, the metatranscriptomes from each patient were further filtered across numerous RNA databases with the SortMeRNA tool. Table 7 shows to what percent, the number of reads found in the pair-end reads were assembled and how much of the reads became mapped to rRNA/tRNA. However, any reads which did not map to the RNA databases were then assumed to be non-rRNA/tRNA and were therefore used for a subsequent mRNA pipeline. Table 8 shows how much of the assembled reads successfully aligned to the various RNA indexes.

	Raw reads (X2)	After QC	Pair-end Assembled %	rRNA/tRNA (%)	Non-rRNA/tRNA (%)
H25361	6975419	5159236	53.677	87.54	12.46
H25362	4972207	3844249	66.858	90.35	9.65
H25363	5451578	3742057	59.148	90.46	9.54
H25364	6351045	4729551	57.382	72.8	27.2
H25365	5976664	5623950	44.19	96.86	3.14

Table 7: Preprocessing/quality control, rRNA or mRNA metrics acquired from metatranscriptomes

	Align %	Bac16s	Bac23s	Euk18s	Euk28s	rfam-5s	rfam-5.8
H25361	91.83	21.5	68.98	0.17	0.22	0.95	0
H25362	90.98	25.42	45.63	6.53	13.13	0.25	0.02
H25363	92.84	0.13	0.79	28.19	63.6	0.02	0.11
H25364	76.73	17.53	36.54	7.03	15.26	0.36	0.02
H25365	97.5	19.63	46.94	10.4	19.98	0.51	0.04

Table 8: Alignment rate of metatranscriptomes across various mRNA databases

2. rRNA Taxonomy Analysis

With regards to data visualization of the OTUs and microbial abundance/taxonomy, several approaches were utilized. First a rarefaction curve of the identified OTUs was used to visualize species richness (Figure 20). This plot can be interpreted as a curve of the total number of unique species annotations as OTUs against the number of rRNA sequences. Naturally, as the curve begins to flatten, it is understood that more taxa have been sampled. These results show a heterogeneity across samples with regards to predicted UTI species. In which, samples H25361 and H25364 have the highest diversity of taxa, while H25363 is low in comparison to the other samples. While a steep curve on the left-side of the rarefaction curve is indicative that a large proportion of species diversity is not uncovered in the samples, it can be seen in the aforementioned H25363 and H25365, that these curves lack a steep slope. Overall, these curves represent the average number of species annotations that are within the community.

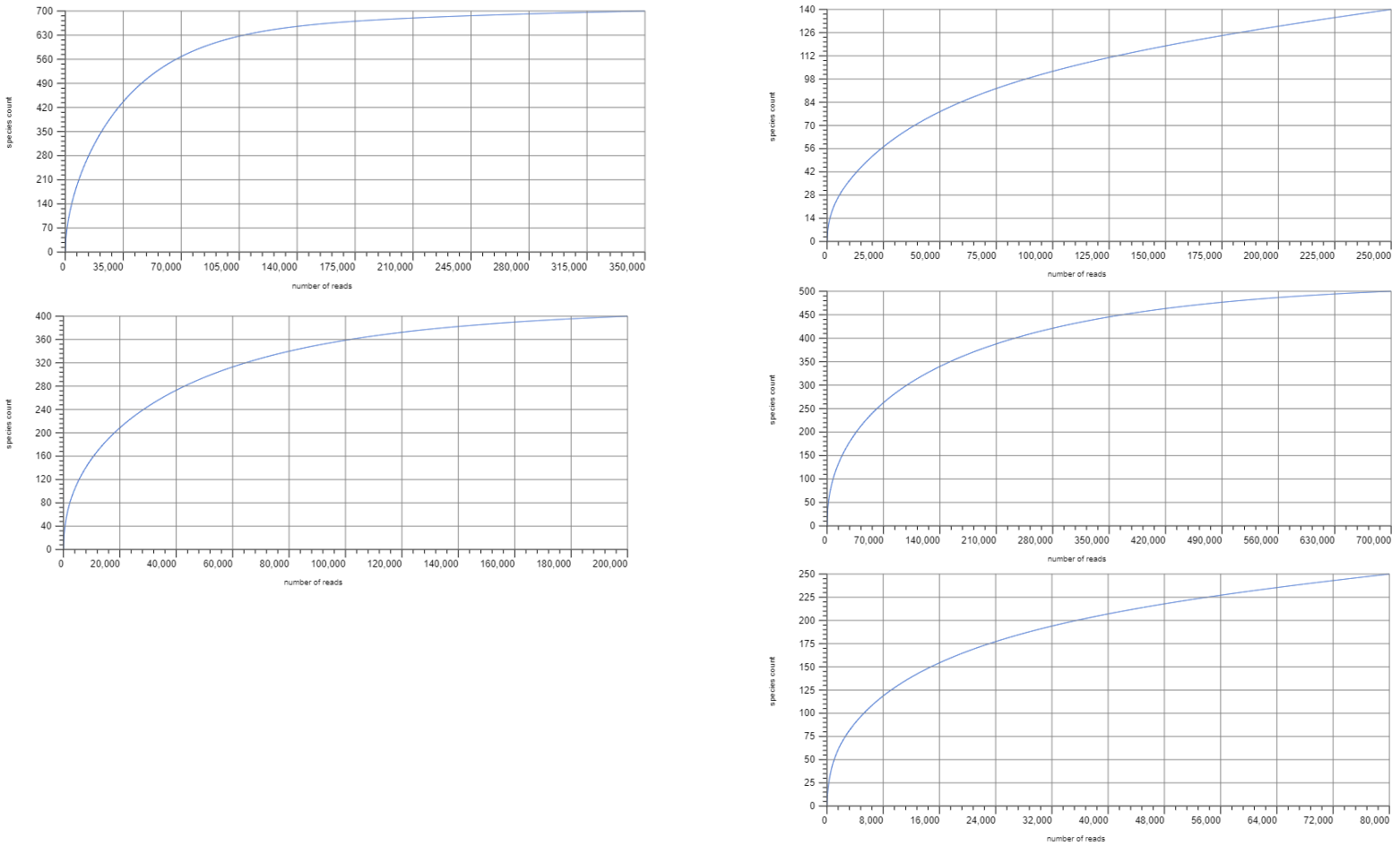

FIGURE 20: Rarefaction curve of rRNA. The curves in all plots show the total number of unique species as a function of the number of sequences found within the samples. The samples are as followed: Sample H25361 (top-left), Sample H25362 (bottom-left), Sample H25363 (top-right), Sample H25364 (middle-right), Sample H25365 (bottom-right).

After normalizing the number of reads and removing low quality reads from all samples, a NMDS plot was used across the top-five main taxa across all samples to assess similarities (Figure 21). This approach demonstrates the clustering of either individual unique OTUs or counts which are representative of species abundance with regards to microbial communities across all five samples. Not surprisingly, is a high abundance of *Proteobacteria* (*Escherichia, Salmonella, Vibrio, Yersinia*, etc.) which dominate this community, more so they appear to be closely related. It is presently understood that a high abundance of *Proteobacteria* are associated with microbial dysbiosis of the urinary tract and lower reproductive tract of women, in addition to promoting host-side inflammation infection (Aragón et al. 2018). In contrast, the healthy female urogenital microbiome normally consists of *Actinobacteria (Actinomyces* & Arthrobacter) and *Bacteroidetes (Bacteroides)* (Lewis et al. 2013) which are presented to have a lower abundance.

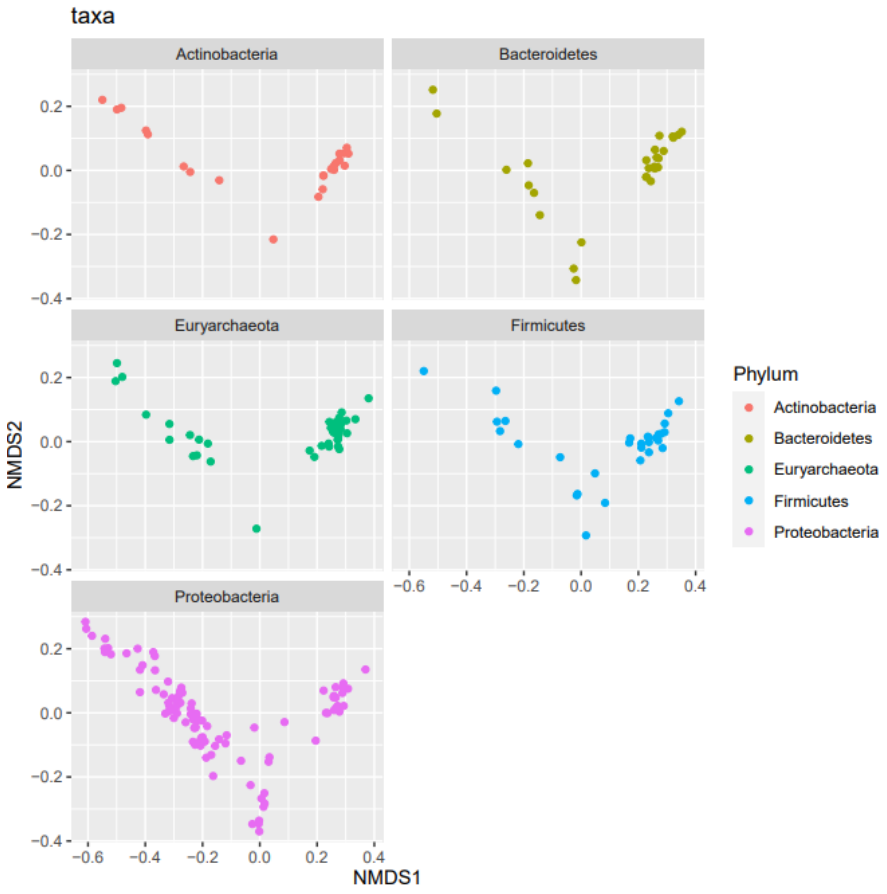

Figure 21: NMDS distribution of individual UTI phyla OTUs across all samples.

To further elaborate on the distribution of microbial abundance, sample-specific genera were plotted to identify the dominant members from each sample (Figure 22). Most samples were dominated by *Proteobacteria* (*Citrobacter, Enterobacter, Escherichia/Shigella, Pluralibacter, Pseudocitrobacter, Salmonella, Serratia, and Yersinia)*. Surprisingly, some samples contained plant-associated pathogens (*Dickeya, Erwinia, Kosakonia,* and *Mangrovibacter*). However, most of these genera were previously classified as *Proteobacter* or closely related to *Enterobacter*, which are understandable false-positives (Brady et al. 2013). As *Escherichia*/*Shigella* dominate the community with regards to the genus level, the species from this clade were further investigated (Figure 22). The *Escherichia* genus was found to mainly consist of both *E. coli* and *S. sonnei*; *E. coli* is generally understood to be the major driving agent of UTI pathogenesis (Flores-Mireles et al. 2015) while *Shigella spp.* are regularly isolated from humans with UTIs (Anatoliotaki et al. 2003; Baka et al. 2013 ; Tufon et al. 2020).

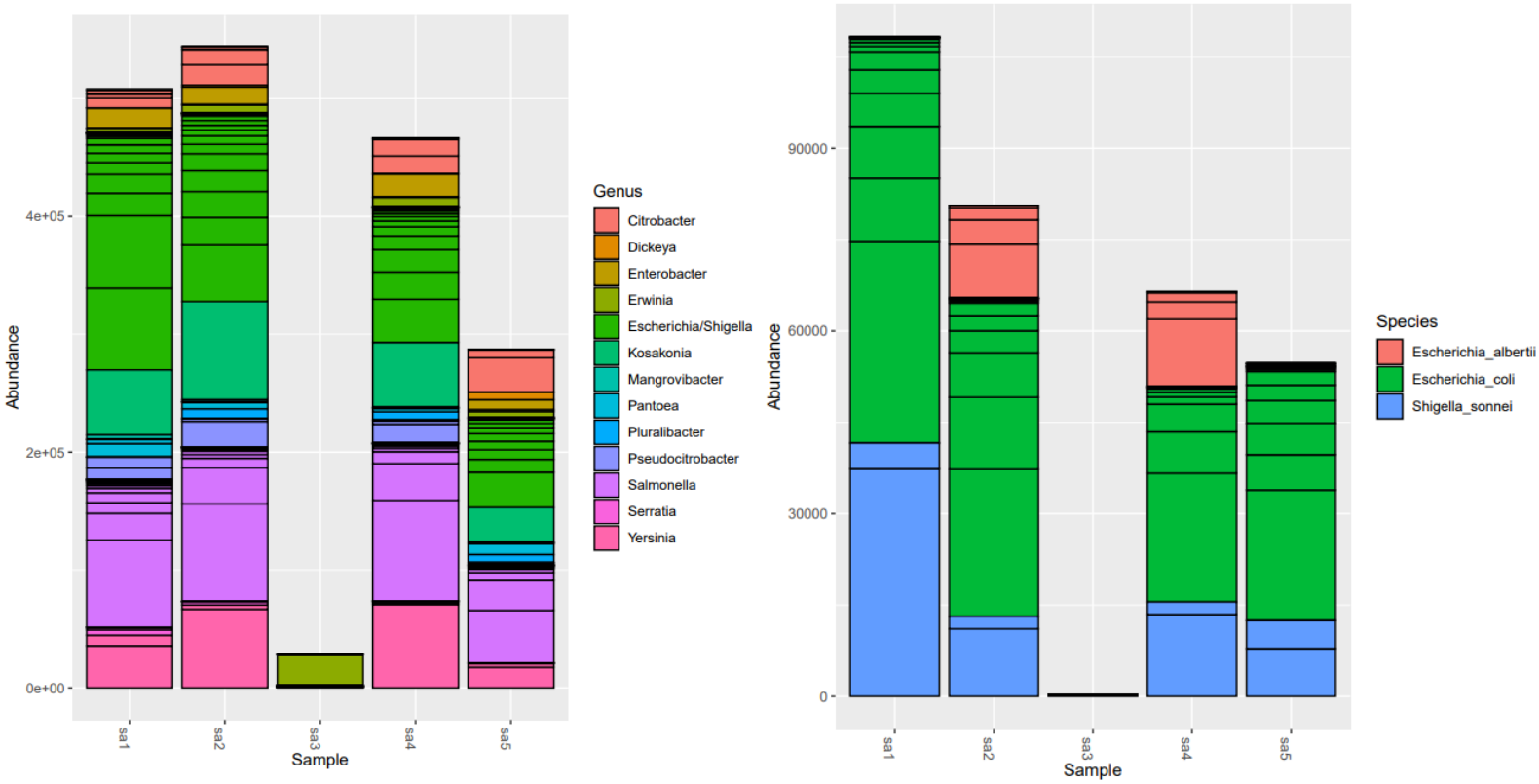

Figure 22: Taxonomic abundance and distribution across all UTI cohort samples.

Next, alpha diversity was calculated to better understand both the species abundance and evenness among each studied UTI patient through the *PhyloSeq* command '*estimate_richness*'; specifically both the diversity measures Chao1 and Shannon diversity index were used (Figure 23). Furthermore, the Shannon index which was derived from the alpha diversity measurement was further used to calculate the effective number of species for deciding the number of species that would be used in the metabolic models. Specifically, the effective number of species analysis provided a range from 2.66 up to 3.52, therefore a total of three species were selected to be included in the simulations for metabolic modeling.

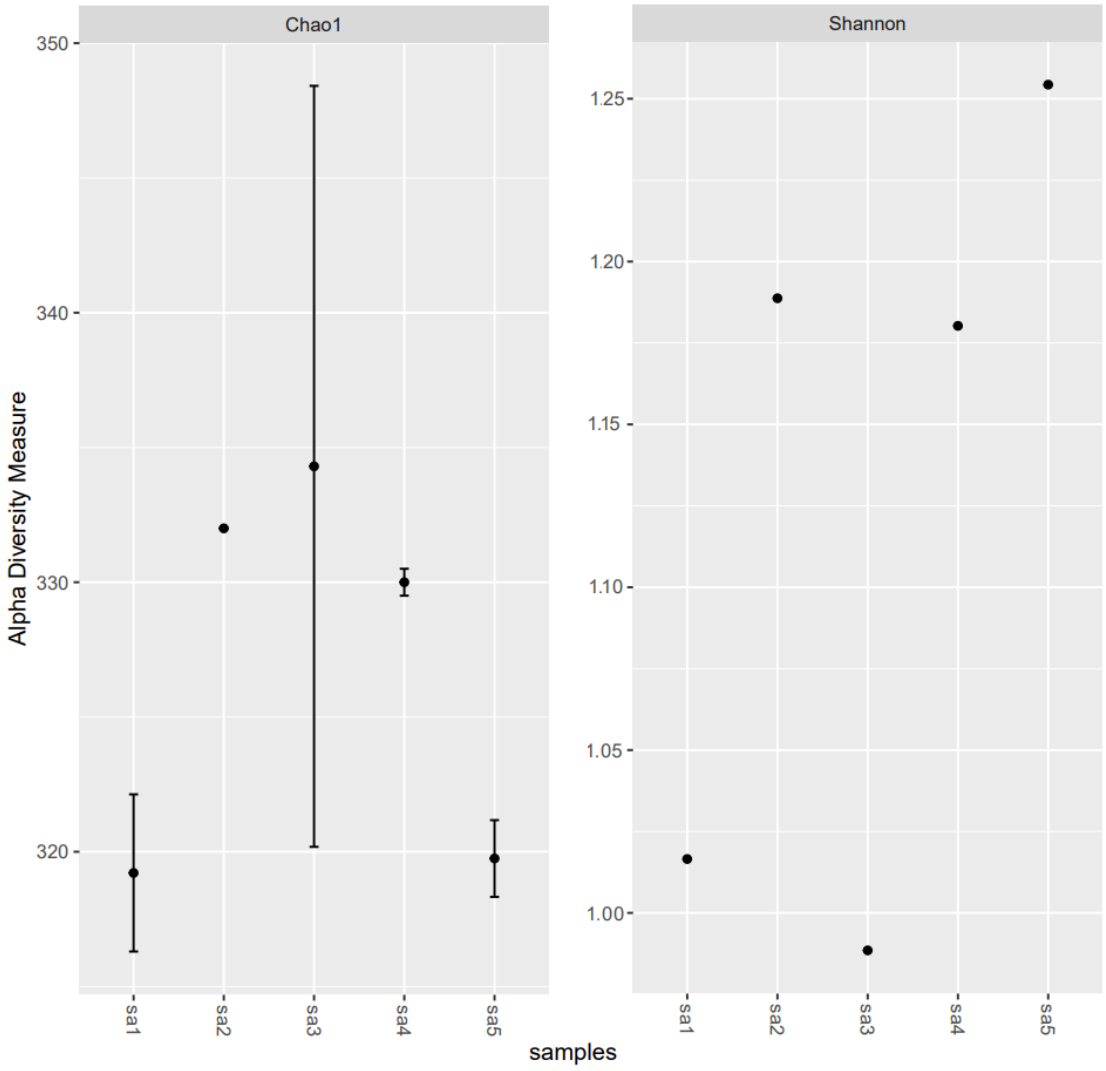

Figure 23: Alpha diversity measures (Chao1 & Shannon Index)

3. Functional mRNA Analysis

Following sorting and isolation of only bacteria mRNA, total mRNA from each sample was uploaded to MG-RAST to predict and quantify annotated biological functions across a wide-range of databases (Figure 24). Primarily, MG-RAST was utilized as a predictive tool to rapidly detail how many proteins could be annotated from the assembled mRNA and to what extent the data would be useful for metabolic modeling. MG-RAST demonstrated that a small proportion of residual rRNA remained in the samples following the technical removal of rRNA and other contaminants through the previously described kits. Furthermore, even through the SortmeRNA software, some rRNA remained with the mRNA.

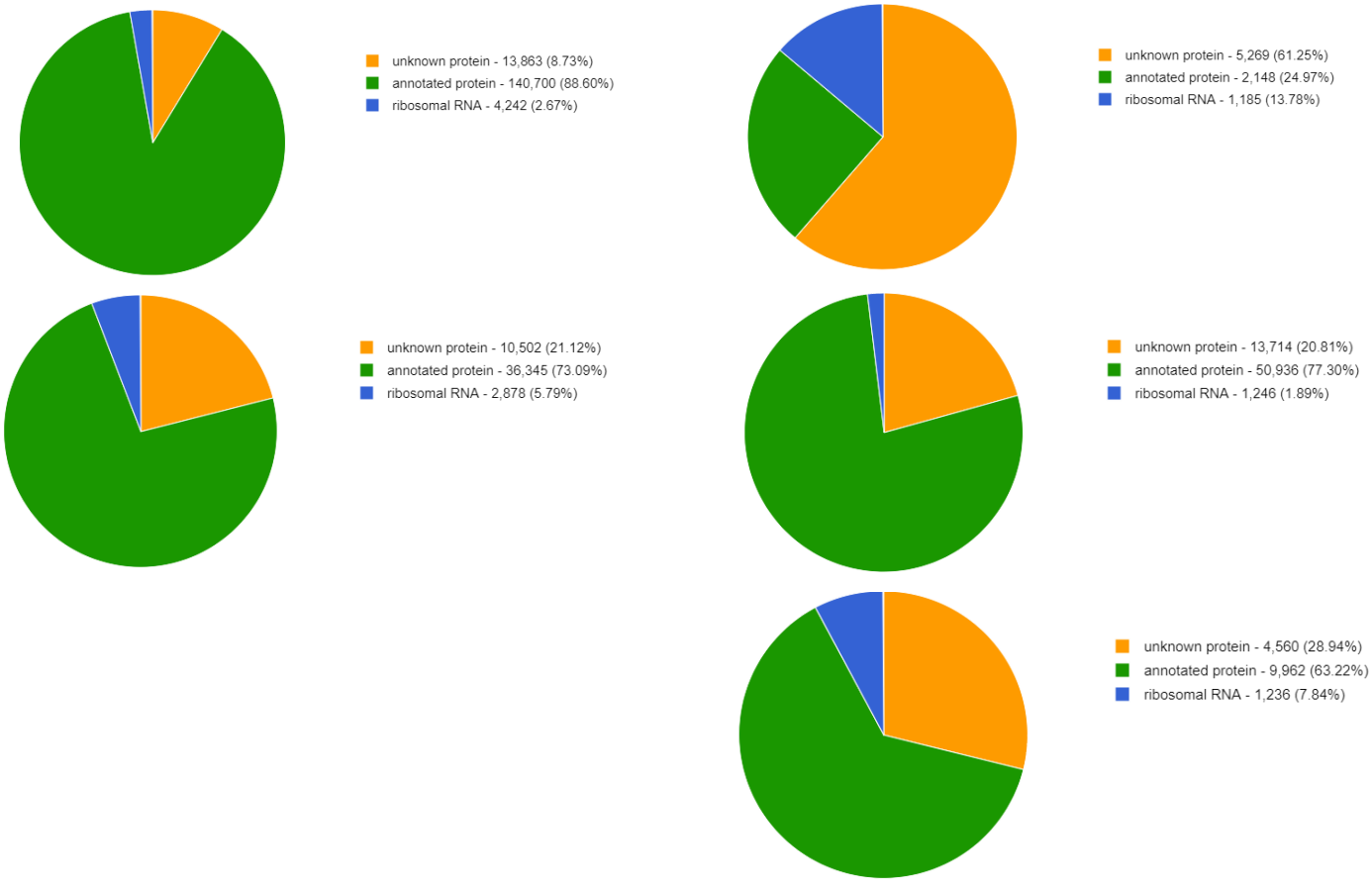

Figure 24: mRNA functional annotation prediction with MG-RAST. The samples are as followed: Sample H25361 (top-left), Sample H25362 (bottom-left), Sample H25363 (top-right), Sample H25364 (middle-right), Sample H25365 (bottom-right).

Next, the individual mRNA samples were cross-checked with KEGG annotation of predicted features to assess the extent of biological function of each sample that would map to metabolism and the usefulness for creating metabolic models (Figure 25). All except for one sample showed the greatest percentage of annotation to metabolism as assessed by KEGG. Specifically, sample H25363 illustrated that a small percentage (18.40%) of the transcriptome could be annotated to metabolism, thus highlighting that this sample may not be as effective as other samples for the reconstruction of metabolic models.

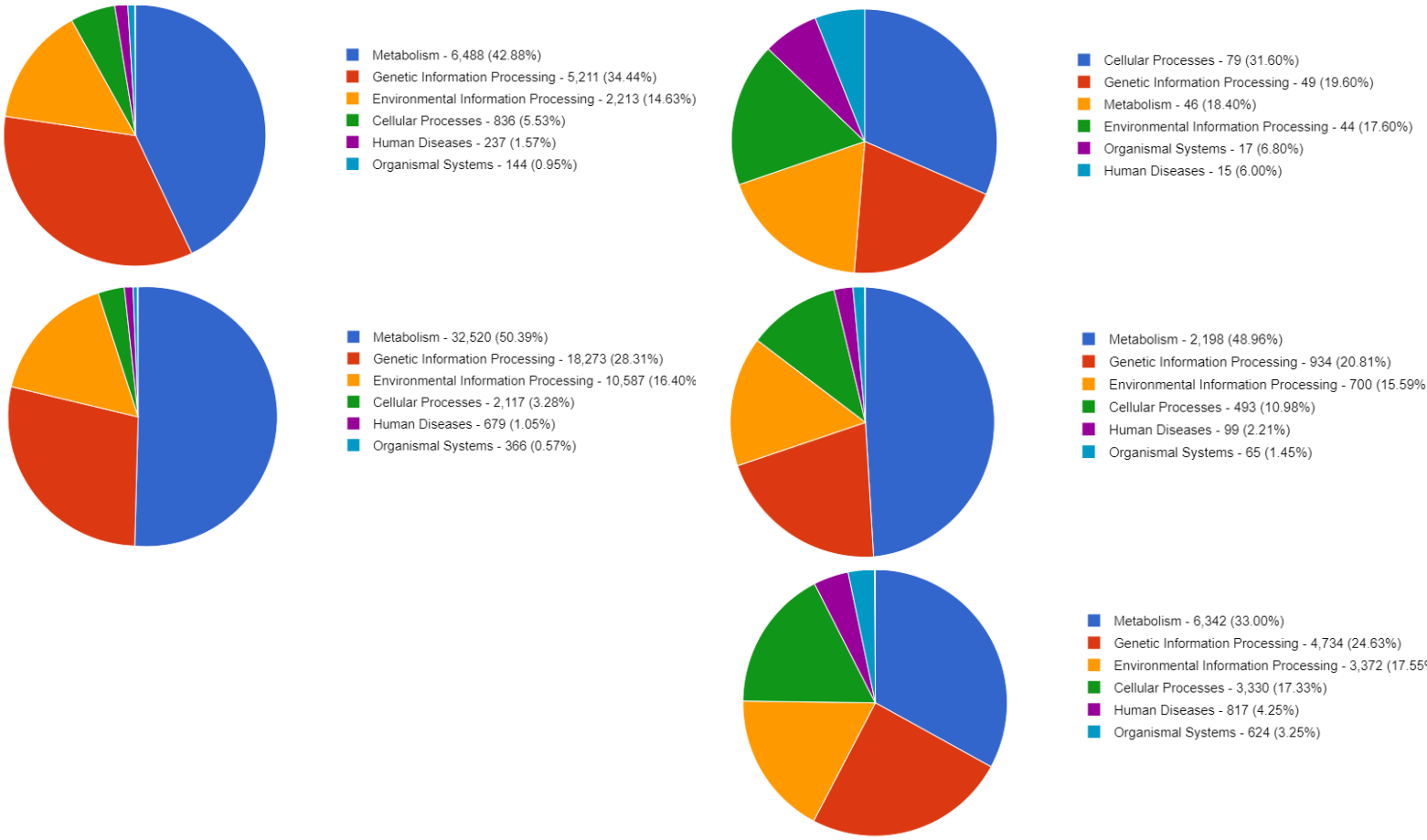

Figure 25: KEGG annotation of predicted features. Each pie chart represents the percentage of reads with predicted protein functions that can be annotated to KEGG functional database, based on various categories. The samples are as followed: Sample H25361 (top-left), Sample H25362 (bottom-left), Sample H25363 (top-right), Sample H25364 (middle-right), Sample H25365 (bottom-right).

Finally with regards to predicting annotated features with MG-RAST, mRNA was then checked against metabolic subsystem functional databases (Figure 26). This was ultimately necessary to uncover the functional aspects of each microbially community at the mRNA level prior to simulation in BacArena. As major metabolic functions are related to biomass reactions and energy growth yields that are required for balanced GEMs, these generally include the utilization of carbohydrates, protein production, amino acid use, and various factors are indeed predicted (Chan et al. 2017). Most interesting in the subsystems assessment is the presence of various factors which are known to be associated with UTI onset and occurrence. Specifically, all assessed mRNA from the patients were able to be annotated for both 'Cell Wall and Capsule' and 'Stress Response', these are essential features in classifying the onset of infection. Furthermore, 'Iron acquisition and metabolism' was identified in all samples (with the exception of sample H25364); acquisition of host-associated Fe is essential for a wide-range of virulence factors such as siderophore biosynthesis, virulence mechanisms in the bladder and kidney, biofilm production, and increase fitness; further metal-derived mechanisms are extensively described in the review article that is also part of this dissertation (Josephs-Spaulding et al. 2021).

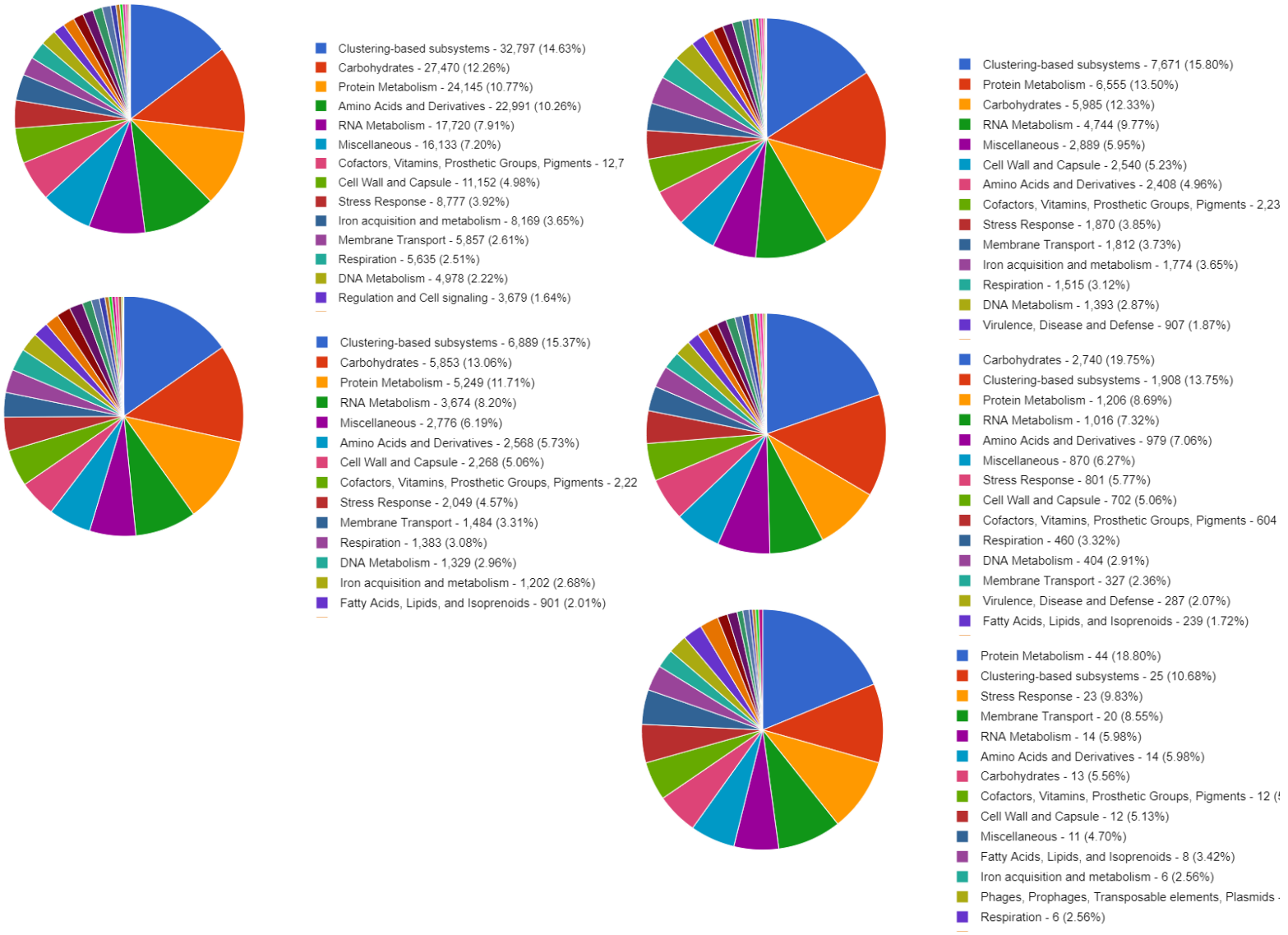

Figure 26: Subsystems annotation of predicted features. Each pie chart represents the percentage of reads with predicted protein functions that can be annotated to metabolic subsystem functional databases, based on various categories. The samples are as followed: Sample H25361 (top-left), Sample H25362 (bottom-left), Sample H25363 (top-right), Sample H25364 (middle-right), Sample H25365 (bottom-right).

4. Microbiome Community Metabolic Modeling

In total, four microbiome community models were assessed over a simulated 5 hour period. In the end, only four out of five samples were further selected for simulation. Specifically, sample 3 was found to have a poor annotation of the mRNA which would be necessary for creating context-specific models. Furthermore, the rRNA taxonomy analysis highlighted that the dominant genus is *Erwinia*, a plant associated pathogen. The remaining four samples were then simulated as context-specific microbiome models; community growth rate and individual bacteria metabolic consumption (represented as negative values and individual bacteria metabolite production (represented as positive values) was assessed. The four community models are interpreted independently, due to the fact that context-specific metabolic models have unique gene expression and thus unique microbial responses. With regards to the presentation of results, first the community simulations without context are displayed and interpreted, then the context-specific simulations, and finally a comparison between the two. It should be noted that the results that are observed from the non-context simulations should be practically similar, but with minor differences in metabolite uptake/production. This is not surprising as the models are based on the same metabolic models, however the abundance of microbes associated with that model will be different between patient simulations.

i. Case 1

1. Non-context simulation

With regards to the non-context-specific simulations, the three species which made up the community were proportionally balanced with an equal number of species for the start of the simulation. However, within 5 hours, it was noted that *E. coli* and *S. flexneri* became the most abundant microbiota, while *S. dysenteriae* was the least abundant organism. Next, the species-specific metabolite uptake / production was assessed. Most surprisingly is the consumption of acetaldehyde by *S. dysenteriae* as a probable energy source. While acetaldehyde is a known mutagenic metabolite to humans and is produced through ethanol metabolism by the liver (Guo and Ren, 2010), acetaldehyde toxicity does not appear to be a significant issue for *Salmonella spp.* (Penrod & Roth, 2020). Specifically, *Salmonella* spp. is able to concentrate and

utilize acetaldehyde not only as an energy source but also for pathogenesis *in vivo* (Burin & Shah, 2020). Similarly, it is also understood that UPEC utilizes acetaldehyde in a comparable fashion as *Salmonella* spp. as a growth advantage to incite infections (Dadswell et al. 2019). However, in the non-context simulations in Case 1, it was not observed that *E.coli* was utilizing acetaldehyde. Acetate was observed to be produced in high abundance from all bacteria within the described community. Specifically, acetic acid and acetate have been identified by NMR metabolomics as a key biomarker for the diagnosis of *E.coli* associated UTIs (Gupta et al. 2012; Lam et al. 2014 ; Lussu et al. 2017). Another interesting observation is the uptake of glycine betaine (BET) by mostly *S. dysenteriae* and to a smaller extent, by *E. coli*. While BET utilization is understood to be used in humans as an osmoprotectant molecule of the kidney, it is additionally utilized by *E. coli*, for initiating pathogenesis in the kidneys (Kunin et al. 1992 ; Peddie et al. 1996). However, the present literature surrounding the role of BET in UTIs remains sparse; although BET as a use for microbial transition into the kidneys should not be overlooked as a potential pathomechanism of rUTIs. Another important osmoregulation metabolite that requires attention in the role of rUTIs is choline (Ly et al. 2020). The simulations from this case demonstrate a production of choline from all microbiota, while it is higher in *S. dysenteriae* the production of choline is far lower in both *S. flexneri* and *E. coli*. While choline production is not directly associated with the onset of UTIs, choline levels are known to play a significant role in overactive bladder syndrome (David et al. 2020 ; David et al. 2020). An additional biomarker of interest is carbon dioxide (CO2) production by all members of the investigated microbial community. CO2 is produced in greater quantities by *S. dysenteriae* in comparison to the other members, this is most likely due to high quantities of sugar that is concentrated in the urine and being utilized as an energy source by the pathogens (Yang & Shen, 1989). Specifically, high quantities of glucose in urine favors bacterial growth and promotes UTI onset (Wilke et al. 2015). For example, in the case of diabetes, it was found that urine with greater glucose concentrations increases biofilm forming potential in diabetic patients (Pillai et al. 2004). While few cases of UTIs that are associated with CO2 dependent *E.* coli have been reported (Tena et al. 2008), the mechanisms of utilizing CO2 is conserved across a wide-range of uropathogens within the family *Enterobacteriaceae* (including uropathogenic

Klebsiella spp.) in addition to *Staphylococcus aureus* (Rahman, 1977 ; Barker et al. 1978). While the true incidence of CO2-associated UTIs may be underrecognized, this may still be a valuable means to identify uropathogenic bacteria which utilize sugars from the host urine. Formate was found to be strongly produced by both *S. flexneri* and *E. coli*, recently it has been identified by NMR metabolics that formate, acetate, lactate, succinate are all able to be used as a biomarker to differentiate those with UTIs, from healthy controls (99.5% accuracy) (Gupta et al. 2012). The uptake of L-aspartate by both *S. flexneri* and *E. coli* is likely involved in biofilm formation. For example, it is understood that the two-component systems, a rapid mediator of stress related stimuli, uses phosphate in tandem with aspartate as a regulator of response to further incite biofilms (Guo et al. 2021). As previously mentioned, uropathogenic bacteria likely utilize sugars from the host urine as a primary growth substrate (Reidl et al. 1991). For example, glucose can be utilized by potential uropathogens such as *Enterococcus faecalis* for the production and regulation of biofilms in host systems (Pillai et al. 2004). It was observed that maltose was consumed by all three microbes and sucrose was mainly consumed by *E.coli* and *S. dysenteriae* to a minor level. However, the effects of resting glucose in non-diabetic individuals in relation to UTI onset and recurrence require further investigation.

2. Context-specific simulation

Within the context-specific simulations of the microbial community leading to UTI from Case 1, there are now some unique aspects that have changed when conditioning the communities with context-specific gene expression. For example, *E. coli* is now the fastest growing bacteria and is closely tied to the growth rate of *S. dysenteriae*, while *S. flexneri* is far lower. Furthermore, it was observed that acetate production is high in all bacteria, with the exception of *S.dysenteriae.* It was previously described that acetate is a significant biomarker of UTI onset in compared to healthy individuals (Gupta et al. 2012; Lam et al. 2014 ; Lussu et al. 2017). Furthermore, the metabolic consumption of BET is now present in all species, indicating the potential of all bacteria to transcend into the kidneys. Choline production is observed in all bacteria, however it is less for *S. dysenteriae* and in a strong abundance by both *S. flexneri* and *E.coli*. These results indicate that the latter two bacteria may be more effective than *S. dysenteriae* with regards to osmoprotective potential. CO2 is also produced in low amounts in

the context-specific models. Most interesting in the context-specific models is the low-level but significant production of the D-amino acid D-alanine by *E.coli,* and not any other microbe. D-alanine is one of the most common amino acids in bacteria cell walls and is used for the synthesis of peptidoglycan. Specifically, when D-alanine is utilized in microbial cell walls, the bacteria may have increased chemical resistance to proteases and antimicrobials (Sasabe & Suzuki, 2018). Formate is observed to be produced only by *S. flexneri* and *E.coli* which is also similar to the non-context-specific model. However within the context-specific models, it is noted that *S. flexneri* began to utilize glycerol as an energy source. Furthermore, there was evidence of cross-feeding of glycerol from *S. dysenteriae* to *S. flexneri*. It is presently understood that uptake and catabolism of glycerol is necessary for bacterial replication during epithelial infection of the intestines for the case of *L. monocytogenes* and *S. flexneri* as it is readily available from host cells (Alteri et al. 2015 ; Doi, 2019). Another notable observation with regards to metabolite production, is the substantial increased production of L-Lactate by *S. dysenteriae* which may act as a biomarker of pathogenesis. L-lactate in the context specific model was greatly produced as a byproduct of bacterial metabolism as an associate of inflammation and thus a biomarker of infection (Rabinowitz & Enerbäck, 2020 ; Wang et al. 2020). Finally, maltose is taken up by all pathogens within this simulation as a likely energy source.

When comparing the differences between the non-context and context-specific communities, growth rate does not appear to be drastically changed. However, metabolic changes when comparing non-context to context-specific community model simulations does highlight some interesting changes. For example, acetaldehyde was observed to be utilized by *S. dysenteriae* in the non-context-specific models, this is not true for context-specific models. Acetate production also seems similar between both communities, however within the context-specific models, only *S. dysenteriae* has a significantly lower production of acetate. BET consumption also drastically changed between the non-context and context. Specifically, *S. dysenteriae* relied heavily on BET uptake, while BET uptake was not observed in *S. flexner* and in small amounts for UTI8 in the non-context simulations. However in contrast with regards to the context-specific models, BET was lowly taken up by *S. dysenteriaie* and taken up in far

greater amounts in both *S. flexneri* and *E. coli*. With regards to choline, the production of this metabolite cut in almost half for *S. dysenteriae* when comparing the non-context specific to context-specific models. Furthermore, *S. flexneri* does not produce choline and *E. coli* produces it in low quantities in the non-context simulations. However in the context-specific simulations, both *S. flexneri* and *E.* coli are producers of choline. The production of D-alanine by *E.coli* is a unique observation in only the context-specific models and should be further investigated in this patient as a potential resistant mechanism for antimicrobial treatment. The production of formate by *S. flexneri* and *E. coli* remains similar between both simulations. However, the utilization of glycerol by *S.flexneri* and apparent cross-feeding which is only observed in the context-specific models is another peculiar biomarker which may require investigation; this in addition to D-alanine production in *E. coli* may point towards a chronic co-infection between both pathogens. While L-aspartate is utilized only in the non-context simulations, L-lactate is rather produced in small amounts by *E. coli* and to a greater extent by *S. dysenteriae*.

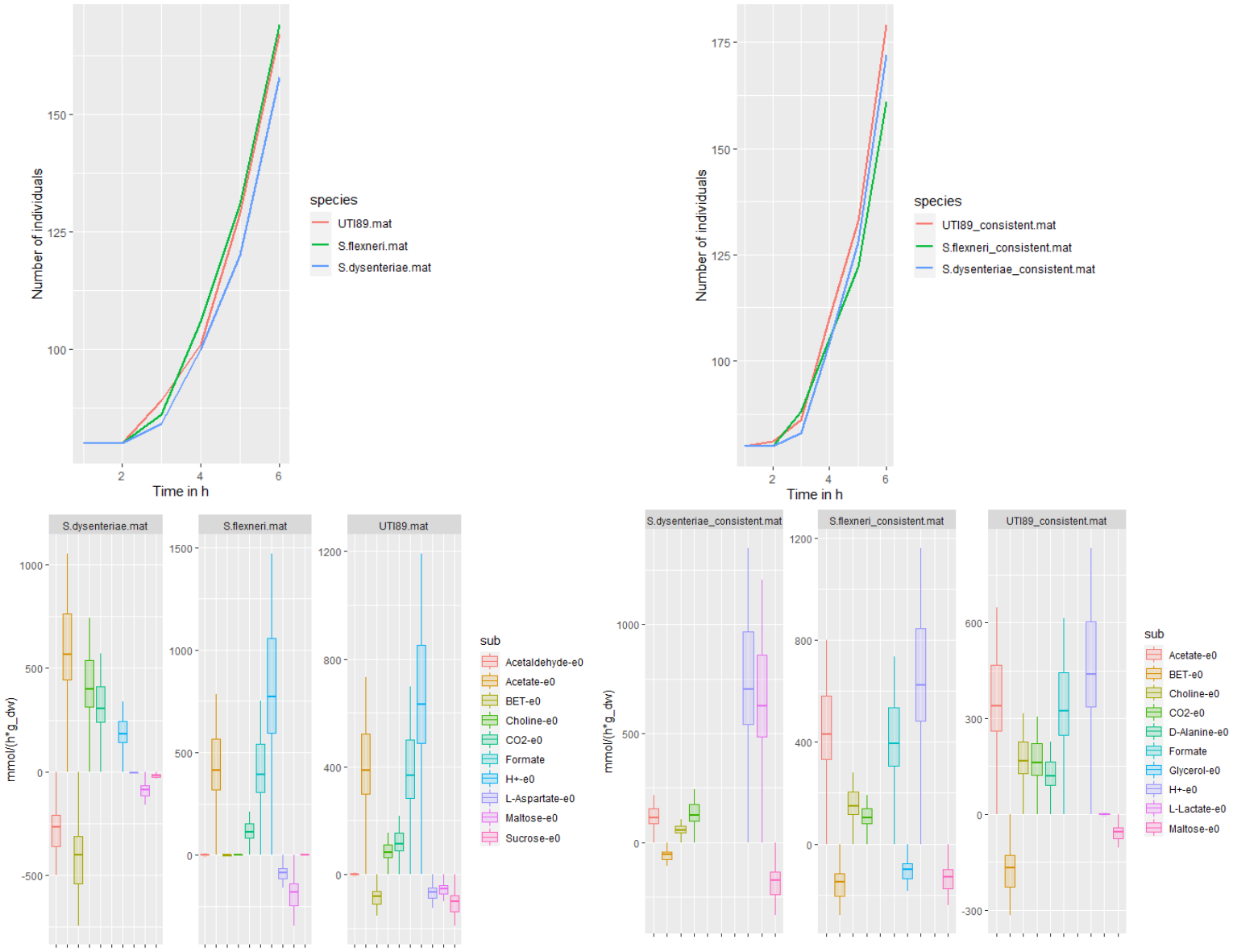

Figure 27: Simulated microbiome community interactions from Case 1 of the UTI cohort.

Left column describes non-context-specific simulations, the right column describes context-specific simulations. Top row shows community growth rate, bottom row shows species-specific top-10 changed substances during the simulation.

ii. Case 2

1. Non-context simulation

With regards to the growth rate of the non-context microbial simulation, *E.coli* remained as the dominant community member while *S. flexneri* and *S. dysenteriae* remained as slowly growing members. One unique metabolite production in these non-context-specific simulations is the production of 1,2 propanediol by all microbes, with a far less extent by *S. dysenteriae*. NMR metabolomics has suggested that UTIs caused by *K. pneumoniae* utilize glycerol from the host and convert this chemical to 1,3-propanediol in addition to acetate as classic biomarkers of UTIs (Gupta et al. 2006). BET is observed to be consumed mainly by *S. dysenteriae* and to a smaller extent, by *E. coli*. Choline production by *S. dysenteriae* and *E. coli* matches previous observations as stated in Case 1. The same is true for the production of formate, and the consumption of L-aspartate, maltose, sucrose as energy sources. However, it is not surprising that the non-context models differ with regards to metabolic potential; all non-context utilize similar models, but with different abundances.

2. Context-specific simulation

With regards to the growth rate of the non-context microbial simulation, *E.coli* remained as the dominant community member while *S. flexneri* and *S. dysenteriae* remained as slowly growing members. Overall, metabolite production and uptake is quite similar between Case 1 and the presently defined Case. However there are a few exceptions which make the investigation of this case unique. For example, it was noted that *E. coli* began to utilize glucuronate. Glucuronate is generally produced in the human kidneys as a means to both detoxify and excrete water products into the urine (Yu et al. 2018). However, this sugar acid is generally derived from glucose and plays an important role in microbial central carbon metabolism and likely improves *E. coli* fitness in the urothelium by inducing chronic inflammation (Alteri & Mobley, 2015). When investigating the cross-feeding interactions in the context-specific models, it was identified that *S. dysenteriae* supports *E. coli* with the production of ornithine (Albersen et al. 2007 ; Keogh et al. 2016). Specifically, it has been

investigated that *E faecalis* is able to promote the pathogenic growth of *E. coli* even if the host limits Fe acquisition to the pathogen. *E. faecalis* supports *E.coli* by providing *E. coli* with L-ornithine which cues *E. coli* to initiate polymicrobial biofilms and further supports the synthesis of siderophores, thus further bolstering Fe acquisition (Keogh et al. 2016). These unique observations in the context-specific simulations highlight specific biomarkers which likely bolster the potential of UTI infections by either increasing pathogen virulence or supporting recurrence through resistance in the cell walls or by biofilm production. More so, both metabolically-derived biomarkers that were observed in this case can act as likely targets to mitigate future patient recurrence.

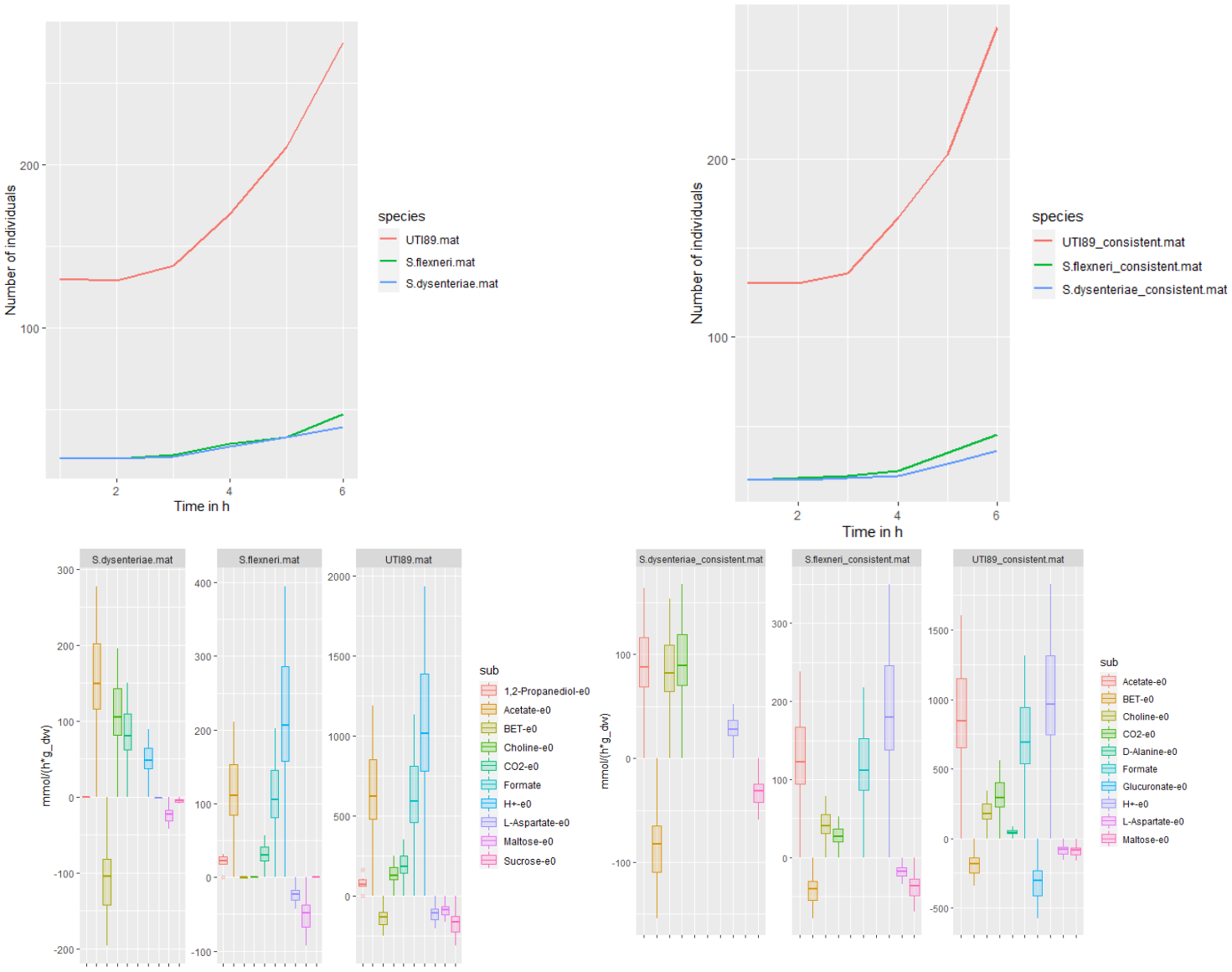

Figure 28: Simulated microbiome community interactions from Case 2 of the UTI cohort.

Left column describes non-context-specific simulations, the right column describes context-specific simulations. Top row shows community growth rate, bottom row shows species-specific top-10 changed substances during the simulation.

iii. Case 3

1. Non-context simulation

With regards to the growth rate of the non-context microbial simulation, *E.coli* remained as the dominant community member while *S. flexneri* and *S. dysenteriae* remained as slowly growing members. As mentioned previously, the simulations within this case are comparable to all aforementioned cases when non-context-specific models are simulated. Therefore for further information on the discussion of previous metabolites in the role of UTI onset, Case 1 should be reviewed.

2. Context-specific simulation

With regards to the growth rate of the non-context microbial simulation, *E.coli* remained as the dominant community member while *S. flexneri* and *S. dysenteriae* remained as slowly growing members. However, *S. dysenteriae* became the dominant member over *S. flexneri* in the context-specific simulation. While the presence of acetate, BET, choline, CO2, formate, maltose, and sucrose remain the same across most context-specific simulations that are presented in this chapter, there is a single unique characteristic that ought to be highlighted. Specifically, sorbitol was identified to be produced by the studied *E. coli.* Specifically, this metabolite has been observed to confer a competitive advantage during chronic cystitis by utilizing free glucose in the host environment; in the case of this context-specific simulation study all studied microbiota are consuming maltose and *E. coli* alone is consuming sucrose (Conover et al. 2016). Furthermore, it has been observed that by deleting major genes which control the consumption of sorbitol leads to a major competitive defect in virulence and fitness of UPEC (Conover et al. 2016).

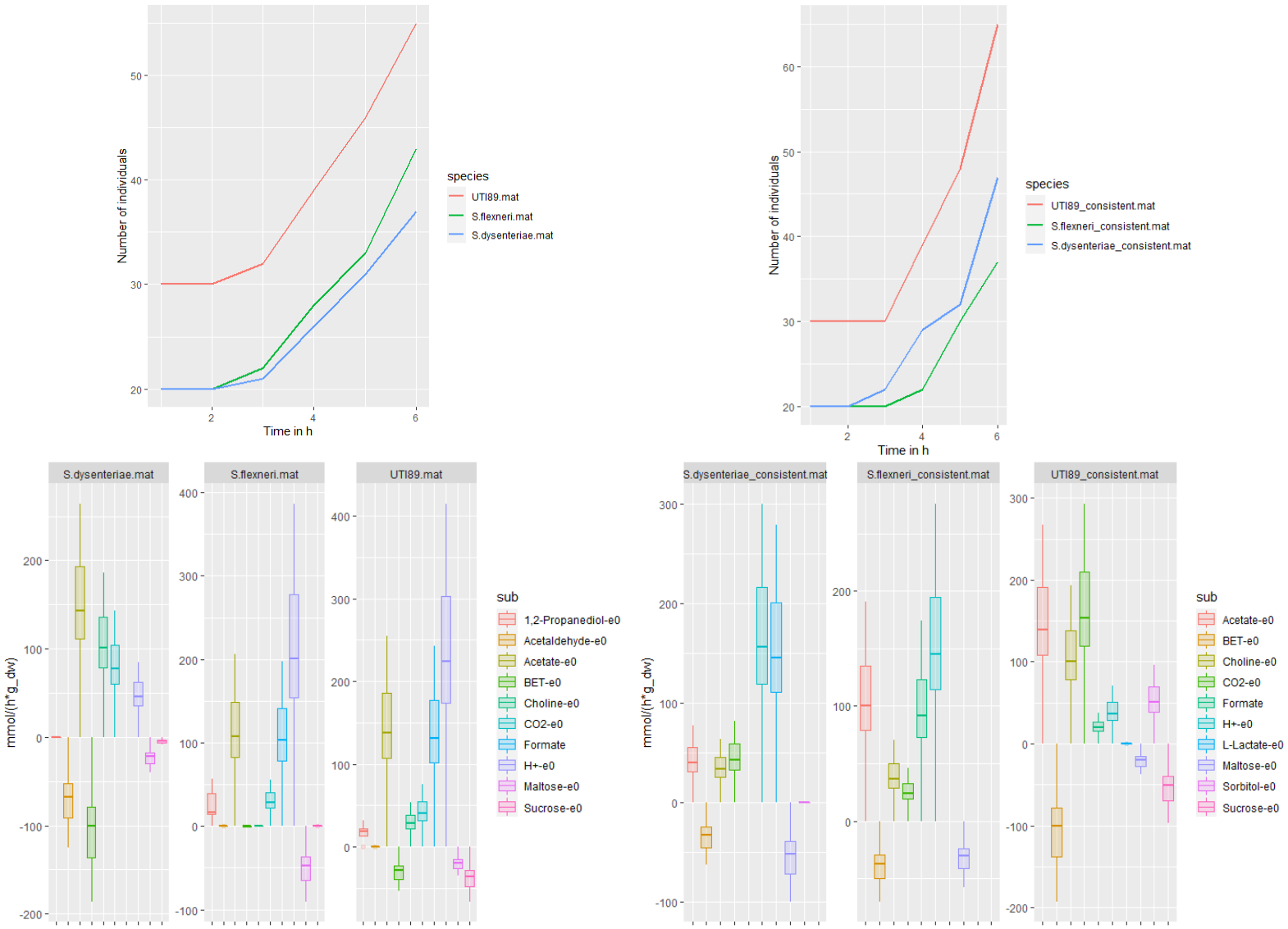

Figure 29: Simulated microbiome community interactions from Case 3 of the UTI cohort.

Left column describes non-context-specific simulations, the right column describes context-specific simulations. Top row shows community growth rate, bottom row shows species-specific top-10 changed substances during the simulation.

iv. Case 4

1. Non-context simulation

With regards to the growth rate of the non-context microbial simulation, *S. dysenteriae* remained a dominant member with *S. flexneri's* growth being closely associated. However, *E. coli* remained as a slow growing pathogen. As mentioned previously, the simulations within this case are comparable to all aforementioned cases when non-context-specific models are simulated. Therefore for further information on the discussion of previous metabolites in the role of UTI onset, Case 1 should be reviewed.

2. Context-specific simulation

With regards to the metabolite uptake and production within the context-specific simulation, this simulation remained fundamentally similar to previous simulations, however there was one notable change. First, there was cross-feeding of glycerol from *S. dysenteriae* to *S. flexneri* which was likely utilized as an energy source by *S. flexneri*. Interestingly, NMR metabolomics has suggested that UTIs caused by *K. pneumoniae* utilize glycerol and convert this chemical to 1,3-propanediol, acetate, ethanol, and succinate (Gupta et al. 2006). It was observed in this simulation that *S. flexneri* does produce both 1,3-propanediol and acetate, suggesting a similar metabolic pathomechanism between both bacteria that are linked to UTIs. With that, this is the first context-specific community model which demonstrated the minor production of 1,3-propanediol which is most likely associated with glycerol cross-feeding.

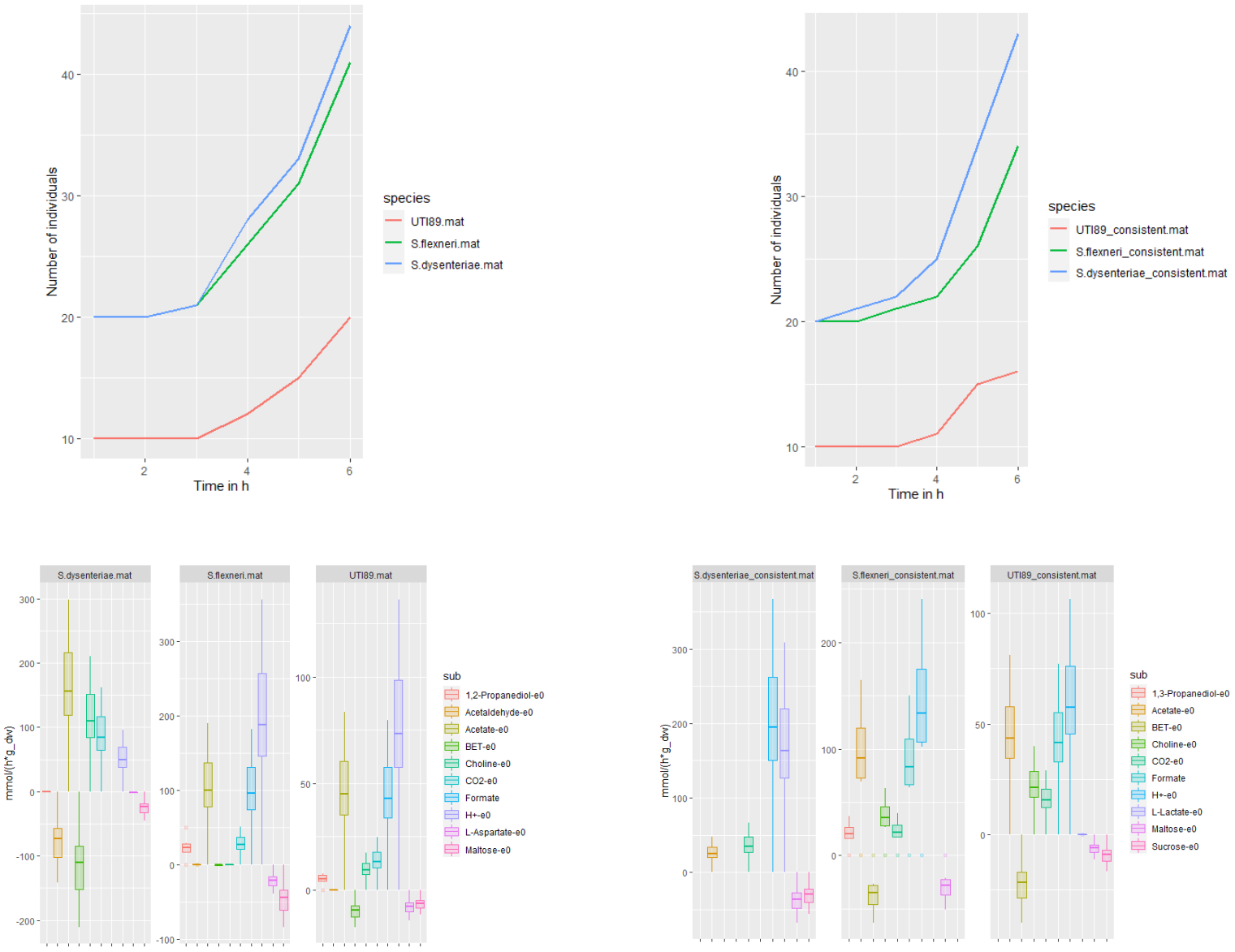

Figure 30: Simulated microbiome community interactions from Case 4 of the UTI cohort.

Left column describes non-context-specific simulations, the right column describes context-specific simulations. Top row shows community growth rate, bottom row shows species-specific top-10 changed substances during the simulation.

V. Summary, Implications, Conclusions, and Suggestions for Future Research

This dissertation seeks to pave the foundation of precision medicine through the application of systems biology to bolster our interpretations of disease onset, treatment, and diagnosis; all host-centric diseases require a holistic and systems-level approach. There is an overarching need to understand human disease as a dynamic system, complicated by host-associated environments and dysbiotic microbial communities. Integrating the ecological interactions between the host and microbial factors is necessary to progress disease diagnosis and therapy in the age of antimicrobial resistance and global pandemics. This integration includes observations of the human microbiome in health and disease, host metabolic dysregulation, and dietary contaminants such as antibiotics or transition metals. This information can be processed through the combination of transcriptomics, *in silico* metabolic modeling or systems biology methods which are representative of the host. Overall, the broad framework of systems medicine in tandem with omics-based analysis can pave the way towards a mechanistic understanding of evidence-based diagnosis and treatment for disease. Thus advancing systems biology applications and precision medicine practices towards understanding disease pathopathology is ultimately necessary to effectively treat patients. Specifically, the previously proposed research question: "how do various pathologies (microbial or viral) drive cell or microbiome-specific metabolic pathways in a way that is either unique to a single patient or a group of closely-related individuals?" has now been answered. Through the application of metabolic network model reconstruction, pathway analysis, and simulations of microbial communities, the impact of microbial infection upon hosts in a patient-specific manner has been elucidated in this dissertation.

With regards to the metabolic model reconstruction of single-cells during the course of COVID-19, the application of metabolic network reconstruction with conditioning both by an artificial blood medium and patient-specific transcriptomes across 358930 led to the creation of 299163 (83.34% model reconstruction success rate) metabolic models from 14 patients and 12 cell types. By assessing metabolic reaction abundance across patients with numerous timepoints, observations which correspond with severe disease status were identified in

erythroid, megakaryocytes, and plasmablast cell types. For example, patients who transitioned towards a severe status were found to have erythroid cells with an increased average of fatty acid oxidation which modulates erythropoietin production and effectively mediates stress through anti-inflammatory properties (Wang et al. 2014). Erythroid cells during severe or complicated disease status were also observed to have increased metabolic pathway abundance which correspond with increased production of inositol and pentose phosphate metabolism, both are essential in the regulation of heme synthesis; platelet formation is a key player in COVID-19 disease severity (Lemke & Silverman, 2020 ; Marcero et al. 2021). Megakaryocytes are also major players in the production of blood platelets and are necessary for clotting (Nayak et al. 2019). However, the results from the metabolic models presented in this dissertation identified that the average bile acid synthesis is almost doubled in a patient during a critical disease status, rather than a less severe complicated status. Bile acid synthesis is important to inhibit the aggregation of platelets and prior to COVID-19 hyperinflammation and may be a preventative mechanism to prevent aggregation of platelets which can lead to severe disease (Cheng et al. 2020). Observations of plasmablast metabolic hyperactivation tends to be associated with this immune cell's response to infection. For example, when plasmablasts recognize viral particles, heme biosynthesis and inositol phosphate metabolism is increased, which was observed in the metabolic models (Li et al. 2017). Furthermore glycolysis and gluconeogenesis is significantly increased during critical disease status as compared to complicated, enhanced glycolysis tends to provoke memory B-cells to transition into plasmablasts during inflammation and increases plasma cell durability (Qi et al. 2021). Overall, there are a wide-range of metabolic subsystems which are increased or decreased as patients transition from health to disease; these observations are well-discussed in the previous results section.

With regards to the reconstruction and simulation of microbiome community models which are representative of patient-specific UTIs, the metatranscriptomic analysis highlighted that there are several bacteria members which are present during a UTI and in most cases, these pathogens collaborate in a community. Specifically, context-specific model reconstruction highlighted unique metabolic observations which are compatible with previous experimental findings that were previously published in the literature. For example, the context-specific

simulations highlighted the production of D-alanine by *E. coli*, this amino acid is utilized in the cell wall of bacteria and can bolster an organism's resistance to antimicrobials; meaning that this bacteria is likely resisting treatment and can incite a recurrent infection (Sasabe & Suzuki, 2018). Additionally, it was found that *S. dysenteriae* was producing glycerol and crossfeeding this metabolite to *S. flexneri*; microbial use this compound by first stealing it from the host and can then be utilized by pathogens to increase bacteria replication (Alteri et al. 2015 ; Doi, 2019). As previously suggested in this dissertation with regards to UTI species collaboration, it was found that *S. dysenteriae* supports E. *coli* with the production of ornithine. This compound allows *E. coli* to further uptake L-ornithine thereby increasing the biosynthesis of siderophores to uptake Fe from the host and to initiate biofilm formation, thereby increasing virulence and persistence (Albersen et al. 2007 ; Keogh et al. 2016). Overall, the conversion of metatranscriptomic datasets towards context-specific metabolic models and simulations identified several valuable biomarkers which can be utilized for patient-specific and targeted treatment options for those with rUTIs.

Systems biology as a science seeks to integrate multiple independent aspects of biology to bolster our understanding of complex biological phenomena. By integrating NGS datasets which are representative of patient-specific factors, such as microbiome, transcriptomes, and metabolomes, the work detailed in this dissertation seeks to move closer towards patient-specific systems medicine. While these approaches and frameworks are holistic and seek to assess the entire picture of the patient, they are not without limitations. Limitations of the methodologies will always remain; no model is truly perfect or without flaws. First, the datasets presented in this study are not all-inclusive. As RNA-Seq was utilized as the major molecular dataset, there remains uncertainty with the effects of individual patient genomes, proteomes, clinical comorbidities, lifestyle, and so forth, have upon the success of metabolic network model reconstruction. Second, is with regards to the discovery of general biomarkers that were flagged in both studies and their usefulness in precision medicine. As information upon each patient is not thoroughly integrated into the GEMs and manually curated (only RNA-seq and general blood or urine metabolome), the usefulness of the identified biomarkers need to be criticized as useful for that patient based on some assumptions. However, this limitation may be solved with

more patient-derived information and machine learning algorithms which may mechanistically predict personalized therapies which further include key biological information that is relevant to the patient in addition to biomarkers (Angione, 2019). Finally, the largest limitation in the use of GEMs for the application of precision medicine is with personal uncertainty or bias in the steps to create models. For example, GEMs reconstruction requires genome annotation, environmental specifications, the formulation of relevant biomass reactions, and gap-filling within the metabolic network (Bernstein et al 2021). Furthermore, models can have a vast variety of interpretations by the choice of flux simulation. All of these factors add high levels of uncertainty to model reconstruction, not to mention the high diversity of bioinformatics tools to preprocess data. As one significant aim for the integration between GEMs and precision medicine is to pave the foundation for *in silico* clinical trials, there is a need to extrapolate these limitations towards findings that can be replicated and useful to the patient.

To date, this dissertation is a cumulation of literature knowledge and systems biology applications which seeks to investigate the application of metabolic network reconstruction within a systems medicine framework to uncover the pathomechanisms underlying COVID-19, UTIs, and PD through the lens of precision medicine. Systems medicine is evolving more rapidly as it becomes available; this recent availability of tools, methods, and datasets is rapidly becoming translated into patient-specific models of biological systems. In particular, while the ailments presented in this manuscript have become some of the most common types of human diseases, they are also poorly understood as a complicated system. Foundational understanding of complex disease mechanisms are expanded with computational and mathematical modeling of biological systems through a systems approach. By integrating and modeling multiple biological properties which underlie metabolic networks, the properties of biological systems are readily uncovered. Metabolic profiles and respective biochemical concentrations are useful for biomarker identification and have an extended value in the creation of metabolic models for systems biology applications. While systems biology methods have numerous applications, in the case of this dissertation they provide a novel outlook to investigate patient-specific disease status within certain contexts. Furthermore, the findings in this dissertation suggest that human metabolic functions drastically change during various states of disease and are useful in the

characterization of disease trajectories or mechanisms. However, there still remains a need to further advance meta-modeling application to humans in a clinical setting to provide new information on human-microbial interactions. Specifically, by further developing patient-specific approaches which include both unique biological data and biomarkers in a personalized approach is the next major step forward for creating the foundation for *in silico* clinical trials.

VI. References

Abat, C., Raoult, D., and Rolain, J.-M. (2016). Low Level of Resistance in Enterococci Isolated in Four Hospitals, Marseille, France. Microb. Drug Resist. 22, 218–222. doi:10.1089/mdr.2015.0121.

Abramov, A. Y., Potapova, E. V, Dremin, V. V, and Dunaev, A. V (2020). Interaction of Oxidative Stress and Misfolded Proteins in the Mechanism of Neurodegeneration. Life (Basel, Switzerland) 10. doi:10.3390/life10070101.

Abubucker, S., Segata, N., Goll, J., Schubert, A. M., Izard, J., Cantarel, B. L., et al. (2012). Metabolic reconstruction for metagenomic data and its application to the human microbiome. PLoS Comput. Biol. 8, e1002358. doi:10.1371/journal.pcbi.1002358.

Aden, K., Rehman, A., Waschina, S., Pan, W. H., Walker, A., Lucio, M., et al. (2019). Metabolic Functions of Gut Microbes Associate With Efficacy of Tumor Necrosis Factor Antagonists in Patients With Inflammatory Bowel Diseases. Gastroenterology 157, 1279-1292.e11. doi:10.1053/j.gastro.2019.07.025.

Agren, R., Bordel, S., Mardinoglu, A., Pornputtapong, N., Nookaew, I., and Nielsen, J. (2012). Reconstruction of genome-scale active metabolic networks for 69 human cell types and 16 cancer types using INIT. PLoS Comput. Biol. 8, e1002518. doi:10.1371/journal.pcbi.1002518.

Ahmad, T., Khan, M., Haroon, Musa, T. H., Nasir, S., Hui, J., et al. (2020). COVID-19: Zoonotic aspects. Travel Med. Infect. Dis. 36, 101607. doi:10.1016/j.tmaid.2020.101607.

Albersen, M., Joniau, S., Van Poppel, H., Cuyle, P.-J., Knockaert, D. C., and Meersseman, W. (2007). Urea-splitting urinary tract infection contributing to hyperammonemic encephalopathy. Nat. Clin. Pract. Urol. 4, 455–458. doi:10.1038/ncpuro0877.

Aller, S., Scott, A., Sarkar-Tyson, M., and Soyer, O. S. (2018). Integrated human-virus metabolic stoichiometric modelling predicts host-based antiviral targets against Chikungunya, Dengue and Zika viruses. J. R. Soc. Interface 15. doi:10.1098/rsif.2018.0125.

Alteri, C. J., and Mobley, H. L. T. (2015). Metabolism and Fitness of Urinary Tract Pathogens. Microbiol. Spectr. 3. doi:10.1128/microbiolspec.mbp-0016-2015.

Alteri, C. J., Himpsl, S. D., and Mobley, H. L. T. (2015). Preferential Use of Central Metabolism In Vivo Reveals a Nutritional Basis for Polymicrobial Infection. PLOS Pathog. 11, e1004601. Available at: https://doi.org/10.1371/journal.ppat.1004601.

Anatoliotaki, M., Galanakis, E., Tsekoura, T., Schinaki, A., Stefanaki, S., and Tsilimigaki, A. (2003). Urinary Tract Infection Caused by Shigella sonnei. Scand. J. Infect. Dis. 35, 431–433. doi:10.1080/00365540310009077.

Anders, S., Pyl, P. T., and Huber, W. (2015). HTSeq—a Python framework to work with high-throughput sequencing data. bioinformatics 31, 166–169.

Andersen, T. E., Khandige, S., Madelung, M., Brewer, J., Kolmos, H. J., and Møller-Jensen, J. (2012). Escherichia coli uropathogenesis in vitro: invasion, cellular escape, and secondary infection analyzed in a human bladder cell infection model. Infect. Immun. 80, 1858–1867. doi:10.1128/IAI.06075-11.

Anderson, G. G., Palermo, J. J., Schilling, J. D., Roth, R., Heuser, J., and Hultgren, S. J. (2003). Intracellular bacterial biofilm-like pods in urinary tract infections. Science 301, 105–107. doi:10.1126/science.1084550.

Andreini, C., Bertini, I., Cavallaro, G., Holliday, G. L., and Thornton, J. M. (2008). Metal ions in biological catalysis: from enzyme databases to general principles. J. Biol. Inorg. Chem. JBIC a Publ. Soc. Biol. Inorg. Chem. 13, 1205–1218. doi:10.1007/s00775-008-0404-5.

Andrews, S. (2017). FastQC: a quality control tool for high throughput sequence data. 2010.

Anger, J., Lee, U., Ackerman, A. L., Chou, R., Chughtai, B., Clemens, J. Q., et al. (2019). Recurrent Uncomplicated Urinary Tract Infections in Women: AUA/CUA/SUFU Guideline. J. Urol. 202, 282–289. doi:10.1097/JU.0000000000000296.

Angione, C. (2019). Human Systems Biology and Metabolic Modelling: A Review-From Disease Metabolism to Precision Medicine. Biomed Res. Int. 2019. doi:10.1155/2019/8304260.

Aragón, I. M., Herrera-Imbroda, B., Queipo-Ortuño, M. I., Castillo, E., Del Moral, J. S.-G., Gómez-Millán, J., et al. (2018). The Urinary Tract Microbiome in Health and Disease. Eur. Urol. Focus 4, 128–138. doi:10.1016/j.euf.2016.11.001.

Ashkar, A. A., Mossman, K. L., Coombes, B. K., Gyles, C. L., and Mackenzie, R. (2008). FimH adhesin of type 1 fimbriae is a potent inducer of innate antimicrobial responses which requires TLR4 and type 1 interferon signalling. PLoS Pathog. 4, e1000233. doi:10.1371/journal.ppat.1000233.

Assefa, S., and Köhler, G. (2020). Intestinal Microbiome and Metal Toxicity. Curr. Opin. Toxicol. 19, 21–27. doi:10.1016/j.cotox.2019.09.009.

Atarashi, K., Tanoue, T., Shima, T., Imaoka, A., Kuwahara, T., Momose, Y., et al. (2011). Induction of colonic regulatory T cells by indigenous Clostridium species. Science (80-.). doi:10.1126/science.1198469.

AUA (2020). Medical Student Curriculum: Adult UTI. Available at: https://www.auanet.org/education/auauniversity/for-medical-students/medical-students-curriculum/medical-student-curriculum/adult-uti%0Ahttps://www.auanet.org/education/auauniversity/for-medical-students/medical-student-curriculum/adult-uti.

Aurich, M. K., Fleming, R. M. T., and Thiele, I. (2016). MetaboTools: A comprehensive toolbox for analysis of genome-scale metabolic models. Front. Physiol. 7. doi:10.3389/fphys.2016.00327.

Aziz, R. K., Bartels, D., Best, A. A., DeJongh, M., Disz, T., Edwards, R. A., et al. (2008). The RAST Server: rapid annotations using subsystems technology. BMC Genomics 9, 1–15.

Baffy, G., Brunt, E. M., and Caldwell, S. H. (2012). Hepatocellular carcinoma in non-alcoholic fatty liver disease: an emerging menace. J. Hepatol. 56, 1384–1391. doi:10.1016/j.jhep.2011.10.027.

Bahadori, M., Motamedifar, M., Derakhshandeh, A., Firouzi, R., Motamedi Boroojeni, A., Alinejad, M., et al. (2019). Genetic relatedness of the Escherichia coli fecal population and strains causing urinary tract infection in the same host. Microbiologyopen 8, e00759. doi:https://doi.org/10.1002/mbo3.759.

Baka, S., Spathi, A., Tsouma, I., and Kouskouni, E. (2013). Symptomatic Shigella sonnei urinary tract infection in pregnancy. Clin. Exp. Obstet. Gynecol. 40, 116–117.

Balashov, V. S., Yan, Y., and Zhu, X. (2021). Using the Newcomb – Benford law to study the association between a country ' s COVID ‐ 19 reporting accuracy and its development. Sci. Rep., 1–11. doi:10.1038/s41598-021-02367-z.

Ballatori, N., Krance, S. M., Notenboom, S., Shi, S., Tieu, K., and Hammond, C. L. (2009). Glutathione dysregulation and the etiology and progression of human diseases. Biol. Chem. 390, 191–214. doi:10.1515/BC.2009.033.

Banan, A., Fields, J. Z., Zhang, Y., and Keshavarzian, A. (2001). iNOS upregulation mediates oxidant-induced disruption of F-actin and barrier of intestinal monolayers. Am. J. Physiol. Gastrointest. Liver Physiol. 280, G1234-46. doi:10.1152/ajpgi.2001.280.6.G1234.

Barichella, M., Severgnini, M., Cilia, R., Cassani, E., Bolliri, C., Caronni, S., et al. (2019). Unraveling gut microbiota in Parkinson's disease and atypical parkinsonism. Mov. Disord. 34, 396–405. doi:10.1002/mds.27581.

Barker, J., Brookes, G., and Johnson, T. (1978). Carbon dioxide-dependent klebsiellae. Br. Med. J. 1, 300. doi:10.1136/bmj.1.6108.300.

Bartl, M., Kötzing, M., Schuster, S., Li, P., and Kaleta, C. (2013). Dynamic optimization identifies optimal programmes for pathway regulation in prokaryotes. Nat. Commun. doi:10.1038/ncomms3243.

Bartoletti, R., Cai, T., Wagenlehner, F. M., Naber, K., and Bjerklund Johansen, T. E. (2016). Treatment of Urinary Tract Infections and Antibiotic Stewardship. Eur. Urol. Suppl. 15, 81–87. doi:https://doi.org/10.1016/j.eursup.2016.04.003.

Bauckman, K. A., Matsuda, R., Higgins, C. B., DeBosch, B. J., Wang, C., and Mysorekar, I. U. (2019). Dietary restriction of iron availability attenuates UPEC pathogenesis in a mouse model of urinary tract infection. Am. J. Physiol. Renal Physiol. 316, F814–F822. doi:10.1152/ajprenal.00133.2018.

Bauer, E., and Thiele, I. (2018). From metagenomic data to personalized in silico microbiotas: predicting dietary supplements for Crohn's disease. NPJ Syst. Biol. Appl. 4, 27. doi:10.1038/s41540-018-0063-2.

Bauer, E., Zimmermann, J., Baldini, F., Thiele, I., and Kaleta, C. (2017). BacArena: Individual-based metabolic modeling of heterogeneous microbes in complex communities. PLoS Comput. Biol. 13, 1–22. doi:10.1371/journal.pcbi.1005544.

Becker, S. A., and Palsson, B. O. (2008). Context-specific metabolic networks are consistent with experiments. PLoS Comput. Biol. 4, e1000082. doi:10.1371/journal.pcbi.1000082.

Beger, R. D., Dunn, W., Schmidt, M. A., Gross, S. S., Kirwan, J. A., Cascante, M., et al. (2016). Metabolomics enables precision medicine: "A White Paper, Community Perspective". Metabolomics 12, 149. doi:10.1007/s11306-016-1094-6.

Bellou, V., Belbasis, L., Tzoulaki, I., Evangelou, E., and Ioannidis, J. P. A. (2016). Environmental risk factors and Parkinson's disease: An umbrella review of meta-analyses. Parkinsonism Relat. Disord. 23, 1–9. doi:10.1016/j.parkreldis.2015.12.008.

Benner, E. J., Banerjee, R., Reynolds, A. D., Sherman, S., Pisarev, V. M., Tsiperson, V., et al. (2008). Nitrated alpha-synuclein immunity accelerates degeneration of nigral dopaminergic neurons. PLoS One 3, e1376. doi:10.1371/journal.pone.0001376.

Bentfeld, M. E., and Bainton, D. F. (1975). Cytochemical localization of lysosomal enzymes in rat megakaryocytes and platelets. J. Clin. Invest. 56, 1635–1649. doi:10.1172/JCI108246.

Bentfeld-Barker, M. E., and Bainton, D. F. (1982). Identification of primary lysosomes in human megakaryocytes and platelets. Blood 59, 472–481.

Bernardes, J. P., Mishra, N., Tran, F., Bahmer, T., Best, L., Blase, J. I., et al. (2020). Longitudinal Multi-omics Analyses Identify Responses of Megakaryocytes, Erythroid Cells, and Plasmablasts as Hallmarks of Severe COVID-19. Immunity 53, 1296-1314.e9. doi:10.1016/j.immuni.2020.11.017.

Bernstein, D. B., Sulheim, S., Almaas, E., and Segrè, D. (2021). Addressing uncertainty in genome-scale metabolic model reconstruction and analysis. Genome Biol. 22, 64. doi:10.1186/s13059-021-02289-z.

Bhattacharyya, A., Chattopadhyay, R., Mitra, S., and Crowe, S. E. (2014). Oxidative stress: an essential factor in the pathogenesis of gastrointestinal mucosal diseases. Physiol. Rev. 94, 329–354. doi:10.1152/physrev.00040.2012.

Bhattacharyya, S., Sinha, K., and Sil, P. C. (2014). Cytochrome P450s: mechanisms and biological implications in drug metabolism and its interaction with oxidative stress. Curr. Drug Metab. 15, 719–742. doi:10.2174/1389200215666141125121659.

Blaecher, C., Smet, A., Flahou, B., Pasmans, F., Ducatelle, R., Taylor, D., et al. (2013). Significantly higher frequency of Helicobacter suis in patients with idiopathic parkinsonism than in control patients. Aliment. Pharmacol. Ther. 38, 1347–1353. doi:10.1111/apt.12520.

Blanco-Melo, D., Nilsson-Payant, B. E., Liu, W.-C., Uhl, S., Hoagland, D., Møller, R., et al. (2020). Imbalanced Host Response to SARS-CoV-2 Drives Development of COVID-19. Cell 181, 1036-1045.e9. doi:10.1016/j.cell.2020.04.026.

Block, M. L., Zecca, L., and Hong, J.-S. (2007). Microglia-mediated neurotoxicity: uncovering the molecular mechanisms. Nat. Rev. Neurosci. 8, 57–69. doi:10.1038/nrn2038.

Bonaz, B., Sinniger, V., Hoffmann, D., Clarençon, D., Mathieu, N., Dantzer, C., et al. (2016). Chronic vagus nerve stimulation in Crohn's disease: A 6-month follow-up pilot study. Neurogastroenterol. Motil. doi:10.1111/nmo.12792.

Bonetto, J., Villaamil Lepori, E., and Puntarulo, S. (2014). Update on the Oxidative Stress Associated with Arsenic Exposure.

Bonnardel, J., and Guilliams, M. (2018). Developmental control of macrophage function. Curr. Opin. Immunol. 50, 64–74. doi:10.1016/j.coi.2017.12.001.

Bordbar, A., and Palsson, B. O. (2012). Using the reconstructed genome-scale human metabolic network to study physiology and pathology. J. Intern. Med. 271, 131–141. doi:10.1111/j.1365-2796.2011.02494.x.

Bordbar, A., Lewis, N. E., Schellenberger, J., Palsson, B. Ø., and Jamshidi, N. (2010). Insight into human alveolar macrophage and M. tuberculosis interactions via metabolic reconstructions. Mol. Syst. Biol. 6, 422. doi:10.1038/msb.2010.68.

Bost, P., De Sanctis, F., Canè, S., Ugel, S., Donadello, K., Castellucci, M., et al. (2021). Deciphering the state of immune silence in fatal COVID-19 patients. Nat. Commun. 12, 1428. doi:10.1038/s41467-021-21702-6.

Bouabid, S., Delaville, C., De Deurwaerdère, P., Lakhdar-Ghazal, N., and Benazzouz, A. (2014). Manganese-induced atypical parkinsonism is associated with altered Basal Ganglia activity and changes in tissue levels of monoamines in the rat. PLoS One 9, e98952. doi:10.1371/journal.pone.0098952.

Bouatra, S., Aziat, F., Mandal, R., Guo, A. C., Wilson, M. R., Knox, C., et al. (2013). The Human Urine Metabolome. PLoS One 8. doi:10.1371/journal.pone.0073076.

Bouhifd, M., Beger, R., Flynn, T., Guo, L., Harris, G., Hogberg, H., et al. (2015). Quality assurance of metabolomics. ALTEX 32, 319–326. doi:10.14573/altex.1509161.

Braak, H., Rüb, U., Gai, W. P., and Del Tredici, K. (2003). Idiopathic Parkinson's disease: possible routes by which vulnerable neuronal types may be subject to neuroinvasion by an unknown pathogen. J. Neural Transm. 110, 517–536. doi:10.1007/s00702-002-0808-2.

Brady, C., Cleenwerck, I., Venter, S., Coutinho, T., and De Vos, P. (2013). Taxonomic evaluation of the genus Enterobacter based on multilocus sequence analysis (MLSA): proposal to reclassify E. nimipressuralis and E. amnigenus into Lelliottia gen. nov. as Lelliottia nimipressuralis comb. nov. and Lelliottia amnigena comb. nov., . Syst. Appl. Microbiol. 36, 309–319.

Branchett, W. J., and Lloyd, C. M. (2019). Regulatory cytokine function in the respiratory tract. Mucosal Immunol. 12, 589–600. doi:10.1038/s41385-019-0158-0.

Braun, J., Loyal, L., Frentsch, M., Wendisch, D., Georg, P., Kurth, F., et al. (2020). SARS-CoV-2-reactive T cells in healthy donors and patients with COVID-19. Nature 587, 270–274. doi:10.1038/s41586-020-2598-9.

Breit, S., Kupferberg, A., Rogler, G., and Hasler, G. (2018). Vagus nerve as modulator of the brain-gut axis in psychiatric and inflammatory disorders. Front. Psychiatry. doi:10.3389/fpsyt.2018.00044.

Breton, J., Daniel, C., Dewulf, J., Pothion, S., Froux, N., Sauty, M., et al. (2013). Gut microbiota limits heavy metals burden caused by chronic oral exposure. Toxicol. Lett. 222, 132–138. doi:10.1016/j.toxlet.2013.07.021.

Breton, J., Daniel, C., Vignal, C., Body-malapel, M., and Garat, A. (2016). Does oral exposure to cadmium and lead mediate susceptibility to colitis ? The dark-and-bright sides of heavy metals in gut ecology. Nat. Publ. Gr., 1–12. doi:10.1038/srep19200.

Breydo, L., Wu, J. W., and Uversky, V. N. (2012). A-synuclein misfolding and Parkinson's disease. Biochim. Biophys. Acta 1822, 261–285. doi:10.1016/j.bbadis.2011.10.002.

Bridges, C. C., and Zalups, R. K. (2005). Molecular and ionic mimicry and the transport of toxic metals. Toxicol. Appl. Pharmacol. doi:10.1016/j.taap.2004.09.007.

Brown, C. T., Olm, M. R., Thomas, B. C., Banfield, J. F., Biology, M., Science, P., et al. (2017). Measurement of bacterial replication rates in microbial communities. 34, 1256–1263. doi:10.1038/nbt.3704.Measurement.

Brubaker, L., and Wolfe, A. J. (2017). The Female Urinary Microbiota/Microbiome: Clinical and Research Implications. Rambam Maimonides Med. J. 8, e0015. doi:10.5041/rmmj.10292.

Brudek, T. (2019). Inflammatory Bowel Diseases and Parkinson's Disease. J. Parkinsons. Dis. 9, S331–S344. doi:10.3233/JPD-191729.

Brumbaugh, A. R., Smith, S. N., and Mobley, H. L. T. (2013). Immunization with the yersiniabactin receptor, FyuA, protects against pyelonephritis in a murine model of urinary tract infection. Infect. Immun. 81, 3309–3316. doi:10.1128/IAI.00470-13.

Brunk, E., Sahoo, S., Zielinski, D. C., Altunkaya, A., Dräger, A., Mih, N., et al. (2018). Recon3D enables a three-dimensional view of gene variation in human metabolism. Nat. Biotechnol. 36, 272–281. doi:10.1038/nbt.4072.

Burin, R., and Shah, D. H. (2020). Global transcriptional profiling of tyramine and d-glucuronic acid catabolism in Salmonella. Int. J. Med. Microbiol. 310, 151452. doi:https://doi.org/10.1016/j.ijmm.2020.151452.

Butler, A., Hoffman, P., Smibert, P., Papalexi, E., and Satija, R. (2018). Integrating single-cell transcriptomic data across different conditions, technologies, and species. Nat. Biotechnol. 36, 411–420. doi:10.1038/nbt.4096.

Byndloss, M. X., Olsan, E. E., Rivera-Chávez, F., Tiffany, C. R., Cevallos, S. A., Lokken, K. L., et al. (2017). Microbiota-activated PPAR-γ signaling inhibits dysbiotic Enterobacteriaceae expansion. Science 357, 570–575. doi:10.1126/science.aam9949.

Cabezas, R., Fidel, M., Torrente, D., Santos El-Bach, R., Morales, L., Gonzalez, J., et al. (2013). "Astrocytes Role in Parkinson: A Double-Edged Sword," in Neurodegenerative Diseases doi:10.5772/54305.

Cai, T., Nesi, G., Mazzoli, S., Meacci, F., Lanzafame, P., Caciagli, P., et al. (2015). Asymptomatic bacteriuria treatment is associated with a higher prevalence of antibiotic resistant strains in women with urinary tract infections. Clin. Infect. Dis. an Off. Publ. Infect. Dis. Soc. Am. 61, 1655–1661. doi:10.1093/cid/civ696.

Cai, T., Yao, T., Zheng, G., Chen, Y., Du, K., Cao, Y., et al. (2010). Manganese induces the overexpression of α-synuclein in PC12 cells via ERK activation. Brain Res. 1359, 201–207. doi:10.1016/j.brainres.2010.08.055.

Cairns, R. A., Harris, I. S., and Mak, T. W. (2011). Regulation of cancer cell metabolism. Nat. Rev. Cancer 11, 85–95. doi:10.1038/nrc2981.

Caito, S., and Aschner, M. (2015). "Neurotoxicity of metals," in Handbook of Clinical Neurology doi:10.1016/B978-0-444-62627-1.00011-1.

Calvani, R., Picca, A., Lo Monaco, M. R., Landi, F., Bernabei, R., and Marzetti, E. (2018). Of microbes and minds: A narrative review on the second brain aging. Front. Med. doi:10.3389/fmed.2018.00053.

Campos-Acuña, J., Elgueta, D., and Pacheco, R. (2019). T-cell-driven inflammation as a mediator of the gut-brain axis involved in Parkinson's disease. Front. Immunol. doi:10.3389/fimmu.2019.00239.

Carabotti, M., Scirocco, A., Maselli, M. A., and Severi, C. (2015). The gut-brain axis: Interactions between enteric microbiota, central and enteric nervous systems. Ann. Gastroenterol.

Cariccio, V. L., Samà, A., Bramanti, P., and Mazzon, E. (2019). Mercury Involvement in Neuronal Damage and in Neurodegenerative Diseases. Biol. Trace Elem. Res. 187, 341–356. doi:10.1007/s12011-018-1380-4.

Carmona, A., Roudeau, S., and Ortega, R. (2021). Molecular Mechanisms of Environmental Metal Neurotoxicity: A Focus on the Interactions of Metals with Synapse Structure and Function. Toxics 9. doi:10.3390/toxics9090198.

Castoldi, A. F., Barni, S., Turin, I., Gandini, C., and Manzo, L. (2000). Early acute necrosis, delayed apoptosis and cytoskeletal breakdown in cultured cerebellar granule neurons exposed to

methylmercury. J. Neurosci. Res. 59, 775–787. doi:10.1002/(SICI)1097-4547(20000315)59:6<775::AID-JNR10>3.0.CO;2-T.

Ceccatelli, S., Daré, E., and Moors, M. (2010). Methylmercury-induced neurotoxicity and apoptosis. Chem. Biol. Interact. 188, 301–308. doi:10.1016/j.cbi.2010.04.007.

Chan, J. F.-W., Yuan, S., Kok, K.-H., To, K. K.-W., Chu, H., Yang, J., et al. (2020). A familial cluster of pneumonia associated with the 2019 novel coronavirus indicating person-to-person transmission: a study of a family cluster. Lancet (London, England) 395, 514–523. doi:10.1016/S0140-6736(20)30154-9.

Chan, S. H. J., Cai, J., Wang, L., Simons-Senftle, M. N., and Maranas, C. D. (2017). Standardizing biomass reactions and ensuring complete mass balance in genome-scale metabolic models. Bioinformatics 33, 3603–3609.

Chang, R. L., Xie, L., Xie, L., Bourne, P. E., and Palsson, B. Ø. (2010). Drug off-target effects predicted using structural analysis in the context of a metabolic network model. PLoS Comput. Biol. 6, e1000938. doi:10.1371/journal.pcbi.1000938.

Channappanavar, R., Fehr, A. R., Vijay, R., Mack, M., Zhao, J., Meyerholz, D. K., et al. (2016). Dysregulated Type I Interferon and Inflammatory Monocyte-Macrophage Responses Cause Lethal Pneumonia in SARS-CoV-Infected Mice. Cell Host Microbe 19, 181–193. doi:10.1016/j.chom.2016.01.007.

Chaturvedi, K. S., Hung, C. S., Crowley, J. R., Stapleton, A. E., and Henderson, J. P. (2012). The siderophore yersiniabactin binds copper to protect pathogens during infection. Nat. Chem. Biol. 8, 731–736. doi:10.1038/nchembio.1020.

Chavali, A. K., D'Auria, K. M., Hewlett, E. L., Pearson, R. D., and Papin, J. A. (2012). A metabolic network approach for the identification and prioritization of antimicrobial drug targets. Trends Microbiol. 20, 113–123. doi:10.1016/j.tim.2011.12.004.

Chen, G., Wu, D., Guo, W., Cao, Y., Huang, D., Wang, H., et al. (2020). Clinical and immunological features of severe and moderate coronavirus disease 2019. J. Clin. Invest. 130, 2620–2629. doi:10.1172/JCI137244.

Chen, H., and Ritz, B. (2018). The Search for Environmental Causes of Parkinson's Disease: Moving Forward. J. Parkinsons. Dis. 8, S9–S17. doi:10.3233/JPD-181493.

Chen, P., Bornhorst, J., and Aschner, M. (2018). Manganese metabolism in humans. Front. Biosci. (Landmark Ed. 23, 1655–1679. doi:10.2741/4665.

Chen, Q. Q., Haikal, C., Li, W., and Li, J. Y. (2019). Gut Inflammation in Association With Pathogenesis of Parkinson's Disease. Front. Mol. Neurosci. doi:10.3389/fnmol.2019.00218.

Chen, Q., Chen, Y., Zhang, Y., Wang, F., Yu, H., Zhang, C., et al. (2019). Iron deposition in Parkinson's disease by quantitative susceptibility mapping. BMC Neurosci. doi:10.1186/s12868-019-0505-9.

Chen, S. L., Wu, M., Henderson, J. P., Hooton, T. M., Hibbing, M. E., Hultgren, S. J., et al. (2013). Genomic diversity and fitness of E. coli strains recovered from the intestinal and urinary tracts of women with recurrent urinary tract infection. Sci. Transl. Med. 5, 184ra60. doi:10.1126/scitranslmed.3005497.

Chen, Y., Liu, Q., and Guo, D. (2020). Emerging coronaviruses: Genome structure, replication, and pathogenesis. J. Med. Virol. 92, 418–423. doi:10.1002/jmv.25681.

Cheng Z, Zhou X, Mei H, H. Y. (2020). Bile Acids Maintain Platelet Homeostasis via p38 and Akt Pathway. Res Pr. Thromb Haemost. 4.

Cheng, H., Guan, X., Chen, D., and Ma, W. (2019). The th17/treg cell balance: A gut microbiota-modulated story. Microorganisms. doi:10.3390/microorganisms7120583.

Cheung, C. C. L., Goh, D., Lim, X., Tien, T. Z., Lim, J. C. T., Lee, J. N., et al. (2021). Residual SARS-CoV-2 viral antigens detected in GI and hepatic tissues from five recovered patients with COVID-19. Gut. doi:10.1136/gutjnl-2021-324280.

Cheung, C. Y., Poon, L. L. M., Ng, I. H. Y., Luk, W., Sia, S.-F., Wu, M. H. S., et al. (2005). Cytokine responses in severe acute respiratory syndrome coronavirus-infected macrophages in vitro: possible relevance to pathogenesis. J. Virol. 79, 7819–7826. doi:10.1128/JVI.79.12.7819-7826.2005.

Chimerel, C., Emery, E., Summers, D. K., Keyser, U., Gribble, F. M., and Reimann, F. (2014). Bacterial Metabolite Indole Modulates Incretin Secretion from Intestinal Enteroendocrine L Cells. Cell Rep. doi:10.1016/j.celrep.2014.10.032.

Choi, J. G., Kim, N., Ju, I. G., Eo, H., Lim, S. M., Jang, S. E., et al. (2018). Oral administration of Proteus mirabilis damages dopaminergic neurons and motor functions in mice. Sci. Rep. doi:10.1038/s41598-018-19646-x.

Chtourou, Y., Trabelsi, K., Fetoui, H., Mkannez, G., Kallel, H., and Zeghal, N. (2011). Manganese induces oxidative stress, redox state unbalance and disrupts membrane bound ATPases on murine neuroblastoma cells in vitro: protective role of silymarin. Neurochem. Res. 36, 1546–1557. doi:10.1007/s11064-011-0483-5.

Chua, R. L., Lukassen, S., Trump, S., Hennig, B. P., Wendisch, D., Pott, F., et al. (2020). COVID-19 severity correlates with airway epithelium-immune cell interactions identified by single-cell analysis. Nat. Biotechnol. 38, 970–979. doi:10.1038/s41587-020-0602-4.

Chung, S. J., Kim, J., Lee, H. J., Ryu, H.-S., Kim, K., Lee, J. H., et al. (2016). Alpha-synuclein in gastric and colonic mucosa in Parkinson's disease: Limited role as a biomarker. Mov. Disord. 31, 241–249. doi:10.1002/mds.26473.

Ciferri, S., Emiliani, C., Guglielmini, G., Orlacchio, A., Nenci, G. G., and Gresele, P. (2000). Platelets release their lysosomal content in vivo in humans upon activation. Thromb. Haemost. 83, 157–164.

Clarke, G., Stilling, R. M., Kennedy, P. J., Stanton, C., Cryan, J. F., and Dinan, T. G. (2014). Minireview: Gut microbiota: the neglected endocrine organ. Mol. Endocrinol. 28, 1221–1238. doi:10.1210/me.2014-1108.

Clarkson, T. W. (2002). The three modern faces of mercury. Environ. Health Perspect. 110 Suppl, 11–23. doi:10.1289/ehp.02110s111.

Claverie, J. M. (2006). Viruses take center stage in cellular evolution. Genome Biol. 7, 1–5. doi:10.1186/gb-2006-7-6-110.

Cobley, J. N., Fiorello, M. L., and Bailey, D. M. (2018). 13 reasons why the brain is susceptible to oxidative stress. Redox Biol. 15, 490–503. doi:10.1016/j.redox.2018.01.008.

Collins, L. M., Toulouse, A., Connor, T. J., and Nolan, Y. M. (2012). Contributions of central and systemic inflammation to the pathophysiology of Parkinson's disease. Neuropharmacology 62, 2154–2168. doi:10.1016/j.neuropharm.2012.01.028.

Conover, M. S., Hadjifrangiskou, M., Palermo, J. J., Hibbing, M. E., Dodson, K. W., and Hultgren, S. J. (2016). Metabolic requirements of Escherichia coli in intracellular bacterial communities during urinary tract infection pathogenesis. MBio 7, 1–13. doi:10.1128/mBio.00104-16.

Corcoran, L. M., and Nutt, S. L. (2016). Long-Lived Plasma Cells Have a Sweet Tooth. Immunity 45, 3–5. doi:10.1016/j.immuni.2016.07.003.

Correia, S., and Rocha, M. (2015). A Critical Evaluation of Methods for the Reconstruction of Tissue-Specific Models. in Progress in Artificial Intelligence, eds. F. Pereira, P. Machado, E. Costa, and A. Cardoso (Cham: Springer International Publishing), 340–352.

Coryell, M., Roggenbeck, B. A., and Walk, S. T. (2019). The Human Gut Microbiome's Influence on Arsenic Toxicity. Curr. Pharmacol. reports 5, 491–504. doi:10.1007/s40495-019-00206-4.

Costa-Mallen, P., Gatenby, C., Friend, S., Maravilla, K. R., Hu, S.-C., Cain, K. C., et al. (2017). Brain iron concentrations in regions of interest and relation with serum iron levels in Parkinson disease. J. Neurol. Sci. 378, 38–44. doi:10.1016/j.jns.2017.04.035.

Cristinelli, S., and Ciuffi, A. (2018). The use of single-cell RNA-Seq to understand virus-host interactions. Curr. Opin. Virol. 29, 39–50. doi:10.1016/j.coviro.2018.03.001.

Cryan, J. F., O'riordan, K. J., Cowan, C. S. M., Sandhu, K. V., Bastiaanssen, T. F. S., Boehme, M., et al. (2019). The microbiota-gut-brain axis. Physiol. Rev. doi:10.1152/physrev.00018.2018.

Cunningham, F., Achuthan, P., Akanni, W., Allen, J., Amode, M. R., Armean, I. M., et al. (2019). Ensembl 2019. Nucleic Acids Res. 47, D745–D751. doi:10.1093/nar/gky1113.

David, L. A., Maurice, C. F., Carmody, R. N., Gootenberg, D. B., Button, J. E., Wolfe, B. E., et al. (2014). Diet rapidly and reproducibly alters the human gut microbiome. Nature 505, 559–63. Available at:

http://www.pubmedcentral.nih.gov/articlerender.fcgi?artid=3957428&tool=pmcentrez&rendertype=abstract.

De Biasi, S., Lo Tartaro, D., Meschiari, M., Gibellini, L., Bellinazzi, C., Borella, R., et al. (2020). Expansion of plasmablasts and loss of memory B cells in peripheral blood from COVID-19 patients with pneumonia. Eur. J. Immunol. 50, 1283–1294. doi:10.1002/eji.202048838.

de Vos, M. G. J., Zagorski, M., McNally, A., and Bollenbach, T. (2017). Interaction networks, ecological stability, and collective antibiotic tolerance in polymicrobial infections. Proc. Natl. Acad. Sci. 114, 10666 LP – 10671. doi:10.1073/pnas.1713372114.

de Wilde, A. H., Wannee, K. F., Scholte, F. E. M., Goeman, J. J., Ten Dijke, P., Snijder, E. J., et al. (2015). A Kinome-Wide Small Interfering RNA Screen Identifies Proviral and Antiviral Host Factors in Severe Acute Respiratory Syndrome Coronavirus Replication, Including Double-Stranded RNA-Activated Protein Kinase and Early Secretory Pathway Proteins. J. Virol. 89, 8318–8333. doi:10.1128/JVI.01029-15.

Deng, X., Hackbart, M., Mettelman, R. C., O'Brien, A., Mielech, A. M., Yi, G., et al. (2017). Coronavirus nonstructural protein 15 mediates evasion of dsRNA sensors and limits apoptosis in macrophages. Proc. Natl. Acad. Sci. U. S. A. 114, E4251–E4260. doi:10.1073/pnas.1618310114.

Deng, Z.-L., Gottschick, C., Bhuju, S., Masur, C., Abels, C., Wagner-Döbler, I., et al. (2018). Metatranscriptome Analysis of the Vaginal Microbiota Reveals Potential Mechanisms for Protection against Metronidazole in Bacterial Vaginosis. mSphere. doi:10.1128/mSphereDirect.00262-18.

Dev, S., and Babitt, J. L. (2017). Overview of iron metabolism in health and disease. Hemodial. Int. 21 Suppl 1, S6–S20. doi:10.1111/hdi.12542.

Devillé, W. L. J. M., Yzermans, J. C., van Duijn, N. P., Bezemer, P. D., van der Windt, D. A. W. M., and Bouter, L. M. (2004). The urine dipstick test useful to rule out infections. A meta-analysis of the accuracy. BMC Urol. 4, 4. doi:10.1186/1471-2490-4-4.

Devos, D., Lebouvier, T., Lardeux, B., Biraud, M., Rouaud, T., Pouclet, H., et al. (2013). Colonic inflammation in Parkinson's disease. Neurobiol. Dis. 50, 42–48. doi:10.1016/j.nbd.2012.09.007.

Dexter, D. T., Wells, F. R., Lees, A. J., Agid, F., Agid, Y., Jenner, P., et al. (1989). Increased nigral iron content and alterations in other metal ions occurring in brain in Parkinson's disease. J. Neurochem. 52, 1830–1836. doi:10.1111/j.1471-4159.1989.tb07264.x.

Dhakal, B. K., and Mulvey, M. A. (2012). The UPEC pore-forming toxin α-hemolysin triggers proteolysis of host proteins to disrupt cell adhesion, inflammatory, and survival pathways. Cell Host Microbe 11, 58–69. doi:10.1016/j.chom.2011.12.003.

Diao, B., Wang, C., Tan, Y., Chen, X., Liu, Y., Ning, L., et al. (2020). Reduction and Functional Exhaustion of T Cells in Patients With Coronavirus Disease 2019 (COVID-19). Front. Immunol. 11, 1–7. doi:10.3389/fimmu.2020.00827.

Dick, F. D., De Palma, G., Ahmadi, A., Scott, N. W., Prescott, G. J., Bennett, J., et al. (2007). Environmental risk factors for Parkinson's disease and parkinsonism: The Geoparkinson study. Occup. Environ. Med. doi:10.1136/oem.2006.027003.

Dirmeier, S., Dächert, C., van Hemert, M., Tas, A., Ogando, N. S., van Kuppeveld, F., et al. (2020). Host factor prioritization for pan-viral genetic perturbation screens using random intercept models and network propagation. PLoS Comput. Biol. 16, e1007587. doi:10.1371/journal.pcbi.1007587.

Doi, Y. (2019). Glycerol metabolism and its regulation in lactic acid bacteria. Appl. Microbiol. Biotechnol. 103, 5079–5093. doi:10.1007/s00253-019-09830-y.

dos Santos, A., Ferrer, B., Marques Gonçalves, F., Tsatsakis, A. M., Renieri, E. A., Skalny, A. V, et al. (2018). Oxidative Stress in Methylmercury-Induced Cell Toxicity. Toxics 6. doi:10.3390/toxics6030047.

Drayman, N., Patel, P., Vistain, L., and Tay, S. (2019). HSV-1 single-cell analysis reveals the activation of anti-viral and developmental programs in distinct sub-populations. Elife 8. doi:10.7554/eLife.46339.

Du, B., Yang, L., Lloyd, C. J., Fang, X., and Palsson, B. O. (2019). Genome-scale model of metabolism and gene expression provides a multi-scale description of acid stress responses in Escherichia coli. PLOS Comput. Biol. 15, e1007525. Available at: https://doi.org/10.1371/journal.pcbi.1007525.

Duan, H., Yu, L., Tian, F., Zhai, Q., Fan, L., and Chen, W. (2020). Gut microbiota: A target for heavy metal toxicity and a probiotic protective strategy. Sci. Total Environ. 742, 140429. doi:10.1016/j.scitotenv.2020.140429.

Duarte, N. C., Becker, S. A., Jamshidi, N., Thiele, I., Mo, M. L., Vo, T. D., et al. (2007). Global reconstruction of the human metabolic network based on genomic and bibliomic data. Proc. Natl. Acad. Sci. U. S. A. 104, 1777–1782. doi:10.1073/pnas.0610772104.

Dumitrescu, L., Popescu-Olaru, I., Cozma, L., Tulbă, D., Hinescu, M. E., Ceafalan, L. C., et al. (2018). Oxidative Stress and the Microbiota-Gut-Brain Axis. Oxid. Med. Cell. Longev. 2018, 2406594. doi:10.1155/2018/2406594.

Durot, M., Le Fèvre, F., de Berardinis, V., Kreimeyer, A., Vallenet, D., Combe, C., et al. (2008). Iterative reconstruction of a global metabolic model of Acinetobacter baylyi ADP1 using high-throughput growth phenotype and gene essentiality data. BMC Syst. Biol. 2, 85. doi:10.1186/1752-0509-2-85.

Ebrahim, A., Lerman, J. A., Palsson, B. O., and Hyduke, D. R. (2013). COBRApy: COnstraints-Based Reconstruction and Analysis for Python. BMC Syst. Biol. 7, 74. doi:10.1186/1752-0509-7-74.

Edgar, R. C. (2010). Search and clustering orders of magnitude faster than BLAST. Bioinformatics 26, 2460–2461. doi:10.1093/bioinformatics/btq461.

Edwards, J. S., and Palsson, B. O. (2000). The Escherichia coli MG1655 in silico metabolic genotype: Its definition, characteristics, and capabilities. Proc. Natl. Acad. Sci. U. S. A. 97, 5528–5533. doi:10.1073/pnas.97.10.5528.

Erickson, K. E., Winkler, J. D., Nguyen, D. T., Gill, R. T., and Chatterjee, A. (2017). The Tolerome: A Database of Transcriptome-Level Contributions to Diverse Escherichia coli Resistance and Tolerance Phenotypes. ACS Synth. Biol., acssynbio.7b00235. doi:10.1021/acssynbio.7b00235.

Ewald, J., Bartl, M., Dandekar, T., and Kaleta, C. (2017). Optimality principles reveal a complex interplay of intermediate toxicity and kinetic efficiency in the regulation of prokaryotic metabolism. PLoS Comput. Biol. 13, 1–19. doi:10.1371/journal.pcbi.1005371.

Fang, L., Karakiulakis, G., and Roth, M. (2020). Are patients with hypertension and diabetes mellitus at increased risk for COVID-19 infection? Lancet. Respir. Med. 8, e21. doi:10.1016/S2213-2600(20)30116-8.

Farina, M., Avila, D. S., Da Rocha, J. B. T., and Aschner, M. (2013). Metals, oxidative stress and neurodegeneration: A focus on iron, manganese and mercury. Neurochem. Int. doi:10.1016/j.neuint.2012.12.006.

Fasano, M., Bergamasco, B., and Lopiano, L. (2006). Modifications of the iron-neuromelanin system in Parkinson's disease. J. Neurochem. 96, 909–916. doi:10.1111/j.1471-4159.2005.03638.x.

Feist, A. M., Herrgård, M. J., Thiele, I., Reed, J. L., and Palsson, B. Ø. (2009). Reconstruction of biochemical networks in microorganisms. Nat. Rev. Microbiol. 7, 129–143. doi:10.1038/nrmicro1949.

Feist, A. M., and Palsson, B. O. (2016). What do cells actually want? Genome Biol. 17, 110. doi:10.1186/s13059-016-0983-3.

Feist, A. M., and Palsson, B. Ø. (2008). The growing scope of applications of genome-scale metabolic reconstructions using Escherichia coli. Nat. Biotechnol. 26, 659–667. doi:10.1038/nbt1401.

Fernandes Azevedo, B., Barros Furieri, L., Peçanha, F. M., Wiggers, G. A., Frizera Vassallo, P., Ronacher Simões, M., et al. (2012). Toxic effects of mercury on the cardiovascular and central nervous systems. J. Biomed. Biotechnol. 2012, 949048. doi:10.1155/2012/949048.

Fernandes, J., Chandler, J. D., Lili, L. N., Uppal, K., Hu, X., Hao, L., et al. (2019). Transcriptome Analysis Reveals Distinct Responses to Physiologic versus Toxic Manganese Exposure in Human Neuroblastoma Cells. Front. Genet. 10, 676. doi:10.3389/fgene.2019.00676.

Fernandes, J., Hao, L., Bijli, K. M., Chandler, J. D., Orr, M., Hu, X., et al. (2017). From the Cover: Manganese Stimulates Mitochondrial H2O2 Production in SH-SY5Y Human Neuroblastoma Cells Over Physiologic as well as Toxicologic Range. Toxicol. Sci. 155, 213–223. doi:10.1093/toxsci/kfw196.

Ferreira, J., Correia, S., and Rocha, M. (2017). Analysing Algorithms and Data Sources for the Tissue-Specific Reconstruction of Liver Healthy and Cancer Cells. Interdiscip. Sci. 9, 36–45. doi:10.1007/s12539-017-0214-y.

Ferruzza, S., Scacchi, M., Scarino, M. L., and Sambuy, Y. (2002). Iron and copper alter tight junction permeability in human intestinal Caco-2 cells by distinct mechanisms. Toxicol. In Vitro 16, 399–404. doi:10.1016/s0887-2333(02)00020-6.

Festa, R. A., and Thiele, D. J. (2011). Copper: an essential metal in biology. Curr. Biol. 21, R877-83. doi:10.1016/j.cub.2011.09.040.

Fink, K. (2012). Origin and function of circulating plasmablasts during acute viral infections. Front. Immunol. 3, 78.

Finkelman, R. B., Orem, W., Castranova, V., Tatu, C. A., Belkin, H. E., Zheng, B., et al. (2002). Health impacts of coal and coal use: possible solutions. Int. J. Coal Geol. 50, 425–443. doi:https://doi.org/10.1016/S0166-5162(02)00125-8.

Fitsanakis, V. A., and Aschner, M. (2005). The importance of glutamate, glycine, and gamma-aminobutyric acid transport and regulation in manganese, mercury and lead neurotoxicity. Toxicol. Appl. Pharmacol. 204, 343–354. doi:10.1016/j.taap.2004.11.013.

Fitsanakis, V. A., Piccola, G., Marreilha dos Santos, A. P., Aschner, J. L., and Aschner, M. (2007). Putative proteins involved in manganese transport across the blood-brain barrier. Hum. Exp. Toxicol. 26, 295–302. doi:10.1177/0960327107070496.

Flores-Mireles, A. L., Walker, J. N., Caparon, M., and Hultgren, S. J. (2015). Urinary tract infections: epidemiology, mechanisms of infection and treatment options. Nat. Rev. Microbiol. 13, 269–284. doi:10.1038/nrmicro3432.

Fond, G., Loundou, A., Hamdani, N., Boukouaci, W., Dargel, A., Oliveira, J., et al. (2014). Anxiety and depression comorbidities in irritable bowel syndrome (IBS): a systematic review and meta-analysis. Eur. Arch. Psychiatry Clin. Neurosci. doi:10.1007/s00406-014-0502-z.

Fonnum, F., and Lock, E. A. (2004). The contributions of excitotoxicity, glutathione depletion and DNA repair in chemically induced injury to neurones: exemplified with toxic effects on cerebellar granule cells. J. Neurochem. 88, 513–531. doi:10.1046/j.1471-4159.2003.02211.x.

Forsyth, V. S., Armbruster, C. E., Smith, S. N., Pirani, A., Springman, A. C., Walters, M. S., et al. (2018). Rapid Growth of Uropathogenic Escherichia coli during Human Urinary Tract Infection. MBio 9. doi:10.1128/mBio.00186-18.

Fouladiha, H., and Marashi, S. A. (2017). Biomedical applications of cell- and tissue-specific metabolic network models. J. Biomed. Inform. 68, 35–49. doi:10.1016/j.jbi.2017.02.014.

Fouts, D. E., Pieper, R., Szpakowski, S., Pohl, H., Knoblach, S., Suh, M.-J., et al. (2012). Integrated next-generation sequencing of 16S rDNA and metaproteomics differentiate the healthy urine

microbiome from asymptomatic bacteriuria in neuropathic bladder associated with spinal cord injury. J. Transl. Med. 10, 174. doi:10.1186/1479-5876-10-174.

Foxman, B. (2002). Epidemiology of urinary tract infections: incidence, morbidity, and economic costs. Am. J. Med. 113, 5–13. doi:10.1016/S0002-9343(02)01054-9.

Frick-Cheng, A. E., Sintsova, A., Smith, S. N., Krauthammer, M., Eaton, K. A., and Mobley, H. L. T. (2020). The Gene Expression Profile of Uropathogenic Escherichia coli in Women with Uncomplicated Urinary Tract Infections Is Recapitulated in the Mouse Model. MBio 11, e01412-20. doi:10.1128/mBio.01412-20.

Friedland, R. P., and Chapman, M. R. (2017). The role of microbial amyloid in neurodegeneration. PLoS Pathog. 13, e1006654. doi:10.1371/journal.ppat.1006654.

Fu, L., Lu, X., Niu, K., Tan, J., and Chen, J. (2019). Bioaccumulation and human health implications of essential and toxic metals in freshwater products of Northeast China. Sci. Total Environ. 673, 768–776. doi:10.1016/j.scitotenv.2019.04.099.

Fujishiro, H., Okugaki, S., Kubota, K., Fujiyama, T., Miyataka, H., and Himeno, S. (2009). The role of ZIP8 down-regulation in cadmium-resistant metallothionein-null cells. J. Appl. Toxicol. doi:10.1002/jat.1419.

Fung, T. C. (2020). The microbiota-immune axis as a central mediator of gut-brain communication. Neurobiol. Dis. doi:10.1016/j.nbd.2019.104714.

Fung, Y. K., Meade, A. G., Rack, E. P., and Blotcky, A. J. (1997). Brain mercury in neurodegenerative disorders. J. Toxicol. Clin. Toxicol. 35, 49–54. doi:10.3109/15563659709001165.

Gaebler, C., Wang, Z., Lorenzi, J. C. C., Muecksch, F., Finkin, S., Tokuyama, M., et al. (2021). Evolution of antibody immunity to SARS-CoV-2. Nature 591, 639–644. doi:10.1038/s41586-021-03207-w.

Galland, L. (2014). The gut microbiome and the brain. J. Med. Food 17, 1261–1272. doi:10.1089/jmf.2014.7000.

Gao, Q., Wang, X., Xu, H., Xu, Y., Ling, J., Zhang, D., et al. (2012). Roles of iron acquisition systems in virulence of extraintestinal pathogenic Escherichia coli: salmochelin and aerobactin contribute more to virulence than heme in a chicken infection model. BMC Microbiol. 12, 143. doi:10.1186/1471-2180-12-143.

Garcia-Albornoz, M. A., and Nielsen, J. (2013). Application of Genome-Scale Metabolic Models in Metabolic Engineering. Ind. Biotechnol. 9, 203–214. doi:10.1089/ind.2013.0011.

Gelders, G., Baekelandt, V., and Van der Perren, A. (2018). Linking Neuroinflammation and Neurodegeneration in Parkinson's Disease. J. Immunol. Res. 2018, 4784268. doi:10.1155/2018/4784268.

Genoud, S., Roberts, B. R., Gunn, A. P., Halliday, G. M., Lewis, S. J. G., Ball, H. J., et al. (2017). Subcellular compartmentalisation of copper, iron, manganese, and zinc in the Parkinson's disease brain. Metallomics 9, 1447–1455. doi:10.1039/c7mt00244k.

Gerlach, M., Double, K. L., Youdim, M. B. H., and Riederer, P. (2006). Potential sources of increased iron in the substantia nigra of parkinsonian patients. J. Neural Transm. Suppl., 133–142. doi:10.1007/978-3-211-45295-0_21.

Ghaisas, S., Maher, J., and Kanthasamy, A. (2016). Gut microbiome in health and disease: Linking the microbiome-gut-brain axis and environmental factors in the pathogenesis of systemic and neurodegenerative diseases. Pharmacol. Ther. 158, 52–62. doi:10.1016/j.pharmthera.2015.11.012.

Giamarellos-Bourboulis, E. J., Netea, M. G., Rovina, N., Akinosoglou, K., Antoniadou, A., Antonakos, N., et al. (2020). Complex Immune Dysregulation in COVID-19 Patients with Severe Respiratory Failure. Cell Host Microbe 27, 992-1000.e3. doi:10.1016/j.chom.2020.04.009.

Giambò, F., Italia, S., Teodoro, M., Briguglio, G., Furnari, N., Catanoso, R., et al. (2021). Influence of toxic metal exposure on the gut microbiota (Review). World Acad. Sci. J. 3, 1–13. doi:10.3892/wasj.2021.90.

Gilbert, N. M., O'Brien, V. P., and Lewis, A. L. (2017). Transient microbiota exposures activate dormant Escherichia coli infection in the bladder and drive severe outcomes of recurrent disease. PLoS Pathog. 13, e1006238. doi:10.1371/journal.ppat.1006238.

Gille, C., Bölling, C., Hoppe, A., Bulik, S., Hoffmann, S., Hübner, K., et al. (2010). HepatoNet1: a comprehensive metabolic reconstruction of the human hepatocyte for the analysis of liver physiology. Mol. Syst. Biol. 6, 411. doi:10.1038/msb.2010.62.

Glass, E. M., Wilkening, J., Wilke, A., Antonopoulos, D., and Meyer, F. (2010). Using the metagenomics RAST server (MG-RAST) for analyzing shotgun metagenomes. Cold Spring Harb. Protoc. 2010, pdb-prot5368.

Godaly, G., Ambite, I., Puthia, M., Nadeem, A., Ho, J., Nagy, K., et al. (2016). Urinary Tract Infection Molecular Mechanisms and Clinical Translation. Pathog. 5. doi:10.3390/pathogens5010024.

González Olmo, B. M., Butler, M. J., and Barrientos, R. M. (2021). Evolution of the Human Diet and Its Impact on Gut Microbiota, Immune Responses, and Brain Health. Nutrients 13. doi:10.3390/nu13010196.

Gottschick, C., Deng, Z.-L., Vital, M., Masur, C., Abels, C., Pieper, D. H., et al. (2017). The urinary microbiota of men and women and its changes in women during bacterial vaginosis and antibiotic treatment. Microbiome 5, 99. doi:10.1186/s40168-017-0305-3.

Graspeuntner, S., Waschina, S., Künzel, S., Twisselmann, N., Rausch, T. K., Cloppenborg-Schmidt, K., et al. (2018). Gut dysbiosis with bacilli dominance and accumulation of fermentation products precedes late-onset sepsis in preterm infants. Clin. Infect. Dis. 69, 268–277. doi:10.1093/cid/ciy882.

Griffiths-Jones, S., Bateman, A., Marshall, M., Khanna, A., and Eddy, S. R. (2003). Rfam: an RNA family database. Nucleic Acids Res. 31, 439–441.

Grifoni, A., Weiskopf, D., Ramirez, S. I., Mateus, J., Dan, J. M., Moderbacher, C. R., et al. (2020). Targets of T Cell Responses to SARS-CoV-2 Coronavirus in Humans with COVID-19 Disease and Unexposed Individuals. Cell 181, 1489-1501.e15. doi:10.1016/j.cell.2020.05.015.

Grochocki, W., Markuszewski, M. J., and Quirino, J. P. (2017). Simultaneous determination of creatinine and acetate by capillary electrophoresis with contactless conductivity detector as a feasible approach for urinary tract infection diagnosis. J. Pharm. Biomed. Anal. 137, 178–181. doi:10.1016/j.jpba.2017.01.032.

Gu, J., Gong, E., Zhang, B., Zheng, J., Gao, Z., Zhong, Y., et al. (2005). Multiple organ infection and the pathogenesis of SARS. J. Exp. Med. 202, 415–424. doi:10.1084/jem.20050828.

Gu, X.-L., Long, C.-X., Sun, L., Xie, C., Lin, X., and Cai, H. (2010). Astrocytic expression of Parkinson's disease-related A53T alpha-synuclein causes neurodegeneration in mice. Mol. Brain 3, 12. doi:10.1186/1756-6606-3-12.

Guan, W.-J., Liang, W.-H., Zhao, Y., Liang, H.-R., Chen, Z.-S., Li, Y.-M., et al. (2020). Comorbidity and its impact on 1590 patients with COVID-19 in China: a nationwide analysis. Eur. Respir. J. 55. doi:10.1183/13993003.00547-2020.

Guan, W.-J., Ni, Z.-Y., Hu, Y., Liang, W.-H., Ou, C.-Q., He, J.-X., et al. (2020). Clinical Characteristics of Coronavirus Disease 2019 in China. N. Engl. J. Med. 382, 1708–1720. doi:10.1056/NEJMoa2002032.

Guiney, S. J., Adlard, P. A., Bush, A. I., Finkelstein, D. I., and Ayton, S. (2017). Ferroptosis and cell death mechanisms in Parkinson's disease. Neurochem. Int. 104, 34–48. doi:10.1016/j.neuint.2017.01.004.

Gunter, T. E., Gerstner, B., Gunter, K. K., Malecki, J., Gelein, R., Valentine, W. M., et al. (2013). Manganese transport via the transferrin mechanism. Neurotoxicology 34, 118–127. doi:10.1016/j.neuro.2012.10.018.

Guo, R., Luo, X., Liu, J., and Lu, H. (2021). Mass spectrometry based targeted metabolomics precisely characterized new functional metabolites that regulate biofilm formation in Escherichia coli. Anal. Chim. Acta 1145, 26–36. doi:https://doi.org/10.1016/j.aca.2020.12.021.

Guo, R., and Ren, J. (2010). Alcohol and Acetaldehyde in Public Health: From Marvel to Menace. Int. J. Environ. Res. Public Heal. 7. doi:10.3390/ijerph7041285.

Gupta, A., Dwivedi, M., Gowda, G. A. N., Mahdi, A. A., Jain, A., Ayyagari, A., et al. (2006). 1H NMR spectroscopy in the diagnosis of Klebsiella pneumoniae-induced urinary tract infection. NMR Biomed. 19, 1055–1061. doi:https://doi.org/10.1002/nbm.1078.

Gupta, A., Dwivedi, M., Mahdi, A. A., Khetrapal, C. L., and Bhandari, M. (2012). Broad Identification of Bacterial Type in Urinary Tract Infection Using 1H NMR Spectroscopy. J. Proteome Res. 11, 1844–1854. doi:10.1021/pr2010692.

Habibi, M., Asadi Karam, M. R., and Bouzari, S. (2017). Evaluation of prevalence, immunogenicity and efficacy of FyuA iron receptor in uropathogenic Escherichia coli isolates as a vaccine target against urinary tract infection. Microb. Pathog. 110, 477–483. doi:10.1016/j.micpath.2017.07.037.

Hadayat, N., De Oliveira, L. M., Da Silva, E., Han, L., Hussain, M., Liu, X., et al. (2018). Assessment of trace metals in five most-consumed vegetables in the US: Conventional vs. organic. Environ. Pollut. 243, 292–300. doi:10.1016/j.envpol.2018.08.065.

Hadjadj, J., Yatim, N., Barnabei, L., Corneau, A., Boussier, J., Smith, N., et al. (2020). Impaired type I interferon activity and inflammatory responses in severe COVID-19 patients. Science 369, 718–724. doi:10.1126/science.abc6027.

Hagan, E. C., Lloyd, A. L., Rasko, D. A., Faerber, G. J., and Mobley, H. L. T. (2010). Escherichia coli global gene expression in urine from women with urinary tract infection. PLoS Pathog. 6. doi:10.1371/journal.ppat.1001187.

Hall, J. A., Bouladoux, N., Sun, C. M., Wohlfert, E. A., Blank, R. B., Zhu, Q., et al. (2008). Commensal DNA Limits Regulatory T Cell Conversion and Is a Natural Adjuvant of Intestinal Immune Responses. Immunity. doi:10.1016/j.immuni.2008.08.009.

Hancock, V., and Klemm, P. (2007). Global gene expression profiling of asymptomatic bacteriuria Escherichia coli during biofilm growth in human urine. Infect. Immun. 75, 966–976. doi:10.1128/IAI.01748-06.

Hanisch, U. K., and Kettenmann, H. (2007). Microglia: Active sensor and versatile effector cells in the normal and pathologic brain. Nat. Neurosci. doi:10.1038/nn1997.

Hare, D. J., Lei, P., Ayton, S., Roberts, B. R., Grimm, R., George, J. L., et al. (2014). An iron-dopamine index predicts risk of parkinsonian neurodegeneration in the substantia nigra pars compacta. Chem. Sci. 5, 2160–2169. doi:10.1039/c3sc53461h.

Hare, D. J., Arora, M., Jenkins, N. L., Finkelstein, D. I., Doble, P. A., and Bush, A. I. (2015). Is early-life iron exposure critical in neurodegeneration? Nat. Rev. Neurol. 11, 536–544. doi:10.1038/nrneurol.2015.100.

Hare, D. J., Cardoso, B. R., Raven, E. P., Double, K. L., Finkelstein, D. I., Szymlek-Gay, E. A., et al. (2017). Excessive early-life dietary exposure: a potential source of elevated brain iron and a risk factor for Parkinson's disease. NPJ Park. Dis. 3, 1. doi:10.1038/s41531-016-0004-y.

Hare, D. J., and Double, K. L. (2016). Iron and dopamine: a toxic couple. Brain 139, 1026–1035. doi:10.1093/brain/aww022.

Hare, D., Ayton, S., Bush, A., and Lei, P. (2013). A delicate balance: Iron metabolism and diseases of the brain. Front. Aging Neurosci. 5, 34. doi:10.3389/fnagi.2013.00034.

Harischandra, D. S., Ghaisas, S., Zenitsky, G., Jin, H., Kanthasamy, A., Anantharam, V., et al. (2019). Manganese-induced neurotoxicity: New insights into the triad of protein misfolding, mitochondrial impairment, and neuroinflammation. Front. Neurosci. 13, 1–19. doi:10.3389/fnins.2019.00654.

Harischandra, D. S., Jin, H., Anantharam, V., Kanthasamy, A., and Kanthasamy, A. G. (2015). α-Synuclein protects against manganese neurotoxic insult during the early stages of exposure in a dopaminergic cell model of Parkinson's disease. Toxicol. Sci. 143, 454–468. doi:10.1093/toxsci/kfu247.

Hartung, T., FitzGerald, R. E., Jennings, P., Mirams, G. R., Peitsch, M. C., Rostami-Hodjegan, A., et al. (2017). Systems Toxicology: Real World Applications and Opportunities. Chem. Res. Toxicol. 30, 870–882. doi:10.1021/acs.chemrestox.7b00003.

Hashim, H., Azmin, S., Razlan, H., Yahya, N. W., Tan, H. J., Manaf, M. R. A., et al. (2014). Eradication of Helicobacter pylori infection improves levodopa action, clinical symptoms and quality of life in patients with Parkinson's disease. PLoS One 9, e112330. doi:10.1371/journal.pone.0112330.

Hashim, H., Azmin, S., Razlan, H., Yahya, N. W., Tan, H. J., Manaf, M. R. A., et al. (2014). Eradication of Helicobacter pylori infection improves levodopa action, clinical symptoms and quality of life in patients with parkinson's disease. PLoS One 9. doi:10.1371/journal.pone.0112330.

Hawkes, C. H., Del Tredici, K., and Braak, H. (2007). Parkinson's disease: A dual-hit hypothesis. Neuropathol. Appl. Neurobiol. doi:10.1111/j.1365-2990.2007.00874.x.

Hawkes, C. H., Del Tredici, K., and Braak, H. (2010). A timeline for Parkinson's disease. Parkinsonism Relat. Disord. 16, 79–84. doi:10.1016/j.parkreldis.2009.08.007.

He, J., Cai, S., Feng, H., Cai, B., Lin, L., Mai, Y., et al. (2020). Single-cell analysis reveals bronchoalveolar epithelial dysfunction in COVID-19 patients. Protein Cell 11, 680–687. doi:10.1007/s13238-020-00752-4.

Hegde, M. L., Shanmugavelu, P., Vengamma, B., Rao, T. S. S., Menon, R. B., Rao, R. V, et al. (2004). Serum trace element levels and the complexity of inter-element relations in patients with Parkinson's disease. J. trace Elem. Med. Biol. organ Soc. Miner. Trace Elem. 18, 163–171. doi:10.1016/j.jtemb.2004.09.003.

Heinken, A., Sahoo, S., Fleming, R. M. T., and Thiele, I. (2013). Systems-level characterization of a host-microbe metabolic symbiosis in the mammalian gut. Gut Microbes 4, 28–40. doi:10.4161/gmic.22370.

Heinken, A., Basile, A., and Thiele, I. (2021). Advances in constraint-based modelling of microbial communities. Curr. Opin. Syst. Biol., 1–10. doi:10.1016/j.coisb.2021.05.007.

Heinken, A., Hertel, J., and Thiele, I. (2021). Metabolic modelling reveals broad changes in gut microbial metabolism in inflammatory bowel disease patients with dysbiosis. npj Syst. Biol. Appl. 7. doi:10.1038/s41540-021-00178-6.

Heirendt, L., Arreckx, S., Pfau, T., Mendoza, S. N., Richelle, A., Heinken, A., et al. (2019). Creation and analysis of biochemical constraint-based models using the COBRA Toolbox v.3.0. Nat. Protoc. 14, 639–702. doi:10.1038/s41596-018-0098-2.

Hiippala, K., Jouhten, H., Ronkainen, A., Hartikainen, A., Kainulainen, V., Jalanka, J., et al. (2018). The potential of gut commensals in reinforcing intestinal barrier function and alleviating inflammation. Nutrients. doi:10.3390/nu10080988.

Hilt, E. E., McKinley, K., Pearce, M. M., Rosenfeld, A. B., Zilliox, M. J., Mueller, E. R., et al. (2014). Urine is not sterile: use of enhanced urine culture techniques to detect resident bacterial flora in the adult female bladder. J. Clin. Microbiol. 52, 871–876. doi:10.1128/JCM.02876-13.

Hiron, A., Posteraro, B., Carrière, M., Remy, L., Delporte, C., La Sorda, M., et al. (2010). A nickel ABC-transporter of Staphylococcus aureus is involved in urinary tract infection. Mol. Microbiol. 77, 1246–1260. doi:10.1111/j.1365-2958.2010.07287.x.

Hirsch, E. C., and Hunot, S. (2009). Neuroinflammation in Parkinson's disease: a target for neuroprotection? Lancet. Neurol. 8, 382–397. doi:10.1016/S1474-4422(09)70062-6.

Hoepel, W., Chen, H.-J., Allahverdiyeva, S., Manz, X., Aman, J., Bonta, P., et al. (2020). Anti-SARS-CoV-2 IgG from severely ill COVID-19 patients promotes macrophage hyper-inflammatory responses. doi:10.1101/2020.07.13.190140.

Hooper, L. V., Littman, D. R., and Macpherson, A. J. (2012). Interactions Between the Microbiota and the Immune System. Science (80-.). 336, 1268–1273.

Hooton, T. M. (2012). Clinical practice. Uncomplicated urinary tract infection. N. Engl. J. Med. 366, 1028–1037. doi:10.1056/NEJMcp1104429.

Horsley, H., Dharmasena, D., Malone-Lee, J., and Rohn, J. L. (2018). A urine-dependent human urothelial organoid offers a potential alternative to rodent models of infection. Sci. Rep. 8, 1238. doi:10.1038/s41598-018-19690-7.

Hsu, M., Srinivas, B., Kumar, J., Subramanian, R., and Andersen, J. (2005). Glutathione depletion resulting in selective mitochondrial complex I inhibition in dopaminergic cells is via an NO-mediated pathway not involving peroxynitrite: implications for Parkinson's disease. J. Neurochem. 92, 1091–1103. doi:10.1111/j.1471-4159.2004.02929.x.

Hu, Y., Chen, D., Zheng, P., Yu, J., He, J., Mao, X., et al. (2019). The Bidirectional Interactions between Resveratrol and Gut Microbiota: An Insight into Oxidative Stress and Inflammatory Bowel Disease Therapy. Biomed Res. Int. 2019, 5403761. doi:10.1155/2019/5403761.

Huang, C., Wang, Y., Li, X., Ren, L., Zhao, J., Hu, Y., et al. (2020). Clinical features of patients infected with 2019 novel coronavirus in Wuhan, China. Lancet (London, England) 395, 497–506. doi:10.1016/S0140-6736(20)30183-5.

Hui, D. S., I Azhar, E., Madani, T. A., Ntoumi, F., Kock, R., Dar, O., et al. (2020). The continuing 2019-nCoV epidemic threat of novel coronaviruses to global health - The latest 2019 novel coronavirus outbreak in Wuhan, China. Int. J. Infect. Dis. IJID Off. Publ. Int. Soc. Infect. Dis. 91, 264–266. doi:10.1016/j.ijid.2020.01.009.

Hunter, P., Chapman, T., Coveney, P. V, de Bono, B., Diaz, V., Fenner, J., et al. (2013). A vision and strategy for the virtual physiological human: 2012 update. Interface Focus 3, 20130004. doi:10.1098/rsfs.2013.0004.

Hyduke, D. R., Lewis, N. E., and Palsson, B. Ø. (2013). Analysis of omics data with genome-scale models of metabolism. Mol. Biosyst. 9, 167–174. doi:10.1039/c2mb25453k.

Hyre, A. N., Kavanagh, K., Kock, N. D., Donati, G. L., and Subashchandrabose, S. (2017). Copper Is a Host Effector Mobilized to Urine during Urinary Tract Infection To Impair Bacterial Colonization. Infect. Immun. 85. doi:10.1128/IAI.01041-16.

Imdahl, F., Vafadarnejad, E., Homberger, C., Saliba, A.-E., and Vogel, J. (2020). Single-cell RNA-sequencing reports growth-condition-specific global transcriptomes of individual bacteria. Nat. Microbiol. 5, 1202–1206. doi:10.1038/s41564-020-0774-1.

Ingrassia, R., Garavaglia, B., and Memo, M. (2019). DMT1 Expression and iron levels at the crossroads between aging and neurodegeneration. Front. Neurosci. doi:10.3389/fnins.2019.00575.

Ipe, D. S., Horton, E., and Ulett, G. C. (2016). The Basics of Bacteriuria: Strategies of Microbes for Persistence in Urine. Front. Cell. Infect. Microbiol. 6, 14. doi:10.3389/fcimb.2016.00014.

Ipe, D. S., Sundac, L., Benjamin, W. H. J., Moore, K. H., and Ulett, G. C. (2013). Asymptomatic bacteriuria: prevalence rates of causal microorganisms, etiology of infection in different patient populations, and recent advances in molecular detection. FEMS Microbiol. Lett. 346, 1–10. doi:10.1111/1574-6968.12204.

Irizar, P., Schäuble, S., Esser, D., Groth, M., Frahm, C., Priebe, S., et al. (2018). Transcriptomic alterations during ageing reflect the shift from cancer to degenerative diseases in the elderly. Nat. Commun. 9, 1–11. doi:10.1038/s41467-017-02395-2.

Jaglin, M., Rhimi, M., Philippe, C., Pons, N., Bruneau, A., Goustard, B., et al. (2018). Indole, a signaling molecule produced by the gut microbiota, negatively impacts emotional behaviors in rats. Front. Neurosci. doi:10.3389/fnins.2018.00216.

Jaishankar, M., Tseten, T., Anbalagan, N., Mathew, B. B., and Beeregowda, K. N. (2014). Toxicity, mechanism and health effects of some heavy metals. Interdiscip. Toxicol. 7, 60–72. doi:10.2478/intox-2014-0009.

Jantunen, M. E., Saxén, H., Lukinmaa, S., Ala-Houhala, M., and Siitonen, A. (2001). Genomic identity of pyelonephritogenic Escherichia coli isolated from blood, urine and faeces of children with urosepsis. J. Med. Microbiol. 50, 650–652. doi:10.1099/0022-1317-50-7-650.

Jerby, L., Shlomi, T., and Ruppin, E. (2010). Computational reconstruction of tissue-specific metabolic models: application to human liver metabolism. Mol. Syst. Biol. 6, 401. doi:10.1038/msb.2010.56.

Jinsmaa, Y., Sullivan, P., Gross, D., Cooney, A., Sharabi, Y., and Goldstein, D. S. (2014). Divalent metal ions enhance DOPAL-induced oligomerization of alpha-synuclein. Neurosci. Lett. 569, 27–32. doi:10.1016/j.neulet.2014.03.016.

Josephs-Spaulding, J., Beeler, E., and Singh, O. V. (2016). Human microbiome versus food-borne pathogens: friend or foe. Appl. Microbiol. Biotechnol. 100, 4845–4863. doi:10.1007/s00253-016-7523-7.

Josephs-Spaulding, J., Krogh, T. J., Rettig, H. C., Lyng, M., Chkonia, M., Waschina, S., et al. (2021). Recurrent Urinary Tract Infections: Unraveling the Complicated Environment of Uncomplicated rUTIs. Front. Cell. Infect. Microbiol. 11, 1–22. doi:10.3389/fcimb.2021.562525.

Joshi, C. J., Schinn, S.-M., Richelle, A., Shamie, I., O'Rourke, E. J., and Lewis, N. E. (2020). StanDep: Capturing transcriptomic variability improves context-specific metabolic models. PLoS Comput. Biol. 16, e1007764. doi:10.1371/journal.pcbi.1007764.

Jost, L. (2007). PARTITIONING DIVERSITY INTO INDEPENDENT ALPHA AND BETA COMPONENTS. Ecology 88, 2427–2439. doi:https://doi.org/10.1890/06-1736.1.

Jost, L. (2006). Entropy and diversity. OIKOS 2.

Jozefczak, M., Remans, T., Vangronsveld, J., and Cuypers, A. (2012). Glutathione is a key player in metal-induced oxidative stress defenses. Int. J. Mol. Sci. 13, 3145–3175. doi:10.3390/ijms13033145.

Jozefczuk, S., Klie, S., Catchpole, G., Szymanski, J., Cuadros-Inostroza, A., Steinhauser, D., et al. (2010). Metabolomic and transcriptomic stress response of Escherichia coli. Mol. Syst. Biol. 6, 364. doi:10.1038/msb.2010.18.

Justice, S. S., Hung, C., Theriot, J. A., Fletcher, D. A., Anderson, G. G., Footer, M. J., et al. (2004). Differentiation and developmental pathways of uropathogenic Escherichia coli in urinary tract pathogenesis. Proc. Natl. Acad. Sci. U. S. A. 101, 1333–1338. doi:10.1073/pnas.0308125100.

Kanehisa, M., Furumichi, M., Sato, Y., Ishiguro-Watanabe, M., and Tanabe, M. (2021). KEGG: Integrating viruses and cellular organisms. Nucleic Acids Res. 49, D545–D551. doi:10.1093/nar/gkaa970.

Kanehisa, M., and Goto, S. (2000). KEGG: kyoto encyclopedia of genes and genomes. Nucleic Acids Res. 28, 27–30.

Karimi, K., Inman, M. D., Bienenstock, J., and Forsythe, P. (2009). Lactobacillus reuteri-induced regulatory T cells protect against an allergic airway response in mice. Am. J. Respir. Crit. Care Med. doi:10.1164/rccm.200806-951OC.

Karlinsky, A., and Kobak, D. (2021). Tracking excess mortality across countries during the covid-19 pandemic with the world mortality dataset. Elife 10, 1–21. doi:10.7554/eLife.69336.

Karri, V., Schuhmacher, M. P., and Kumar, V. (2020). A systems toxicology approach to compare the heavy metal mixtures (Pb, As, MeHg) impact in neurodegenerative diseases. Food Chem. Toxicol. an Int. J. Publ. Br. Ind. Biol. Res. Assoc. 139, 111257. doi:10.1016/j.fct.2020.111257.

Katherine, D., Sinead, C., Edward, M., Mingzhi, L., R., B. I., J., W. M., et al. (2019). Bacterial Microcompartment-Mediated Ethanolamine Metabolism in Escherichia coli Urinary Tract Infection. Infect. Immun. 87, e00211-19. doi:10.1128/IAI.00211-19.

Ke, T., Sidoryk-Wegrzynowicz, M., Pajarillo, E., Rizor, A., Soares, F. A. A., Lee, E., et al. (2019). Role of Astrocytes in Manganese Neurotoxicity Revisited. Neurochem. Res. 44, 2449–2459. doi:10.1007/s11064-019-02881-7.

Keogh, D., Tay, W. H., Ho, Y. Y., Dale, J. L., Chen, S., Umashankar, S., et al. (2016). Enterococcal Metabolite Cues Facilitate Interspecies Niche Modulation and Polymicrobial Infection. Cell Host Microbe 20, 493–503. doi:https://doi.org/10.1016/j.chom.2016.09.004.

Keshavarzian, A., Green, S. J., Engen, P. A., Voigt, R. M., Naqib, A., Forsyth, C. B., et al. (2015). Colonic bacterial composition in Parkinson's disease. Mov. Disord. 30, 1351–1360. doi:10.1002/mds.26307.

Khasheii, B., Anvari, S., and Jamalli, A. (2016). Frequency evaluation of genes encoding siderophores and the effects of different concentrations of Fe ions on growth rate of uropathogenic Escherichia coli. Iran. J. Microbiol. 8, 359–365.

Khoury, M. J., Iademarco, M. F., and Riley, W. T. (2016). Precision Public Health for the Era of Precision Medicine. Am. J. Prev. Med. 50, 398–401. doi:10.1016/j.amepre.2015.08.031.

Kim, D., Paggi, J. M., Park, C., Bennett, C., and Salzberg, S. L. (2019). Graph-based genome alignment and genotyping with HISAT2 and HISAT-genotype. Nat. Biotechnol. 37, 907–915.

Kim, M. Y., Kim, J. H., Cho, M. H., Choi, Y. H., Kim, S. H., Im, Y. J., et al. (2019). Urological Problems in Patients with Menkes Disease. J Korean Med Sci 34. Available at: https://doi.org/10.3346/jkms.2019.34.e4.

Kim, S. H., Johnson, V. J., and Sharma, R. P. (2002). Mercury inhibits nitric oxide production but activates proinflammatory cytokine expression in murine macrophage: differential modulation of NF-kappaB and p38 MAPK signaling pathways. Nitric oxide Biol. Chem. 7, 67–74. doi:10.1016/s1089-8603(02)00008-3.

King, Z. A., Lloyd, C. J., Feist, A. M., and Palsson, B. O. (2015). Next-generation genome-scale models for metabolic engineering. Curr. Opin. Biotechnol. 35, 23–29. doi:10.1016/j.copbio.2014.12.016.

Klitgord, N., and Segrè, D. (2011). Ecosystems biology of microbial metabolism. Curr. Opin. Biotechnol. 22, 541–546. doi:10.1016/j.copbio.2011.04.018.

Knudsen, T. B., Keller, D. A., Sander, M., Carney, E. W., Doerrer, N. G., Eaton, D. L., et al. (2015). FutureTox II: In vitro Data and In Silico Models for Predictive Toxicology. Toxicol. Sci. 143, 256–267. doi:10.1093/toxsci/kfu234.

Kopylova, E., Noé, L., and Touzet, H. (2012). SortMeRNA: fast and accurate filtering of ribosomal RNAs in metatranscriptomic data. Bioinformatics 28, 3211–3217.

Kortekaas, R., Leenders, K. L., Van Oostrom, J. C. H., Vaalburg, W., Bart, J., Willemsen, A. T. M., et al. (2005). Blood-brain barrier dysfunction in Parkinsonian midbrain in vivo. Ann. Neurol. doi:10.1002/ana.20369.

Kostakioti, M., Hultgren, S. J., and Hadjifrangiskou, M. (2012). Molecular blueprint of uropathogenic Escherichia coli virulence provides clues toward the development of anti-virulence therapeutics. Virulence 3, 592–594. doi:10.4161/viru.22364.

Kouli, A., Torsney, K. M., and Kuan, W.-L. (2018). "Parkinson's Disease: Etiology, Neuropathology, and Pathogenesis.," in, eds. T. B. Stoker and J. C. Greenland (Brisbane (AU)). doi:10.15586/codonpublications.parkinsonsdisease.2018.ch1.

Kuchina, A., Brettner, L. M., Paleologu, L., Roco, C. M., Rosenberg, A. B., Carignano, A., et al. (2021). Microbial single-cell RNA sequencing by split-pool barcoding. Science (80-.). 371, eaba5257. doi:10.1126/science.aba5257.

Kunin, C. M., Hua, T. H., Van Arsdale White, L., and Villarejo, M. (1992). Growth of Escherichia coli in Human Urine: Role of Salt Tolerance and Accumulation of Glycine Betaine. J. Infect. Dis. 166, 1311–1315. doi:10.1093/infdis/166.6.1311.

Kuri-Cervantes, L., Pampena, M. B., Meng, W., Rosenfeld, A. M., Ittner, C. A. G., Weisman, A. R., et al. (2020). Comprehensive mapping of immune perturbations associated with severe COVID-19. Sci. Immunol. 5. doi:10.1126/sciimmunol.abd7114.

Kustrimovic, N., Comi, C., Magistrelli, L., Rasini, E., Legnaro, M., Bombelli, R., et al. (2018). Parkinson's disease patients have a complex phenotypic and functional Th1 bias: Cross-sectional studies of CD4+ Th1/Th2/T17 and Treg in drug-naïve and drug-treated patients. J. Neuroinflammation. doi:10.1186/s12974-018-1248-8.

Kwakye, G. F., Paoliello, M. M. B., Mukhopadhyay, S., Bowman, A. B., and Aschner, M. (2015). Manganese-induced parkinsonism and Parkinson's disease: Shared and distinguishable features. Int. J. Environ. Res. Public Health. doi:10.3390/ijerph120707519.

Kwon, H. S., and Koh, S.-H. (2020). Neuroinflammation in neurodegenerative disorders: the roles of microglia and astrocytes. Transl. Neurodegener. 9, 42. doi:10.1186/s40035-020-00221-2.

Laing, A. G., Lorenc, A., Del Molino Del Barrio, I., Das, A., Fish, M., Monin, L., et al. (2020). A consensus Covid-19 immune signature combines immuno-protection with discrete sepsis-like traits associated with poor prognosis. medRxiv. doi:10.1101/2020.06.08.20125112.

Lam, C.-W., Law, C.-Y., To, K. K.-W., Cheung, S. K.-K., Lee, K., Sze, K.-H., et al. (2014). NMR-based metabolomic urinalysis: A rapid screening test for urinary tract infection. Clin. Chim. Acta 436, 217–223. doi:https://doi.org/10.1016/j.cca.2014.05.014.

Lamont, R. F., Sobel, J. D., Akins, R. A., Hassan, S. S., Chaiworapongsa, T., Kusanovic, J. P., et al. (2011). The vaginal microbiome: new information about genital tract flora using molecular based techniques. BJOG An Int. J. Obstet. Gynaecol. 118, 533–549. doi:https://doi.org/10.1111/j.1471-0528.2010.02840.x.

Lamtai, M., Zghari, O., Ouakki, S., Marmouzi, I., Mesfioui, A., El Hessni, A., et al. (2020). Chronic copper exposure leads to hippocampus oxidative stress and impaired learning and memory in male and female rats. Toxicol. Res. 36, 359–366. doi:10.1007/s43188-020-00043-4.

Larsen, M. D., de Graaf, E. L., Sonneveld, M. E., Plomp, H. R., Nouta, J., Hoepel, W., et al. (2021). Afucosylated IgG characterizes enveloped viral responses and correlates with COVID-19 severity. Science (80-.). 371, eabc8378. doi:10.1126/science.abc8378.

Latorre, R., Sternini, C., De Giorgio, R., and Greenwood-Van Meerveld, B. (2016). Enteroendocrine cells: A review of their role in brain-gut communication. Neurogastroenterol. Motil. doi:10.1111/nmo.12754.

Lebouvier, T., Chaumette, T., Paillusson, S., Duyckaerts, C., Bruley Des Varannes, S., Neunlist, M., et al. (2009). The second brain and Parkinson's disease. Eur. J. Neurosci. doi:10.1111/j.1460-9568.2009.06873.x.

Lee, I. T., Nakayama, T., Wu, C.-T., Goltsev, Y., Jiang, S., Gall, P. A., et al. (2020). Robust ACE2 protein expression localizes to the motile cilia of the respiratory tract epithelia and is not increased by ACE inhibitors or angiotensin receptor blockers. medRxiv Prepr. Serv. Heal. Sci. doi:10.1101/2020.05.08.20092866.

Lee, Y. K., Menezes, J. S., Umesaki, Y., and Mazmanian, S. K. (2011). Proinflammatory T-cell responses to gut microbiota promote experimental autoimmune encephalomyelitis. Proc. Natl. Acad. Sci. U. S. A. doi:10.1073/pnas.1000082107.

Lemke, G., and Silverman, G. J. (2020). Blood clots and TAM receptor signalling in COVID-19 pathogenesis. Nat. Rev. Immunol. 20, 395–396. doi:10.1038/s41577-020-0354-x.

Letko, M., Marzi, A., and Munster, V. (2020). Functional assessment of cell entry and receptor usage for SARS-CoV-2 and other lineage B betacoronaviruses. Nat. Microbiol. 5, 562–569. doi:10.1038/s41564-020-0688-y.

Léveillé, S., Caza, M., Johnson, J. R., Clabots, C., Sabri, M., and Dozois, C. M. (2006). Iha from an Escherichia coli urinary tract infection outbreak clonal group A strain is expressed in vivo in the

mouse urinary tract and functions as a catecholate siderophore receptor. Infect. Immun. 74, 3427–3436. doi:10.1128/IAI.00107-06.

Levi, S., and Finazzi, D. (2014). Neurodegeneration with brain iron accumulation: update on pathogenic mechanisms. Front. Pharmacol. 5, 99. doi:10.3389/fphar.2014.00099.

Lewis, D. A., Brown, R., Williams, J., White, P., Jacobson, S. K., Marchesi, J. R., et al. (2013). The human urinary microbiome; bacterial DNA in voided urine of asymptomatic adults. Front. Cell. Infect. Microbiol. 3, 41. doi:10.3389/fcimb.2013.00041.

Lewis, N. E., Schramm, G., Bordbar, A., Schellenberger, J., Andersen, M. P., Cheng, J. K., et al. (2010). Large-scale in silico modeling of metabolic interactions between cell types in the human brain. Nat. Biotechnol. 28, 1279–1285. doi:10.1038/nbt.1711.

Lewis, N. E., Nagarajan, H., and Palsson, B. O. (2012). Constraining the metabolic genotype-phenotype relationship using a phylogeny of in silico methods. Nat. Rev. Microbiol. 10, 291–305. doi:10.1038/nrmicro2737.

Li, C., Menoret, A., Farragher, C., Ouyang, Z., Bonin, C., Holvoet, P., et al. (2019). Single-cell transcriptomics-based MacSpectrum reveals macrophage activation signatures in diseases. JCI Insight 4. doi:10.1172/jci.insight.126453.

Li, H., Handsaker, B., Wysoker, A., Fennell, T., Ruan, J., Homer, N., et al. (2009). The sequence alignment/map format and SAMtools. Bioinformatics 25, 2078–2079.

Li, H., Liu, L., Zhang, D., Xu, J., Dai, H., Tang, N., et al. (2020). SARS-CoV-2 and viral sepsis: observations and hypotheses. Lancet (London, England) 395, 1517–1520. doi:10.1016/S0140-6736(20)30920-X.

Li, S., Sullivan, N. L., Rouphael, N., Yu, T., Banton, S., Maddur, M. S., et al. (2017). Metabolic phenotypes of response to vaccination in humans. Cell 169, 862–877.

Li, W., Wu, X., Hu, X., Wang, T., Liang, S., Duan, Y., et al. (2017). Structural changes of gut microbiota in Parkinson's disease and its correlation with clinical features. Sci. China. Life Sci. 60, 1223–1233. doi:10.1007/s11427-016-9001-4.

Li, X., and Ma, X. (2020). Acute respiratory failure in COVID-19: Is it "typical" ARDS? Crit. Care 24, 1–5. doi:10.1186/s13054-020-02911-9.

Li, X., Brejnrod, A. D., Ernst, M., Rykær, M., Herschend, J., Olsen, N. M. C., et al. (2019). Heavy metal exposure causes changes in the metabolic health-associated gut microbiome and metabolites. Environ. Int. doi:10.1016/j.envint.2019.02.048.

Lian, T.-H., Guo, P., Zuo, L.-J., Hu, Y., Yu, S.-Y., Yu, Q.-J., et al. (2019). Tremor-Dominant in Parkinson Disease: The Relevance to Iron Metabolism and Inflammation. Front. Neurosci. 13, 255. doi:10.3389/fnins.2019.00255.

Liao, M., Liu, Y., Yuan, J., Wen, Y., Xu, G., Zhao, J., et al. (2020). Single-cell landscape of bronchoalveolar immune cells in patients with COVID-19. Nat. Med. 26, 842–844. doi:10.1038/s41591-020-0901-9.

Lin, Y., Vogt, R., and Larssen, T. (2012). Environmental mercury in China: a review. Environ. Toxicol. Chem. 31, 2431–2444. doi:10.1002/etc.1980.

Litvak, Y., Byndloss, M. X., and Bäumler, A. J. (2018). Colonocyte metabolism shapes the gut microbiota. Science 362. doi:10.1126/science.aat9076.

Liu, F., Ling, Z., Xiao, Y., Lv, L., Yang, Q., Wang, B., et al. (2017). Dysbiosis of urinary microbiota is positively correlated with type 2 diabetes mellitus. Oncotarget 8, 3798–3810. doi:10.18632/oncotarget.14028.

Liu, J. T., Dong, M. H., Zhang, J. Q., Bai, Y., Kuang, F., and Chen, L. W. (2015). Microglia and astroglia: The role of neuroinflammation in lead toxicity and neuronal injury in the brain. Neuroimmunol. Neuroinflammation 2, 131–137. doi:10.4103/2347-8659.156980.

Liu, X., Su, P., Meng, S., Aschner, M., Cao, Y., Luo, W., et al. (2017). Role of matrix metalloproteinase-2/9 (MMP2/9) in lead-induced changes in an in vitro blood-brain barrier model. Int. J. Biol. Sci. 13, 1351–1360. doi:10.7150/ijbs.20670.

Liu, Y. Y., Wang, Y., Walsh, T. R., Yi, L. X., Zhang, R., Spencer, J., et al. (2016). Emergence of plasmid-mediated colistin resistance mechanism MCR-1 in animals and human beings in China: A microbiological and molecular biological study. Lancet Infect. Dis. 16, 161–168. doi:10.1016/S1473-3099(15)00424-7.

Lloyd, K. G., Steen, A. D., Ladau, J., Yin, J., and Crosby, L. (2018). Phylogenetically Novel Uncultured Microbial Cells Dominate Earth Microbiomes. mSystems 3. doi:10.1128/mSystems.00055-18.

Logroscino, G., Marder, K., Graziano, J., Freyer, G., Slavkovich, V., LoIacono, N., et al. (1997). Altered systemic iron metabolism in Parkinson's disease. Neurology 49, 714–717. doi:10.1212/wnl.49.3.714.

Long, Q.-X., Liu, B.-Z., Deng, H.-J., Wu, G.-C., Deng, K., Chen, Y.-K., et al. (2020). Antibody responses to SARS-CoV-2 in patients with COVID-19. Nat. Med. 26, 845–848. doi:10.1038/s41591-020-0897-1.

López-Maury, L., Marguerat, S., and Bähler, J. (2008). Tuning gene expression to changing environments: From rapid responses to evolutionary adaptation. Nat. Rev. Genet. 9, 583–593. doi:10.1038/nrg2398.

Lotfipour, A. K., Wharton, S., Schwarz, S. T., Gontu, V., Schäfer, A., Peters, A. M., et al. (2012). High resolution magnetic susceptibility mapping of the substantia nigra in Parkinson's disease. J. Magn. Reson. Imaging 35, 48–55. doi:10.1002/jmri.22752.

Lu, L., Barbi, J., and Pan, F. (2017). The regulation of immune tolerance by FOXP3. Nat. Rev. Immunol. 17, 703–717. doi:10.1038/nri.2017.75.

Lu, Z., Huang, L., Li, Y., Xu, Y., Zhang, R., Zhou, Q., et al. (2021). Fine‐Tuning of Cholesterol Homeostasis Controls Erythroid Differentiation. Adv. Sci., 2102669.

Lund, M. L., Sorrentino, G., Egerod, K. L., Kroone, C., Mortensen, B., Knop, F. K., et al. (2020). L-cell differentiation is induced by bile acids through GpBAR1 and paracrine GLP-1 and serotonin signaling. Diabetes. doi:10.2337/db19-0764.

Luo, X., Yang, X., Li, J., Zou, G., Lin, Y., Qing, G., et al. (2018). The procalcitonin/albumin ratio as an early diagnostic predictor in discriminating urosepsis from patients with febrile urinary tract infection. Medicine (Baltimore). 97. Available at: https://journals.lww.com/md-journal/Fulltext/2018/07130/The_procalcitonin_albumin_ratio_as_an_early.2.aspx.

Luo, Y., Ma, Y., Zhao, Q., Wang, L., Guo, L., Ye, L., et al. (2012). Similarity and divergence of phylogenies, antimicrobial susceptibilities, and virulence factor profiles of Escherichia coli isolates causing recurrent urinary tract infections that persist or result from reinfection. J. Clin. Microbiol. 50, 4002–4007. doi:10.1128/JCM.02086-12.

Lussu, M., Camboni, T., Piras, C., Serra, C., Del Carratore, F., Griffin, J., et al. (2017). 1H NMR spectroscopy-based metabolomics analysis for the diagnosis of symptomatic E. coli-associated urinary tract infection (UTI). BMC Microbiol. 17, 201. doi:10.1186/s12866-017-1108-1.

Ly, A., James, H., Annie, L., E., C. D., and M., W. J. (2004). Osmoregulatory Systems of Escherichia coli:Identification of Betaine-Carnitine-Choline Transporter Family MemberBetU and Distributions of betU and trkG amongPathogenic and NonpathogenicIsolates. J. Bacteriol. 186, 296–306. doi:10.1128/JB.186.2.296-306.2004.

Lyons, A., O'Mahony, D., O'Brien, F., MacSharry, J., Sheil, B., Ceddia, M., et al. (2010). Bacterial strain-specific induction of Foxp3+ T regulatory cells is protective in murine allergy models. Clin. Exp. Allergy. doi:10.1111/j.1365-2222.2009.03437.x.

M, J., RJ, C., S, R., and D, M. (2018). Medullary Sponge Kidney with Distal Renal Tubular Acidosis: A Case Report and Review of the Literature. SAJ Case Reports 5, 1–5. doi:10.18875/2375-7043.5.204.

Ma, L., Gholam Azad, M., Dharmasivam, M., Richardson, V., Quinn, R. J., Feng, Y., et al. (2021). Parkinson's disease: Alterations in iron and redox biology as a key to unlock therapeutic strategies. Redox Biol. 41, 101896. doi:10.1016/j.redox.2021.101896.

MacDonald, T. T., and Monteleone, G. (2005). Immunity, inflammation, and allergy in the gut. Science (80-.). doi:10.1126/science.1106442.

Machado, A., Jefferson, K. K., and Cerca, N. (2013). Interactions between Lactobacillus crispatus and bacterial vaginosis (BV)-associated bacterial species in initial attachment and biofilm formation. Int. J. Mol. Sci. 14, 12004–12012. doi:10.3390/ijms140612004.

Machado, D., and Herrgård, M. (2014). Systematic evaluation of methods for integration of transcriptomic data into constraint-based models of metabolism. PLoS Comput. Biol. 10, e1003580. doi:10.1371/journal.pcbi.1003580.

Magnúsdóttir, S., Heinken, A., Kutt, L., Ravcheev, D. A., Bauer, E., Noronha, A., et al. (2017). Generation of genome-scale metabolic reconstructions for 773 members of the human gut microbiota. Nat. Biotechnol. 35, 81–89. doi:10.1038/nbt.3703.

Magruder, M., Sholi, A. N., Gong, C., Zhang, L., Edusei, E., Huang, J., et al. (2019). Gut uropathogen abundance is a risk factor for development of bacteriuria and urinary tract infection. Nat. Commun. 10, 5521. doi:10.1038/s41467-019-13467-w.

Marashi, S.-A., Kouhestani, H., and Mahdavi, M. (2013). Studying the relationship between robustness against mutations in metabolic networks and lifestyle of organisms. ScientificWorldJournal. 2013, 615697. doi:10.1155/2013/615697.

Marcero, J. R., Cox, J. E., Bergonia, H. A., Medlock, A. E., Phillips, J. D., and Dailey Jr, H. A. (2021). The immunometabolite itaconate inhibits heme synthesis and remodels cellular metabolism in erythroid precursors. Blood Adv. 5, 4831–4841.

Mardinoglu, A., and Nielsen, J. (2012). Systems medicine and metabolic modelling. J. Intern. Med. 271, 142–154. doi:10.1111/j.1365-2796.2011.02493.x.

Mardinoglu, A., Agren, R., Kampf, C., Asplund, A., Uhlen, M., and Nielsen, J. (2014). Genome-scale metabolic modelling of hepatocytes reveals serine deficiency in patients with non-alcoholic fatty liver disease. Nat. Commun. 5, 1–11. doi:10.1038/ncomms4083.

Marinos, G., Kaleta, C., and Waschina, S. (2020). Defining the nutritional input for genome-scale metabolic models: A roadmap. PLoS One 15, 1–17. doi:10.1371/journal.pone.0236890.

Martin, C. R., Osadchiy, V., Kalani, A., and Mayer, E. A. (2018). The Brain-Gut-Microbiome Axis. CMGH. doi:10.1016/j.jcmgh.2018.04.003.

Martin, H. L., Richardson, B. A., Nyange, P. M., Lavreys, L., Hillier, S. L., Chohan, B., et al. (1999). Vaginal lactobacilli, microbial flora, and risk of human immunodeficiency virus type 1 and sexually transmitted disease acquisition. J. Infect. Dis. 180, 1863–1868. doi:10.1086/315127.

Martin, M. (2011). Cutadapt removes adapter sequences from high-throughput sequencing reads. EMBnet. J. 17, 10–12.

Martinez-Finley, E. J., Chakraborty, S., Fretham, S. J. B., and Aschner, M. (2012). Cellular transport and homeostasis of essential and nonessential metals. Metallomics 4, 593–605. doi:10.1039/c2mt00185c.

Martín-Rodríguez, A. J., Rhen, M., Melican, K., and Richter-Dahlfors, A. (2020). Nitrate Metabolism Modulates Biosynthesis of Biofilm Components in Uropathogenic Escherichia coli and Acts as a Fitness Factor During Experimental Urinary Tract Infection . Front. Microbiol. 11, 26. Available at: https://www.frontiersin.org/article/10.3389/fmicb.2020.00026.

Masid, M., Ataman, M., and Hatzimanikatis, V. (2020). Analysis of human metabolism by reducing the complexity of the genome-scale models using redHUMAN. Nat. Commun. 11, 1–12. doi:10.1038/s41467-020-16549-2.

Mathew, D., Giles, J. R., Baxter, A. E., Oldridge, D. A., Greenplate, A. R., Wu, J. E., et al. (2020). Deep immune profiling of COVID-19 patients reveals distinct immunotypes with therapeutic implications. Science 369. doi:10.1126/science.abc8511.

McConnell, J. R., and Edwards, R. (2008). Coal burning leaves toxic heavy metal legacy in the Arctic. Proc. Natl. Acad. Sci. U. S. A. 105, 12140–12144. doi:10.1073/pnas.0803564105.

McGarrity, S., Karvelsson, S. T., Sigurjónsson, Ó. E., and Rolfsson, Ó. (2020). Comparative Metabolic Network Flux Analysis to Identify Differences in Cellular Metabolism. Methods Mol. Biol. 2088, 223–269. doi:10.1007/978-1-0716-0159-4_11.

McMurdie, P. J., and Holmes, S. (2013). Phyloseq: An R Package for Reproducible Interactive Analysis and Graphics of Microbiome Census Data. PLoS One 8. doi:10.1371/journal.pone.0061217.

Mediavilla, J. R., Patrawalla, A., Chen, L., Chavda, K. D., Mathema, B., Vinnard, C., et al. (2016). Colistin- and Carbapenem-Resistant Escherichia coli Harboring mcr-1 and blaNDM-5, Causing a Complicated Urinary Tract Infection in a Patient from the United States. MBio 7. doi:10.1128/mBio.01191-16.

Mehta, P., McAuley, D. F., Brown, M., Sanchez, E., Tattersall, R. S., and Manson, J. J. (2020). COVID-19: consider cytokine storm syndromes and immunosuppression. Lancet (London, England) 395, 1033–1034. doi:10.1016/S0140-6736(20)30628-0.

Mejia‐Pous, C., Damiola, F., and Gandrillon, O. (2011). Cholesterol synthesis‐related enzyme oxidosqualene cyclase is required to maintain self‐renewal in primary erythroid progenitors. Cell Prolif. 44, 441–452.

Mick, E., and Sorek, R. (2014). High-resolution metagenomics. Nat. Biotechnol. 32, 750–751. doi:10.1038/nbt.2962.

Miclean, M., Cadar, O., Levei, E. A., Roman, R., Ozunu, A., and Levei, L. (2019). Metal (Pb, Cu, Cd, and Zn) Transfer along Food Chain and Health Risk Assessment through Raw Milk Consumption from Free-Range Cows. Int. J. Environ. Res. Public Health 16. doi:10.3390/ijerph16214064.

Min, S. H., Suzuki, A., Stalker, T. J., Zhao, L., Wang, Y., McKennan, C., et al. (2014). Loss of PIKfyve in platelets causes a lysosomal disease leading to inflammation and thrombosis in mice. Nat. Commun. 5, 1–12.

Miranda, M., López-Alonso, M., Castillo, C., Hernández, J., and Benedito, J. L. (2005). Effects of moderate pollution on toxic and trace metal levels in calves from a polluted area of northern Spain. Environ. Int. 31, 543–548. doi:10.1016/j.envint.2004.09.025.

Mirmonsef, P., Hotton, A. L., Gilbert, D., Burgad, D., Landay, A., Weber, K. M., et al. (2014). Free glycogen in vaginal fluids is associated with Lactobacillus colonization and low vaginal pH. PLoS One 9, e102467. doi:10.1371/journal.pone.0102467.

Mo, M. L., Jamshidi, N., and Palsson, B. Ø. (2007). A genome-scale, constraint-based approach to systems biology of human metabolism. Mol. Biosyst. 3, 598–603. doi:10.1039/b705597h.

Mobley, H. (2016). Measuring Escherichia coli Gene Expression during Human Urinary Tract Infections. Pathogens 5, 7. doi:10.3390/pathogens5010007.

Möller, H. E., Bossoni, L., Connor, J. R., Crichton, R. R., Does, M. D., Ward, R. J., et al. (2019). Iron, Myelin, and the Brain: Neuroimaging Meets Neurobiology. Trends Neurosci. 42, 384–401. doi:10.1016/j.tins.2019.03.009.

Moons, R., Konijnenberg, A., Mensch, C., Van Elzen, R., Johannessen, C., Maudsley, S., et al. (2020). Metal ions shape α-synuclein. Sci. Rep. 10, 16293. doi:10.1038/s41598-020-73207-9.

Moore, J. B., and June, C. H. (2020). Cytokine release syndrome in severe COVID-19. Science 368, 473–474. doi:10.1126/science.abb8925.

Moos, T., Rosengren Nielsen, T., Skjørringe, T., and Morgan, E. H. (2007). Iron trafficking inside the brain. J. Neurochem. 103, 1730–1740. doi:10.1111/j.1471-4159.2007.04976.x.

Moreno-Altamirano, M. M. B., Kolstoe, S. E., and Sánchez-García, F. J. (2019). Virus control of cell metabolism for replication and evasion of host immune responses. Front. Cell. Infect. Microbiol. 9, 1–15. doi:10.3389/fcimb.2019.00095.

Mosley, R. L., Hutter-Saunders, J. A., Stone, D. K., and Gendelman, H. E. (2012). Inflammation and adaptive immunity in Parkinson's disease. Cold Spring Harb. Perspect. Med. 2, a009381. doi:10.1101/cshperspect.a009381.

Muhleisen, A. L., and Herbst-Kralovetz, M. M. (2016). Menopause and the vaginal microbiome. Maturitas 91, 42–50. doi:10.1016/j.maturitas.2016.05.015.

Muir, E. M., and Bowyer, D. E. (1984). Inhibition of pinocytosis and induction of release of lysosomal contents by lysosomal overload of arterial smooth muscle cells in vitro. Atherosclerosis 50, 85–92.

Mulak, A., and Bonaz, B. (2015). Brain-gut-microbiota axis in Parkinson's disease. World J. Gastroenterol. doi:10.3748/wjg.v21.i37.10609.

Muñoz, P., and Humeres, A. (2012). Iron deficiency on neuronal function. Biometals an Int. J. role Met. ions Biol. Biochem. Med. 25, 825–835. doi:10.1007/s10534-012-9550-x.

Nayak, M. K., Ghatge, M., Dhanesha, N., Flora, G. D., Jain, M., Rodriguez, O., et al. (2019). Targeting Metabolic Enzyme Pyruvate Kinase M2: A Novel Strategy to Inhibit Platelet Function and Arterial Thrombosis. Blood 134, 1056. doi:10.1182/blood-2019-129027.

Ni, L., Ye, F., Cheng, M.-L., Feng, Y., Deng, Y.-Q., Zhao, H., et al. (2020). Detection of SARS-CoV-2-Specific Humoral and Cellular Immunity in COVID-19 Convalescent Individuals. Immunity 52, 971-977.e3. doi:10.1016/j.immuni.2020.04.023.

Nielsen, K. L., Stegger, M., Godfrey, P. A., Feldgarden, M., Andersen, P. S., and Frimodt-Møller, N. (2016). Adaptation of Escherichia coli traversing from the faecal environment to the urinary tract. Int. J. Med. Microbiol. 306, 595–603. doi:10.1016/j.ijmm.2016.10.005.

Nielsen, S. C. A., Yang, F., Jackson, K. J. L., Hoh, R. A., Röltgen, K., Jean, G. H., et al. (2020). Human B Cell Clonal Expansion and Convergent Antibody Responses to SARS-CoV-2. Cell Host Microbe 28, 516-525.e5. doi:https://doi.org/10.1016/j.chom.2020.09.002.

Nordstrom, L., Liu, C. M., and Price, L. B. (2013). Foodborne urinary tract infections: a new paradigm for antimicrobial-resistant foodborne illness. Front. Microbiol. 4, 29. doi:10.3389/fmicb.2013.00029.

Noronha, A., Modamio, J., Jarosz, Y., Guerard, E., Sompairac, N., Preciat, G., et al. (2019). The Virtual Metabolic Human database: Integrating human and gut microbiome metabolism with nutrition and disease. Nucleic Acids Res. 47, D614–D624. doi:10.1093/nar/gky992.

Notz, Q., Herrmann, J., Schlesinger, T., Kranke, P., Sitter, M., Helmer, P., et al. (2021). Vitamin D deficiency in critically ill COVID-19 ARDS patients. Clin. Nutr.

Oberhardt, M. A., Palsson, B. Ø., and Papin, J. A. (2009). Applications of genome-scale metabolic reconstructions. Mol. Syst. Biol. 5, 320. doi:10.1038/msb.2009.77.

Oberhardt, M. A., Yizhak, K., and Ruppin, E. (2013). Metabolically re-modeling the drug pipeline. Curr. Opin. Pharmacol. 13, 778–785. doi:10.1016/j.coph.2013.05.006.

O'Brien, E. J., Monk, J. M., and Palsson, B. O. (2015). Using Genome-scale Models to Predict Biological Capabilities. Cell 161, 971–987. doi:10.1016/j.cell.2015.05.019.

Oertel, W. H. (2017). Recent advances in treating Parkinson's disease. F1000Research 6, 260. doi:10.12688/f1000research.10100.1.

O'Hanlon, D. E., Come, R. A., and Moench, T. R. (2019). Vaginal pH measured in vivo: lactobacilli determine pH and lactic acid concentration. BMC Microbiol. 19, 13. doi:10.1186/s12866-019-1388-8.

Onderdonk, A. B., Delaney, M. L., and Fichorova, R. N. (2016). The Human Microbiome during Bacterial Vaginosis. Clin. Microbiol. Rev. 29, 223–238. doi:10.1128/CMR.00075-15.

O'Neal, S. L., and Zheng, W. (2015). Manganese Toxicity Upon Overexposure: a Decade in Review. Curr. Environ. Heal. reports 2, 315–328. doi:10.1007/s40572-015-0056-x.

Opdam, S., Richelle, A., Kellman, B., Li, S., Zielinski, D. C., and Lewis, N. E. (2017). A Systematic Evaluation of Methods for Tailoring Genome-Scale Metabolic Models. Cell Syst. 4, 318-329.e6. doi:10.1016/j.cels.2017.01.010.

Orsini, M., Chateauvieux, S., Rhim, J., Gaigneaux, A., Cheillan, D., Christov, C., et al. (2019). Sphingolipid-mediated inflammatory signaling leading to autophagy inhibition converts erythropoiesis to myelopoiesis in human hematopoietic stem/progenitor cells. Cell Death Differ. 26, 1796–1812.

Orth, Jeffrey D., Ines Thiele, B. Ø. P. (2011). What is flux balance Analysis? 28, 245–248. doi:10.1038/nbt.1614.What.

Ottman, N., Reunanen, J., Meijerink, M., Pietilä, T. E., Kainulainen, V., Klievink, J., et al. (2017). Pili-like proteins of Akkermansia muciniphila modulate host immune responses and gut barrier function. PLoS One 12, e0173004. doi:10.1371/journal.pone.0173004.

Özoğul, F. (2004). Production of biogenic amines by Morganella morganii, Klebsíella pneumoniae and Hafnia alvei using a rapid HPLC method. Eur. Food Res. Technol. doi:10.1007/s00217-004-0988-0.

Paalanne, N., Husso, A., Salo, J., Pieviläinen, O., Tejesvi, M. V, Koivusaari, P., et al. (2018). Intestinal microbiome as a risk factor for urinary tract infections in children. Eur. J. Clin. Microbiol. Infect. Dis. Off. Publ. Eur. Soc. Clin. Microbiol. 37, 1881–1891. doi:10.1007/s10096-018-3322-7.

Pacheco, M. P., Pfau, T., and Sauter, T. (2015). Benchmarking Procedures for High-Throughput Context Specific Reconstruction Algorithms. Front. Physiol. 6, 410. doi:10.3389/fphys.2015.00410.

Pál, C., Papp, B., Lercher, M. J., Csermely, P., Oliver, S. G., and Hurst, L. D. (2006). Chance and necessity in the evolution of minimal metabolic networks. Nature 440, 667–670. doi:10.1038/nature04568.

Palsson, B. Ø. (2011). Systems Biology: Simulation of Dynamic Network States. Cambridge: Cambridge University Press doi:DOI: 10.1017/CBO9780511736179.

Panwar, H., Calderwood, D., Gillespie, A. L., Wylie, A. R., Graham, S. F., Grant, I. R., et al. (2016). Identification of lactic acid bacteria strains modulating incretin hormone secretion and gene expression in enteroendocrine cells. J. Funct. Foods. doi:10.1016/j.jff.2016.02.040.

Parada Venegas, D., De la Fuente, M. K., Landskron, G., González, M. J., Quera, R., Dijkstra, G., et al. (2019). Short Chain Fatty Acids (SCFAs)-Mediated Gut Epithelial and Immune Regulation and Its Relevance for Inflammatory Bowel Diseases. Front. Immunol. 10, 277. doi:10.3389/fimmu.2019.00277.

Paraskevis, D., Kostaki, E. G., Magiorkinis, G., Panayiotakopoulos, G., Sourvinos, G., and Tsiodras, S. (2020). Full-genome evolutionary analysis of the novel corona virus (2019-nCoV) rejects the hypothesis of emergence as a result of a recent recombination event. Infect. Genet. Evol. J. Mol. Epidemiol. Evol. Genet. Infect. Dis. 79, 104212. doi:10.1016/j.meegid.2020.104212.

Peddie, B. A., Chambers, S. T., and Lever, M. (1996). Is the ability of urinary tract pathogens to accumulate glycine betaine a factor in the virulence of pathogenic strains? J. Lab. Clin. Med. 128, 417–422. doi:https://doi.org/10.1016/S0022-2143(96)80014-X.

Pelzer, E. S., Allan, J. A., Theodoropoulos, C., Ross, T., Beagley, K. W., and Knox, C. L. (2012). Hormone-dependent bacterial growth, persistence and biofilm formation--a pilot study investigating human follicular fluid collected during IVF cycles. PLoS One 7, e49965. doi:10.1371/journal.pone.0049965.

Pendergrass, J. C., and Haley, B. E. (1997). Inhibition of brain tubulin-guanosine 5'-triphosphate interactions by mercury: similarity to observations in Alzheimer's diseased brain. Met. Ions Biol. Syst. 34, 461–478.

Perlman, S., and Netland, J. (2009). Coronaviruses post-SARS: update on replication and pathogenesis. Nat. Rev. Microbiol. 7, 439–450. doi:10.1038/nrmicro2147.

Pertea, M., Pertea, G. M., Antonescu, C. M., Chang, T.-C., Mendell, J. T., and Salzberg, S. L. (2015). StringTie enables improved reconstruction of a transcriptome from RNA-seq reads. Nat. Biotechnol. 33, 290–295.

Peter, I., Dubinsky, M., Bressman, S., Park, A., Lu, C., Chen, N., et al. (2018). Anti-Tumor Necrosis Factor Therapy and Incidence of Parkinson Disease Among Patients With Inflammatory Bowel Disease. JAMA Neurol. 75, 939–946. doi:10.1001/jamaneurol.2018.0605.

Peters, M. A., McLaren, P., and Jandrić, P. (2020). A viral theory of post-truth. Educ. Philos. Theory 0, 1–9. doi:10.1080/00131857.2020.1750090.

Petersen, M. S., Halling, J., Bech, S., Wermuth, L., Weihe, P., Nielsen, F., et al. (2008). Impact of dietary exposure to food contaminants on the risk of Parkinson's disease. Neurotoxicology 29, 584–590. doi:10.1016/j.neuro.2008.03.001.

Pfeiffer, R. F. (2016). Non-motor symptoms in Parkinson's disease. Parkinsonism Relat. Disord. 22 Suppl 1, S119-22. doi:10.1016/j.parkreldis.2015.09.004.

Pillai, S. K., Sakoulas, G., Eliopoulos, G. M., Moellering, R. C. J., Murray, B. E., and Inouye, R. T. (2004). Effects of glucose on fsr-mediated biofilm formation in Enterococcus faecalis. J. Infect. Dis. 190, 967–970. doi:10.1086/423139.

Ping, W. S., A., R. L., H., D. S., E., D. G., Grietje, H., Galiana, L., et al. (2021). Pivotal Roles for pH, Lactate, and Lactate-Utilizing Bacteria in the Stability of a Human Colonic Microbial Ecosystem. mSystems 5, e00645-20. doi:10.1128/mSystems.00645-20.

Playdon, M. C., Sampson, J. N., Cross, A. J., Sinha, R., Guertin, K. A., Moy, K. A., et al. (2016). Comparing metabolite profiles of habitual diet in serum and urine. Am. J. Clin. Nutr. 104, 776–789. doi:10.3945/ajcn.116.135301.

Poirault-Chassac, S., Nivet-Antoine, V., Houvert, A., Kauskot, A., Lauret, E., Lai-Kuen, R., et al. (2021). Mitochondrial dynamics and reactive oxygen species initiate thrombopoiesis from mature megakaryocytes. Blood Adv. 5, 1706–1718.

Pott, J., and Hornef, M. (2012). Innate immune signalling at the intestinal epithelium in homeostasis and disease. EMBO Rep. doi:10.1038/embor.2012.96.

Prabhakaran, K., Chapman, G. D., and Gunasekar, P. G. (2011). α-Synuclein overexpression enhances manganese-induced neurotoxicity through the NF-κB-mediated pathway. Toxicol. Mech. Methods 21, 435–443. doi:10.3109/15376516.2011.560210.

Priyadarshi, A., Khuder, S. A., Schaub, E. A., and Priyadarshi, S. S. (2001). Environmental risk factors and parkinson's disease: A metaanalysis. Environ. Res. doi:10.1006/enrs.2001.4264.

Pryor, R., Norvaisas, P., Marinos, G., Best, L., Thingholm, L. B., Quintaneiro, L. M., et al. (2019). Host-Microbe-Drug-Nutrient Screen Identifies Bacterial Effectors of Metformin Therapy. Cell 178, 1299-1312.e29. doi:10.1016/j.cell.2019.08.003.

Psichas, A., Sleeth, M. L., Murphy, K. G., Brooks, L., Bewick, G. A., Hanyaloglu, A. C., et al. (2015). The short chain fatty acid propionate stimulates GLP-1 and PYY secretion via free fatty acid receptor 2 in rodents. Int. J. Obes. doi:10.1038/ijo.2014.153.

Qamar, M. A., Sauerbier, A., Politis, M., Carr, H., Loehrer, P., and Chaudhuri, K. R. (2017). Presynaptic dopaminergic terminal imaging and non-motor symptoms assessment of Parkinson's disease: evidence for dopaminergic basis? NPJ Park. Dis. 3, 5. doi:10.1038/s41531-016-0006-9.

Qi, F., Zhang, W., Huang, J., Fu, L., and Zhao, J. (2021). Single-Cell RNA Sequencing Analysis of the Immunometabolic Rewiring and Immunopathogenesis of Coronavirus Disease 2019. Front. Immunol. 12, 1261.

Quigley, E. M. M. (2017). Microbiota-Brain-Gut Axis and Neurodegenerative Diseases. Curr. Neurol. Neurosci. Rep. doi:10.1007/s11910-017-0802-6.

Rabinowitz, J. D., and Enerbäck, S. (2020). Lactate: the ugly duckling of energy metabolism. Nat. Metab. 2, 566–571. doi:10.1038/s42255-020-0243-4.

Racette, B. A., Searles Nielsen, S., Criswell, S. R., Sheppard, L., Seixas, N., Warden, M. N., et al. (2017). Dose-dependent progression of parkinsonism in manganese-exposed welders. Neurology 88, 344–351. doi:10.1212/WNL.0000000000003533.

Rahman, M. (1977). Carbon dioxide-dependent Staphylococcus aureus from abscess. Br. Med. J. 2, 319. doi:10.1136/bmj.2.6082.319-b.

Raj, K., Kaur, P., Gupta, G. D., and Singh, S. (2021). Metals associated neurodegeneration in Parkinson's disease: Insight to physiological, pathological mechanisms and management. Neurosci. Lett. 753, 135873. doi:10.1016/j.neulet.2021.135873.

Rajewsky, N., Almouzni, G., Gorski, S. A., Aerts, S., Amit, I., Bertero, M. G., et al. (2020). LifeTime and improving European healthcare through cell-based interceptive medicine. Nature 587, 377–386. doi:10.1038/s41586-020-2715-9.

Rani, A., Ranjan, R., McGee, H. S., Andropolis, K. E., Panchal, D. V, Hajjiri, Z., et al. (2017). Urinary microbiome of kidney transplant patients reveals dysbiosis with potential for antibiotic resistance. Transl. Res. 181, 59–70. doi:10.1016/j.trsl.2016.08.008.

Rao, R. K., Li, L., Baker, R. D., Baker, S. S., and Gupta, A. (2000). Glutathione oxidation and PTPase inhibition by hydrogen peroxide in Caco-2 cell monolayer. Am. J. Physiol. Gastrointest. Liver Physiol. 279, G332-40. doi:10.1152/ajpgi.2000.279.2.G332.

Rao, R. (2008). Oxidative stress-induced disruption of epithelial and endothelial tight junctions. Front. Biosci. doi:10.2741/3223.

Ratner, M. H., and Fitzgerald, E. (2017). Understanding of the role of manganese in parkinsonism and Parkinson disease. Neurology 88, 338–339. doi:10.1212/WNL.0000000000003543.

Ravel, J., Gajer, P., Abdo, Z., Schneider, G. M., Koenig, S. S. K., McCulle, S. L., et al. (2011). Vaginal microbiome of reproductive-age women. Proc. Natl. Acad. Sci. U. S. A. 108 Suppl, 4680–4687. doi:10.1073/pnas.1002611107.

Ravindra, N. G., Alfajaro, M. M., Gasque, V., Huston, N. C., Wan, H., Szigeti-Buck, K., et al. (2021). Single-cell longitudinal analysis of SARS-CoV-2 infection in human airway epithelium identifies target cells, alterations in gene expression, and cell state changes. PLoS Biol. 19, e3001143. doi:10.1371/journal.pbio.3001143.

Reidl, J., and Boos, W. (1991). The malX malY operon of Escherichia coli encodes a novel enzyme II of the phosphotransferase system recognizing glucose and maltose and an enzyme abolishing the endogenous induction of the maltose system. J. Bacteriol. 173, 4862–4876. doi:10.1128/jb.173.15.4862-4876.1991.

Remy, L., Carrière, M., Derré-Bobillot, A., Martini, C., Sanguinetti, M., and Borezée-Durant, E. (2013). The Staphylococcus aureus Opp1 ABC transporter imports nickel and cobalt in zinc-depleted conditions and contributes to virulence. Mol. Microbiol. 87, 730–743. doi:10.1111/mmi.12126.

Rendu, F., and Brohard-Bohn, B. (2001). The platelet release reaction: granules' constituents, secretion and functions. Platelets 12, 261–273.

Renz, A., Widerspick, L., and Dräger, A. (2020). FBA reveals guanylate kinase as a potential target for antiviral therapies against SARS-CoV-2. Bioinformatics 36, i813–i821. doi:10.1093/bioinformatics/btaa813.

Rice, G., MacDonell, M., Hertzberg, R. C., Teuschler, L., Picel, K., Butler, J., et al. (2008). An approach for assessing human exposures to chemical mixtures in the environment. Toxicol. Appl. Pharmacol. 233, 126–136. doi:https://doi.org/10.1016/j.taap.2008.05.004.

Rice, J. C., Peng, T., Spence, J. S., Wang, H.-Q., Goldblum, R. M., Corthésy, B., et al. (2005). Pyelonephritic Escherichia coli Expressing P Fimbriae Decrease Immune Response of the Mouse Kidney. J. Am. Soc. Nephrol. 16, 3583 LP – 3591. doi:10.1681/ASN.2005030243.

Richelle, A., Joshi, C., and Lewis, N. E. (2019). Assessing key decisions for transcriptomic data integration in biochemical networks. PLOS Comput. Biol. 15, e1007185. Available at: https://doi.org/10.1371/journal.pcbi.1007185.

Robinson, A. E., Lowe, J. E., Koh, E.-I., and Henderson, J. P. (2018). Uropathogenic enterobacteria use the yersiniabactin metallophore system to acquire nickel. J. Biol. Chem. 293, 14953–14961. doi:10.1074/jbc.RA118.004483.

Robinson, J. L., Kocabaş, P., Wang, H., Cholley, P.-E., Cook, D., Nilsson, A., et al. (2020). An atlas of human metabolism. Sci. Signal. 13.

Rodda, L. B., and Pepper, M. (2020). Metabolic constraints on the B cell response to malaria. Nat. Immunol. 21, 722–724.

Rooney, J. P. K. (2007). The role of thiols, dithiols, nutritional factors and interacting ligands in the toxicology of mercury. Toxicology 234, 145–156. doi:10.1016/j.tox.2007.02.016.

Rose, C., Parker, A., Jefferson, B., and Cartmell, E. (2015). The Characterization of Feces and Urine: A Review of the Literature to Inform Advanced Treatment Technology. Crit. Rev. Environ. Sci. Technol. 45, 1827–1879. doi:10.1080/10643389.2014.1000761.

Russell, A. B., Trapnell, C., and Bloom, J. D. (2018). Extreme heterogeneity of influenza virus infection in single cells. Elife 7. doi:10.7554/eLife.32303.

Sabri, M., Houle, S., and Dozois, C. M. (2009). Roles of the extraintestinal pathogenic Escherichia coli ZnuACB and ZupT zinc transporters during urinary tract infection. Infect. Immun. 77, 1155–1164. doi:10.1128/IAI.01082-08.

Salvo Romero, E., Alonso Cotoner, C., Pardo Camacho, C., Casado Bedmar, M., and Vicario, M. (2015). The intestinal barrier function and its involvement in digestive disease. Rev. Española Enfermedades Dig. doi:10.17235/reed.2015.3846/2015.

Sampson, T. R., Debelius, J. W., Thron, T., Janssen, S., Shastri, G. G., Ilhan, Z. E., et al. (2016). Gut Microbiota Regulate Motor Deficits and Neuroinflammation in a Model of Parkinson's Disease. Cell 167, 1469-1480.e12. doi:10.1016/j.cell.2016.11.018.

Sanders, K. M., and Ward, S. M. (2019). Nitric oxide and its role as a non-adrenergic, non-cholinergic inhibitory neurotransmitter in the gastrointestinal tract. Br. J. Pharmacol. 176, 212–227. doi:10.1111/bph.14459.

Sarafian, T. A., Bredesen, D. E., and Verity, M. A. (1996). Cellular resistance to methylmercury. Neurotoxicology 17, 27–36.

Sarigiannis, D. A., and Hansen, U. (2012). Considering the cumulative risk of mixtures of chemicals – A challenge for policy makers. Environ. Heal. 11, S18. doi:10.1186/1476-069X-11-S1-S18.

Sas, K. M., Kayampilly, P., Byun, J., Nair, V., Hinder, L. M., Hur, J., et al. (2016). Tissue-specific metabolic reprogramming drives nutrient flux in diabetic complications. JCI insight 1.

Sasabe, Jumpei, and Masataka Suzuki. "Emerging role of d-amino acid metabolism in the innate defense." *Frontiers in microbiology* 9 (2018): 933.

Savica, R., Grossardt, B. R., Carlin, J. M., Icen, M., Bower, J. H., Ahlskog, J. E., et al. (2009). Anemia or low hemoglobin levels preceding Parkinson disease: a case-control study. Neurology 73, 1381–1387. doi:10.1212/WNL.0b013e3181bd80c1.

Scheperjans, F., Aho, V., Pereira, P. A. B., Koskinen, K., Paulin, L., Pekkonen, E., et al. (2015). Gut microbiota are related to Parkinson's disease and clinical phenotype. Mov. Disord. 30, 350–358. doi:10.1002/mds.26069.

Schmelzer, C., Niklowitz, P., Okun, J. G., Haas, D., Menke, T., and Döring, F. (2011). Ubiquinol‐induced gene expression signatures are translated into altered parameters of erythropoiesis and reduced low density lipoprotein cholesterol levels in humans. IUBMB Life 63, 42–48.

Schneider, C. B., Donix, M., Linse, K., Werner, A., Fauser, M., Klingelhoefer, L., et al. (2017). Accelerated age-dependent hippocampal volume loss in Parkinson disease with mild cognitive impairment. Am. J. Alzheimers. Dis. Other Demen. doi:10.1177/1533317517698794.

Scholes, D., Hooton, T. M., Roberts, P. L., Stapleton, A. E., Gupta, K., and Stamm, W. E. (2000). Risk factors for recurrent urinary tract infection in young women. J. Infect. Dis. 182, 1177–1182. doi:10.1086/315827.

Scholz, J., Kuhrau, J., Heinrich, F., Heinz, G. A., Hutloff, A., Worm, M., et al. (2021). Vitamin A controls the allergic response through T follicular helper cell as well as plasmablast differentiation. Allergy 76, 1109–1122.

Schreiber, H. L., Conover, M. S., Chou, W.-C., Hibbing, M. E., Manson, A. L., Dodson, K. W., et al. (2017). Bacterial virulence phenotypes of Escherichia coli and host susceptibility determine risk for urinary tract infections. Sci. Transl. Med. 9, eaaf1283. doi:10.1126/scitranslmed.aaf1283.

Schulte-Schrepping, J., Reusch, N., Paclik, D., Baßler, K., Schlickeiser, S., Zhang, B., et al. (2020). Severe COVID-19 Is Marked by a Dysregulated Myeloid Cell Compartment. Cell 182, 1419-1440.e23. doi:10.1016/j.cell.2020.08.001.

Schultz, A., and Qutub, A. A. (2016). Reconstruction of Tissue-Specific Metabolic Networks Using CORDA. PLoS Comput. Biol. 12, e1004808. doi:10.1371/journal.pcbi.1004808.

Schwartz, M. H., Waldbauer, J. R., Zhang, L., and Pan, T. (2016). Global tRNA misacylation induced by anaerobiosis and antibiotic exposure broadly increases stress resistance in Escherichia coli. Nucleic Acids Res. 44, 10292–10303. doi:10.1093/nar/gkw856.

Selvarasu, S., Karimi, I. A., Ghim, G.-H., and Lee, D.-Y. (2010). Genome-scale modeling and in silico analysis of mouse cell metabolic network. Mol. Biosyst. 6, 152–161. doi:10.1039/b912865d.

Seo, S. W., Kim, D., Szubin, R., and Palsson, B. O. (2015). Genome-wide Reconstruction of OxyR and SoxRS Transcriptional Regulatory Networks under Oxidative Stress in Escherichia coli K-12 MG1655. Cell Rep. 12, 1289–1299. doi:https://doi.org/10.1016/j.celrep.2015.07.043.

Sewankambo, N., Gray, R. H., Wawer, M. J., Paxton, L., McNaim, D., Wabwire-Mangen, F., et al. (1997). HIV-1 infection associated with abnormal vaginal flora morphology and bacterial vaginosis. Lancet (London, England) 350, 546–550. doi:10.1016/s0140-6736(97)01063-5.

Shakya, M., Lo, C.-C., and Chain, P. S. G. (2019). Advances and Challenges in Metatranscriptomic Analysis. Front. Genet. 10, 904. doi:10.3389/fgene.2019.00904.

Sharma, R. P., Schuhmacher, M., and Kumar, V. (2017). Review on crosstalk and common mechanisms of endocrine disruptors: Scaffolding to improve PBPK/PD model of EDC mixture. Environ. Int. 99, 1–14. doi:https://doi.org/10.1016/j.envint.2016.09.016.

Sheyn, D., Hijaz, A. K., Hazlett Jr, F. E., Dawodu, K., El-Nashar, S., Mangel, J. M., et al. (2020). Evaluation of urine choline levels in women with and without overactive bladder syndrome. Female Pelvic Med. Reconstr. Surg. 26, 644–648.

Sheyn, D., Hijaz, A. K., Hazlett Jr, F. E., El-Nashar, S., Mangel, J. M., Li, X., et al. (2020). Evaluation of choline and acetylcholine levels in responders and nonresponders to anticholinergic therapy for overactive bladder syndrome. Female Pelvic Med. Reconstr. Surg. 26, e91–e96.

Shields-Cutler, R. R., Crowley, J. R., Hung, C. S., Stapleton, A. E., Aldrich, C. C., Marschall, J., et al. (2015). Human Urinary Composition Controls Antibacterial Activity of Siderocalin*, ♦. J. Biol. Chem. 290, 15949–15960. doi:https://doi.org/10.1074/jbc.M115.645812.

Shishov, V. A., Kirovskaya, T. A., Kudrin, V. S., and Oleskin, A. V. (2009). Amine neuromediators, their precursors, and oxidation products in the culture of Escherichia coli k-12. Appl. Biochem. Microbiol. doi:10.1134/S0003683809050068.

Shlomi, T., Eisenberg, Y., Sharan, R., and Ruppin, E. (2007). A genome-scale computational study of the interplay between transcriptional regulation and metabolism. Mol. Syst. Biol. 3, 101. doi:10.1038/msb4100141.

Shnayder, M., Nachshon, A., Krishna, B., Poole, E., Boshkov, A., Binyamin, A., et al. (2018). Defining the Transcriptional Landscape during Cytomegalovirus Latency with Single-Cell RNA Sequencing. MBio 9. doi:10.1128/mBio.00013-18.

Shoskes, D. A., Altemus, J., Polackwich, A. S., Tucky, B., Wang, H., and Eng, C. (2016). The Urinary Microbiome Differs Significantly Between Patients With Chronic Prostatitis/Chronic Pelvic Pain Syndrome and Controls as Well as Between Patients With Different Clinical Phenotypes. Urology 92, 26–32. doi:10.1016/j.urology.2016.02.043.

Sian-Hülsmann, J., Mandel, S., Youdim, M. B. H., and Riederer, P. (2011). The relevance of iron in the pathogenesis of Parkinson's disease. J. Neurochem. 118, 939–957. doi:10.1111/j.1471-4159.2010.07132.x.

Sibon, D., Coman, T., Rossignol, J., Lamarque, M., Kosmider, O., Bayard, E., et al. (2019). Enhanced renewal of erythroid progenitors in myelodysplastic anemia by peripheral serotonin. Cell Rep. 26, 3246–3256.

Sidoryk-Wegrzynowicz, M., and Aschner, M. (2013). Manganese toxicity in the central nervous system: the glutamine/glutamate-γ-aminobutyric acid cycle. J. Intern. Med. 273, 466–477. doi:10.1111/joim.12040.

Sigmundsdottir, H., and Butcher, E. C. (2008). Environmental cues, dendritic cells and the programming of tissue-selective lymphocyte trafficking. Nat. Immunol. 9, 981–987.

Sigurdsson, M. I., Jamshidi, N., Steingrimsson, E., Thiele, I., and Palsson, B. Ø. (2010). A detailed genome-wide reconstruction of mouse metabolism based on human Recon 1. BMC Syst. Biol. 4, 140. doi:10.1186/1752-0509-4-140.

Sintsova, A., Frick-Cheng, A. E., Smith, S., Pirani, A., Subashchandrabose, S., Snitkin, E. S., et al. (2019). Genetically diverse uropathogenic Escherichia coli adopt a common transcriptional program in patients with utis. Elife 8, 1–26. doi:10.7554/eLife.49748.

Sintsova, A., Smith, S., Subashchandrabose, S., and Mobley, H. L. (2018). Role of Ethanolamine Utilization Genes in Host Colonization during Urinary Tract Infection. Infect. Immun. 86. doi:10.1128/IAI.00542-17.

Smart, A., de Lacy Costello, B., White, P., Avison, M., Batty, C., Turner, C., et al. (2019). Sniffing out resistance – Rapid identification of urinary tract infection-causing bacteria and their antibiotic susceptibility using volatile metabolite profiles. J. Pharm. Biomed. Anal. 167, 59–65. doi:https://doi.org/10.1016/j.jpba.2019.01.044.

Sommer, F., and Bäckhed, F. (2013). The gut microbiota-masters of host development and physiology. Nat. Rev. Microbiol. doi:10.1038/nrmicro2974.

Stapleton, A. E., Au-Yeung, M., Hooton, T. M., Fredricks, D. N., Roberts, P. L., Czaja, C. A., et al. (2011). Randomized, Placebo-Controlled Phase 2 Trial of a Lactobacillus crispatus Probiotic Given Intravaginally for Prevention of Recurrent Urinary Tract Infection. Clin. Infect. Dis. 52, 1212–1217. doi:10.1093/cid/cir183.

Stephens, D. S., and McElrath, M. J. (2020). COVID-19 and the Path to Immunity. JAMA 324, 1279–1281. doi:10.1001/jama.2020.16656.

Stewart, P. S., and Franklin, M. J. (2008). Physiological heterogeneity in biofilms. Nat. Rev. Microbiol. 6, 199–210. doi:10.1038/nrmicro1838.

Stilling, R. M., Moloney, G. M., Ryan, F. J., Hoban, A. E., Bastiaanssen, T. F., Shanahan, F., et al. (2018). Social interaction-induced activation of RNA splicing in the amygdala of microbiome-deficient mice. Elife 7. doi:10.7554/eLife.33070.

Strandwitz, P. (2018). Neurotransmitter modulation by the gut microbiota. Brain Res. doi:10.1016/j.brainres.2018.03.015.

Stuart, T., Butler, A., Hoffman, P., Hafemeister, C., Papalexi, E., Mauck, W. M. 3rd, et al. (2019). Comprehensive Integration of Single-Cell Data. Cell 177, 1888-1902.e21. doi:10.1016/j.cell.2019.05.031.

Subashchandrabose, S., Hazen, T. H., Brumbaugh, A. R., Himpsl, S. D., Smith, S. N., Ernst, R. D., et al. (2014). Host-specific induction of Escherichia coli fitness genes during human urinary tract infection. Proc. Natl. Acad. Sci. 111, 18327–18332. doi:10.1073/pnas.1415959112.

Subashchandrabose, S., and Mobley, H. L. T. (2015). Back to the metal age: battle for metals at the host-pathogen interface during urinary tract infection. Metallomics 7, 935–942. doi:10.1039/c4mt00329b.

Suganya, K., and Koo, B.-S. (2020). Gut-Brain Axis: Role of Gut Microbiota on Neurological Disorders and How Probiotics/Prebiotics Beneficially Modulate Microbial and Immune Pathways to Improve Brain Functions. Int. J. Mol. Sci. 21. doi:10.3390/ijms21207551.

Swainston, N., Smallbone, K., Hefzi, H., Dobson, P. D., Brewer, J., Hanscho, M., et al. (2016). Recon 2.2: from reconstruction to model of human metabolism. Metabolomics 12. doi:10.1007/s11306-016-1051-4.

T., P. J., and R., R. J. (2006). Conserving a Volatile Metabolite: a Role for Carboxysome-Like Organelles in Salmonella enterica. J. Bacteriol. 188, 2865–2874. doi:10.1128/JB.188.8.2865-2874.2006.

Tachedjian, G., Aldunate, M., Bradshaw, C. S., and Cone, R. A. (2017). The role of lactic acid production by probiotic Lactobacillus species in vaginal health. Res. Microbiol. 168, 782–792. doi:10.1016/j.resmic.2017.04.001.

Tai, Y. K., Chew, K. C. M., Tan, B. W. Q., Lim, K.-L., and Soong, T. W. (2016). Iron mitigates DMT1-mediated manganese cytotoxicity via the ASK1-JNK signaling axis: Implications of iron supplementation for manganese toxicity. Sci. Rep. 6, 21113. doi:10.1038/srep21113.

Takahashi, T., and Shimohata, T. (2019). Vascular dysfunction induced by mercury exposure. Int. J. Mol. Sci. doi:10.3390/ijms20102435.

Takiishi, T., Fenero, C. I. M., and Câmara, N. O. S. (2017). Intestinal barrier and gut microbiota: Shaping our immune responses throughout life. Tissue Barriers. doi:10.1080/21688370.2017.1373208.

Tan, P. M., Buchholz, K. S., Omens, J. H., McCulloch, A. D., and Saucerman, J. J. (2017). Predictive model identifies key network regulators of cardiomyocyte mechano-signaling. PLoS Comput. Biol. 13, 1–17. doi:10.1371/journal.pcbi.1005854.

Tanaka, T., Kai, S., Matsuyama, T., Adachi, T., Fukuda, K., and Hirota, K. (2013). General anesthetics inhibit LPS-induced IL-1β expression in glial cells. PLoS One 8, e82930. doi:10.1371/journal.pone.0082930.

Tang, J. (2017). Microbiome in the urinary system-a review. AIMS Microbiol. 3, 143–154. doi:10.3934/microbiol.2017.2.143.

Tang, X. C., Zhang, J. X., Zhang, S. Y., Wang, P., Fan, X. H., Li, L. F., et al. (2006). Prevalence and genetic diversity of coronaviruses in bats from China. J. Virol. 80, 7481–7490. doi:10.1128/JVI.00697-06.

Tena, D., González-Praetorius, A., Sáez-Nieto, J. A., Valdezate, S., and Bisquert, J. (2008). Urinary tract infection caused by capnophilic Escherichia coli. Emerg. Infect. Dis. 14, 1163–1164. doi:10.3201/eid1407.071053.

Thaker, S. K., Ch'ng, J., and Christofk, H. R. (2019). Viral hijacking of cellular metabolism. BMC Biol. 17, 59. doi:10.1186/s12915-019-0678-9.

Thänert, R., Reske, K. A., Hink, T., Wallace, M. A., Wang, B., Schwartz, D. J., et al. (2019). Comparative Genomics of Antibiotic-Resistant Uropathogens Implicates Three Routes for Recurrence of Urinary Tract Infections. MBio 10. doi:10.1128/mBio.01977-19.

Thiele, I., Heinken, A., and Fleming, R. M. T. (2013). A systems biology approach to studying the role of microbes in human health. Curr. Opin. Biotechnol. 24, 4–12. doi:https://doi.org/10.1016/j.copbio.2012.10.001.

Thiele, I., and Palsson, B. Ø. (2010). A protocol for generating a high-quality genome-scale metabolic reconstruction. Nat. Protoc. 5, 93–121. doi:10.1038/nprot.2009.203.

Thiele, I., Sahoo, S., Heinken, A., Hertel, J., Heirendt, L., Aurich, M. K., et al. (2020). Personalized whole‐body models integrate metabolism, physiology, and the gut microbiome. Mol. Syst. Biol. 16, 1–24. doi:10.15252/msb.20198982.

Thiele, I., Swainston, N., Fleming, R. M. T., Hoppe, A., Sahoo, S., Aurich, M. K., et al. (2013). A community-driven global reconstruction of human metabolism. Nat. Biotechnol. 31, 419–425. doi:10.1038/nbt.2488.

Thiele, I., Vo, T. D., Price, N. D., and Palsson, B. Ø. (2005). Expanded metabolic reconstruction of Helicobacter pylori (iIT341 GSM/GPR): an in silico genome-scale characterization of single- and double-deletion mutants. J. Bacteriol. 187, 5818–5830. doi:10.1128/JB.187.16.5818-5830.2005.

Thomas-White, K., Forster, S. C., Kumar, N., Van Kuiken, M., Putonti, C., Stares, M. D., et al. (2018). Culturing of female bladder bacteria reveals an interconnected urogenital microbiota. Nat. Commun. 9, 1557. doi:10.1038/s41467-018-03968-5.

Tilocca, B., Pieroni, L., Soggiu, A., Britti, D., Bonizzi, L., Roncada, P., et al. (2020). Gut-Brain Axis and Neurodegeneration: State-of-the-Art of Meta-Omics Sciences for Microbiota Characterization. Int. J. Mol. Sci. 21. doi:10.3390/ijms21114045.

Timm, A., and Yin, J. (2012). Kinetics of virus production from single cells. Virology 424, 11–17. doi:10.1016/j.virol.2011.12.005.

Tinkov, A. A., Gritsenko, V. A., Skalnaya, M. G., Cherkasov, S. V, Aaseth, J., and Skalny, A. V (2018). Gut as a target for cadmium toxicity. Environ. Pollut. 235, 429–434. doi:10.1016/j.envpol.2017.12.114.

Tisoncik, J. R., Korth, M. J., Simmons, C. P., Farrar, J., Martin, T. R., and Katze, M. G. (2012). Into the eye of the cytokine storm. Microbiol. Mol. Biol. Rev. 76, 16–32. doi:10.1128/MMBR.05015-11.

Tiwari, P. C., and Pal, R. (2017). The potential role of neuroinflammation and transcription factors in Parkinson disease. Dialogues Clin. Neurosci. 19, 71–80. doi:10.31887/DCNS.2017.19.1/rpal.

Tremaroli, V., and Bäckhed, F. (2012). Functional interactions between the gut microbiota and host metabolism. Nature 489, 242–249. doi:10.1038/nature11552.

Trist, B. G., Hare, D. J., and Double, K. L. (2019). Oxidative stress in the aging substantia nigra and the etiology of Parkinson's disease. Aging Cell 18, e13031. doi:10.1111/acel.13031.

Troncoso-Escudero, P., Parra, A., Nassif, M., and Vidal, R. L. (2018). Outside in: Unraveling the role of neuroinflammation in the progression of Parkinson's disease. Front. Neurol. doi:10.3389/fneur.2018.00860.

Tsavkelova, E. A., Botvinko, I. V., Kudrin, V. S., and Oleskin, A. V. (2000). Detection of neurotransmitter amines in microorganisms with the use of high-performance liquid chromatography. Dokl. Biochem.

Tschopp, J., and Schroder, K. (2010). NLRP3 inflammasome activation: The convergence of multiple signalling pathways on ROS production? Nat. Rev. Immunol. doi:10.1038/nri2725.

Tshala-Katumbay, D., Mwanza, J. C., Rohlman, D. S., Maestre, G., and Oria, R. B. (2015). A global perspective on the influence of environmental exposures on the nervous system. Nature. doi:10.1038/nature16034.

Tufon, K. A., Fokam, D. P. Y., Kouanou, Y. S., and Meriki, H. D. (2020). Case report on a swift shift in uropathogens from Shigella flexneri to Escherichia coli: A thin line between bacterial persistence and reinfection. Ann. Clin. Microbiol. Antimicrob. 19, 1–6. doi:10.1186/s12941-020-00374-y.

Tümer, Z., and Møller, L. B. (2010). Menkes disease. Eur. J. Hum. Genet. 18, 511–518. doi:10.1038/ejhg.2009.187.

Turner, J. R. (2009). Intestinal mucosal barrier function in health and disease. Nat. Rev. Immunol. doi:10.1038/nri2653.

Turner, J. R. (2009). Intestinal mucosal barrier function in health and disease. Nat. Rev. Immunol. doi:10.1038/nri2653.

Tysnes, O.-B., and Storstein, A. (2017). Epidemiology of Parkinson's disease. J. Neural Transm. 124, 901–905. doi:10.1007/s00702-017-1686-y.

Uhlén, M., Fagerberg, L., Hallström, B. M., Lindskog, C., Oksvold, P., Mardinoglu, A., et al. (2015). Proteomics. Tissue-based map of the human proteome. Science 347, 1260419. doi:10.1126/science.1260419.

Ulla, M., Bonny, J. M., Ouchchane, L., Rieu, I., Claise, B., and Durif, F. (2013). Is R2* a new MRI biomarker for the progression of Parkinson's disease? A longitudinal follow-up. PLoS One 8, e57904. doi:10.1371/journal.pone.0057904.

Unger, M. M., Spiegel, J., Dillmann, K.-U., Grundmann, D., Philippeit, H., Bürmann, J., et al. (2016). Short chain fatty acids and gut microbiota differ between patients with Parkinson's disease and age-matched controls. Parkinsonism Relat. Disord. 32, 66–72. doi:10.1016/j.parkreldis.2016.08.019.

Valet, C., Batut, A., Vauclard, A., Dortignac, A., Bellio, M., Payrastre, B., et al. (2020). Adipocyte fatty acid transfer supports megakaryocyte maturation. Cell Rep. 32, 107875.

Valko, M., Morris, H., and Cronin, M. T. D. (2005). Metals, toxicity and oxidative stress. Curr. Med. Chem. 12, 1161–1208. doi:10.2174/0929867053764635.

van de Wijgert, J. H. H. M., Borgdorff, H., Verhelst, R., Crucitti, T., Francis, S., Verstraelen, H., et al. (2014). The vaginal microbiota: what have we learned after a decade of molecular characterization? PLoS One 9, e105998. doi:10.1371/journal.pone.0105998.

van Vliet, E. (2011). Current standing and future prospects for the technologies proposed to transform toxicity testing in the 21st century. ALTEX 28, 17–44. doi:10.14573/altex.2011.1.017.

Vancamelbeke, M., and Vermeire, S. (2017). The intestinal barrier: a fundamental role in health and disease. Expert Rev. Gastroenterol. Hepatol. doi:10.1080/17474124.2017.1343143.

Vandeputte, D., Falony, G., Vieira-Silva, S., Tito, R. Y., Joossens, M., and Raes, J. (2016). Stool consistency is strongly associated with gut microbiota richness and composition, enterotypes and bacterial growth rates. Gut 65, 57–62. doi:10.1136/gutjnl-2015-309618.

Vesey, D. A. (2010). Transport pathways for cadmium in the intestine and kidney proximal tubule: Focus on the interaction with essential metals. Toxicol. Lett. doi:10.1016/j.toxlet.2010.05.004.

Viceconti, M., Henney, A., and Morley-Fletcher, E. (2016). In silico clinical trials: how computer simulation will transform the biomedical industry. Int. J. Clin. Trials 3, 37. doi:10.18203/2349-3259.ijct20161408.

Vijay, R., Guthmiller, J. J., Sturtz, A. J., Surette, F. A., Rogers, K. J., Sompallae, R. R., et al. (2020). Infection-induced plasmablasts are a nutrient sink that impairs humoral immunity to malaria. Nat. Immunol. 21, 790–801. doi:10.1038/s41590-020-0678-5.

Visanji, N. P., Brooks, P. L., Hazrati, L.-N., and Lang, A. E. (2013). The prion hypothesis in Parkinson's disease: Braak to the future. Acta Neuropathol. Commun. 1, 2. doi:10.1186/2051-5960-1-2.

Vlassis, N., Pacheco, M. P., and Sauter, T. (2014). Fast reconstruction of compact context-specific metabolic network models. PLoS Comput. Biol. 10, e1003424. doi:10.1371/journal.pcbi.1003424.

Vodstrcil, L. A., Twin, J., Garland, S. M., Fairley, C. K., Hocking, J. S., Law, M. G., et al. (2017). The influence of sexual activity on the vaginal microbiota and Gardnerella vaginalis clade diversity in young women. PLoS One 12, e0171856. doi:10.1371/journal.pone.0171856.

Wallin, C., Friedemann, M., Sholts, S. B., Noormägi, A., Svantesson, T., Jarvet, J., et al. (2019). Mercury and Alzheimer's Disease: Hg(II) Ions Display Specific Binding to the Amyloid-β Peptide and Hinder Its Fibrillization. Biomolecules 10. doi:10.3390/biom10010044.

Wan, Y., Shang, J., Graham, R., Baric, R. S., and Li, F. (2020). Receptor Recognition by the Novel Coronavirus from Wuhan: an Analysis Based on Decade-Long Structural Studies of SARS Coronavirus. J. Virol. 94. doi:10.1128/JVI.00127-20.

Wang, A., Luan, H. H., and Medzhitov, R. (2019). An evolutionary perspective on immunometabolism. Science (80-.). 363.

Wang, L., Di, L., and Noguchi, C. T. (2014). Erythropoietin, a novel versatile player regulating energy metabolism beyond the erythroid system. Int. J. Biol. Sci. 10, 921.

Wang, Q., Liu, Y., and Zhou, J. (2015). Neuroinflammation in Parkinson's disease and its potential as therapeutic target. Transl. Neurodegener. doi:10.1186/s40035-015-0042-0.

Wang, X., Yan, M., Zhao, L., Wu, Q., Wu, C., Chang, X., et al. (2016). Low-Dose Methylmercury-Induced Apoptosis and Mitochondrial DNA Mutation in Human Embryonic Neural Progenitor Cells. Oxid. Med. Cell. Longev. 2016, 5137042. doi:10.1155/2016/5137042.

Wang, Y., Eddy, J. A., and Price, N. D. (2012). Reconstruction of genome-scale metabolic models for 126 human tissues using mCADRE. BMC Syst. Biol. 6, 153. doi:10.1186/1752-0509-6-153.

Wanichthanarak, K., Fahrmann, J. F., and Grapov, D. (2015). Genomic, Proteomic, and Metabolomic Data Integration Strategies. Biomark. Insights 10s4, BMI.S29511. doi:10.4137/BMI.S29511.

Watanabe, S., Masangkay, J. S., Nagata, N., Morikawa, S., Mizutani, T., Fukushi, S., et al. (2010). Bat coronaviruses and experimental infection of bats, the Philippines. Emerg. Infect. Dis. 16, 1217–1223. doi:10.3201/eid1608.100208.

Watts, R. E., Totsika, M., Challinor, V. L., Mabbett, A. N., Ulett, G. C., Voss, J. J. D., et al. (2012). Contribution of siderophore systems to growth and urinary tract colonization of asymptomatic bacteriuria escherichia coli. Infect. Immun. 80, 333–344. doi:10.1128/IAI.05594-11.

Wen, W., Su, W., Tang, H., Le, W., Zhang, X., Zheng, Y., et al. (2020). Immune cell profiling of COVID-19 patients in the recovery stage by single-cell sequencing. Cell Discov. 6, 31. doi:10.1038/s41421-020-0168-9.

Wessely, F., Bartl, M., Guthke, R., Li, P., Schuster, S., and Kaleta, C. (2011). Optimal regulatory strategies for metabolic pathways in Escherichia coli depending on protein costs. Mol. Syst. Biol. doi:10.1038/msb.2011.46.

Whiteside, S. A., Razvi, H., Dave, S., Reid, G., and Burton, J. P. (2015). The microbiome of the urinary tract--a role beyond infection. Nat. Rev. Urol. 12, 81–90. doi:10.1038/nrurol.2014.361.

Wilke, T., Boettger, B., Berg, B., Groth, A., Mueller, S., Botteman, M., et al. (2015). Epidemiology of urinary tract infections in type 2 diabetes mellitus patients: An analysis based on a large sample

of 456,586 German T2DM patients. J. Diabetes Complications 29, 1015–1023. doi:10.1016/j.jdiacomp.2015.08.021.

Wolfe, A. J., Toh, E., Shibata, N., Rong, R., Kenton, K., Fitzgerald, M., et al. (2012). Evidence of uncultivated bacteria in the adult female bladder. J. Clin. Microbiol. 50, 1376–1383. doi:10.1128/JCM.05852-11.

Wong, J. M. W., de Souza, R., Kendall, C. W. C., Emam, A., and Jenkins, D. J. A. (2006). Colonic health: fermentation and short chain fatty acids. J. Clin. Gastroenterol. 40, 235–243. doi:10.1097/00004836-200603000-00015.

Wong, M. L., Inserra, A., Lewis, M. D., Mastronardi, C. A., Leong, L., Choo, J., et al. (2016). Inflammasome signaling affects anxiety- and depressive-like behavior and gut microbiome composition. Mol. Psychiatry. doi:10.1038/mp.2016.46.

Woźniak, D., Cichy, W., Przysławski, J., and Drzymała-Czyż, S. (2021). The role of microbiota and enteroendocrine cells in maintaining homeostasis in the human digestive tract. Adv. Med. Sci. 66, 284–292. doi:10.1016/j.advms.2021.05.003.

Wu, Z., and McGoogan, J. M. (2020). Characteristics of and Important Lessons From the Coronavirus Disease 2019 (COVID-19) Outbreak in China: Summary of a Report of 72 314 Cases From the Chinese Center for Disease Control and Prevention. JAMA 323, 1239–1242. doi:10.1001/jama.2020.2648.

Wyler, E., Franke, V., Menegatti, J., Kocks, C., Boltengagen, A., Praktiknjo, S., et al. (2019). Single-cell RNA-sequencing of herpes simplex virus 1-infected cells connects NRF2 activation to an antiviral program. Nat. Commun. 10, 4878. doi:10.1038/s41467-019-12894-z.

Wyler, E., Mösbauer, K., Franke, V., Diag, A., Gottula, L. T., Arsiè, R., et al. (2021). Transcriptomic profiling of SARS-CoV-2 infected human cell lines identifies HSP90 as target for COVID-19 therapy. iScience 24, 102151. doi:10.1016/j.isci.2021.102151.

Xie, S. Z.-J., Kaufmann, K., Gan, O. I., Zandi, S., Takayama, N., and Dick, J. E. (2016). Sphingolipids Regulate Myeloid-Erythroid Fate Determination in Human Hematopoiesis. Blood 128, 3865.

Xiong, Y., Liu, Y., Cao, L., Wang, D., Guo, M., Jiang, A., et al. (2020). Transcriptomic characteristics of bronchoalveolar lavage fluid and peripheral blood mononuclear cells in COVID-19 patients. Emerg. Microbes Infect. 9, 761–770. doi:10.1080/22221751.2020.1747363.

Xu, X., Nie, S., Ding, H., and Hou, F. F. (2018). Environmental pollution and kidney diseases. Nat. Rev. Nephrol. 14, 313–324. doi:10.1038/nrneph.2018.11.

Xuan, M., Guan, X., Gu, Q., Shen, Z., Yu, X., Qiu, T., et al. (2017). Different iron deposition patterns in early- and middle-late-onset Parkinson's disease. Parkinsonism Relat. Disord. 44, 23–27. doi:10.1016/j.parkreldis.2017.08.013.

Yamamoto, S., Tsukamoto, T., Terai, A., Kurazono, H., Takeda, Y., and Yoshida, O. (1997). Genetic evidence supporting the fecal-perineal-urethral hypothesis in cystitis caused by Escherichia coli. J. Urol. 157, 1127–1129.

Yan, B., Chu, H., Yang, D., Sze, K.-H., Lai, P.-M., Yuan, S., et al. (2019). Characterization of the Lipidomic Profile of Human Coronavirus-Infected Cells: Implications for Lipid Metabolism Remodeling upon Coronavirus Replication. Viruses 11. doi:10.3390/v11010073.

Yang, W.-H., and Shen, N.-C. (1990). Gas-Forming Infection of the Urinary Tract: An Investigation of Fermentation As a Mechanism. J. Urol. 143, 960–964. doi:https://doi.org/10.1016/S0022-5347(17)40151-0.

Yen, Y., Cheng, B., Chan, C., Lin, C., and Chen, H. (2018). Heavy Metal Components in Blood and Urinary Stones of Urolithiasis Patients. Biol. Trace Elem. Res. 185, 266–274. doi:10.1007/s12011-018-1253-x.

Yilmaz, P., Parfrey, L. W., Yarza, P., Gerken, J., Pruesse, E., Quast, C., et al. (2014). The SILVA and "all-species living tree project (LTP)" taxonomic frameworks. Nucleic Acids Res. 42, D643–D648.

Yizhak, K., Tuller, T., Papp, B., and Ruppin, E. (2011). Metabolic modeling of endosymbiont genome reduction on a temporal scale. Mol. Syst. Biol. 7, 479. doi:10.1038/msb.2011.11.

Yofe, I., Dahan, R., and Amit, I. (2020). Single-cell genomic approaches for developing the next generation of immunotherapies. Nat. Med. 26, 171–177. doi:10.1038/s41591-019-0736-4.

Yu, X., Du, T., Song, N., He, Q., Shen, Y., Jiang, H., et al. (2013). Decreased iron levels in the temporal cortex in postmortem human brains with Parkinson disease. Neurology 80, 492–495. doi:10.1212/WNL.0b013e31827f0ebb.

Yu, Y., Tsitrin, T., Singh, H., Doerfert, S. N., Sizova, M. V, Epstein, S. S., et al. (2018). Actinobaculum massiliense Proteome Profiled in Polymicrobial Urethral Catheter Biofilms. Proteomes 6. doi:10.3390/proteomes6040052.

Zang, R., Gomez Castro, M. F., McCune, B. T., Zeng, Q., Rothlauf, P. W., Sonnek, N. M., et al. (2020). TMPRSS2 and TMPRSS4 promote SARS-CoV-2 infection of human small intestinal enterocytes. Sci. Immunol. 5. doi:10.1126/sciimmunol.abc3582.

Zanini, F., Pu, S.-Y., Bekerman, E., Einav, S., and Quake, S. R. (2018). Single-cell transcriptional dynamics of flavivirus infection. Elife 7. doi:10.7554/eLife.32942.

Zengler, K., and Palsson, B. O. (2012). A road map for the development of community systems (CoSy) biology. Nat. Rev. Microbiol. 10, 366–372. doi:10.1038/nrmicro2763.

Zhang, J., Cai, T., Zhao, F., Yao, T., Chen, Y., Liu, X., et al. (2012). The role of α-synuclein and tau hyperphosphorylation-mediated autophagy and apoptosis in lead-induced learning and memory injury. Int. J. Biol. Sci. 8, 935–944. doi:10.7150/ijbs.4499.

Zhang, L., Shimoji, M., Thomas, B., Moore, D. J., Yu, S.-W., Marupudi, N. I., et al. (2005). Mitochondrial localization of the Parkinson's disease related protein DJ-1: implications for pathogenesis. Hum. Mol. Genet. 14, 2063–2073. doi:10.1093/hmg/ddi211.

Zhang, T., Ruan, J., Zhang, B., Lu, S., Gao, C., Huang, L., et al. (2019). Heavy metals in human urine, foods and drinking water from an e-waste dismantling area: Identification of exposure sources and metal-induced health risk. Ecotoxicol. Environ. Saf. 169, 707–713. doi:https://doi.org/10.1016/j.ecoenv.2018.10.039.

Zhao, D., Liu, R.-Y., Xiang, P., Juhasz, A. L., Huang, L., Luo, J., et al. (2017). Applying Cadmium Relative Bioavailability to Assess Dietary Intake from Rice to Predict Cadmium Urinary Excretion in Nonsmokers. Environ. Sci. Technol. 51, 6756–6764. doi:10.1021/acs.est.7b00940.

Zhao, L., Gao, S., Huan, H., Xu, X., Zhu, X., Yang, W., et al. (2009). Comparison of virulence factors and expression of specific genes between uropathogenic Escherichia coli and avian pathogenic E. coli in a murine urinary tract infection model and a chicken challenge model. Microbiology 155, 1634–1644. doi:10.1099/mic.0.024869-0.

Zheng, H.-Y., Zhang, M., Yang, C.-X., Zhang, N., Wang, X.-C., Yang, X.-P., et al. (2020). Elevated exhaustion levels and reduced functional diversity of T cells in peripheral blood may predict severe progression in COVID-19 patients. Cell. Mol. Immunol. 17, 541–543. doi:10.1038/s41423-020-0401-3.

Zhou, F., Yu, T., Du, R., Fan, G., Liu, Y., Liu, Z., et al. (2020). Clinical course and risk factors for mortality of adult inpatients with COVID-19 in Wuhan, China: a retrospective cohort study. Lancet (London, England) 395, 1054–1062. doi:10.1016/S0140-6736(20)30566-3.

Zhou, P., Yang, X.-L., Wang, X.-G., Hu, B., Zhang, L., Zhang, W., et al. (2020). A pneumonia outbreak associated with a new coronavirus of probable bat origin. Nature 579, 270–273. doi:10.1038/s41586-020-2012-7.

Zhou, Y., Fu, B., Zheng, X., Wang, D., Zhao, C., Qi, Y., et al. (2020). Pathogenic T-cells and inflammatory monocytes incite inflammatory storms in severe COVID-19 patients. Natl. Sci. Rev. 7, 998–1002. doi:10.1093/nsr/nwaa041.

Zhu, L., Pei, W., Thiele, I., and Mahadevan, R. (2021). Integration of a physiologically-based pharmacokinetic model with a whole-body, organ-resolved genome-scale model for characterization of ethanol and acetaldehyde metabolism. PLOS Comput. Biol. 17, e1009110. doi:10.1371/journal.pcbi.1009110.

Zilberberg, M. D., Nathanson, B. H., Sulham, K., Fan, W., and Shorr, A. F. (2017). Carbapenem resistance, inappropriate empiric treatment and outcomes among patients hospitalized with Enterobacteriaceae urinary tract infection, pneumonia and sepsis. BMC Infect. Dis. 17, 279. doi:10.1186/s12879-017-2383-z.

Zimmermann, J., Kaleta, C., and Waschina, S. (2020). Gapseq: Informed prediction of bacterial metabolic pathways and reconstruction of accurate metabolic models. bioRxiv, 1–35. doi:10.1101/2020.03.20.000737.

Zozaya, M., Ferris, M. J., Siren, J. D., Lillis, R., Myers, L., Nsuami, M. J., et al. (2016). Bacterial communities in penile skin, male urethra, and vaginas of heterosexual couples with and without bacterial vaginosis. Microbiome 4, 16. doi:10.1186/s40168-016-0161-6.

Zur, H., Ruppin, E., and Shlomi, T. (2010). iMAT: an integrative metabolic analysis tool. Bioinformatics 26, 3140–3142. doi:10.1093/bioinformatics/btq602.

VII. Supplementary Data

A. Figures

Co_002_TA
Complicated w/ Hyperinflammatory Syndrome

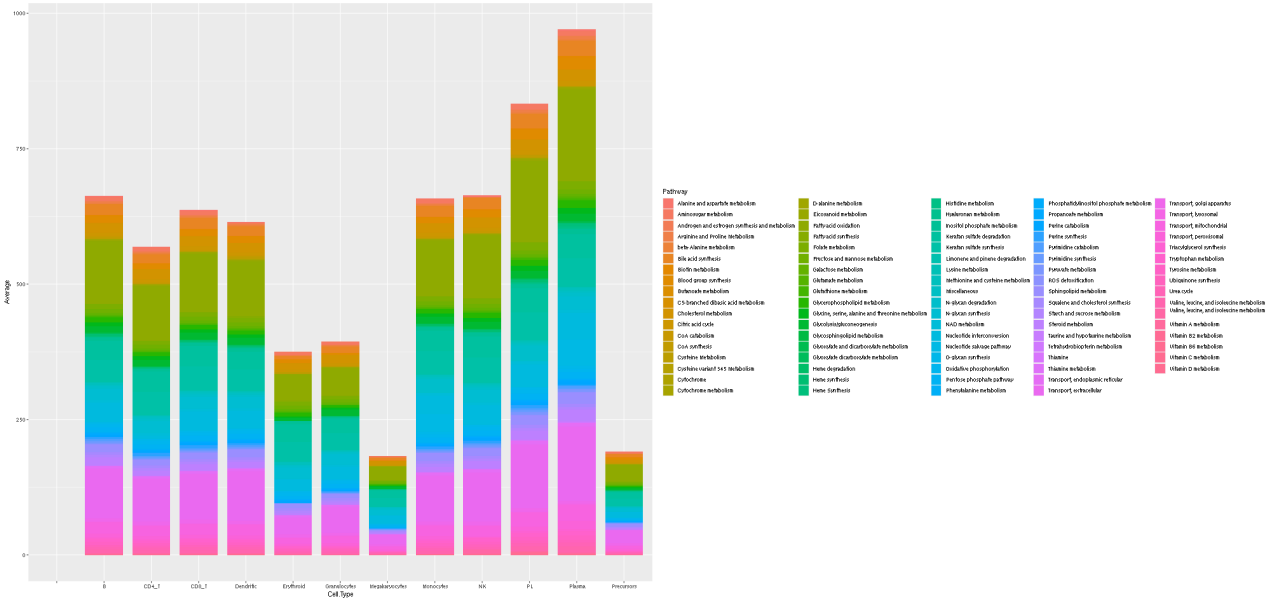

Co_003_TA
Complicated (Recovering)

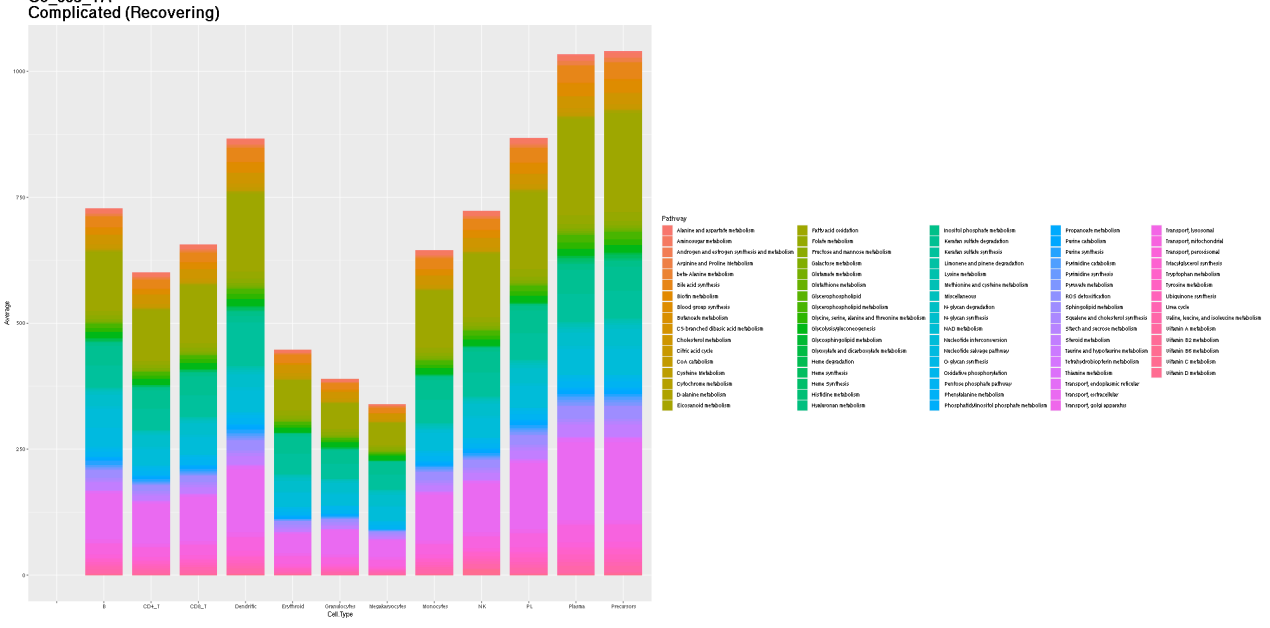

Co_003_TB
Recovery (Asymptomatic)

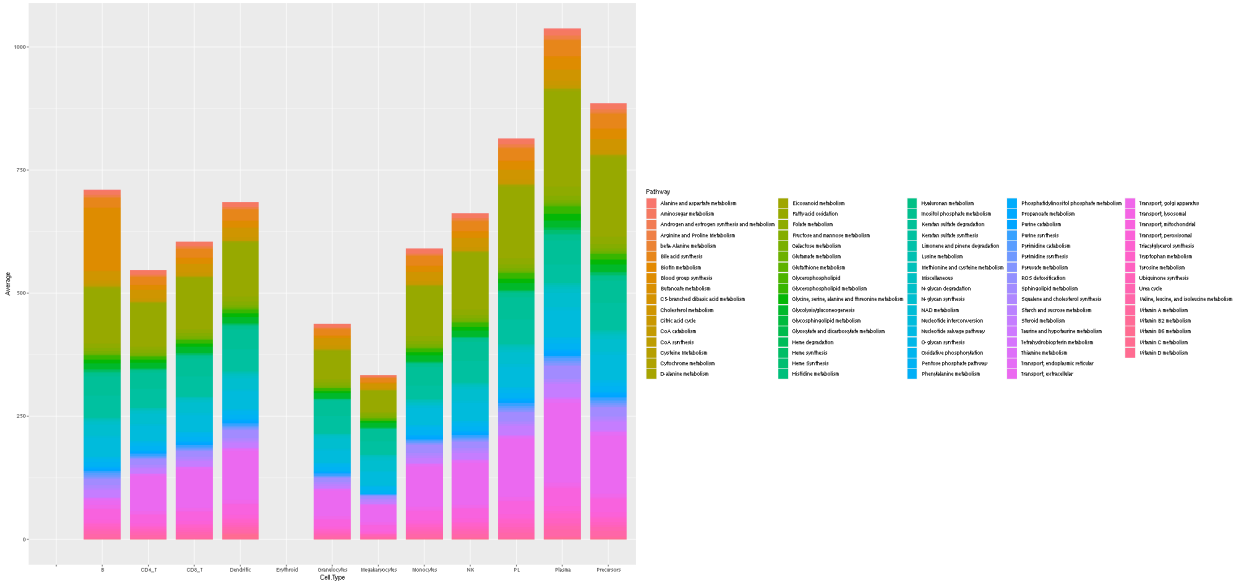

Co_004_TC
Mild (Recovering)

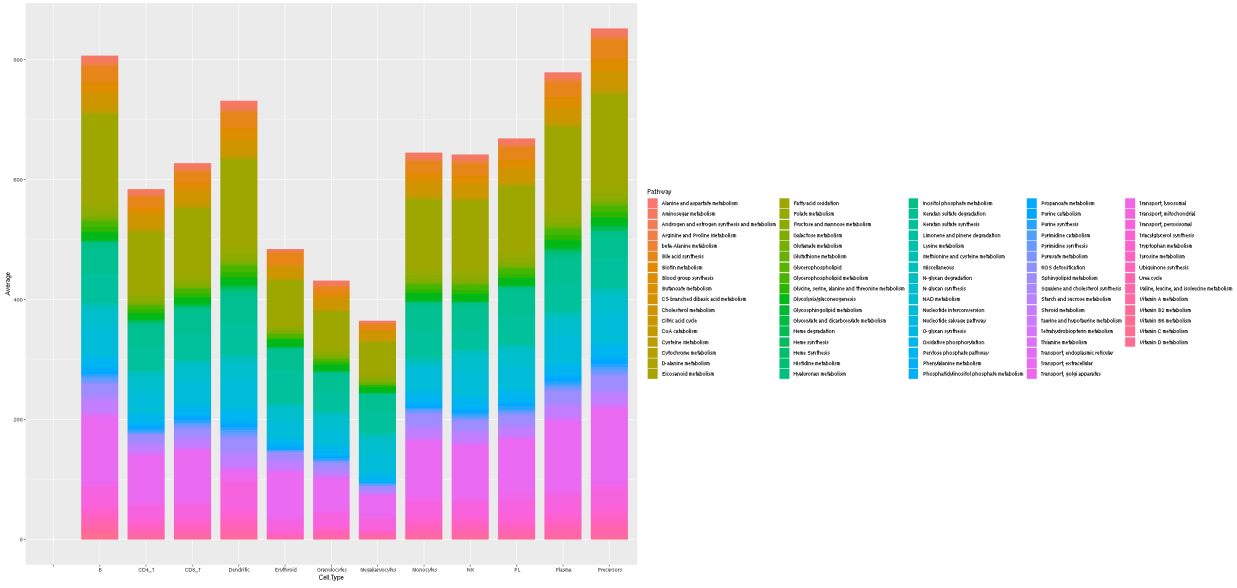

Co_011_TA
Recovery / Asymptomatic

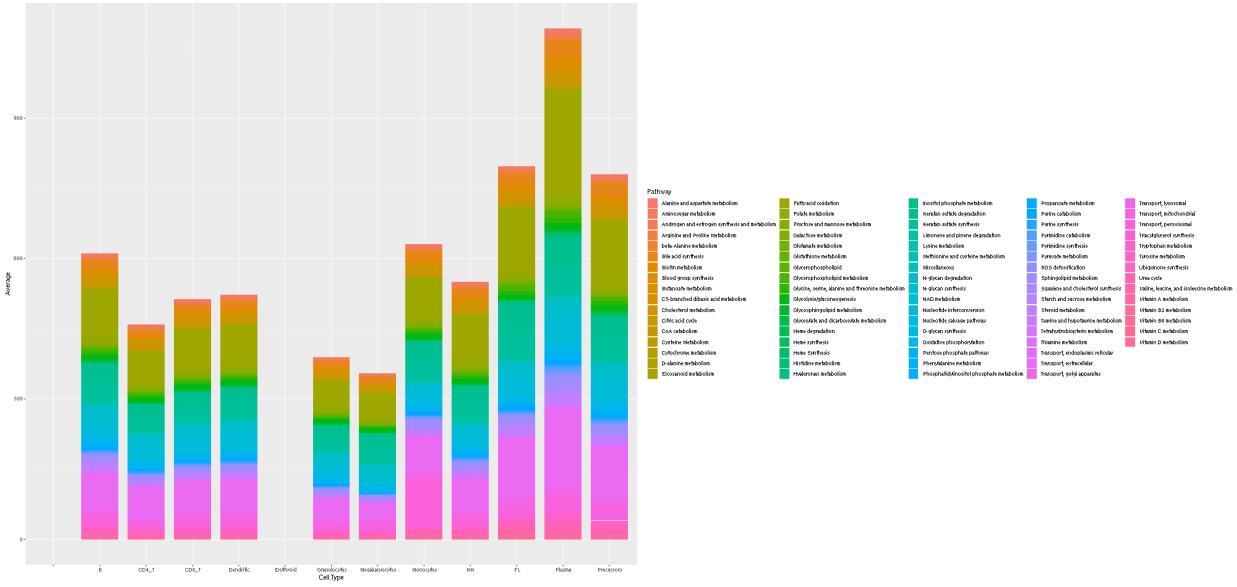

Co_011_TB
Recovery / Asymptomatic

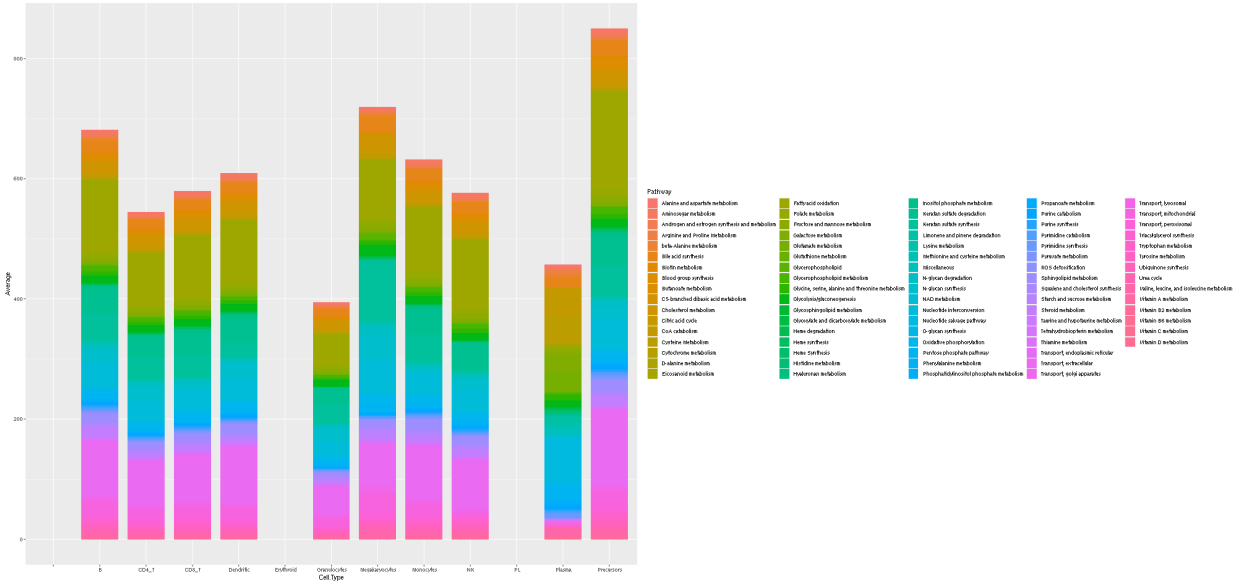

Co_012_TA
Critical

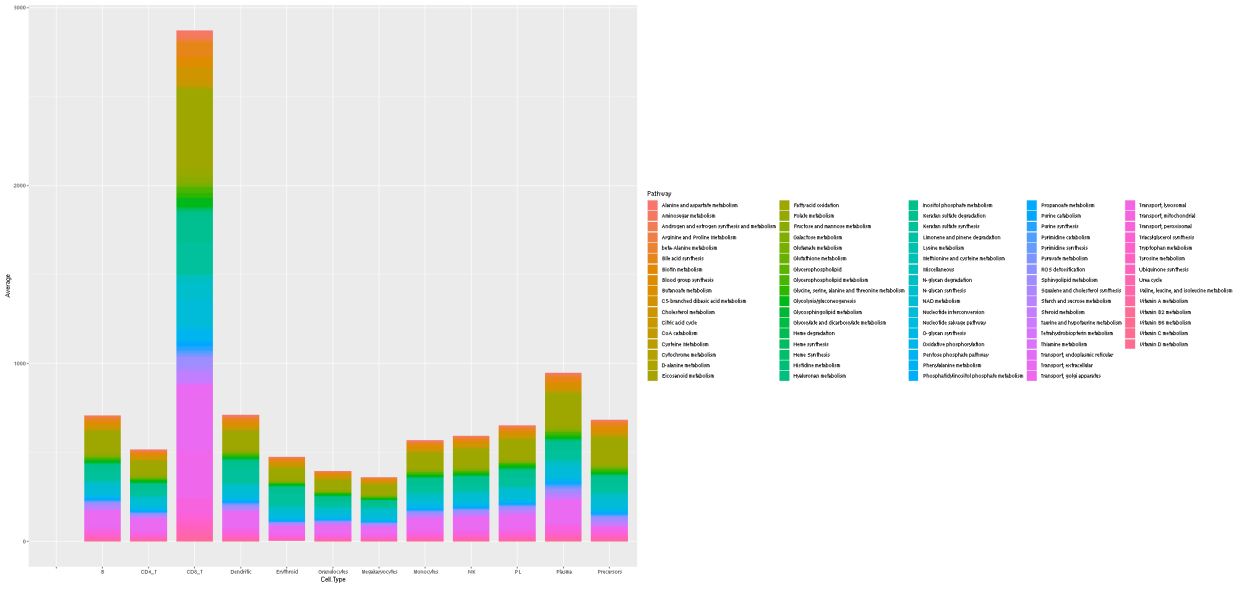

Co_012_TB
Complicated w/ Hyperinflammatory Syndrome

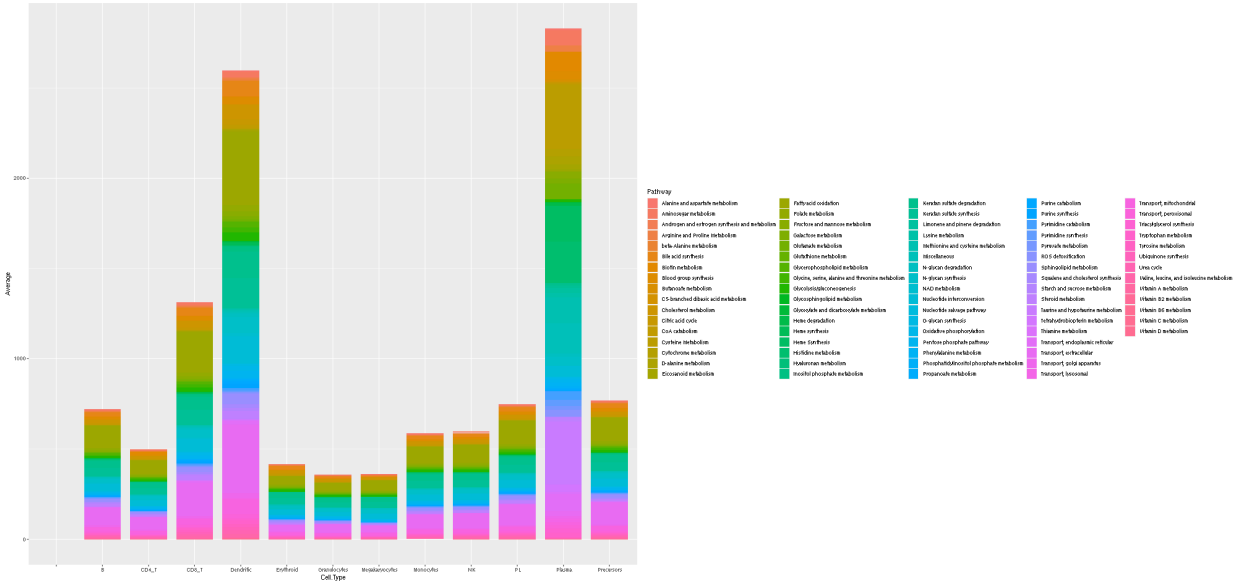

Co_012_TC
Mild (Recovering)

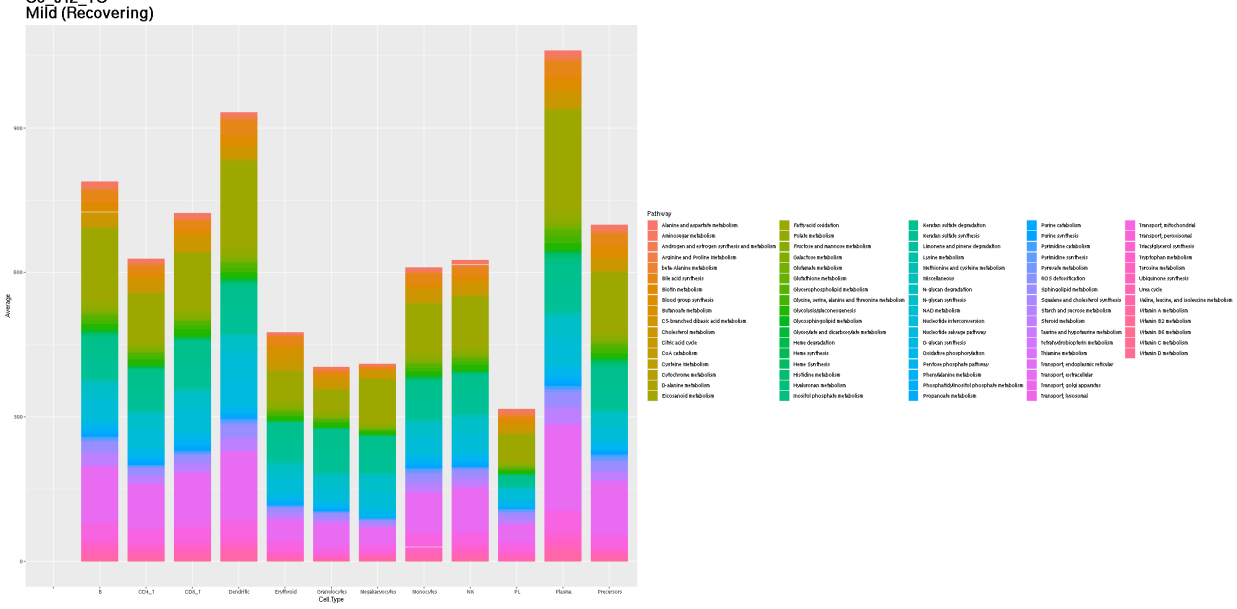

Co_012_TE
Mild (Recovering)

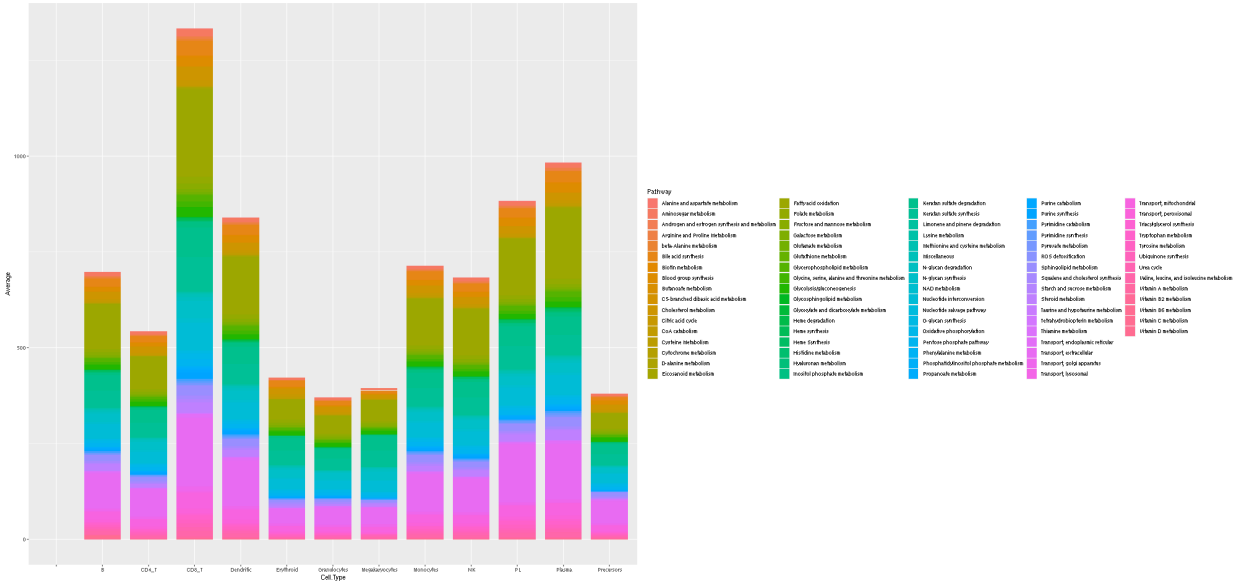

Co_022_TA
Complicated (Recovering)

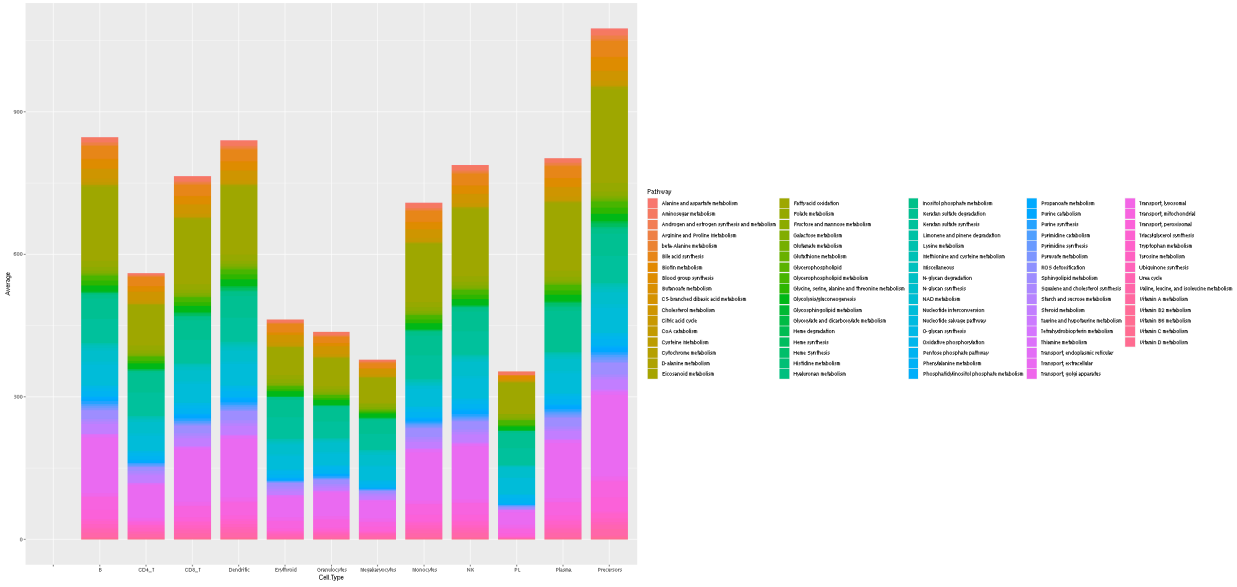

Ki_001_TA
Complicated (Recovering)

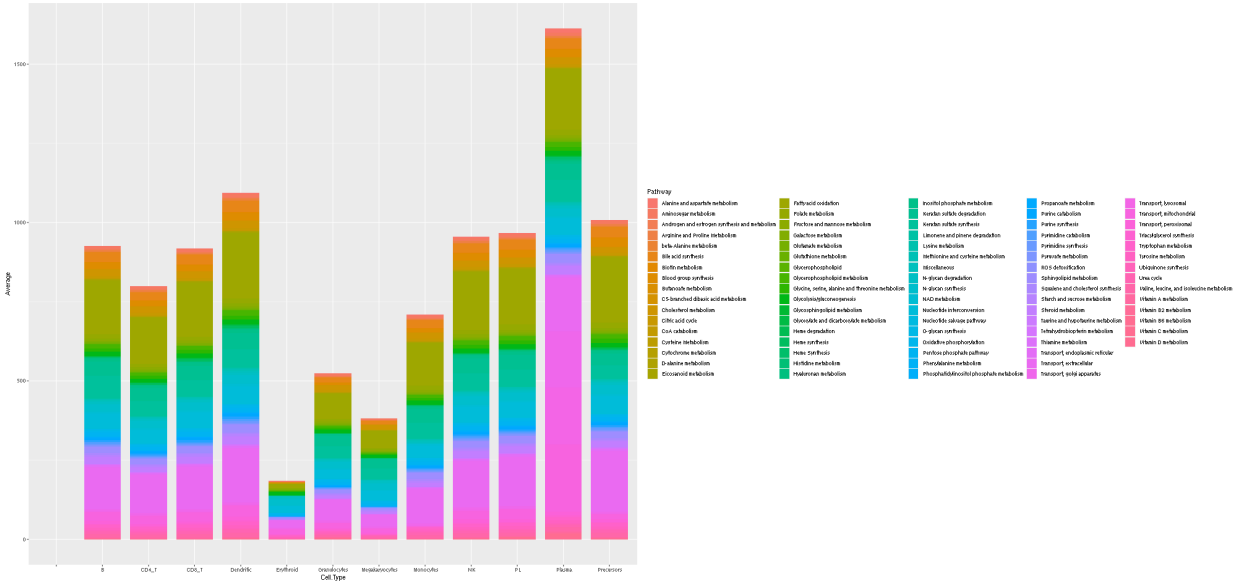

Ki_001_TA2
Complicated w/ Hyperinflammatory Syndrome

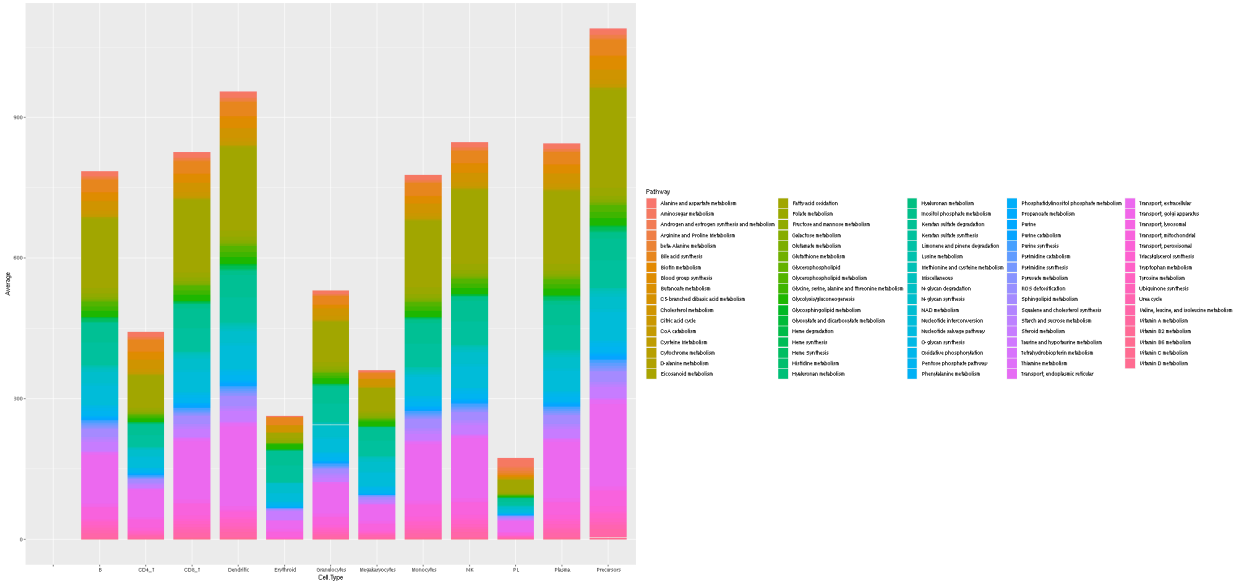

Ki_001_TB
Mild (Recovering)

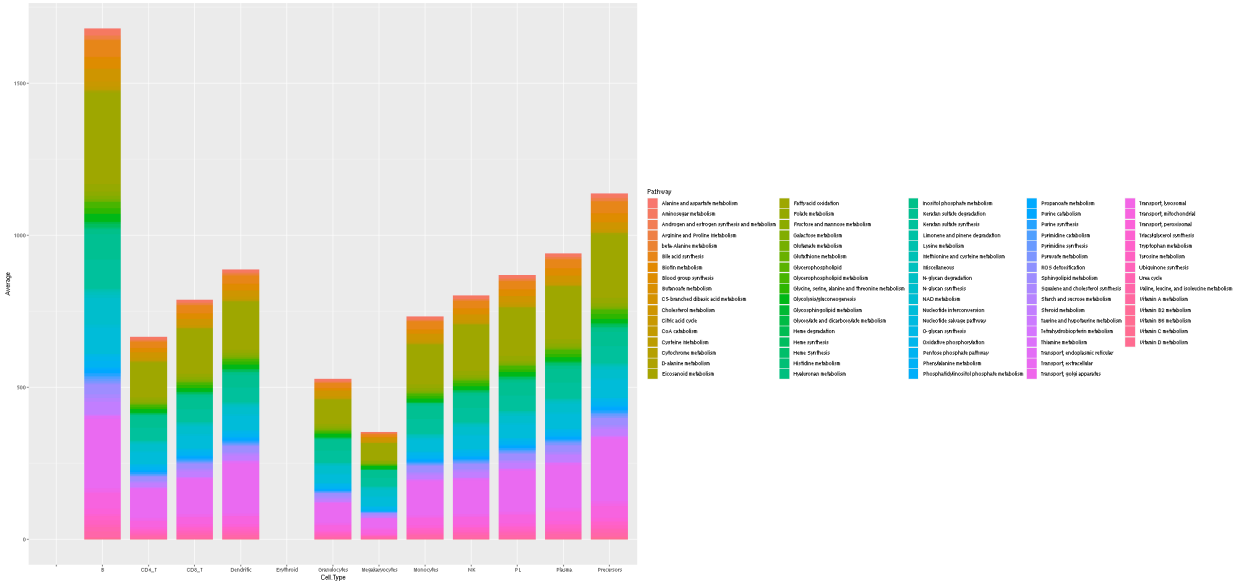

Ki_001_TC
Recovery / Asymptomatic

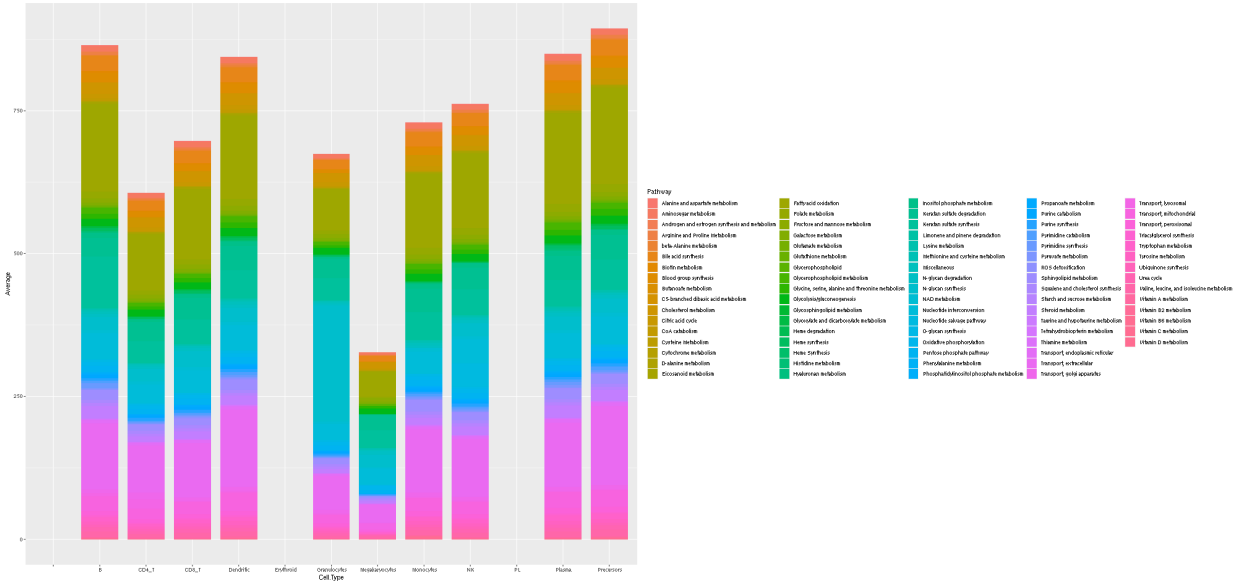

Ki_002_TA
Complicated (Incremental)

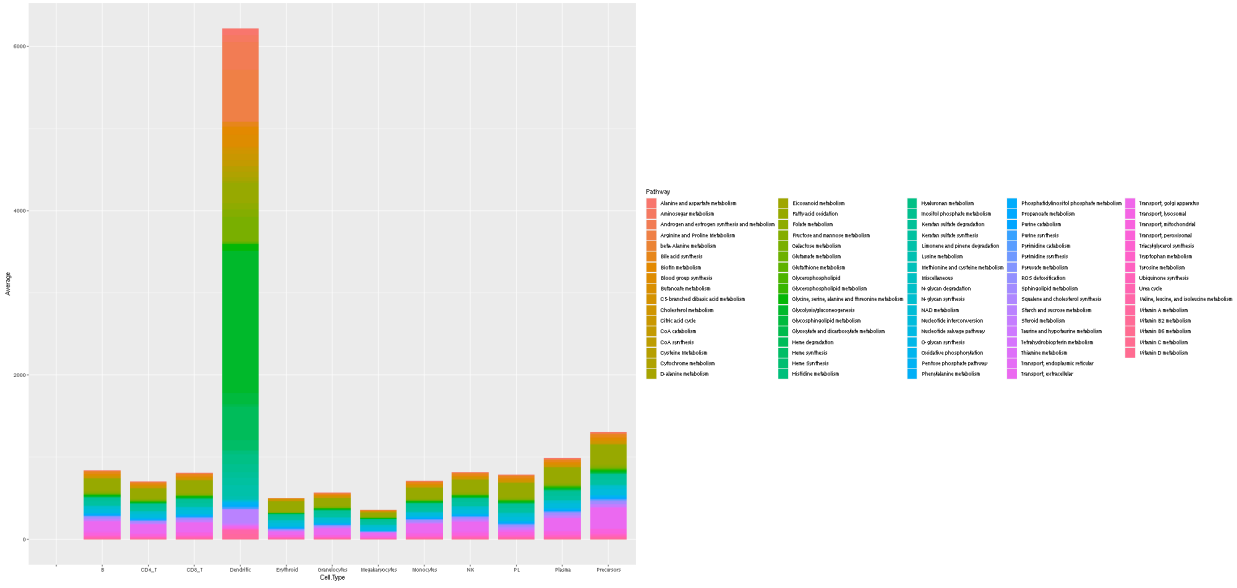

Ki_002_TA2
Critical

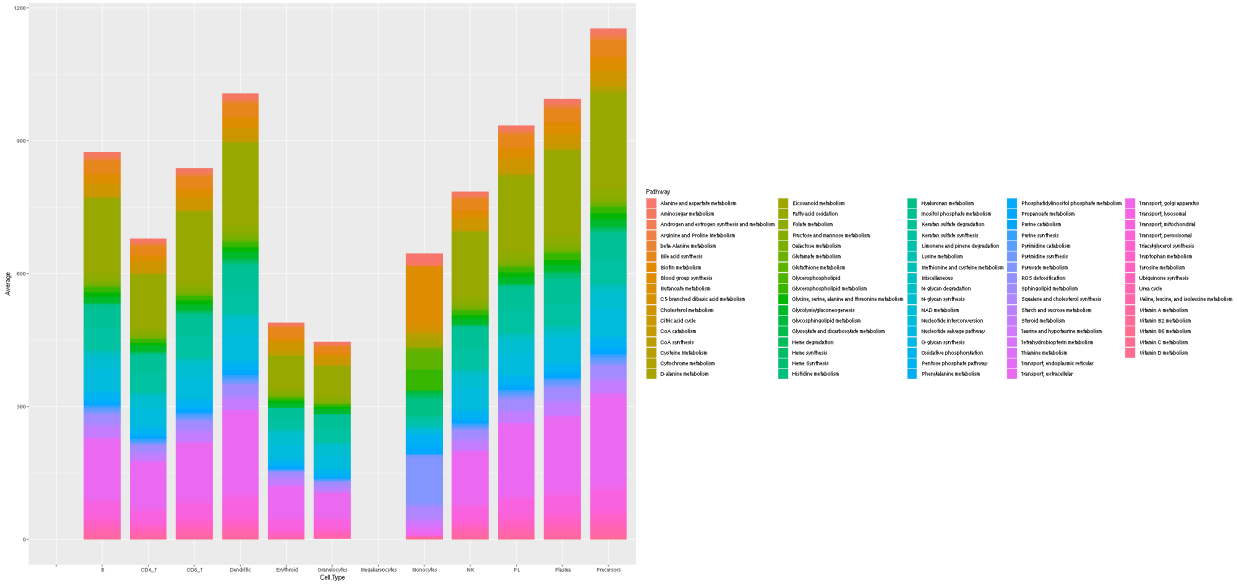

Ki_003_Control
Healthy

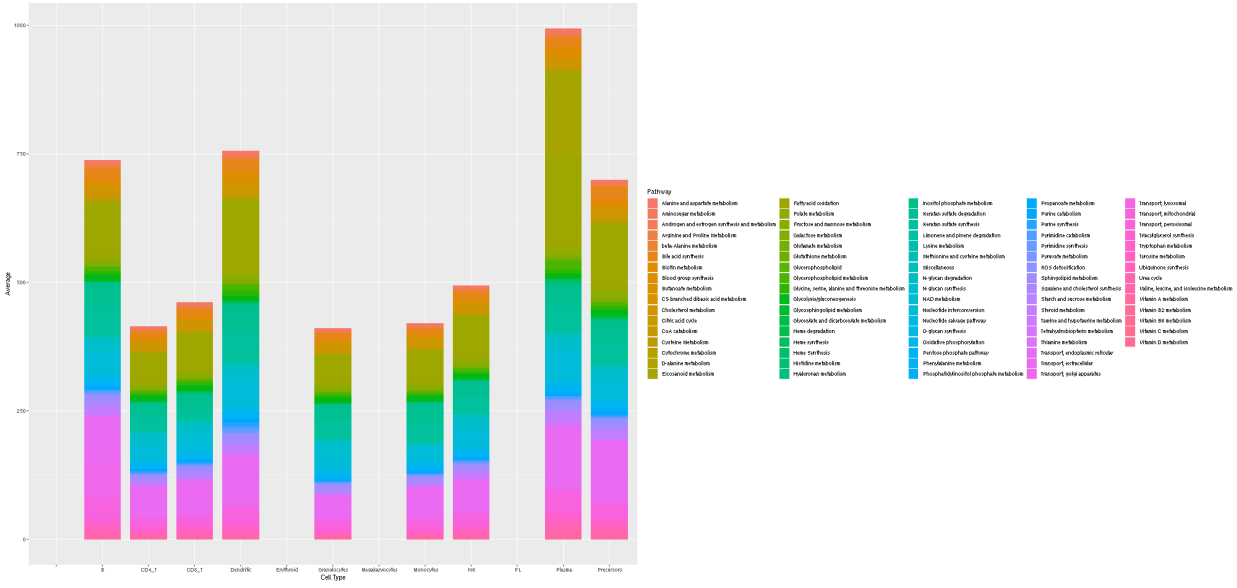

Ki_004_TA
Complicated / Incremental

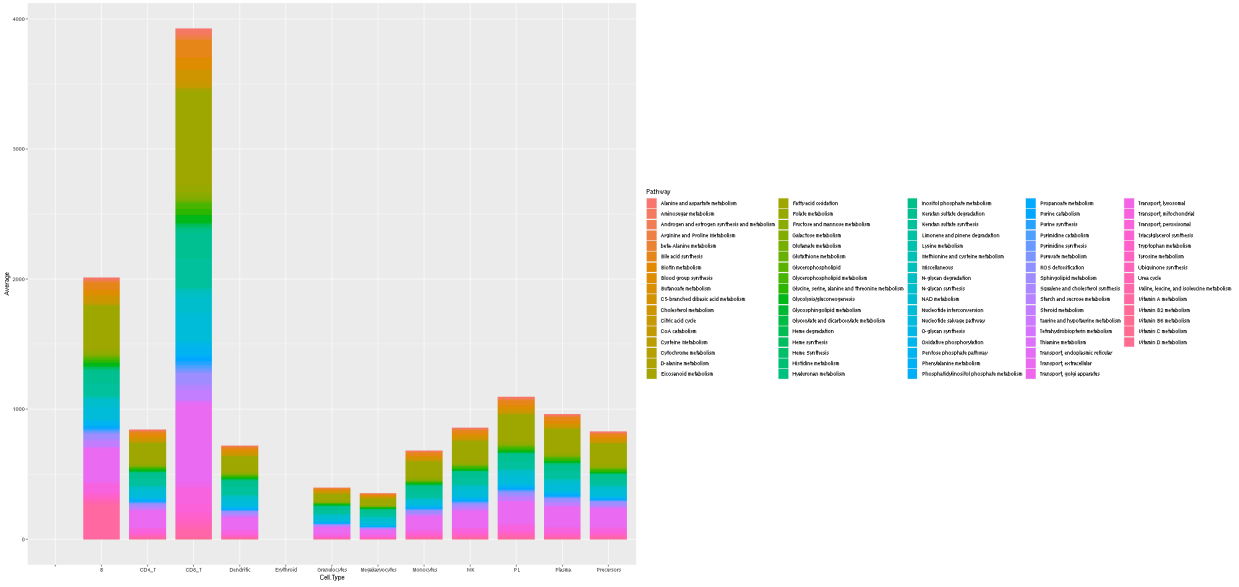

Ki_004_TA2
Complicated w/ Hyperinflammatory Syndrome

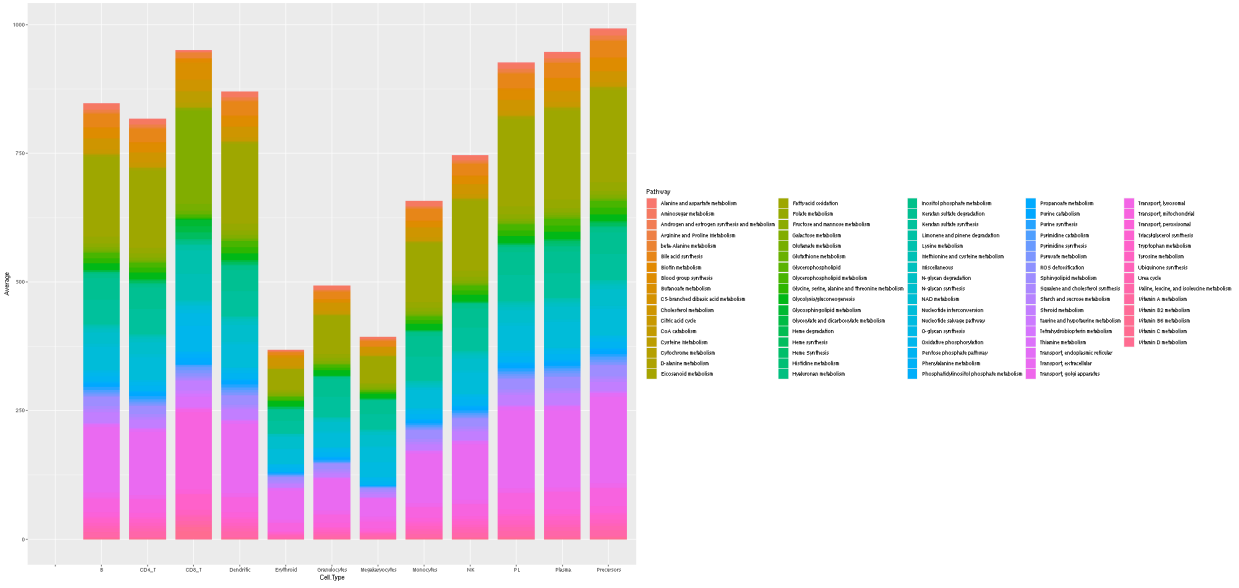

Ki_004_TB
Mild (Recovering)

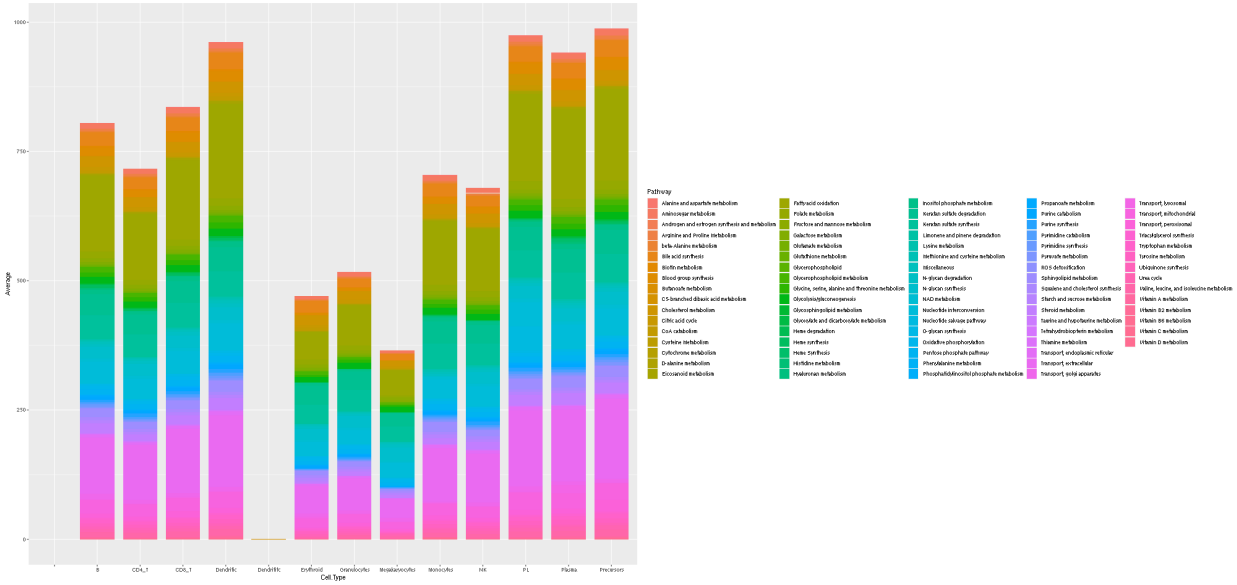

Ki_005_Control
Healthy

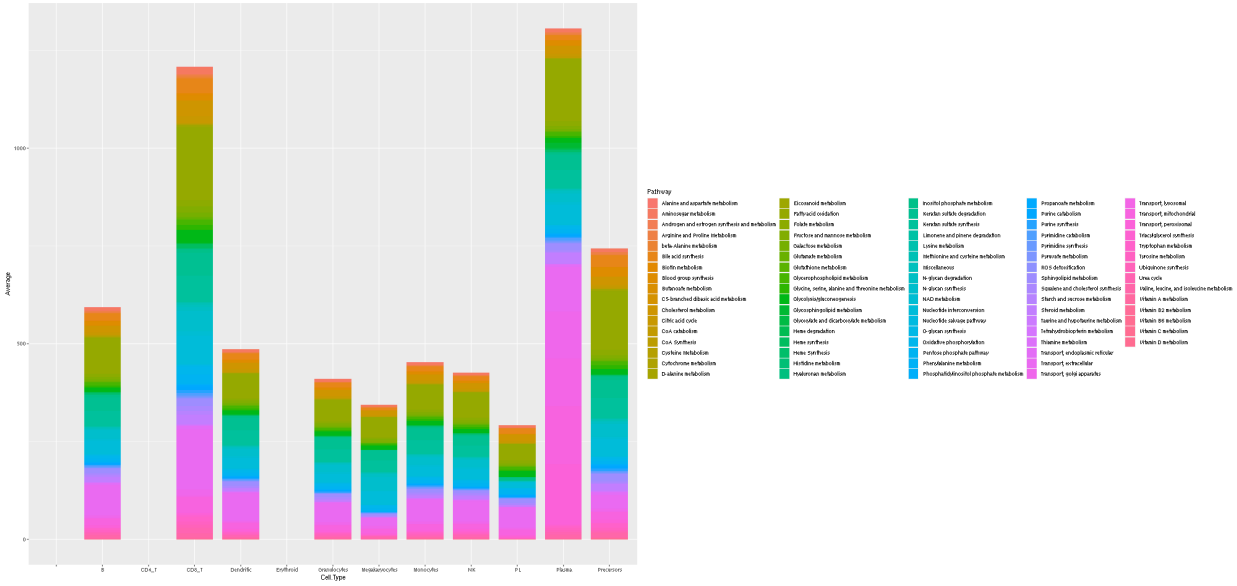

Ki_005_TA
Complicated (Incremental)

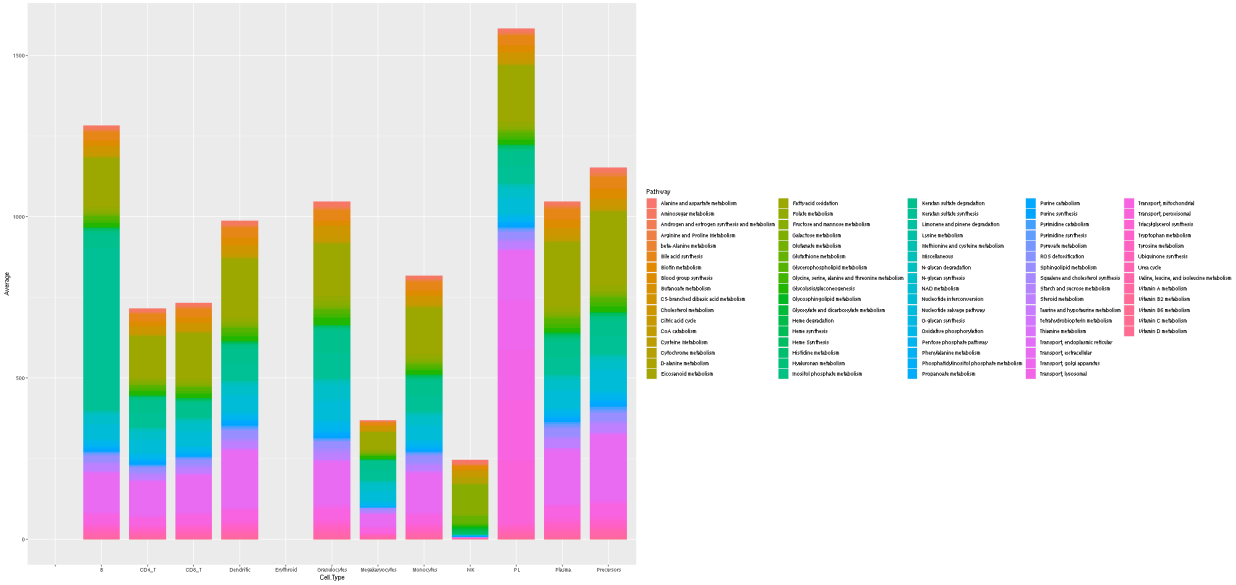

Ki_005_TA2
Complicated w/ Hyperinflammatory Syndrome

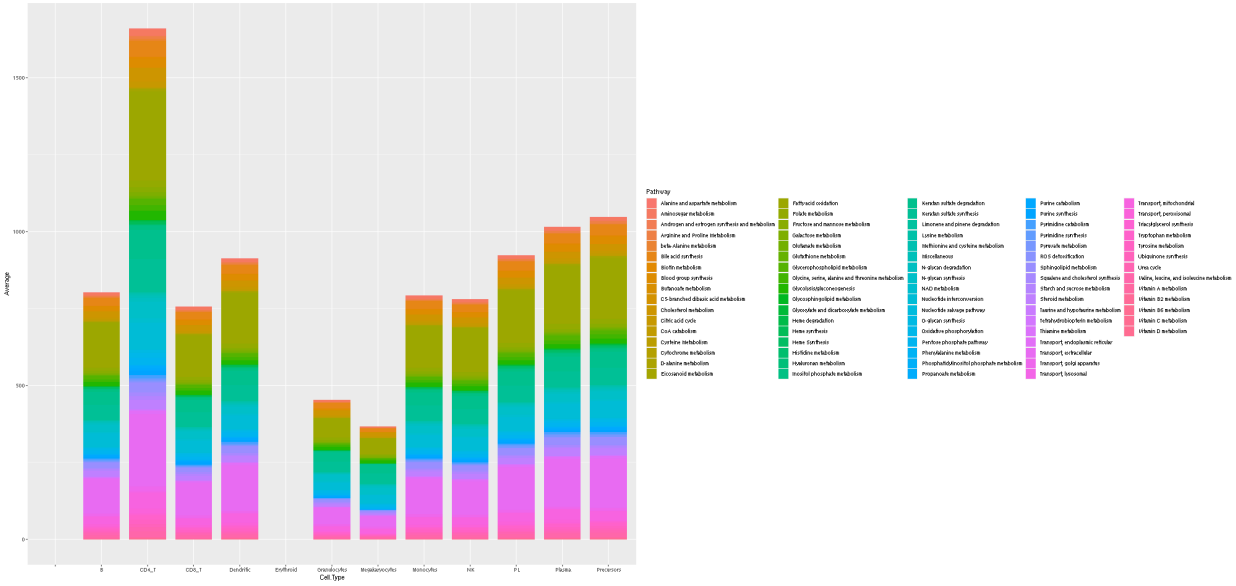

Ki_005_TB
Recovery / Asymptomatic

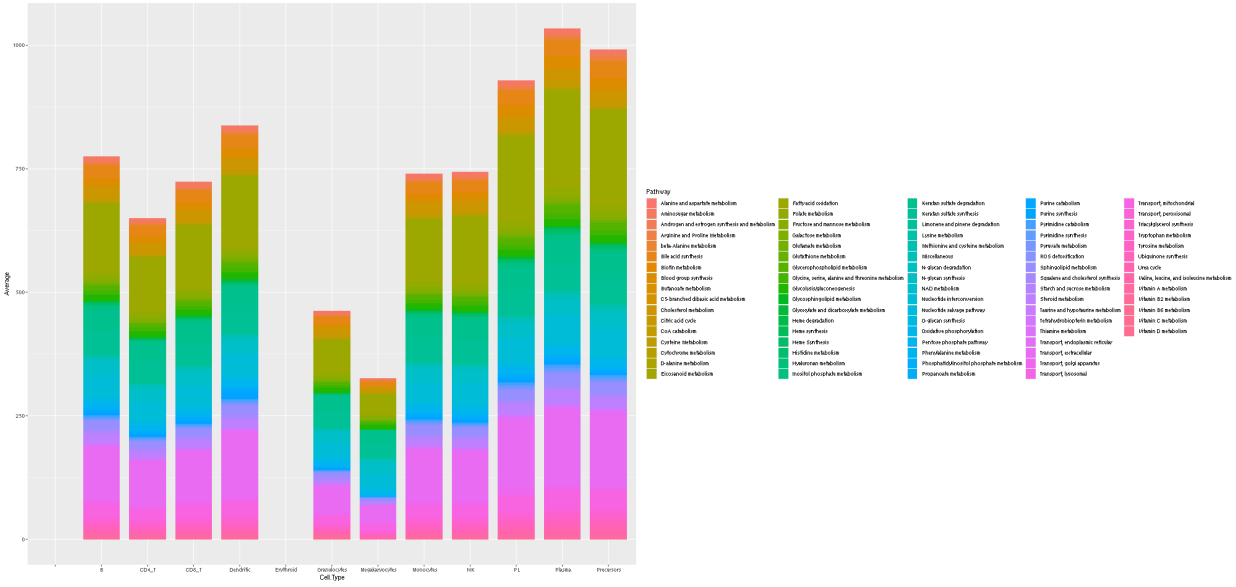

Ki_006_TA
Mild (Recovering)

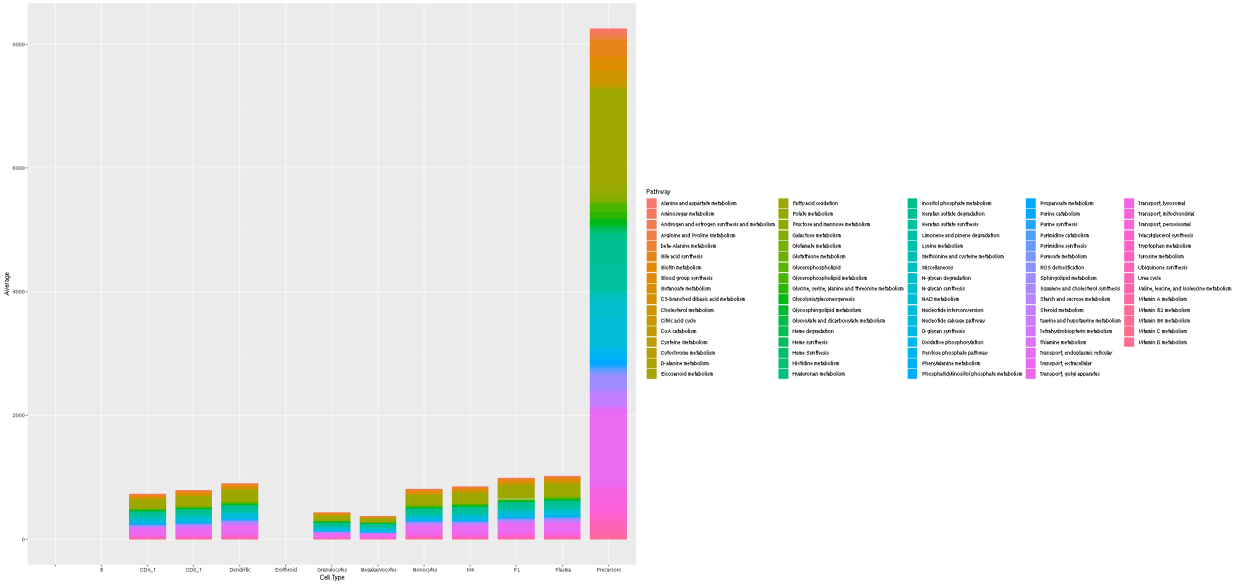

Ki_006_TA2
Mild (Recovering)

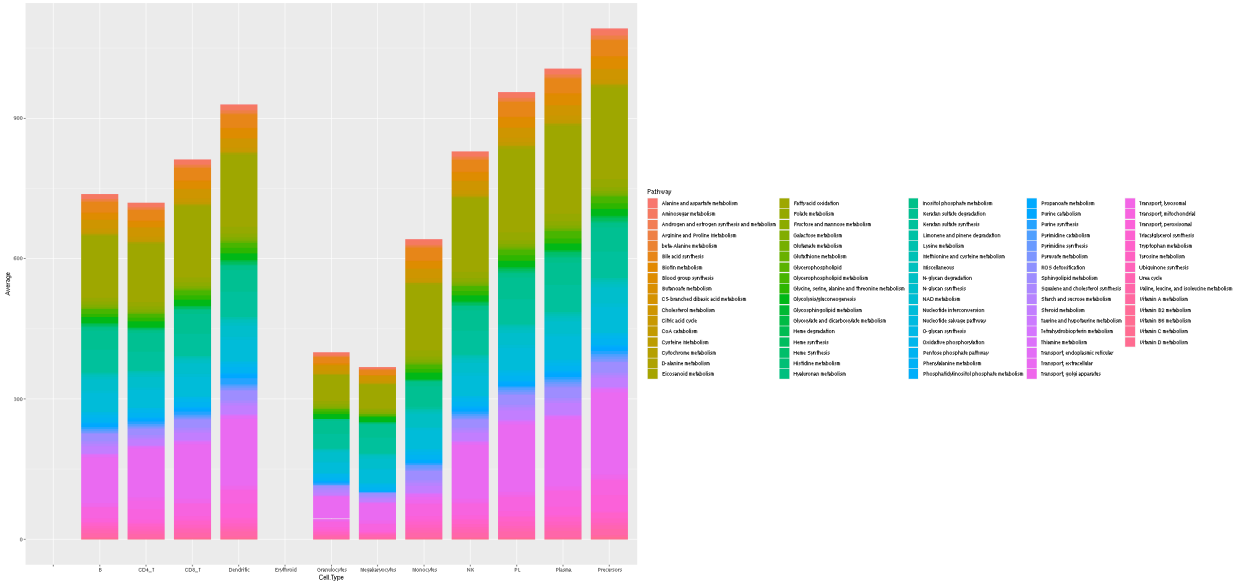

Ki_006_TB
Recovery / Asymptomatic

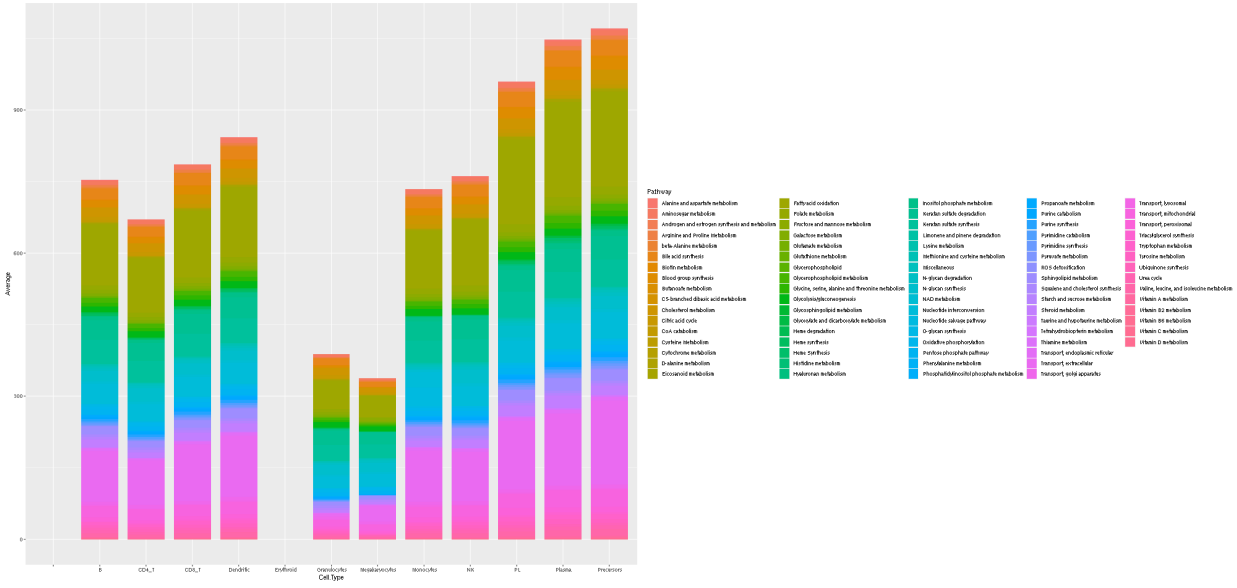

Ki_006_TE
Recovered

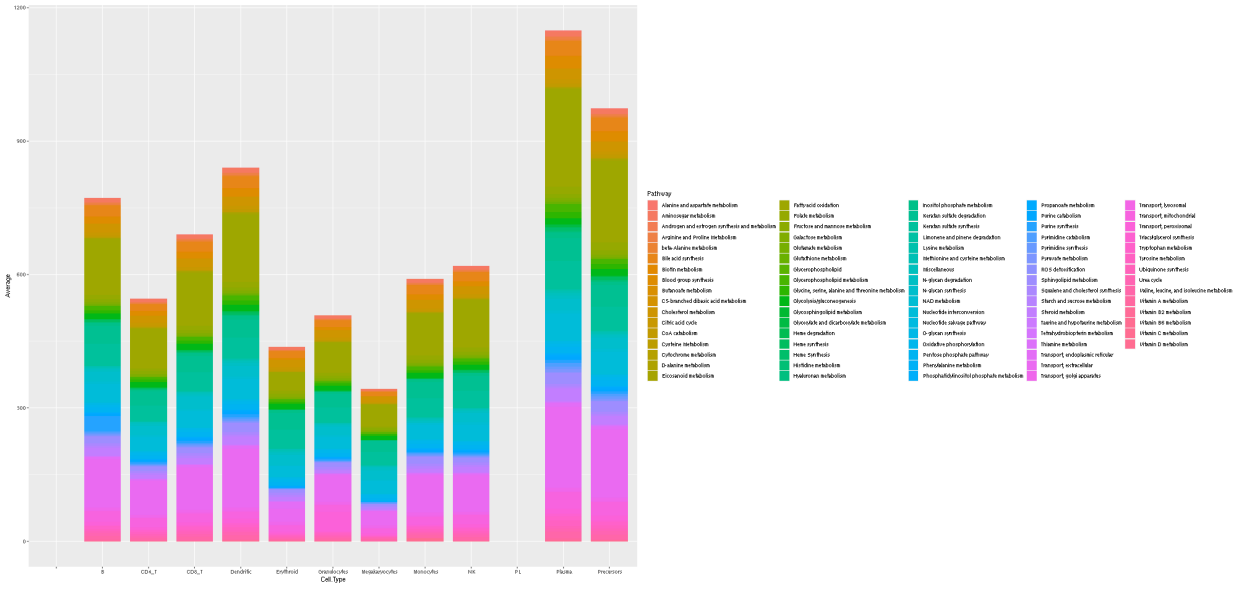

Ki_007_Control
Healthy

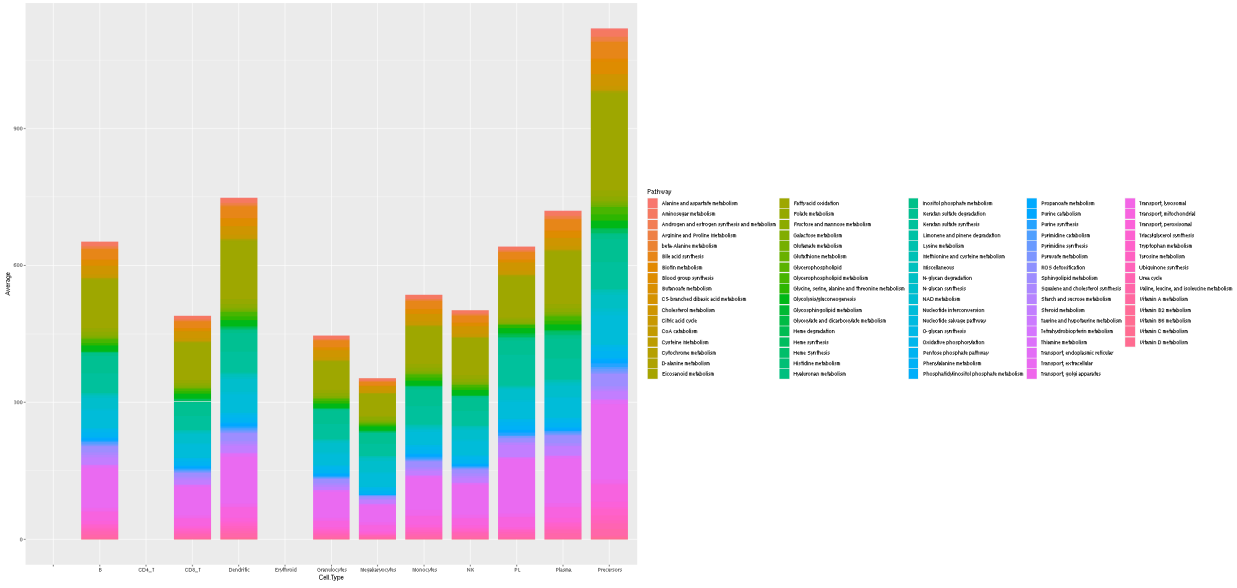

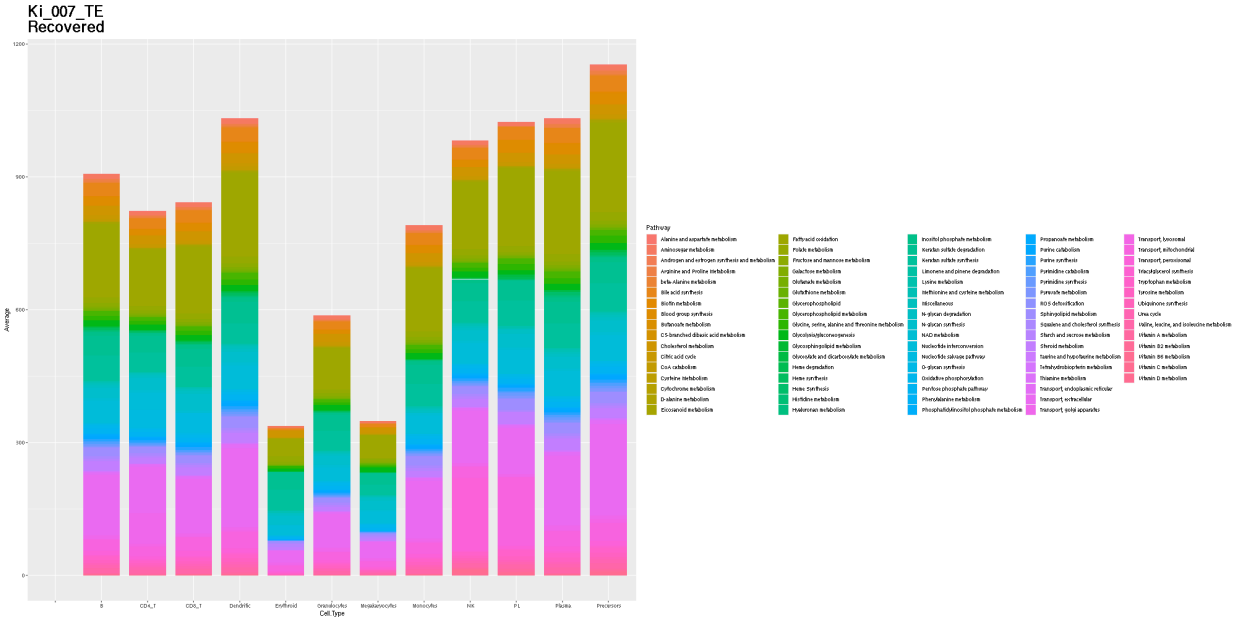
Ki_007_TE
Recovered
Average
1200
900
600
300
0
B
CD4_T
CD8_T
Dendritic
Erythroid
Granulocytes
Megakaryocytes
Monocytes
NK
PL
Plasma
Precursors
Cell Type
Pathway
Alanine and aspartate metabolism
Aminosugar metabolism
Androgen and estrogen synthesis and metabolism
Arginine and Proline metabolism
Beta-Alanine metabolism
Bile acid synthesis
Biotin metabolism
Blood group synthesis
Butanoate metabolism
C5-branched dibasic acid metabolism
Cholesterol metabolism
Citric acid cycle
Cox catabolism
Cortisine metabolism
Cytochrome metabolism
D-alanine metabolism
Eicosanoid metabolism
Fatty acid oxidation
Folate metabolism
Fructose and mannose metabolism
Galactose metabolism
Glutamate metabolism
Glutathione metabolism
Glycerophospholipid
Glycerophospholipid metabolism
Glycine, serine, alanine and threonine metabolism
Glycosphingolipid metabolism
Glycosylate and dicarboxylate metabolism
Heme degradation
Heme synthesis
Heme Synthesis
Histidine metabolism
Hyaluronan metabolism
Inositol phosphate metabolism
Keratan sulfate degradation
Keratan sulfate synthesis
Limonene and pinene degradation
Lysine metabolism
Methionine and cortisine metabolism
Miscellaneous
N-glycan degradation
N-glycan synthesis
NAD metabolism
Nucleotide interconversion
Nucleotide salvage pathway
O-glycan synthesis
Oxidative phosphorylation
Pentose phosphate pathway
Phenylalanine metabolism
Phosphatidylinositol phosphate metabolism
Propanoate metabolism
Purine catabolism
Purine synthesis
Pyrimidine catabolism
Pyrimidine synthesis
Pyruvate metabolism
ROS detoxification
Sphingolipid metabolism
Squalene and cholesterol synthesis
Starch and sucrose metabolism
Steroid metabolism
Taurine and hypotaurine metabolism
Tetrahydrobiopterin metabolism
Thiamine metabolism
Transport, endoplasmic reticular
Transport, extracellular
Transport, golgi apparatus
Transport, lysosomal
Transport, mitochondrial
Transport, peroxisomal
Triacylglycerol synthesis
Tryptophan metabolism
Tyrosine metabolism
Ubiquinone synthesis
Urea cycle
Valine, leucine, and isoleucine metabolism
Vitamin A metabolism
Vitamin B2 metabolism
Vitamin B6 metabolism
Vitamin C metabolism
Vitamin D metabolism

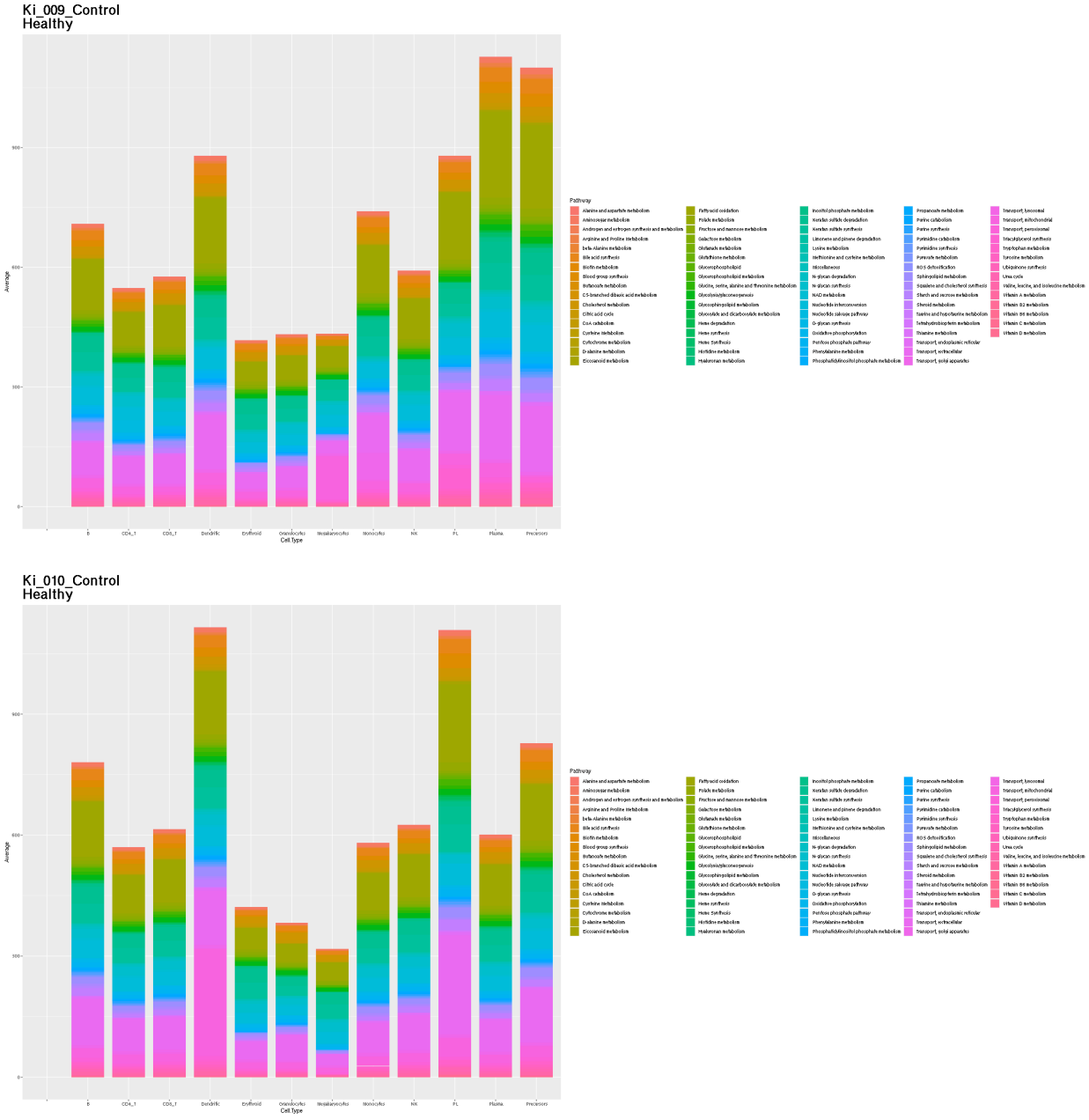

Supplementary Figures 1-33: Metabolic reaction activities across cell-types for the remaining COVID-19 cohort

B. Tables

Software / Package	Version	Link
ape	5.5	http://ape-package.ird.fr/
BacArena	1.8.2	https://github.com/euba/bacarena
BiocManager	1.30.16	https://github.com/Bioconductor/
COBRA Toolbox	3.3	https://github.com/opencobra/cobratoolbox
CobraPy	0.22.0	https://opencobra.github.io/cobrapy/
CPLEX	12.7.1	https://www.ibm.com/analytics/cplex-optimizer
Cutadapt	1.5	https://github.com/marcelm/cutadapt
data.table	1.14.0	https://github.com/Rdatatable/data.table
dendextend	1.15.1	10.1093/bioinformatics/btv428
DESeq2	1.28.1	https://git.bioconductor.org/packages/DESeq2
fastcc	N/A	https://journals.plos.org/ploscompbiol/article?id=10.1371/journal.pcbi.1003424
fastcore	N/A	https://journals.plos.org/ploscompbiol/article?id=10.1371/journal.pcbi.1003424
FASTQC	3	http://www.bioinformatics.babraham.ac.uk/projects/fastqc/
GapSeq	1.1	https://github.com/jotech/gapseq
ggplot2	3.3.5	https://github.com/tidyverse/ggplot2
git	2.21.0	https://git-scm.com/
hdf5	1.3.3	https://github.com/HDFGroup/hdf5
HISAT2	2.1.0	http://ccb.jhu.edu/software/hisat2
htseq	0.11.1	https://academic.oup.com/bioinformatics/article/31/2/166/2366196
MATLAB	R2021b	https://www.mathworks.com
Mendeley Desktop	1.19.8	https://www.mendeley.com/

miniconda3	4.7.12.1	https://www.anaconda.com.
openmpi	3.1.5	https://www.open-mpi.org/
Pandas	1.3.4	https://pandas.pydata.org/
PhyloSeq	1.32.0	https://git.bioconductor.org/packages/phyloseq
plyr	1.8.6	https://github.com/hadley/plyr
Prinseq-lite	0.20.4	http://prinseq.sourceforge.net
Python	3.8.1	https://www.python.org/
R Version	4.0.0	https://cran.r-project.org/
R.matlab	3.6.2	https://github.com/HenrikBengtsson/R.matlab
reshape	0.8.8	http://had.co.nz/reshape
SAMtools	1.1	http://samtools.sourceforge.net
sbml	5.18.0	https://pubmed.ncbi.nlm.nih.gov/31219795/
SciPy	1.7.1	https://scipy.org/
Seurat	4.0.3	https://github.com/satijalab/seurat
SortmeRNA	2.1	http://bioinfo.lifl.fr/RNA/sortmerna/
StanDep	1.0.0	https://github.com/LewisLabUCSD/StanDep
stringtie	2.0.3	http://ccb.jhu.edu/software/stringtie/
sybil	2.2.0	https://www.cs.hhu.de/lehrstuehle-und-arbeitsgruppen/computational-cell-biology/software-contributions/sybil
tidyr	1.1.3	https://github.com/tidyverse/tidyr
USEARCH	11.0.667	https://drive5.com/usearch/
vctrs	0.3.8	https://github.com/r-lib/vctrs
Vegan	2.5-7	https://github.com/vegandevs/vegan/
viridis	0.6.1	https://sjmgarnier.github.io/viridis/

Supplementary Table 1: A compilation of all software utilized in this study.

C. Dedication

I am eternally grateful to the committed mentors who supported my interests in the interdisciplinary fields underlying health science during my academic career. I am especially grateful to my Doktorvater Christoph Kaleta who supported my journey during the doctorate and provided me with an environment to express creativity in a challenging, but rewarding environment. The opportunity to explore natural sciences through the lens of computing has pushed my viewpoint to be deeper and broader than I could have expected, for that I am eternally grateful and motivated. I have also received extensive support from my family and friends to pursue my academic and personal dreams abroad, even if it means leaving home behind. I dedicate this dissertation to my Grandmother Thrity Spaulding who instilled the academic spirit into me at a young age. Whether it be her stories of cultures, religion, literature, or providing books and a creative area to explore natural sciences. Her continued support has extended from my childhood towards my present research, where her editing support has been acknowledged in a published manuscript that is discussed in the body of this dissertation. It is true that the objective of previous generations is to further support the growth of the next and to create a better future for their children. Therefore I am sure that this dissertation will make her and the elders of my family proud; these are people who immigrated between numerous countries and gave up their dreams, to give me this opportunity. These supporters and many others, have helped me down various physical and emotional roads towards the development of this dissertation. With their motivation I hope to continue to support scholarly endeavors to bolster the pursuit of science for future generations ahead.

D. Acknowledgments

This dissertation would not be possible with the combined roles of unnamed patients, physicians, medical students, and laboratory technicians who contributed to this work directly or indirectly. Specifically Samer Kadib Alban, Lena Best, Daniella Esser, Lady Johanna, Forero-Rodriguez, Stefano Flor, Simon Graspeunter, Christoph Kaleta, Georgios Marinos, Alina Renz, Hannah Clara Rettig, Jan Rupp, Jan Taubenheim, and Johannes Zimmermann have been instrumental in the creation of this doctoral dissertation. Johannes Zimmermann has exceeded his expectations as a friend and roommate by providing extra help with software support, translating the dissertation abstract from English to German, and reading through the large volume of text that is presented as my dissertation. I acknowledge the referees of the Disputation jury, Dr. Prof .Tal Dagan, Dr. Prof. Andre Franke, and Dr. Prof. Hinrich Schulenburg, who devoted their valuable time to examine and discuss this thesis. I am also in debt to Lena Best and Rebecca Höög for keeping me sane with regular and healthy breaks during the time-intensive period of preparing this dissertation. Furthermore, the work presented here could not be completed without continuous motivation from my family back home and in Germany: Rebecca, Melissa, Christian, Dominic, Mathieu, David, Zhouji, and Hakan. It truly takes a village to create something extraordinary, as well stated in a traditional African proverb: "*If you want to go fast, go alone. If you want to go far, go **together***."

E. Erklärung

Ich, Jonathan Josephs-Spaulding, erkläre hiermit, dass

- ich die Abhandlung - abgesehen von der Beratung durch die Betreuerin oder den Betreuer - nach Inhalt und Form eigenständig und nur mit den angegebenen Hilfsmitteln verfasst habe,
- die Arbeit weder in Gänze noch zum Teil einer anderen Stelle im Rahmen eines Prüfungsverfahrens vorgelegt wurde, veröffentlicht worden ist oder zur Veröffentlichung eingereicht wurde;
- die Arbeit unter Einhaltung der Regeln guter wissenschaftlicher Praxis der Deutschen Forschungsgemeinschaft entstanden ist;
- kein akademischer Grad entzogen wurde.

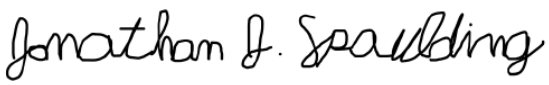

Jonathan Josephs-Spaulding

Kiel, 20.01.2022